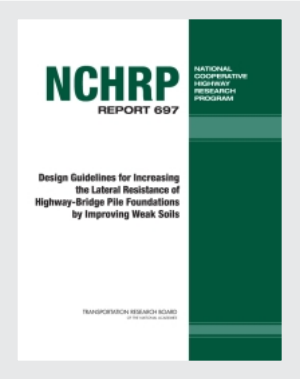

Design Guidelines for Increasing the Lateral Resistance of Highway-Bridge Pile Foundations by Improving Weak Soils

DETAILS

108 pages | | PAPERBACK

ISBN 978-0-309-21341-7 | DOI 10.17226/14574

AUTHORS

Dan Brown; Kyle Rollins; Transportation Research Board

NATIONAL COOPERATIVE HIGHWAY RESEARCH PROGRAM

NCHRP REPORT 697

Design Guidelines for Increasing the Lateral Resistance of Highway-Bridge Pile Foundations by Improving Weak Soils

Kyle Rollins
BRIGHAM YOUNG UNIVERSITY
Provo, UT

Dan Brown
DAN BROWN & ASSOCIATES
Sequatchie, TN

Subscriber Categories
Bridges and Other Structures • Design • Geotechnology

Research sponsored by the American Association of State Highway and Transportation Officials
in cooperation with the Federal Highway Administration

TRANSPORTATION RESEARCH BOARD

WASHINGTON, D.C.
2011
www.TRB.org

NATIONAL COOPERATIVE HIGHWAY RESEARCH PROGRAM

Systematic, well-designed research provides the most effective approach to the solution of many problems facing highway administrators and engineers. Often, highway problems are of local interest and can best be studied by highway departments individually or in cooperation with their state universities and others. However, the accelerating growth of highway transportation develops increasingly complex problems of wide interest to highway authorities. These problems are best studied through a coordinated program of cooperative research.

In recognition of these needs, the highway administrators of the American Association of State Highway and Transportation Officials initiated in 1962 an objective national highway research program employing modern scientific techniques. This program is supported on a continuing basis by funds from participating member states of the Association and it receives the full cooperation and support of the Federal Highway Administration, United States Department of Transportation.

The Transportation Research Board of the National Academies was requested by the Association to administer the research program because of the Board's recognized objectivity and understanding of modern research practices. The Board is uniquely suited for this purpose as it maintains an extensive committee structure from which authorities on any highway transportation subject may be drawn; it possesses avenues of communications and cooperation with federal, state and local governmental agencies, universities, and industry; its relationship to the National Research Council is an insurance of objectivity; it maintains a full-time research correlation staff of specialists in highway transportation matters to bring the findings of research directly to those who are in a position to use them.

The program is developed on the basis of research needs identified by chief administrators of the highway and transportation departments and by committees of AASHTO. Each year, specific areas of research needs to be included in the program are proposed to the National Research Council and the Board by the American Association of State Highway and Transportation Officials. Research projects to fulfill these needs are defined by the Board, and qualified research agencies are selected from those that have submitted proposals. Administration and surveillance of research contracts are the responsibilities of the National Research Council and the Transportation Research Board.

The needs for highway research are many, and the National Cooperative Highway Research Program can make significant contributions to the solution of highway transportation problems of mutual concern to many responsible groups. The program, however, is intended to complement rather than to substitute for or duplicate other highway research programs.

NCHRP REPORT 697

Project 24-30
ISSN 0077-5614
ISBN 978-0-309-21341-7
Library of Congress Control Number 2011934448

COPYRIGHT INFORMATION

NOTICE

The project that is the subject of this report was a part of the National Cooperative Highway Research Program, conducted by the Transportation Research Board with the approval of the Governing Board of the National Research Council.

The members of the technical panel selected to monitor this project and to review this report were chosen for their special competencies and with regard for appropriate balance. The report was reviewed by the technical panel and accepted for publication according to procedures established and overseen by the Transportation Research Board and approved by the Governing Board of the National Research Council.

The opinions and conclusions expressed or implied in this report are those of the researchers who performed the research and are not necessarily those of the Transportation Research Board, the National Research Council, or the program sponsors.

The Transportation Research Board of the National Academies, the National Research Council, and the sponsors of the National Cooperative Highway Research Program do not endorse products or manufacturers. Trade or manufacturers' names appear herein solely because they are considered essential to the object of the report.

Published reports of the

NATIONAL COOPERATIVE HIGHWAY RESEARCH PROGRAM

are available from:

Transportation Research Board
Business Office
500 Fifth Street, NW
Washington, DC 20001

and can be ordered through the Internet at:

http://www.national-academies.org/trb/bookstore

Printed in the United States of America

THE NATIONAL ACADEMIES

Advisers to the Nation on Science, Engineering, and Medicine

The **National Academy of Sciences** is a private, nonprofit, self-perpetuating society of distinguished scholars engaged in scientific and engineering research, dedicated to the furtherance of science and technology and to their use for the general welfare. On the authority of the charter granted to it by the Congress in 1863, the Academy has a mandate that requires it to advise the federal government on scientific and technical matters. Dr. Ralph J. Cicerone is president of the National Academy of Sciences.

The **National Academy of Engineering** was established in 1964, under the charter of the National Academy of Sciences, as a parallel organization of outstanding engineers. It is autonomous in its administration and in the selection of its members, sharing with the National Academy of Sciences the responsibility for advising the federal government. The National Academy of Engineering also sponsors engineering programs aimed at meeting national needs, encourages education and research, and recognizes the superior achievements of engineers. Dr. Charles M. Vest is president of the National Academy of Engineering.

The **Institute of Medicine** was established in 1970 by the National Academy of Sciences to secure the services of eminent members of appropriate professions in the examination of policy matters pertaining to the health of the public. The Institute acts under the responsibility given to the National Academy of Sciences by its congressional charter to be an adviser to the federal government and, on its own initiative, to identify issues of medical care, research, and education. Dr. Harvey V. Fineberg is president of the Institute of Medicine.

The **National Research Council** was organized by the National Academy of Sciences in 1916 to associate the broad community of science and technology with the Academy's purposes of furthering knowledge and advising the federal government. Functioning in accordance with general policies determined by the Academy, the Council has become the principal operating agency of both the National Academy of Sciences and the National Academy of Engineering in providing services to the government, the public, and the scientific and engineering communities. The Council is administered jointly by both Academies and the Institute of Medicine. Dr. Ralph J. Cicerone and Dr. Charles M. Vest are chair and vice chair, respectively, of the National Research Council.

The **Transportation Research Board** is one of six major divisions of the National Research Council. The mission of the Transportation Research Board is to provide leadership in transportation innovation and progress through research and information exchange, conducted within a setting that is objective, interdisciplinary, and multimodal. The Board's varied activities annually engage about 7,000 engineers, scientists, and other transportation researchers and practitioners from the public and private sectors and academia, all of whom contribute their expertise in the public interest. The program is supported by state transportation departments, federal agencies including the component administrations of the U.S. Department of Transportation, and other organizations and individuals interested in the development of transportation. **www.TRB.org**

www.national-academies.org

CRP STAFF FOR NCHRP REPORT 697

Christopher W. Jenks, *Director, Cooperative Research Programs*
Crawford F. Jencks, *Deputy Director, Cooperative Research Programs*
Andrew C. Lemer, *Senior Program Officer*
Sheila A. Moore, *Senior Program Assistant*
Eileen P. Delaney, *Director of Publications*
Hilary Freer, *Senior Editor*

NCHRP PROJECT 24-30 PANEL
Field of Soils and Geology—Area of Mechanics and Foundations

Jon E. Bischoff, *Utah DOT, Salt Lake City, UT* (Chair)
Mark DeSalvatore, *California DOT, Sacramento, CA*
Manoj B. Chopra, *University of Central Florida, Orlando, FL*
Nicholas E. Harman, *South Carolina DOT, Columbia, SC*
Michael G. Katona, *Washington State University (Retired), Gig Harbor, WA*
Daehyeon Kim, *Chosun University, Gwangju, Korea*
Lianyang Zhang, *University of Arizona, Tucson, AZ*
Silas Nichols, *FHWA Liaison*
G. P. Jayaprakash, *TRB Liaison*

AUTHOR ACKNOWLEDGMENTS

The research reported herein was performed under NCHRP Project 24-30 by the Department of Civil and Environmental Engineering at Brigham Young University (BYU) in Provo, Utah. Kyle M. Rollins, Ph.D., professor of civil and environmental engineering, was the project director and principal investigator. Dan Brown, Ph.D., P.E., principal engineer at Dan Brown & Associates in Sequatchie, Tennessee, was co-principal investigator. The other authors of this report are Hubert Law, Ph.D., P.E., and Dr. Zhao (Joe) Chang, Ph.D., of Earth Mechanics Inc. of Fountain Valley, California. Matthew Adsero, Mark Herbst, Nathan Lemme, and Dustin Miner performed the field load testing reported in this study under the supervision of Dr. Rollins of BYU with the assistance of David Anderson, chief technician for the Civil & Environmental Engineering Department at BYU.

FOREWORD

By Andrew C. Lemer
Staff Officer
Transportation Research Board

NCHRP Report 697: Design Guidelines for Increasing the Lateral Resistance of Highway-Bridge Pile Foundations by Improving Weak Soils presents design guidance for strengthening of soils to resist lateral forces on bridge pile foundations. Lateral loads may be produced by wave action, wind, seismic events, ship impact, or traffic. Strengthening of soil surrounding the upper portions of piles and pile groups—for example by compaction, replacement of native soil with granular material, or mixing of cement with soil—may be more cost-effective than driving additional piles and extending pile caps as ways to increase the bridge foundation's capacity to resist lateral forces associated with these loads. This report presents computational methods for assessing soil-strengthening options using finite-element analysis of single piles and pile groups and a simplified approach employing commercially available software. The analysis methodology and design guidelines will be helpful to designers responsible for bridge foundations likely to be exposed to significant lateral loads.

Lateral resistance of pile foundations typically is controlled by the stiffness and strength of the materials in the vicinity of the pile cap and surrounding the upper portion of the piles. When these materials are weak in comparison to the lateral loads that may be placed on the foundation, the foundation's design may be controlled by these lateral loads. A larger number of piles or larger diameter piles and larger caps may be required and construction costs will be increased.

Previous studies have shown that improving the strength of the weak materials may significantly increase pile lateral resistance. Improvements to be considered typically include removal and replacement of the in-situ materials, in-situ densification, grouting, or soil mixing using more granular materials or a binder such as Portland cement. Soil improvement extending a relatively limited distance around the piles and below the pile cap may be a cost-effective method for meeting foundation design requirements.

Bridge foundation engineers have been hampered by a lack of verified design guidelines for estimating the increase in pile lateral resistance to be gained from soil improvement. The objective of NCHRP Project 24-30 was to develop such design guidelines.

A team led by Brigham Young University first reviewed recent practice, test data, existing specifications, and research findings from both foreign and domestic sources concerning the use of soil improvement techniques to increase the lateral resistance of piles. From this review, the research team developed a descriptive cataloging of soil improvement techniques to be addressed by the design guidelines. The catalog included likely applicability of each technique to specific weak soil types, such as soft cohesive soils, loose granular soils, or organic materials.

The team then described analytical methods that may be used to estimate the increased lateral resistance achievable through soil improvement around single piles and pile groups. A set of prototypical foundation designs was developed for testing to calibrate and verify analysis estimates. These designs were then field tested in weak soils near Interstate 15 in Salt Lake City, Utah. This report describes the experimental design and field testing.

The research team used finite-element methods and field-test results to perform a comprehensive parametric analysis to quantify the effect of soil improvement on the lateral resistance of piles in bridge foundations. Through this analysis, the researchers developed design guidelines and found that simplified computational methods employing widely used, commercially available software generally will provide acceptably accurate results for highway-bridge design.

The guidelines and analysis methods presented in this report may be useful to bridge foundation designers facing the problem of ensuring that foundations will perform acceptably under lateral loads produced by wave action, wind, seismic events, ship impact, or traffic.

CONTENTS

1 Summary

3 **Chapter 1** Introduction

5 **Chapter 2** Available Ground Improvement Case Histories and Approaches

14 **Chapter 3** Field Load Testing

14 3.1 Test Site Location
14 3.2 Geotechnical Site Characterization
15 3.3 Single Pile Test in Untreated Soil
23 3.4 Pile Group Properties
23 3.5 Pile Group Testing Procedure
25 3.6 Pile Group Tests in Untreated Clay
32 3.7 Pile Group Load Tests Involving Jet Grouting
36 3.8 Pile Group Load Tests Involving Soil Mixing
37 3.9 Pile Group Load Tests Involving Flowable Fill
39 3.10 Pile Group Load Tests Involving Excavation and Replacement
48 3.11 Summary of Increased Resistance from Soil Improvement Methods and Cost Considerations

51 **Chapter 4** Finite Element Modeling of Single Pile Load Test

54 **Chapter 5** Finite Element Modeling of Pile Group Load Tests

54 5.1 Pile Group FEM Mesh Design
56 5.2 FEM Model for Pile Group Model in Virgin Clay
56 5.3 Pile Group Model in Virgin Clay with Excavation
57 5.4 FEM Model of Pile Group with Mass Mixing
57 5.5 Pile Group Model with Jet Grouting

61 **Chapter 6** Parametric Studies

61 6.1 Mass Mix Depth Effect (Beside the Cap) on Lateral Resistance
61 6.2 Mass Mix Depth Effect (Below the Cap) on Lateral Resistance
65 6.3 Mass Mix Length Effect (Beside the Cap) on Lateral Resistance
66 6.4 Jet Grout Depth Effect (Beside the Cap) on Lateral Resistance
68 6.5 Jet Grout Depth Effect (Below the Cap) on Soil Improvement
68 6.6 Jet Grout Length Effect (Beside the Cap) on Soil Improvement
71 6.7 Material Strength Effect on Lateral Pile Group Resistance
72 6.8 Conclusions Based on Parametric Studies

76 **Chapter 7** Development of Simplified Model

76 7.1 Calibration GROUP Analysis Model
76 7.2 Comparison with Results from Tests in Virgin Soil
79 7.3 Comparison with Results from Tests Involving Mass Mixing
79 7.4 Development of Simplified Method

85 7.5 Evaluation for Jet Grouting Cases
89 7.6 Design Recommendations

96 **Chapter 8** Conclusions

97 References

99 **Appendix A** Schematic Drawings Showing the Layout of the 16 Lateral Pile Group Tests

Note: Many of the photographs, figures, and tables in this report have been converted from color to grayscale for printing. The electronic version of the report (posted on the Web at www.trb.org) retains the color versions.

SUMMARY

Design Guidelines for Increasing the Lateral Resistance of Highway-Bridge Pile Foundations by Improving Weak Soils

The objective of this study was to determine the viability of ground improvement methods for increasing lateral resistance of bridge foundations and to develop simple design approaches for predicting the increased resistance. The lateral resistance of bridge foundations is often a critical component in the design of highway bridges. Lateral loads can be produced by earthquakes, wind, wave action, ship impact, and traffic. The foundation designer must verify that the lateral capacity of a foundation exceeds the lateral demand transmitted by the column. When the lateral capacity of a new foundation is inadequate, the designer typically increases the number or diameter of piles. For existing bridge foundations, additional piles, drilled shafts, or micro-piles are added to increase the lateral resistance. Furthermore, an expanded pile cap or connecting beam often is required to structurally connect the new piles to the existing pile group. Although these structural approaches provide the required lateral resistance, they may also be relatively expensive and time consuming.

An alternative approach is to use soil improvement techniques to increase the strength and stiffness of the soil surrounding the foundation and thereby increase the lateral resistance of the pile group. For new construction, the improvement could readily be performed on the entire block of soil below the pile cap footprint and extending laterally several pile diameters from the perimeter pile. For retrofit of the existing foundations, soil improvement would be easier to accomplish around the perimeter of the pile group, but some techniques such as jet grouting also could treat the zone below the footprint of the pile cap. Typically, soil improvement would be only needed to extend to relatively shallow depths in the range from 10 to 20 ft.

To evaluate the ability of ground improvement to increase lateral pile group resistance, 16 full-scale lateral load tests were performed on pile groups in soft clay after using ground improvement methods that included soil mixing, jet grouting, replacement with compacted sand, replacement with flowable fill, and replacement with rammed aggregate piers. The tests clearly demonstrated that significant increases in the lateral resistance of bridge foundations can be achieved by soil improvement techniques with the potential for cost savings. The greatest benefits typically will be achieved when improving soft clays; however, significant improvement is also possible with loose sands.

Excavating soft clay and replacing it with compacted granular fill increases the lateral pile-soil resistance, as well as the lateral passive resistance on the pile cap. Typical increases in lateral resistance are 10% to 50%, with the highest increases occurring when the contrast in strength is the greatest. The compacted granular fill should extend 5 pile diameters below the ground surface and 10 pile diameters beyond the face of the piles to obtain the full lateral resistance of the granular soil.

Ground improvement techniques such as soil mixing and jet grouting can create a cemented volume of "soilcrete" in-situ with compressive strengths of 100 to 600 psi. This soilcrete block is most effective when it encompasses the entire pile group below the cap; although

significant improvement also can be obtained with soilcrete walls around the periphery of the pile group. During full-scale lateral load testing, jet grouting below a pile cap increased lateral resistance by 500 kips or (160%) relative to the 280 kip lateral resistance in untreated clay. Soilcrete walls produced by jet grouting and soil mixing adjacent to a pile group produced increases of 400 kips (185%) and 170 kips (60%), respectively, relative to untreated conditions.

Under lateral loading the soilcrete zone tends to move as a block and develop increased lateral resistance from passive force on the back of the block and adhesion on the sides of the block, rather than increased pile-soil resistance. This lateral resistance can be computed using basic soil mechanics principles for passive force and side shear under undrained conditions with some adjustments to account for limits on depth. Numerical analyses suggest that soilcrete block depths greater than about 10 ft will provide limited increased benefit for a lateral deflection limit of 1.5 in. at the pile cap. They also indicate that the lateral resistance of the soilcrete block is relatively insensitive to the strength of the soilcrete. Therefore, soil improvement techniques that can produce a compressive strength greater than 100 psi may be sufficient for practical purposes. Shear calculations can be used to check the minimum strength requirement.

A cemented block also can be efficiently created by excavating soft clay and replacing it with flowable fill. The flowable fill can be placed below a pile cap prior to pile driving or around the periphery of the pile group after driving. In comparison with in-situ treatments, it is necessary to maintain a stable excavation after excavation, which may be difficult in soft clay. In this study, problems were also encountered in obtaining a consistent compressive strength of the flowable fill. In addition, tests performed 2 years after treatment showed strength degradation in test specimens.

Full-scale field tests and finite-element methods (FEM) analyses indicate that placement of a narrow dense compacted granular zone adjacent to a pile cap or abutment in loose sand can significantly increase the lateral passive resistance provided by the cap. Typically, when the width of the dense zone is equal to the cap height, the passive resistance is increased to about 60% of that which would be obtained for a homogenous dense backfill extending about four times the height of the cap. A generalized equation can be used to compute the percentage of the passive force as a function of backfill width, dense sand friction angle, and loose sand friction angle.

Simple cost comparisons indicate that ground improvement techniques have the potential to produce increased lateral pile group resistance at significantly less cost than would be obtained by simply driving more piles and extending the pile cap. Although costs are expected to vary with locality, these results make it clear that engineers should investigate this alternative as part of their overall effort to produce a cost-effective foundation solution.

CHAPTER 1

Introduction

The lateral resistance of bridge foundations is often a critical component in the design of highway bridges. Lateral loads can be produced by earthquakes, wind, wave action, ship impact, and traffic. In practice, bridge foundation design often is governed by load demands of the bridge column. The size and number of piles as well as the pile group layout are designed to resist service level moments, shears, and axial loads and the moment demands induced by the column plastic hinge mechanism. The foundation designer must verify that the lateral capacity of the foundation exceeds the lateral demand transmitted by the column. When the lateral capacity of the foundation is inadequate, the designer develops a strategy for increasing the lateral resistance of the foundation. These strategies typically include thickening the pile cap to increase passive resistance or increasing the number or diameter of piles. When existing bridge foundations are found to have inadequate lateral resistance, additional piles, drilled shafts or micro-piles are added to increase the lateral resistance. Furthermore, an expanded pile cap or connecting beam often is required to structurally connect the new piles to the existing pile group. Although these structural approaches provide the required lateral resistance, they may also be relatively expensive and time consuming

An alternative approach is to use soil improvement techniques to increase the strength and stiffness of the surrounding soil and thereby increase the lateral resistance of the pile group. Ground improvement methods have the potential to increase (1) the passive resistance of the pile cap and (2) the lateral resistance of the underlying piles. The improved zone could potentially be relatively shallow because the lateral resistance of piles is typically transferred within 5 to 10 pile diameters. Although soil improvement techniques have the potential for being cost-effective and reducing construction time, relatively few tests have been performed to guide engineers in evaluating the actual effectiveness of this approach. In addition, numerical models to evaluate this approach have not been validated. As a result, no general procedures are available for designing pile foundations in soils that have been improved in zones surrounding the piles. For these reasons, soil improvement methods for increasing lateral pile group resistance have rarely been implemented in practice.

Two different improvement schemes might be employed depending on whether the pile foundation is a new foundation or an existing foundation. Soil improvement for a new pile foundation is relatively straightforward since it can take place prior to installing the piles using a variety of techniques. Lateral pile stiffness is typically affected by the soil stiffness within the zone of significant soil-pile interaction, which in most poor sites is approximately 4 to 5 pile diameters from the ground surface. For this case, soil improvement could be performed on the entire block of soil within the pile cap footprint, extending laterally about 3 to 4 pile diameters from the perimeter pile and vertically about 4 to 5 pile diameters as illustrated in Figure 1-1. In this case, all of the piles would be located in improved soil and increased resistance could be substantial.

For the case of existing pile foundations, the soil improvement frequently would be limited to the perimeter of the pile group because of practical access to the interior piles as shown in Figure 1-2. In this case, increased lateral resistance might be concentrated in piles at the edge of the group, and relatively little increase could occur for the interior piles. Alternatively, the soil under the foundation could be improved for a new foundation or even for an existing foundation with a technique such as jet grouting. Improving the soil under the foundation would have the potential for producing greater increases in lateral resistance than just improving around the perimeter because the improvement would reach interior piles. In addition, the process of creating a cemented "soilcrete" zone around pile foundations could potentially produce a zone that would behave like a reinforced "superpile" with increased structural stiffness.

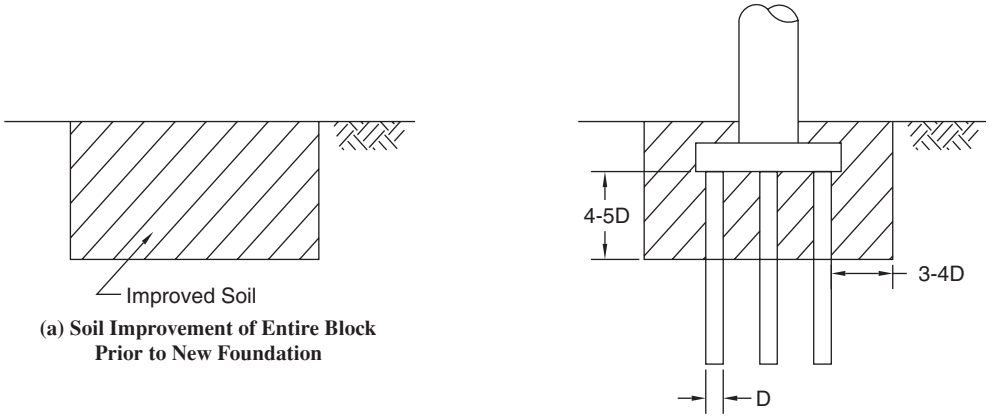

(a) Soil Improvement of Entire Block Prior to New Foundation

(b) Construct New Foundations

Figure 1-1. Soil improvement around new foundation.

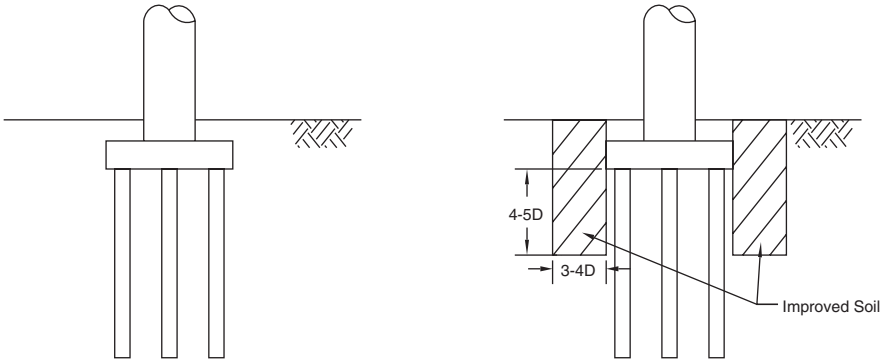

(a) Existing Foundation

(b) Soil Improvement at Perimeter

Figure 1-2. Soil improvement around existing footing.

CHAPTER 2

Available Ground Improvement Case Histories and Approaches

Publications on ground improvement methods and their applications to foundation design are extensive. However, engineering practice typically has not used soil improvement techniques in combination with deep foundations to increase the lateral resistance of bridge foundations. If soil improvement has been undertaken, it has generally been with the goal of preventing liquefaction or increasing soil resistance so that deep foundations were not required. Three excellent publications that summarize the state of the art in soil improvement are provided by Mitchell (1981), Terashi and Juran (2000), and ASCE (1997). Based on a review of methods documented in these and other publications, specific improvement methods or technologies appropriate for applications to improve the lateral resistance of soils (stiffness and strength) associated with pile foundations are summarized in Tables 2-1 and 2-2.

A review of the literature indicates that there are also a number of case histories that provide some insight regarding the degree of increased lateral pile resistance that could be obtained by employing soil improvement in concert with deep foundations. In connection with research studies, field load tests have been performed on two pile groups where the native clay soil was excavated and replaced with compacted granular soil. These studies were primarily undertaken to evaluate group interaction factors under lateral loading. Brown et al. (1987) conducted lateral load tests on a nine-pile group in saturated stiff clay. Later, Brown et al. (1988) excavated the clay, compacted sand around the pile group, and repeated the lateral load test. Rollins et al. (2005) performed cyclic lateral load tests on a 15-pile group in medium-consistency clay. Rollins, Snyder et al. (2010) excavated the clay, replaced it with clean sand, and performed additional lateral pile group load tests. Although these tests were not designed to evaluate the effect of excavation and replacement on lateral pile group resistance, the test results can be compared to provide this information.

The pile group tested by Brown et al. (1987, 1988) was a nine-pile group consisting of 0.25-m (10-in.) diameter steel pipe piles filled with grout. The piles were driven in a 3 × 3 arrangement with a 0.75-m center-to-center (3D) spacing in both directions. The original clay profile consisted of stiff, overconsolidated clay with an undrained shear strength of about 1150 psf (57 kPa) at the ground surface, which increased to about 3000 psf (150 kPa) at a depth of 18 ft (5.5 m) below the ground. Approximately 9 ft of the clay was excavated and replaced with a relatively uniform clean sand compacted to a dry unit weight (γ_d) of 98 pcf (15.4 kN/m^3), which is a relative density of about 50%. A direct shear test indicated a friction angle of 38.5°, but back-calculated friction angles using LPILE (Reese, Wang, Isenhower et al., 2004a) suggest a friction angle of around 50°. A plot showing the total load versus deflection curves for the pile group in both clay and sand is presented in Figure 2-1. At deflections less than about 20 mm, the lateral resistance of the pile group in clay is about the same as that in sand. However, at greater deflections, the lateral resistance of the pile group in sand eventually exceeds that for the pile group in clay by over 28%, despite the fact that the clay was relatively stiff.

The pile group tested by Rollins et al. (2005) and Rollins, Snyder et al. (2010) consisted of 15 12.75-in. diameter steel pipe piles driven closed-ended to a depth of about 40 ft. The piles were driven in a 3 × 5 grouping with a center-to-center spacing of 4.17 ft (3.92D) in the direction of loading and 3.5 ft (3.29D) transverse to loading. The upper 2.5 m of clay in the original soil profile had an undrained shear strength of about 900 psf. The pile group reacted against two 4-ft diameter drilled shafts. Prior to the second set of tests, the upper 1 m of clay was excavated and replaced with compacted clean sand. In addition, an extra 1.5 m of sand was compacted above the original ground elevation so that the upper 2.5 of the profile consisted of clean sand compacted to 93% of the modified Proctor maximum density. The load versus deflection curves for the pile group in clay and sand are compared in Figure 2-2.

Because the clay strength was relatively soft, the lateral resistance of the pile group in sand was considerably higher than that for the pile group in clay. Analyses using the computer

Table 2-1. Summary of soil improvement methods in loose cohesionless soils.

Method	Advantages	Disadvantages	Strength Gain	Cost
Excavate and Replace				
Compacted Fill	•Simple, widely used method •Equipment widely available •Compaction can be measured easily	•May require excavation support or dewatering	Low to mod.	Low to mod.
Flowable Fill	•No special equipment or personnel required •No compaction necessary	•Must dispose of excavated material	Mod. to high	Mod. to high
In-Situ Densification				
Dynamic Compaction	Densification to 25-ft depth from surface impact	•Decrease in improvement with depth •Produces vibration and noise •Could produce downdrag in existing piles •Requires overhead clearance for dropping weight	Low	Low
Vibro Compaction	•Relatively uniform improvement with depth	•Could produce downdrag in existing piles	Low	Moderate
Stone Columns	•Increased densification relative to vibrocompaction •Increased shear resistance of reinforced soil mass •Drainage provided by columns in the event of liquefaction concerns	•Must install stone through entire layer to treat loose sand at depth •Could produce downdrag in existing piles	Low	Moderate
Stone Columns with Wick Drains	•Improved effectiveness with high fines content soils •Does not produce spoils	•Increased cost and logistical effort of installing wick drains prior to stone column treatment	Low	Moderate
Compaction Grouting	•Can be used for retrofit below a pile cap •Can treat zones of interest without treating all soil above the zone •Does not produce spoils	•Less effective at shallow depths where pressure is restricted •More difficult to evaluate improvement for retrofit conditions below pile	Moderate	Moderate
Soil Mixing				
Deep Soil Mixing	•Mixing can occur to 60- to 80-ft depths •Significant strength gain can be achieved • Can produce columns (3-ft dia.) or wall panels at desired depths	•Can decrease the strength of sensitive clays •Produces spoils	Mod. to high	Mod. to high
Grouting				
Permeation Grouting	•Can be used for retrofit below a pile cap •Can treat zones of interest without treating all soil above the zone •Does not produce spoils	•Limited to very coarse sands •More difficult to evaluate improvement for retrofit conditions below pile than in areas around periphery of pile group •Uniformity of treatment is often difficult	Moderate	Moderate
Jet Grouting	•Low noise and vibration •Can treat soil under pile cap after construction •Can transform pile group into equivalent pier for scour resistance	•Creates spoil material •Requires mobilization of specialized equipment and personnel	High	High

Table 2-2. Summary of soil improvement techniques in soft cohesive soils.

Method	Advantages	Disadvantages	Strength Gain	Cost
Excavate and Replace				
Compacted Fill	•Simple, widely used method •Equipment widely available •Compaction can be easily measured	•Must dispose of excavated material •May require excavation support or dewatering	Low to mod.	Low to mod.
Flowable Fill	•No special equipment or personnel required •No compaction necessary	May need to dispose of excavated material	Mod. to high	Mod. to high
Cement Treated Excavated Clay	•Strength can be increased by 3 to 5 times the in-situ strength	•Requires special care in mixing operations •Significant laboratory testing necessary to develop treatment plan •Field strength gain usually much less than laboratory because of less efficient mixing	Mod. to high	Mod. to high
Lime Treated Compacted Clay	•Strength can be increased 3 to 5 times the in-situ strength •Requires less cement to achieve same strength as using cement alone	•Requires special care in mixing operations •Significant laboratory testing necessary to develop treatment plan •Field strength gain usually much less than laboratory because of less efficient mixing •Difficult to treat soils with high sulfate content	Mod. to High	Mod. to High
Rammed Aggregate Piers	•Can be constructed above or below water table •Creates extremely dense gravel columns with high-friction angle •Increases lateral pressure in surrounding soil •Increases shear resistance of the reinforced soil mass	Creates relatively little increase in density of surrounding soil •Columns provide no flexural resistance. •Creates extremely dense high-friction angle columns	Low	Low
In-Situ Soil Mixing				
Vibro Replacement	•Increases shear resistance of the reinforced soil mass	•Can cause heave of surrounding ground	Low	Low
Compaction Grouting	•Can be used for retrofit below a pile cap •Can treat zones of interest without treating all soil above the zone •Does not produce spoils	•Less effective at shallow depths where pressure is restricted •Can decrease the strength of sensitive clays •More difficult to evaluate improvement for retrofit conditions below pile	Moderate	Low
Deep Soil Mixing	•Mixing can occur to 60- to 80-ft depths •Significant strength gain can be achieved •Can produce columns (3 ft dia.) or wall panels at desired depths	•Can decrease the strength of sensitive clays •Produces spoils	Mod. to high	Mod. to high
Mass Mixing	•Mixing can occur in-situ to 10- to 15-ft depths •No need for excavation or recompaction •Strength increase of 3 to 5 times original shear strength	•Significant laboratory testing necessary to develop treatment plan •Field strength gain usually much less than laboratory because of less efficient mixing	Mod. to high	Mod. to high
Grouting				
Jet Grouting	•In-situ treatment with flexibility to produce variety of geometries (columns and panels) •Flexibility to treat only zones of interest •Can treat soil under pile cap after construction •Can transform pile group into equivalent pier for resistance during scour events	•Creates spoil material •Requires mobilization of specialized equipment and personnel	High	High

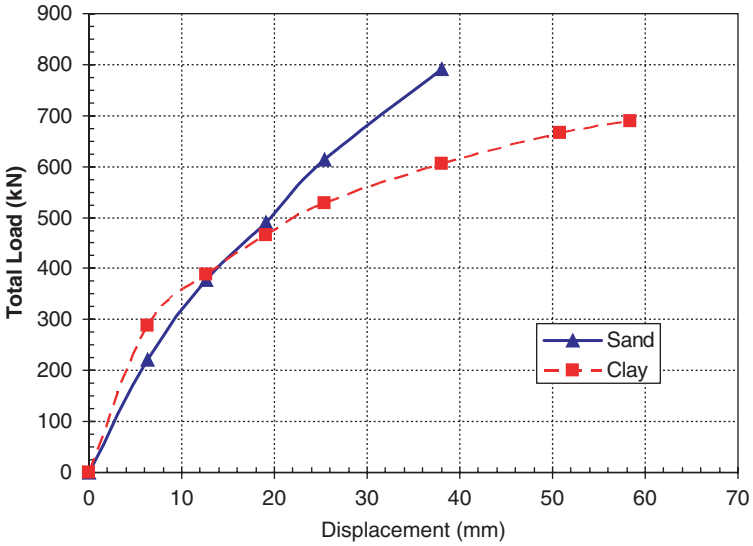

Figure 2-1. Load vs deflection curves for nine-pile groups in stiff clay and dense sand based on Brown et al. (1987, 1988).

program GROUP (Reese, Wang, and Arrellaga et al., 2004b) were successful in matching the measured response of the pile groups in clay. However, for the pile groups in sand, successful agreement with measured response generally required the use of friction angles that are somewhat higher than would normally be used in engineering practice. The potential for improved resistance using excavation and replacement increases as the clay becomes softer and compacted granular soil becomes denser. Increases of 60% are possible (Rollins, Snyder et al., 2010).

Two field test studies have evaluated the passive force on a pile cap as a function of soil type and density. Mokwa and Duncan (2001) performed tests on a 1.1-m (3.5-ft) deep and 1.9-m (6.3-ft) wide anchor block. The block was originally poured flush against an excavation into partially saturated stiff clay and a lateral load test was performed. The clay was then excavated and replaced with a compacted sandy gravel backfill and the test was repeated. Rollins, Gerber, and Kwon (2010) evaluated the passive force provided by various soils against a pile cap that was 1.1 m (3.67 ft) deep and 5.2 m (17 ft) wide. Tests were conducted on a silty sand at two densities and on loose silty sand with a 1- to 2-m wide zone of dense compacted gravel immediately adjacent to the pile cap.

The native clay in the tests performed by Mokwa and Duncan (2001) was partially saturated. Triaxial shear tests on the clay at the natural moisture content indicate that the cohesion

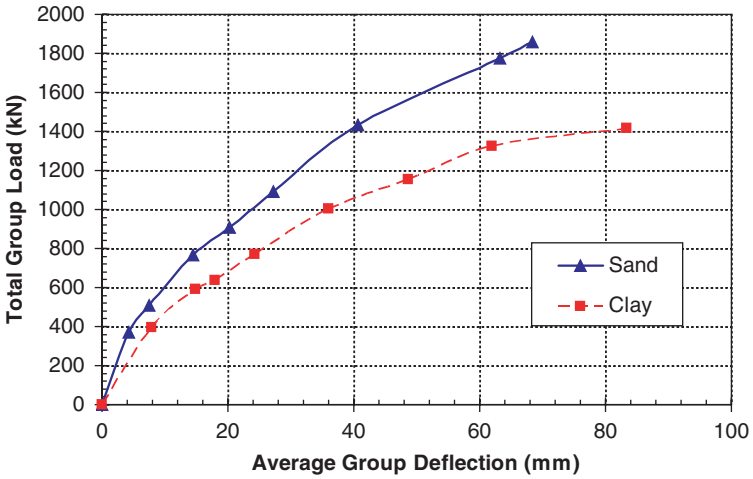

Figure 2-2. Load vs deflection curves for 15-pile group in medium stiff clay and dense sand based on Rollins et al. (2005) and Rollins, Snyder et al. (2010).

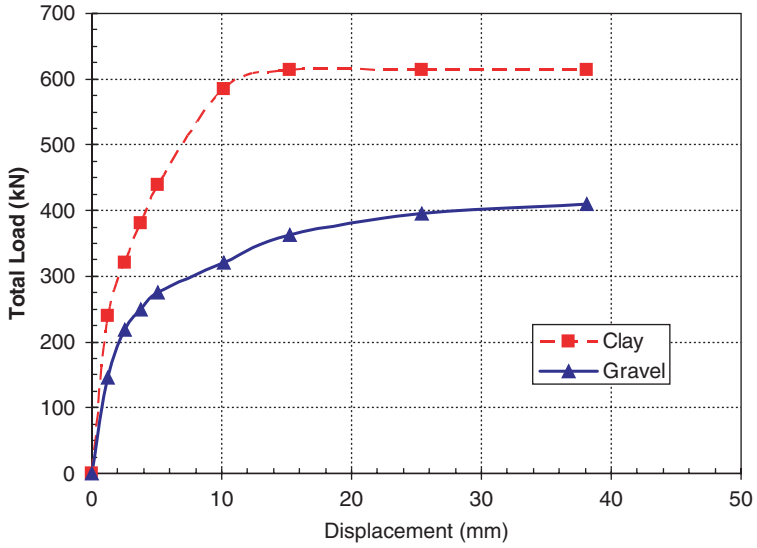

Figure 2-3. Comparison of passive force provided by stiff, partially saturated clay and compacted sandy gravel against 1.1-m deep × 1.9-m wide cap block.

was 1 ksf and that the friction angle ranged from 32° to 38°. The clay was excavated to the base of the cap block and replaced by a compacted, sandy gravel. The sandy gravel (GW-GM in the Unified Soil Classification System) was compacted to a relative density of approximately 80%. Triaxial shear tests indicate that the friction angle could range from a low of 48° to a high of 52°. A comparison between the passive force-deflection curves for the clay and gravel is provided in Figure 2-3. In this case, the lateral resistance provided by the stiff, partially saturated clay was considerably higher than that for the gravel at the shallow depths involved. As a result, the lateral resistance actually decreased substantially when the compacted gravel was used in place of the clay. Duncan and Mokwa (2001) concluded that the log-spiral method provided the best estimate of the ultimate capacity and that the passive force-deflection relationship could be estimated reasonably using a hyperbolic curve. This conclusion was supported by analyses of additional large-scale tests by Rollins and Cole (2006) and Cole and Rollins (2006).

Rollins, Gerber, and Kwon (2010) performed lateral load tests on a pile cap supported by 12 0.324-m diameter pipe piles. The piles provided sufficient vertical resistance so that the full wall friction force could develop. Basic passive force-deflection relationships were developed for two tests involving silty sand compacted at 88% and 98% of the modified Proctor maximum unit weight as shown in Figure 2-4. The increased compactive effort produced a considerable increase in passive resistance. Preliminary analyses indicate that this behavior is predicted quite well using the Duncan and Mokwa (2001) approach along with the soil properties measured in the field.

Tests also were performed using the loose silty sand backfill along with a well-compacted zone of sandy gravel adjacent to the pile cap. The compacted zones were 0.9 m (3 ft) and 1.83 m (6 ft) thick. These tests indicate that compacting relatively thin zones (3 to 6 ft wide) of sandy gravel around a pile cap can significantly increase the passive resistance as illustrated in Figure 2-5. In this case, replacing a 0.9 m (3 ft) zone of loose silty sand around the pile cap with compacted gravel increased the lateral resistance on the pile cap from an initial value of 70 kips to more than 180 kips, which is an increase of over 200%. Crack patterns from the tests, shown in Figure 2-6 indicate that the compacted gravel zones increase the effective

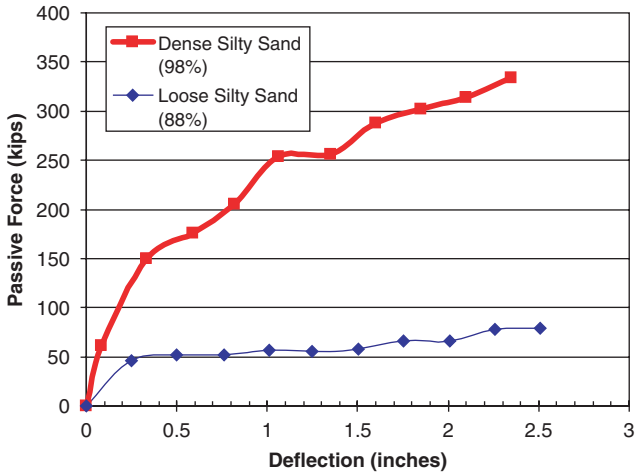

Figure 2-4. Measured passive force vs deflection relationships for two full-scale tests with silty sand compacted to 88% and 98% of the modified Proctor maximum unit weight.

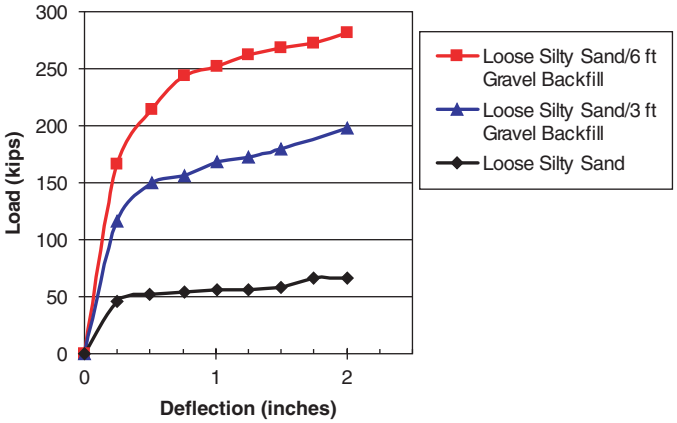

Figure 2-5. Passive force vs deflection curves for loose silty sand against a 17-ft wide by 3.67-ft high pilecap after excavation and replacement with 3-ft and 6-ft zones of compacted gravel backfill against the cap.

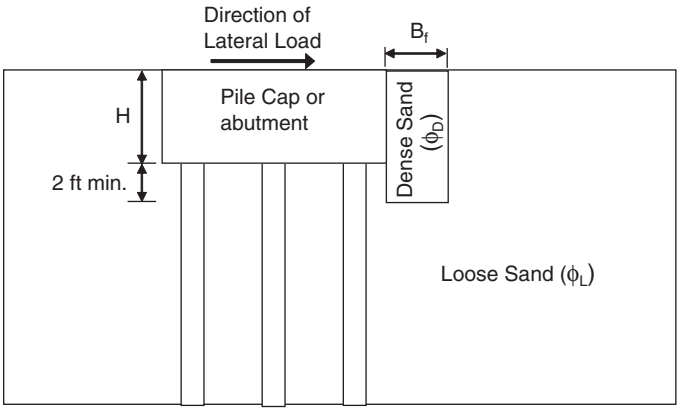

Figure 2-7. Layout of geometry for limited width dense backfill zone adjacent to pile cap or abutment.

width of the pile cap and reduce the pressure on the loose silty sand behind it, thereby increasing passive resistance. Rollins and Nasr (2010) completed a follow-up study to develop a generalized equation to predict the increased passive resistance that could be obtained by constructing a narrow dense granular zone adjacent to a pile cap or abutment surrounded by loose sand. This investigation followed the same pattern employed in this NCHRP study. The full-scale load tests reported by Rollins, Gerber et al. (2010) and Gerber et al. (2010) were used to calibrate soil parameters within the finite element computer program PLAXIS. In addition, the computer model was verified against analytical solutions for computing passive force (e.g., Duncan and Mokwa, 2001). Once the FEM analysis model was calibrated, parametric studies were performed to evaluate the influence of changes in wall height (H), the dense zone width (B_f), the friction angle of the dense zone (ϕ_D) and the friction angle of the looser surrounding sand (ϕ_L). Figure 2-7 shows the layout of the improved zone relative to the pile cap or abutment and defines the basic parameters involved. To facilitate generalization, the width of the dense zone is normalized by the height of the pile cap. In addition, the ultimate passive resistance provided by the limited-width dense granular backfill (P_{LW}) is normalized by the ultimate passive resistance for a homogeneous dense backfill (P_{FW}) that fully encloses the passive failure surface. This ratio is defined as the passive force ratio (PFR). PFR is plotted as a function of normalized width (B_f/H) for a number of cases in Figure 2-8 where the dense zone consisted of gravel. As the normalized width increases, the PFR increases. When B_f/H exceeds 1.0, the PFR is normally greater than 60%, and the PFR increases as the friction angle of the surrounding sand increases. Typically, the B_f/H ratio would need to be around 4.0 to fully enclose the failure surface; therefore, the narrow dense zone is relatively effective in mobilizing the majority of the total passive resistance. Based on the result from the FEM parametric study, Equation 1

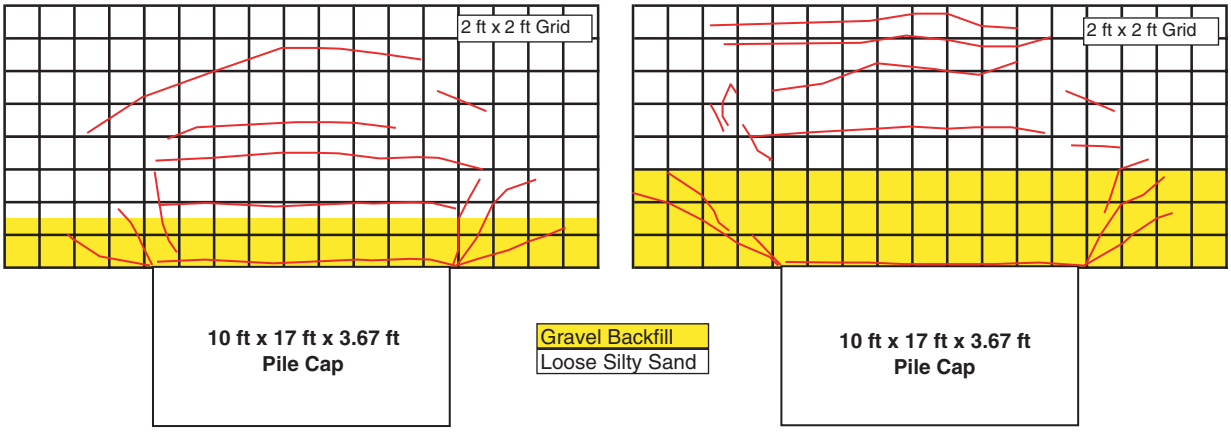

(a) 3 ft sandy gravel zone plus loose silty sand backfill

(b) 6 ft sandy gravel zone plus loose silty sand backfill

Figure 2-6. Plan view of crack patterns behind a pile cap after excavation and replacement of loose silty sand with (a) a 3-ft and (b) a 6-ft zone of compacted sandy gravel behind the pile cap.

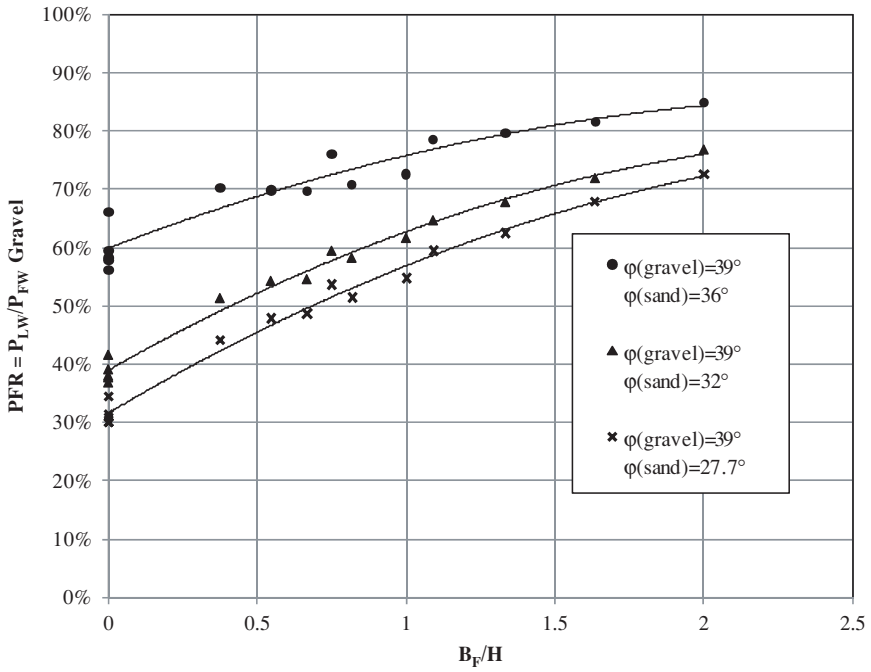

Figure 2-8. Percentage of total passive resistance developed by a narrow dense gravel zone adjacent to an abutment relative to that for a homogenous dense gravel zone.

was developed to predict the PFR for a limited-width dense granular backfill.

$$PFR = 3.1418 - 0.139\phi_D - 0.033\phi_D + 0.484\left(B_f/H\right) - 0.043\left(B_f/H\right)^2 + 0.003\phi_2^L - 0.007\phi_L\left(B_f/H\right) \quad (1)$$

At a test site on Treasure Island in San Francisco Bay, stone column treatment was used to improve a 6-m-thick liquefiable sand layer around two test foundations (Ashford, Rollins, and Baez 2000a; Ashford, Rollins, Bradford et al., 2000b; and Weaver et al., 2005). One test foundation was a 0.6-m diameter cast-in-steel shell (CISS) shaft that reacted against a group of four 0.324-m diameter driven steel pipe piles. Lateral load tests were first performed on the test foundations prior to treatment, then comparable lateral load tests were performed after treatment for comparison. A high-speed hydraulic actuator was used to apply load. In addition to the conventional static lateral load tests, a pattern of small explosive charges was detonated sequentially to produce a liquefied volume of soil within which the test foundations also could be laterally loaded to large displacement levels (9 in.). The layout of the test foundations is shown in Figure 2-9. The 0.9-m diameter stone columns were installed in a square pattern with a spacing of 2.5 m from center to center (see Figure 2-9) using the dry, bottom feed method. The sand had a mean grain size of about 0.2 mm with a fines content between 5% and 10% and was initially placed using hydraulic filling techniques. Prior to treatment, correlations with SPT and CPT test results (Kulhawy and Mayne, 1990) indicated that the sand had a relative density of about 50%; however, after treatment, the relative density was increased to between 85% and 100%.

A comparison of the load versus deflection curves for the CISS pile and the pile group before and after treatment but prior to blast liquefaction are shown in Figure 2-10. The lateral resistance was increased by about 25% for the pile group and about 33% for the CISS pile. Back-analyses using the computer program LPILE indicate that the friction angle was increased from about 39° prior to treatment to about 48° after treatment.

Prior to stone column treatment the sand layer liquefied (excess pore pressure ratios of 100%) following blasting and remained liquefied for at least 10 minutes. Settlement following dissipation of excess pore pressures amounted to about 12 in. A plot of the load-deflection curve for the CISS pile following blast-induced liquefaction is provided in Figure 2-11(a). The pre-blast load-deflection curve also is shown for comparison. Following liquefaction, about 11 times more movement was required to develop the same lateral resistance as that prior to liquefaction. After treatment, high excess pore pressure developed initially after the blasting but dissipated within a few seconds, presumably due to the increased drainage provided by the stone columns. The load-deflection curve after blasting is presented in Figure 2-11(b) for comparison and the stiffness of the curve is several hundred percent higher in comparison to that prior to treatment.

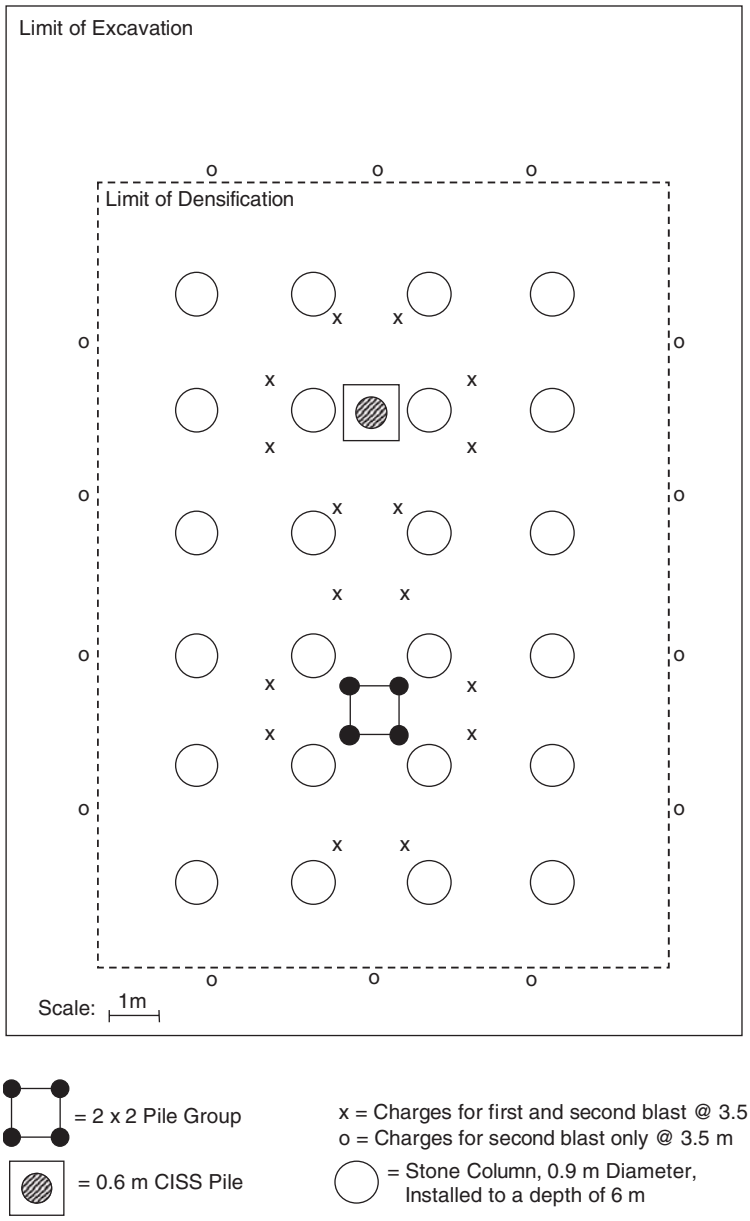

Figure 2-9. Layout of test foundations, stone columns, and explosive charges.

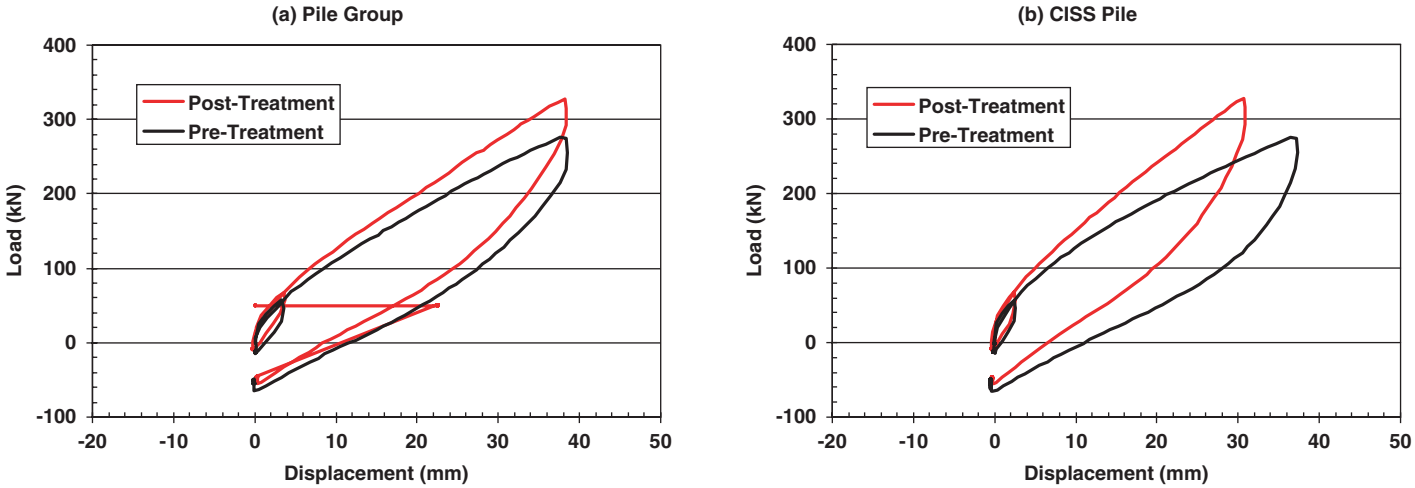

Figure 2-10. Static load vs deflection curves before and after stone column treatment for (a) pile group and (b) 0.6-m CISS pile.

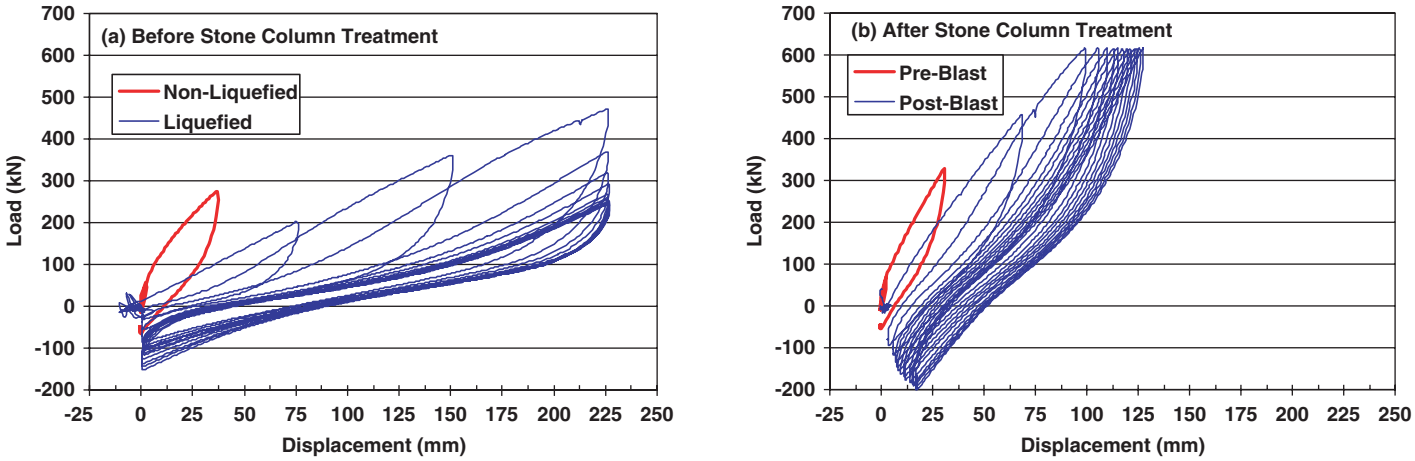

Figure 2-11. Pre- and post-blast cyclic load-deflection curves (a) before and (b) after stone column treatment for a 0.6-m CISS pile.

CHAPTER 3

Field Load Testing

Based on preliminary lateral pile load analyses, improvement of soft clay was considered to provide the greatest potential for increasing the lateral resistance of pile foundations. Therefore, a test site was selected where a variety of soil improvement methods appropriate for treating soft clay around a pile group could be investigated. The field load tests provided basic performance data that also could be used to calibrate and verify computer models.

3.1 Test Site Location

The test site was located north of Salt Lake City, Utah, at the interchange of Redwood Road and I-215 on a Utah Department of Transportation right of way. An aerial view of the site is provided in Figure 3-1. The site offered several advantages including the following:

1. Presence of a consistent layer of relatively soft saturated cohesive soil near the ground surface,
2. Fill over the soft clay to allow easy access for construction equipment,
3. Access to water, and
4. Permission to drive piles and use ground improvement methods.

Four pile groups were constructed at this site according to the basic layout shown in Figure 3-2 and discussed subsequently.

3.2 Geotechnical Site Characterization

Geotechnical site conditions were evaluated using field and laboratory testing. Field testing included one drilled hole with undisturbed sampling, four cone penetration test (CPT) soundings, and shear wave velocity testing. Laboratory testing included unit weight and moisture content determination, Atterberg limits testing, and undrained shear testing.

A generalized soil boring log at the test site is provided in Figure 3-3. The depth is referenced to the top of the excavation, which was 2.5 ft above the base of the pile cap as shown in the figure. The soil profile consists predominantly of cohesive soils; however, some thin sand layers are located throughout the profile. The cohesive soils typically classify as CL or CH materials with plasticity indices of about 20 as shown in Figure 3-3(b). In contrast, the soil layer from a depth of 15 to 25 ft consists of interbedded silt (ML) and sand (SM) layers as will be highlighted by the subsequent plots of CPT cone tip resistance.

The liquid limit, plastic limit, and natural moisture content are plotted in Figure 3-3(b) at each depth where Atterberg limit testing was performed. The water table is at a depth of 1.5 ft. The natural water content is less than the liquid limit near the ground surface, suggesting that the soil is overconsolidated, but the water content is greater than the liquid limit for soil specimens from a depth of 5 to 27 ft suggesting that these materials may be sensitive. Below a depth of 30 ft the water content is approximately equal to the liquid limit suggesting that the soils are close to normally consolidated.

The undrained shear strength is plotted as a function of depth in Figure 3-3(c). Undrained shear strength was measured using a miniature vane shear test or Torvane test on undisturbed samples immediately after they were obtained in the field. In addition, unconfined compression tests were performed on most of the undisturbed samples. Both the Torvane and unconfined compression tests indicate that the undrained shear strength decreases rapidly from the ground surface to a depth of about 6 ft but then tends to increase with depth. This profile is typical of a soil profile with a surface crust that has been overconsolidated by desiccation. However, the undrained shear strength from the unconfined compression tests is typically about 30% lower than that from the Torvane tests. The unconfined compression tests at a depth of 27 and 48 ft appear to have been conducted on soil with sand lenses because the measured strength is substantially lower than that from the

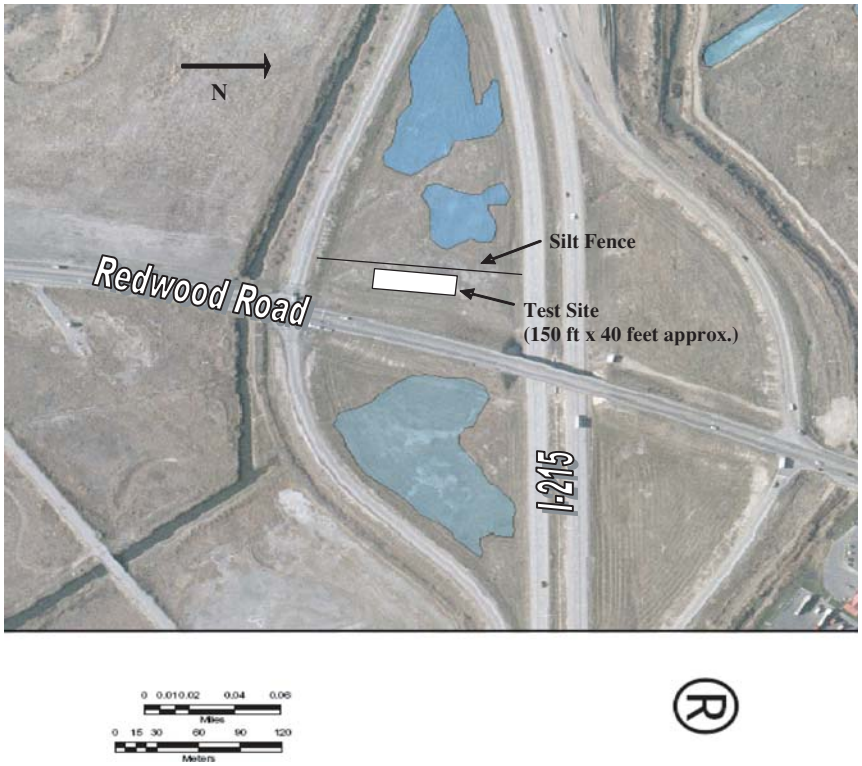

Figure 3-1. Aerial view of the test site and surrounding area.

Torvane test and are not likely to be representative of the soil in-situ. The undrained shear strength was also computed from the cone tip resistance using the following correlation equation:

$$s_u = \frac{(q_c - \sigma)}{N_k} \quad (2)$$

where q_c is the cone tip resistance, σ is the total vertical stress, and N_k is a variable which was taken to be 15 for this study. The undrained shear strength obtained from Equation 2 also is plotted versus depth in Figure 3-3(c) and the agreement with the strengths obtained from the Torvane and unconfined compression tests is reasonably good. Nevertheless, there is much greater variability and the drained strength in the interbedded sand layers is ignored. A summary of laboratory test results is provided Table 3-1.

Four cone penetration tests were performed across the test site and plots of cone tip resistance, friction ratio, and pore pressure are provided as a function of depth in Figure 3-4. In addition, the interpreted soil profile also is shown. From the ground surface to a depth of about 15 ft the soil profile appears to be relatively consistent with a cone tip resistance of about 6 tons per square foot (tsf) and a friction ratio of about 1%. However, one thin sand layer is clearly evident between 6 and 8 ft. The cone tip resistance, friction ratio, and pore pressure plots clearly show the interbedded silt and sand layering in the soil profile between 15 and 27 ft. below the ground surface.

Figure 3-5 provides plots of the cone tip resistance, friction ratio, and pore pressure versus depth as a function of depth for all four of the CPT soundings. The measured parameters and layering are generally very consistent for all four soundings, which indicates that the lateral pile load tests can be fairly compared from one site to the next.

Figure 3-6 provides a plot of the shear wave velocity as a function of depth obtained from the downhole seismic cone testing. The interpreted soil profile and cone tip resistance are also provided in Figure 3-6 for reference. The shear wave velocity in the upper 10 ft of the profile is between 300 and 400 ft/sec, which is relatively low, and suggests a low shear strength. Between a depth of 10 to 20 ft, the velocity increases to about 550 ft/sec. This increase in velocity is likely associated with the interbedded layer that contains significant sand layers. Below 20 ft, the velocity drops to a value of around 500 ft/sec and remains relatively constant to a depth of 45 ft.

3.3 Single Pile Test in Untreated Soil

Test Pile Properties

A 12.75-in. OD pipe pile with a 0.375-in. wall thickness was driven closed-ended with a hydraulic hammer to a depth of 45 ft below the excavated ground surface on June 15, 2007. The test pile had a beveled end that allowed a 1.5-in. thick

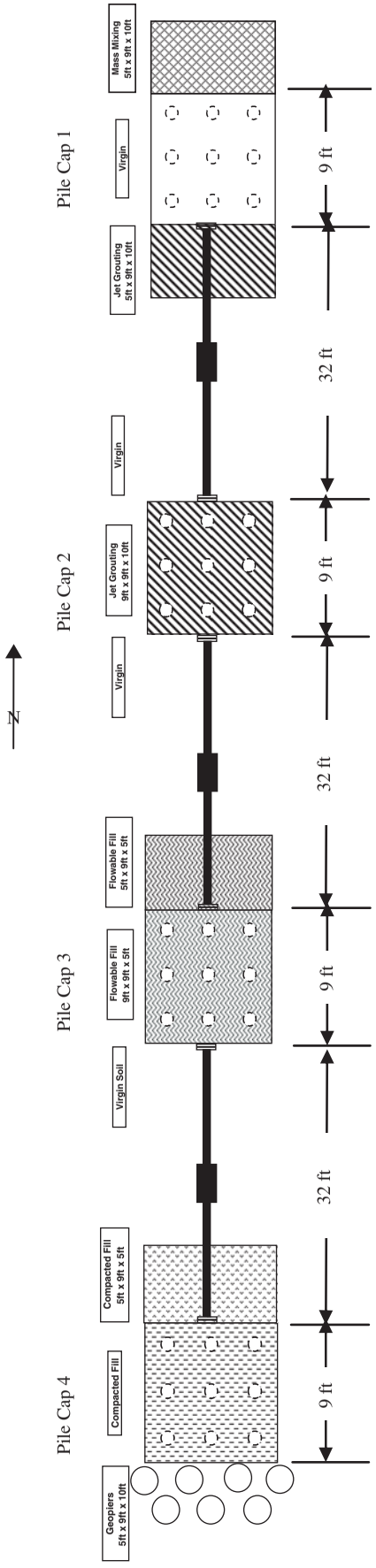

Figure 3-2. Generalized layout of test pile groups at the test site.

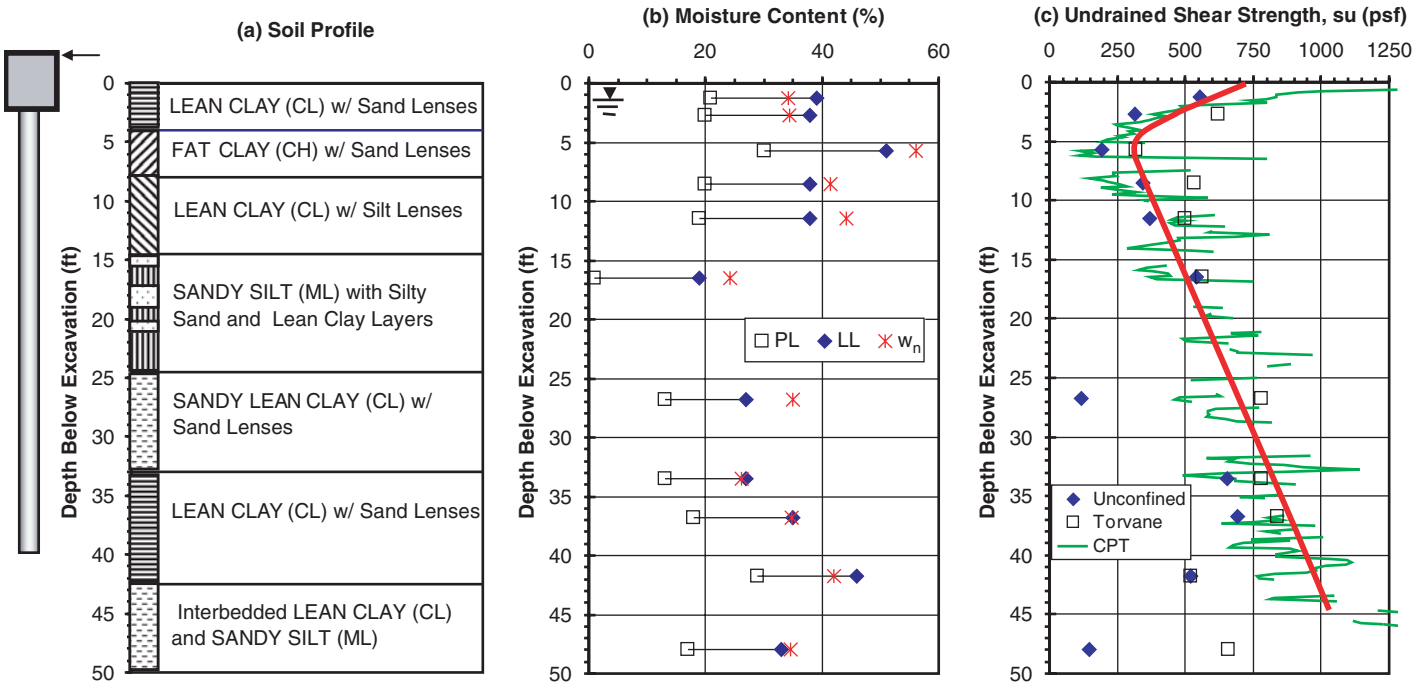

Figure 3-3. Borehole log, plot of Atterberg limits and natural water content vs depth, and plot of undrained shear strength vs depth.

plate to be welded flush with the edge of the pile at the bottom. The steel conformed to ASTM A252 Grade 3 specifications and had a yield strength of 58,700 psi based on the 0.2% offset criteria. The moment of inertia of the pile itself was 279 in.^{4}; however, angle irons were welded on opposite sides of the test pile, which increased the moment of inertia to 342 in.^{4}. A steel reinforcing cage was installed at the top of the test pile to replicate the reinforcing cages in the test piles within the pile groups. The reinforcing cage consisted of six #8 reinforcing bars that were confined within a #4 bar spiral with a diameter of 8 in. The reinforcing cage extended to a depth of 10 ft. The steel pipe pile was filled with concrete that had an average unconfined compressive strength of 5150 psi based on tests of four specimens. A drawing of the cross-section for the test pile is provided in Figure 3-7.

Test Layout, Instrumentation, and Procedure

The lateral load test was conducted on October 10, 2007, after the pile had been in the ground for about 4 months. The ground around the test pile was excavated to the elevation of

Table 3-1. Summary of laboratory soil test data.

Depth (ft)	In-Place		Atterberg Limits			Unconfined Compressive Strength (lb/ft^2)	Miniature Vane Shear Strength (Torvane) (lb/ft^2)	Unified Soil Classification System Symbol
	Dry Unit Weight γ_d (lb/ft^3)	Natural Moisture Content w_n (%)	Liquid Limit (LL) (%)	Plastic Limit (PL) (%)	Plasticity Index (PI) (%)			
1.25	117.6	34.2	39	18	21	1104	-	CL
2.75	117.4	34.4	38	18	20	626	620	CL
5.75	104.6	56.0	51	21	30	384	320	CH
8.5	112.4	41.5	38	18	20	684	534	CL
11.5	110.8	44.1	38	19	19	741	500	CL
16.5	126.6	24.2	19	18	1	1081	560	ML
26.75	116.9	35.0	27	14	13	237	780	CL
33.5	124.6	26.1	27	14	13	1306	780	CL
36.75	117.1	34.8	35	17	18	1381	840	CL
41.75	112.0	42.1	46	17	29	1037	520	CL
48	117.2	34.6	33	16	17	297	660	CL

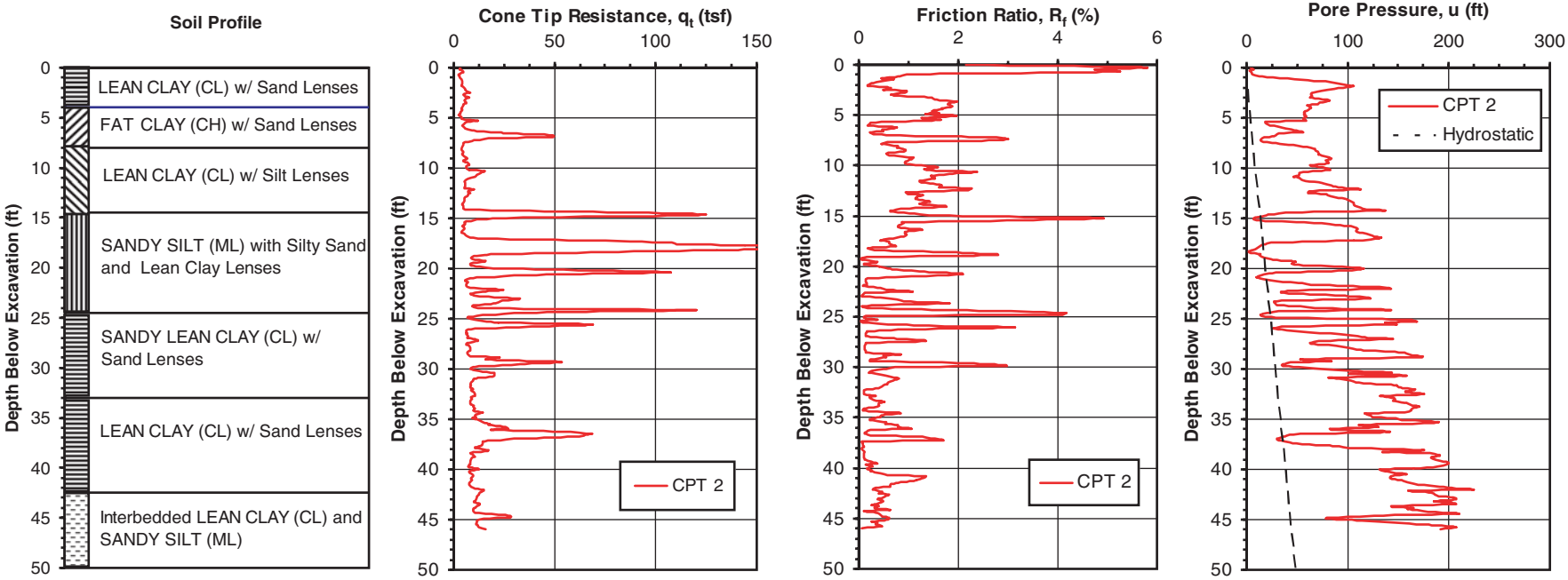

Figure 3-4. Plots of cone tip resistance, friction ratio and pore pressure vs depth curves from cone penetration test (CPT) Sounding 2 near the center of the site along with soil profile.

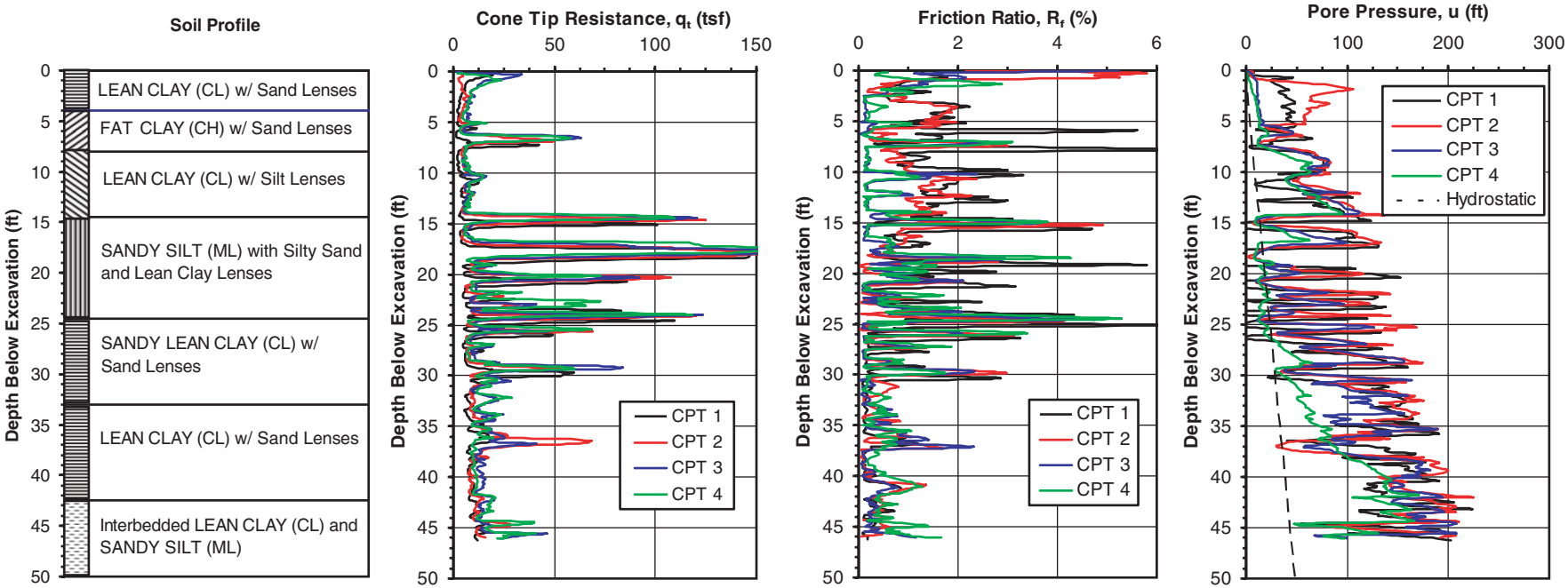

Figure 3-5. Plots of cone tip resistance, friction ratio, and pore pressure vs depth curves from all CPT soundings at the site along with soil profile.

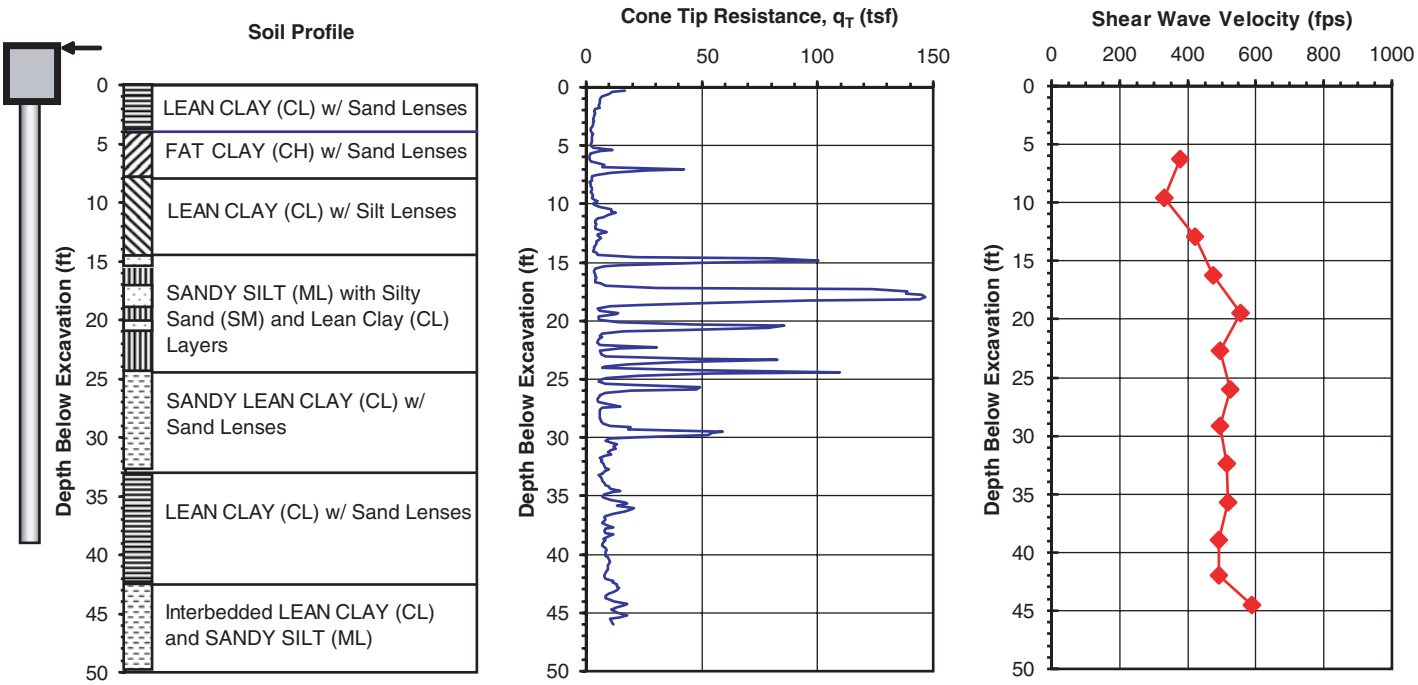

Figure 3-6. Plots of cone tip resistance and shear wave velocity versus depth from seismic cone testing along with soil profile.

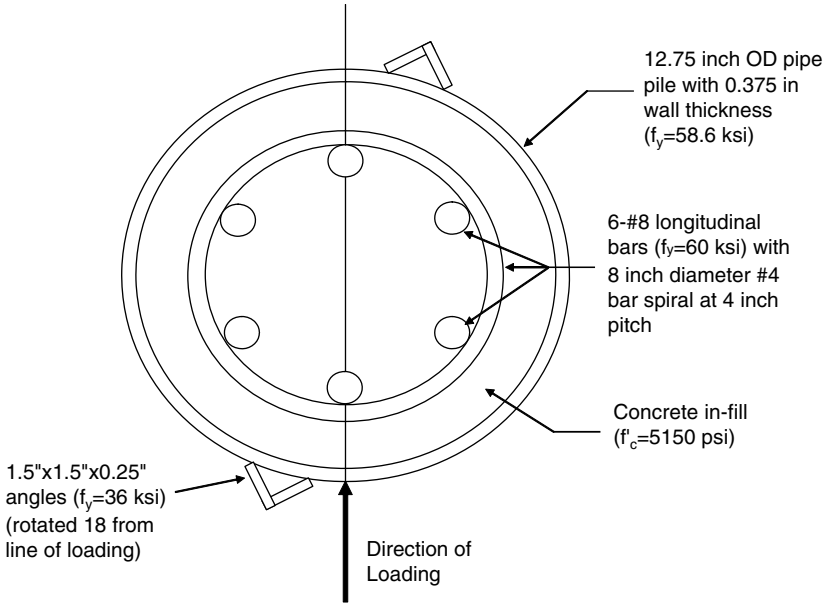

Figure 3-7. Cross-section of single pipe pile.

Figure 3-8. Photograph of lateral load test on single pipe pile.

the base of the pile caps used in the pile group testing, which was approximately 2.5 ft below the ground surface shown in Figure 3-9. Load was applied at a height of 1.5 ft above the surrounding ground surface. In contrast to the pile group tests where the pile head was restrained (fixed-head), the pile head for the single pile test was unrestrained (free-head). A free-head lateral load test for a single pile is common because it is very difficult to create a truly fixed-head condition for a single pile. Because the purpose of the test was to calibrate the analysis model, it was considered more important to know the pile head fixity condition than whether it was a free-head or fixed-head. The boundary condition can be changed easily for subsequent analyses once the soil model is established.

The load was applied to the test pile using a hydraulic jack attached to an electric pump. Hemispherical plates were used to prevent the application of moment to the pile and account for any eccentricity in the loading. Load was measured using a resistance-type strain gauge load cell that had been calibrated previously in the laboratory. Pile head deflection was measured at the elevation of the load point with a string potentiometer attached to an independent reference frame. In addition, pile head deflection was measured at an elevation 3.31 ft above the load point so that pile head rotation could be computed. Prior to placing concrete in the test pile, a 1-in. diameter conduit was installed to a depth of 30 ft. A shape accelerometer array was inserted into this conduit at the beginning of the load test so that deflection versus depth profiles could be determined at various load increments. Data was recorded using computer data acquisition systems. A photograph of the test pile during testing is provided in Figure 3-8.

The load test was performed incrementally using a deflection control approach. The load in the hydraulic jack was increased to deflection increments of 0.125, 0.25, 0.50, 0.75, 1.0, 1.5, 2.0, and 2.5 in. The maximum deflection was somewhat larger than that used for the pile group testing to facilitate calibration of the numerical models. After reaching each target deflection, the deflection was maintained for 3 minutes and then load was reduced to zero prior to loading the pile to the next increment.

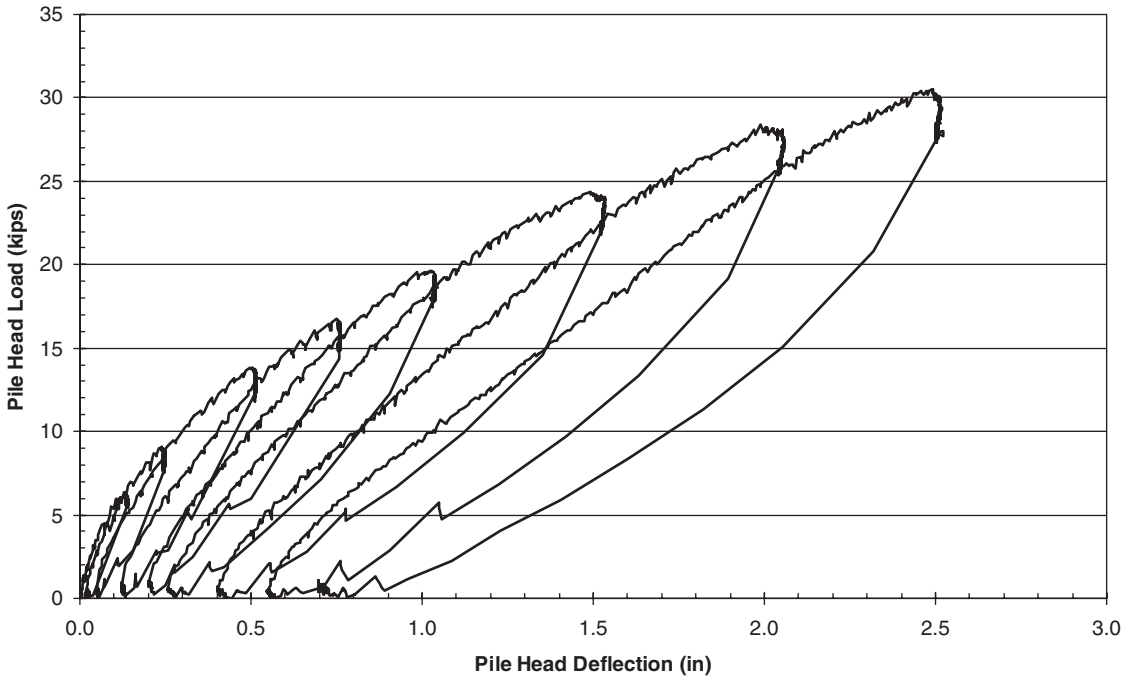

Figure 3-9. Complete pile head load vs pile head deflection curve.

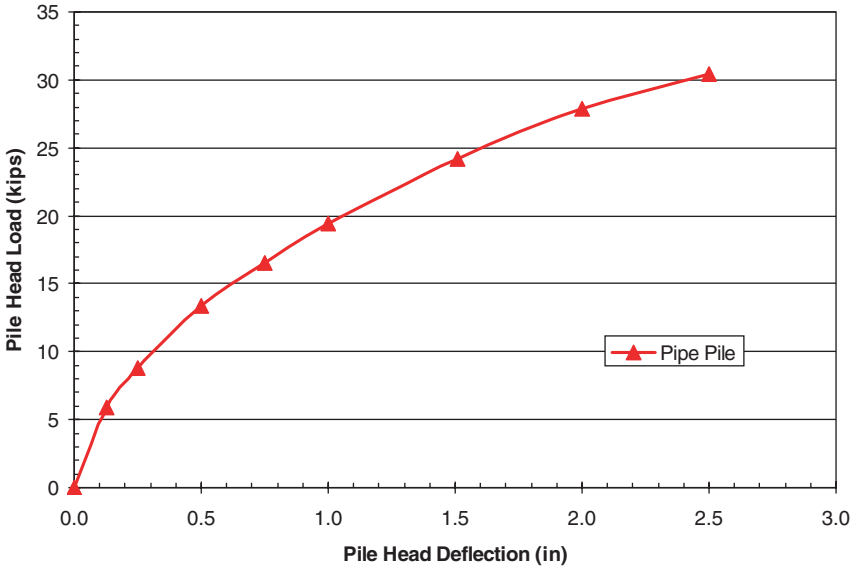

Figure 3-10. Peak pile head load vs pile head deflection.

Test Results

A plot of the complete pile head load versus deflection curve for the entire test is presented in Figure 3-9. This curve provides the load path taken during loading, unloading, and reloading for each cycle. While the load was decreased to zero after each increment, the pile did not return to its initial zero deflection level, but exhibited a residual deflection. This may have been due to side friction and soil falling into the gap behind the pile. During reloading, the load-defection curve was stiffer than that observed during virgin loading at the same deflection.

The virgin pile head load versus deflection curve is plotted in Figure 3-10. This plot was developed by plotting the peak values and eliminating the unload and reload segments. The curve exhibits the conventional hyperbolic shape that would be expected for a pile in soft clay. The peak pile head load versus rotation curve is also plotted in Figure 3-11. The rotation, θ, was determined using the following equation:

$$\theta = \tan^{-1}\left(\frac{(\Delta_1 - \Delta_2)}{H}\right) \quad (3)$$

where Δ_1 is the pile deflection 3 ft above the load point, Δ_2 is the pile deflection at the load point, and H is the distance between the measurements (3.31 ft).

Deflection versus depth curves obtained from the shape accelerometer arrays are provided in Figure 3-12 for a number

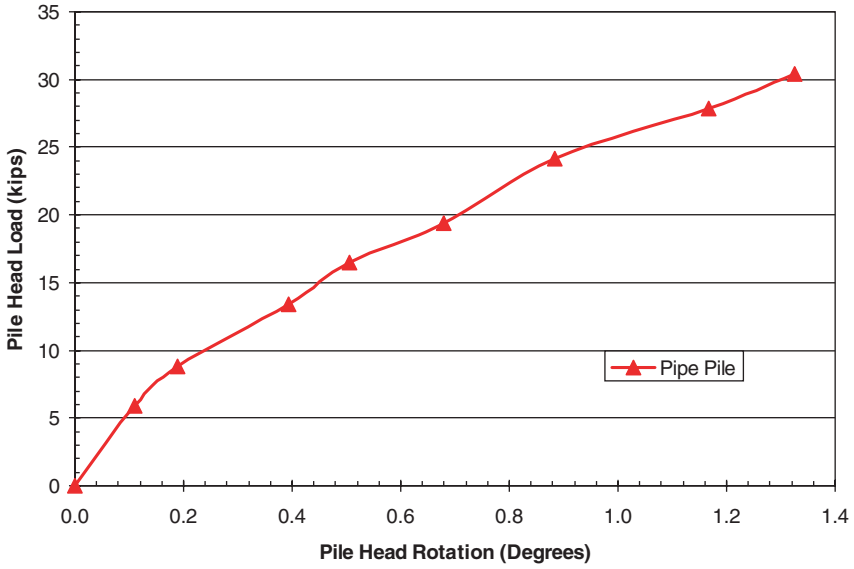

Figure 3-11. Peak pile head load vs pile head rotation.

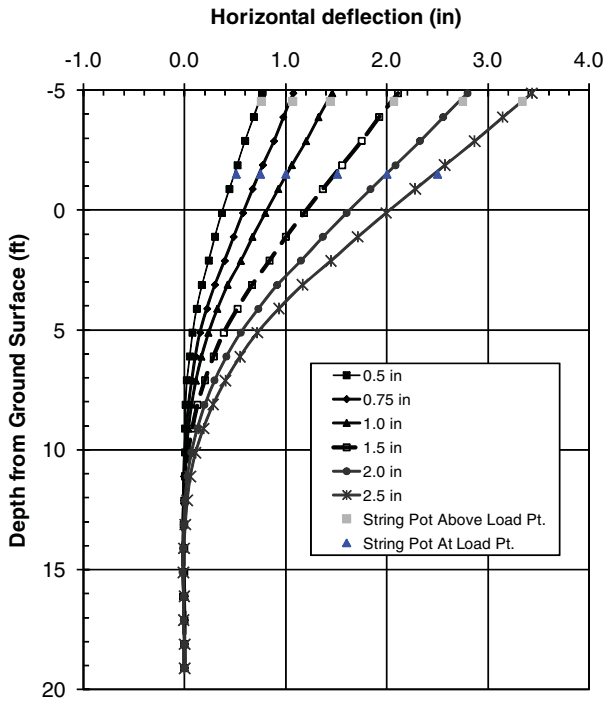

Figure 3-12. Deflection vs depth curves at several deflection increments for single pile lateral load test.

of deflection increments. The shape array provides horizontal deflection values at 1 ft intervals from the top of the pile, which was approximately 40 in. above the load point. Without any corrections, the computed deflection curves obtained from the shape arrays are consistent with the maximum pile head deflections measured by the string potentiometers at the load point. The deflected shape curves also are consistent with the free-head (zero-moment) boundary condition.

3.4 Pile Group Properties

A total of 16 lateral load tests were performed on the 4 pile groups. Schematic drawings of the pile group layout and the soil improvement geometries are provided in Appendix A. All pile groups consisted of nine test piles, which were driven in a 3×3 arrangement with a nominal center to center spacing of 3 ft. The tests piles were 12.75-in. outside diameter pipe piles with a 0.375-in. wall thickness and they were driven closed-ended with a hydraulic hammer to a depth of approximately 44 ft below the excavated ground surface. The steel conformed to ASTM A252 Grade 3 specifications and had a yield strength of 58.6 ksi based on the 0.2% offset criteria. The moment of inertia of the pile itself was 279 in.^{4}; however, angle irons were welded on opposite sides of two to three test piles within each group, which increased the moment of inertia to 324 in.^{4}.

A steel reinforcing cage was installed at the top of each test pile to connect the test piles to the pile cap. The reinforcing cage consisted of six #8 reinforcing bars that were confined within a #4 bar spiral with a diameter of 8 in. and a pitch of 6 in. The test piles typically extended about 2 ft above the base of the pile cap and the reinforcing cage extended 2.25 ft above the base of the cap and 8.75 ft below the base. The steel pipe pile was filled with concrete that had an average unconfined compressive strength of 5000 psi.

A pile cap was constructed by excavating 2.5 ft below the surface of the surface clay layer. The concrete was poured directly against vertical soil faces on the front and back sides of each pile cap. This procedure made it possible to evaluate passive force against the front and back faces of the pile caps. In contrast, plywood forms were used along the sides of each cap and were braced laterally against the adjacent soil faces. This construction procedure created a gap between the cap sidewall and the soil so that side friction would be eliminated. Steel reinforcing mats were placed in the top and bottom of each cap.

3.5 Pile Group Testing Procedure

Lateral load was applied using MTS actuators with the load centered at a height of 11 in. above the top of the pile cap. Each actuator could produce 600 kips in compression and 450 kips in tension. Another pile group or groups provided a reaction for the applied load. In all cases, the reaction pile group or groups were located 32 ft away from the test pile group to minimize interference between the two pile groups during lateral loading. Each actuator was fitted with two 8.67-ft extension pieces to span the 32.1-ft gap between the pile groups. The actuator was attached to a concrete corbel atop each pile cap using steel tie-rods that extended through PVC sleeves in the corbel and were bolted to the back face of the corbel. This allowed load to be applied without affecting the soil around the pile group. The tie-rods were prestressed to minimize displacement of the steel during the load tests. A three-dimensional swivel head was located at each end of the actuator to provide a zero moment or "pinned" connection. Each swivel could accommodate $\pm 5°$ of pile cap rotation about a horizontal line and $\pm 15°$ of pile cap rotation about a vertical line.

The lateral load tests were carried out with a displacement control approach with target pile cap displacement increments of 0.25, 0.5, 0.75, 1.0, and 1.5 in. During this process, the actuator extended or contracted at a rate of about 40 mm/min. Additionally, at each increment, 10 cycles with a peak pile cap amplitude of ± 0.1 in. were applied with a frequency of approximately 1 Hz to evaluate dynamic response of the pile cap. After this cyclic loading at each increment, the pile group was pulled back to the initial starting point prior to loading to the next higher displacement increment.

Load Test Instrumentation

Applied load was measured directly by the load cell on the actuator, which was calibrated in the laboratory prior to testing in the field. Lateral pile cap displacement was measured using two string potentiometers attached to the pile cap at the elevation of the loading point (0.92 ft above the top of the cap) on the east and west sides of the actuator attachment point as shown in Figure 3-13. Lateral pile cap displacement also was measured on the back side of each corbel with two string potentiometers attached 1.75 ft (21 in.) and 0.375 ft (4.5 in.) above the top of the pile cap directly in line with the load direction. Therefore, the vertical distance between these two string pots was 1.375 ft (16.5 in.) as shown in Figure 3-13. Finally, vertical pile cap displacement was measured at two points along the length of each pile cap to evaluate pile cap rotation. On both caps, string potentiometers were located 2 in. from the north and south edges of the corbel, with a distance of 44.72 in. between the potentiometers on Cap 1 and a distance of 108 in. (9 ft) for Cap 2 as shown in Figure 3-13. Each potentiometer was attached to an independent reference beam supported at a distance of about 6 ft from the side of the pile cap. The pile rotation, θ, was determined using the following equation:

$$\theta = \tan^{-1}\left(\frac{\Delta_1 - \Delta_2}{H}\right) \quad (4)$$

where Δ_1 and Δ_2 are the vertical pile cap deflection at two points on the pile cap and H is the distance between the measurements.

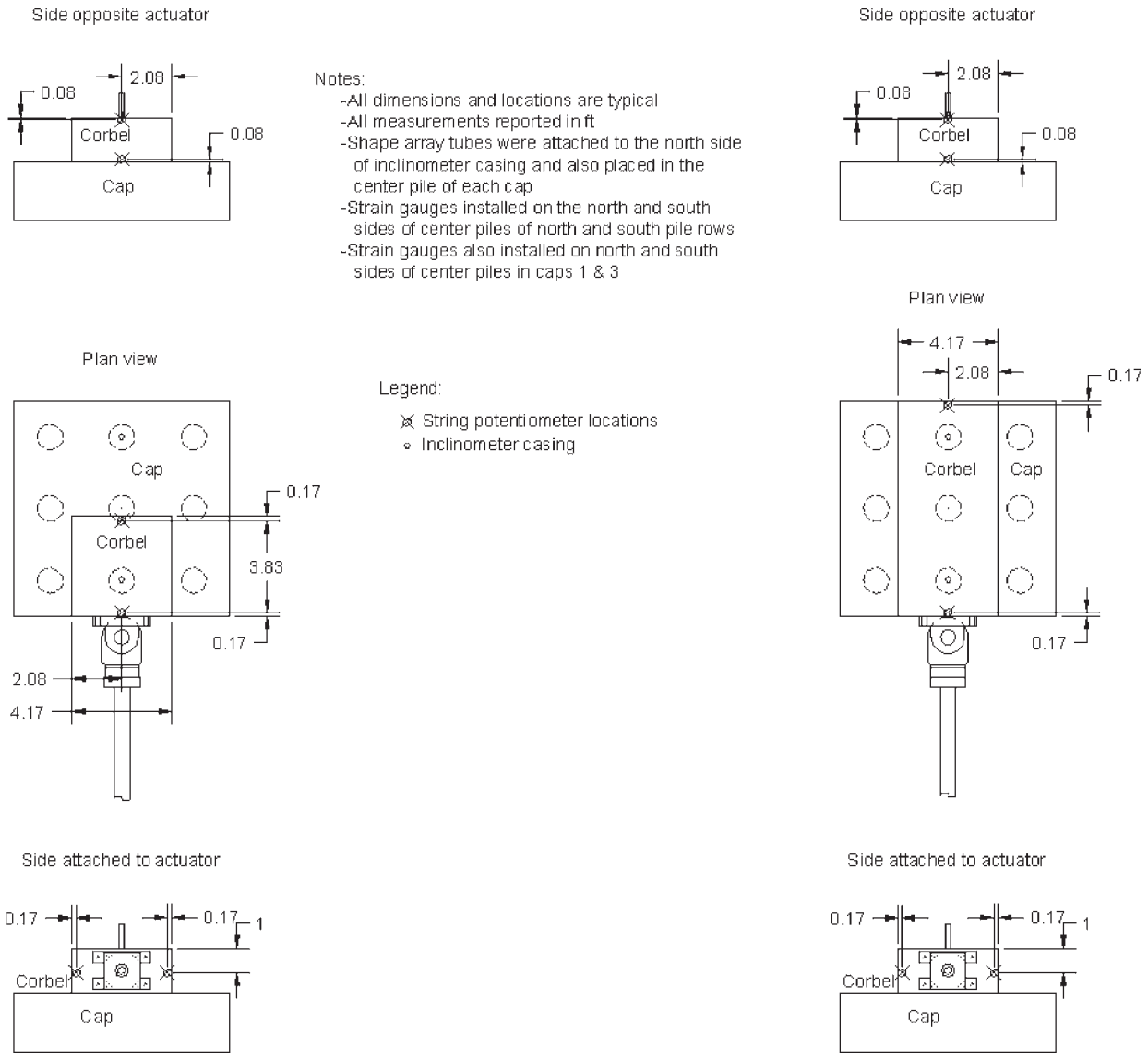

Figure 3-13. Typical instrumentation layout for piles caps with a partial-length corbel (Caps 1 and 4) and a full-length corbel (Caps 2 and 3).

Prior to placing concrete in the test piles, a 1-in. diameter PVC pipe was installed to a depth of 30 ft in the middle pile in each row of each pile group. A shape accelerometer array could be inserted into this pipe at the beginning of the load tests so that deflection versus depth profiles could be determined at various load increments. Using triaxial accelerometers embedded into a flexible cable at 1-ft intervals, the shape arrays provided real-time displacement versus depth profiles throughout the process of testing. To provide some check on the accuracy of the shape array measurements, inclinometer pipes were also installed in the middle pile in the front and back rows of each pile group. Inclinometer measurements were typically performed before testing and then again once the 1.5-in. or final displacement increment had been reached. Bending moment along the length of the piles was evaluated using two complementary procedures. First, the deflection versus depth curves obtained from the shape array data were used to determine bending moment versus depth profiles along the length of the pile. The moment, M, was computed using the following equation:

$$M = \frac{EI\left(y_{-1} - 2y_0 + y_1\right)}{h^2} \tag{5}$$

where

E is the elastic modulus of the pile;
I is the moment of inertia of the pile;
y_{-1}, y_o, and y_1 are the horizontal pile deflections at locations 12 in. above, at the depth, and 12 in. below the depth of interest; and
h is the vertical spacing between the deflection (12 in.).

For the steel pipe pile with concrete fill, this required a calculation of the composite properties. These calculations indicated that EI was 1.415×10^7 kip-in^2 using a compressive strength of 5100 psi based on compression tests on concrete cylinders at the time of testing. The moment computed using Equation 5 is very sensitive to minor variations or errors in the measured displacement versus depth curves. To reduce the influence of minor variances in the measured displacement data on the computed moment, a 5th-order polynomial equation was developed based on the measured data to smooth the displacement versus depth curves. The displacements used in Equation 5 were then based on values computed with the polynomial equation. Although the difference in the displacement values at any depth were generally very small, this procedure produced moment versus depth curves with more realistic shapes.

Secondly, waterproof electrical resistance type strain gauges were placed at depths of 2, 6, 11, and 13.5 ft below the top of two to three piles within each group. For Pile Cap 1, the middle piles within each row were instrumented with strain gauges while for Pile Cap 2, the middle piles within the front and back row piles were instrumented. The strain gauge depths were selected to provide the maximum negative and positive moments along the pile. For a fixed-head or restrained-head pile, the maximum negative moment is expected to occur at the pile-pile cap interface. Preliminary LPILE analyses suggested that the maximum positive moment would likely occur between 11 and 13 ft below the top of the piles. Angle irons were welded on opposite sides of the instrumented piles to a depth of 20 ft to protect the strain gauges during pile driving. Data was recorded using two computer data acquisition systems.

3.6 Pile Group Tests in Untreated Clay

Plan and profile drawings showing the layout of the pile group in untreated clay for Tests 1 and 2 are provided in Figure 3-14. Tests 1 and 2 were performed to provide a baseline of the lateral load behavior of the pile caps in virgin soil conditions prior to any soil treatment. Test 1 was conducted by pulling the caps together using the actuator while the untreated native soil was in place adjacent to the pile cap. At the completion of Test 1, the pile cap was pulled back to zero deflection, but after the actuator load was released some residual deflection remained. Prior to Test 2, the soil immediately adjacent to the opposite face of the pile cap was excavated by hand to create roughly a 1-ft-wide gap between the pile cap face and the adjacent soil as shown in Figure 3-14. This excavation eliminated passive force against the pile cap for the subsequent test. After excavation was complete, which required less than an hour to accomplish, Test 2 was carried out by pushing the pile caps apart using the actuator. The testing was performed using the same procedure described previously. Test 2 was designed to define the passive force provided by the unsaturated clay soil against the pile cap.

Load versus Displacement

Plots of the complete pile cap load versus displacement curves for Cap 1 are provided in Figure 3-15. This plot provides the load path taken during loading, unloading, and reloading for each cycle. At the end of each loading cycle it was necessary to apply a tensile force to bring the actuator deflection back to zero. This does not appear to be a result of yielding in the pile based on measured moments. The behavior could result from a flow of weak soil into the gap behind the pile during loading or lateral resistance due to side shear on the pile as it moves in the opposite direction. During reloading, the load is typically less than that obtained during virgin loading and considerably more linear, but after the load exceeds the maximum previous load, the load increase and the load deflection transitions into what appears to be the virgin curve.

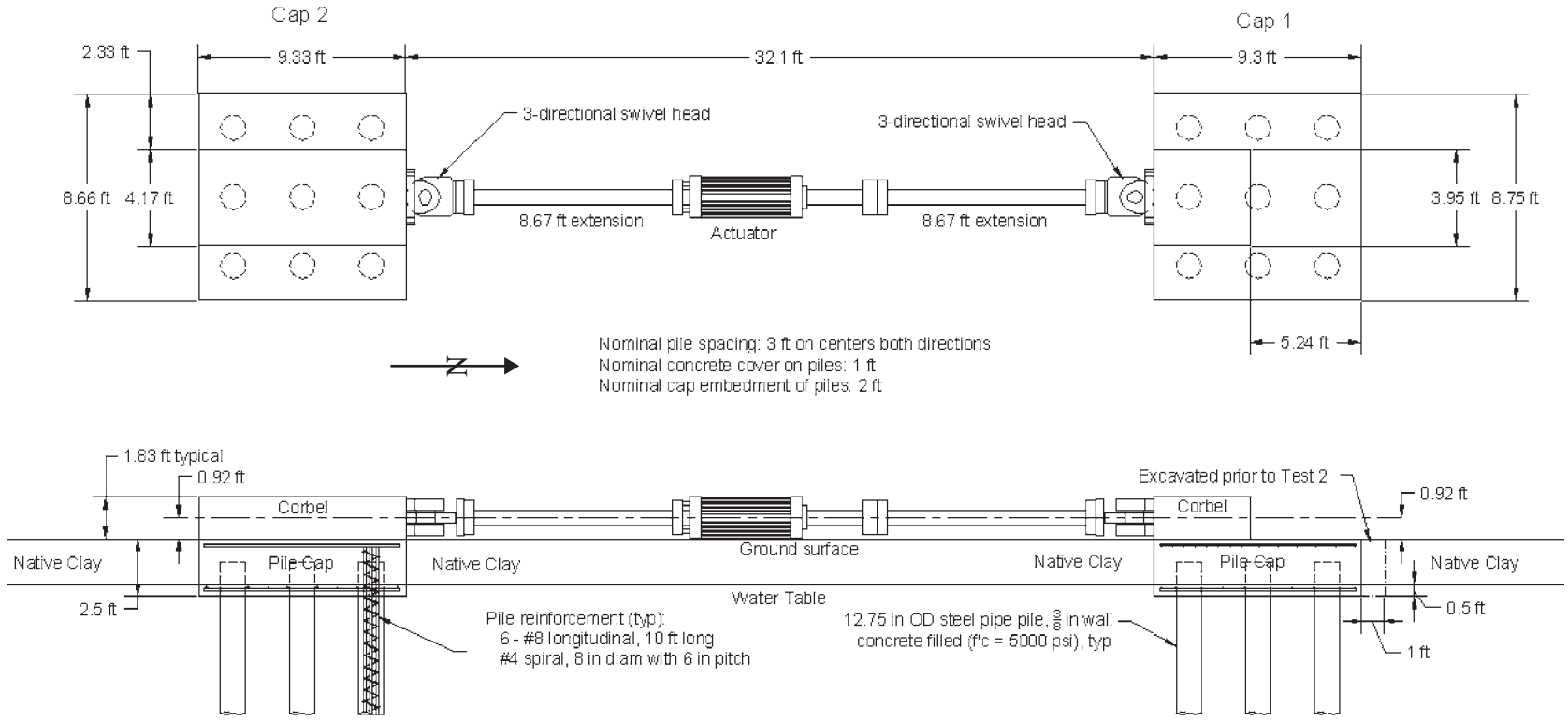

Figure 3-14. Plan and profile drawings of Pile Caps 1 and 2 during Test 1 when the pile groups were pulled together by the actuator. (During Test 2, the soil adjacent to the pile cap was excavated to the base of the cap and the pile caps were pushed apart by the actuator.)

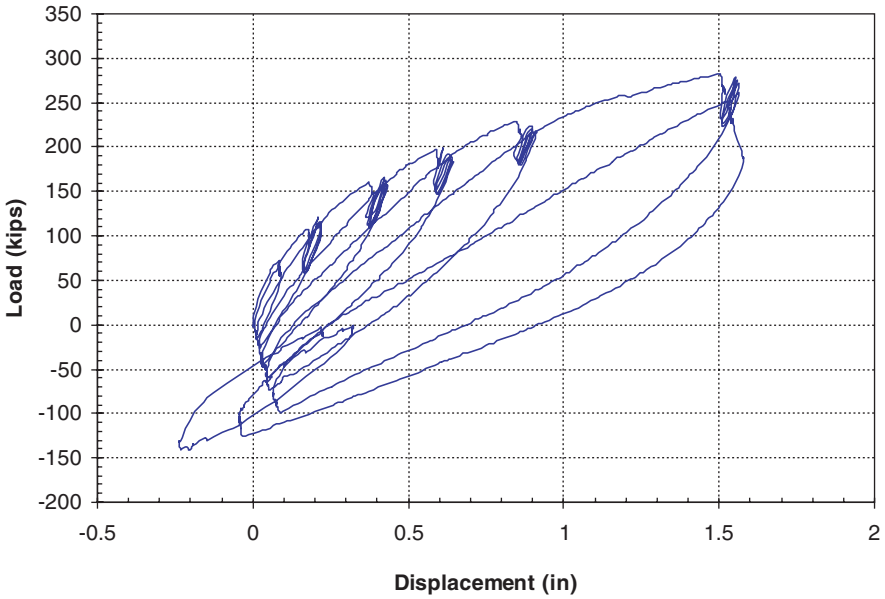

Figure 3-15. Complete pile cap load vs pile head deflection curve for Cap 1 during Test 1.

The virgin pile head load versus displacement curves for each pile group have been developed in Figure 3-16 by plotting the peak values and eliminating the unload and reload segments. The curve exhibits the conventional hyperbolic shape that would be expected for a pile in soft clay. Despite the fact that the two pile groups are 32 ft apart and have minor variations in construction details, the two load-displacement curves are nearly identical. These results suggest that the soil properties across the site are sufficiently uniform for valid comparisons to be made between the pile caps with various soil improvement techniques relative to the untreated conditions.

Rotation versus Load

Pile cap rotation versus load curves based on the string potentiometer and shape arrays for Cap 1 are provided in

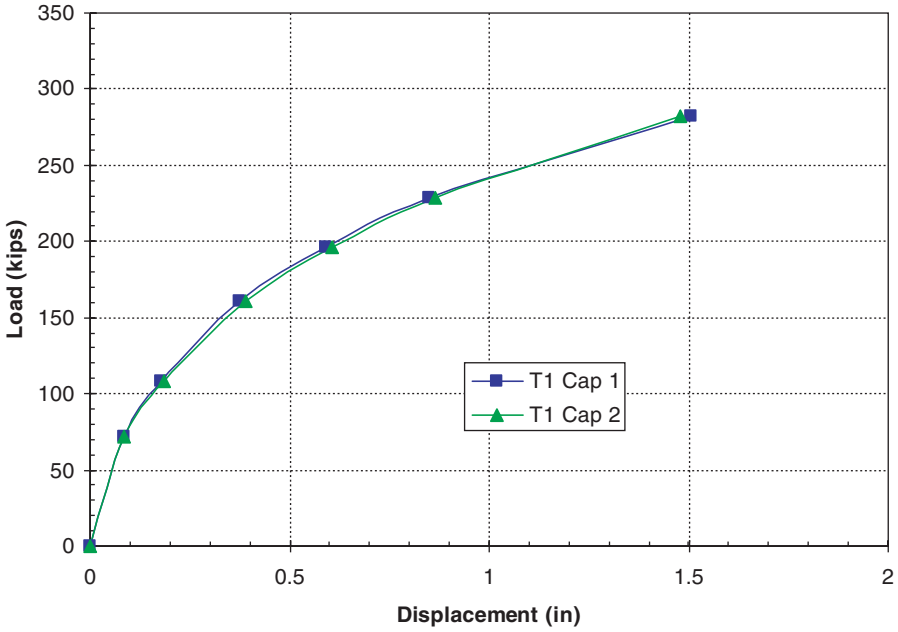

Figure 3-16. Peak pile cap load vs pile head deflection curves for Caps 1 and 2 during Test 1.

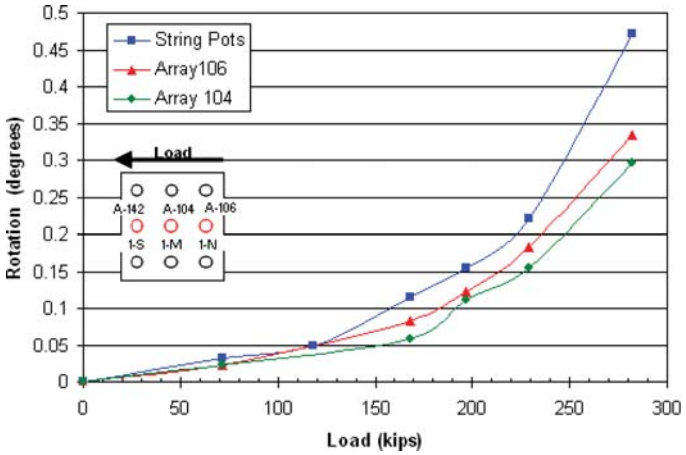

Figure 3-17. Peak pile cap rotation vs load for Caps 1 and 2 during Test 1.

Figure 3-17. The curves are fairly linear up to a load of about 170 kips after which the rotation begins to increase more rapidly with load. The measured rotations are fairly consistent for both caps, although the rotation of Cap 1 is somewhat greater than that for Cap 2. Although pile cap rotation is clearly observed, it is considerably lower than the rotation of the single pile under free-head conditions.

Displacement versus Depth Curves

Displacement versus depth curves obtained from the shape accelerometer arrays in the piles within Pile Cap 1 are provided in Figure 3-18. One of the shape arrays in each pile cap appeared to be providing unrealistic information, which was likely due to damage from previous field testing. As a result, profiles are only provided for two shape arrays in each cap. The location of the shape arrays relative to the piles in the group and the loading direction are shown by the legends in each figure. The average displacements measured by the string potentiometers at the elevation of the load application for each load increment are also shown in these figures for comparison purposes. The displacements obtained from the shape arrays are generally quite consistent with those measured by the string potentiometers; however, in some cases, variations are observed. The discrepancies appear to be related to the difficulty of providing a tight fit between the shape array and the surrounding PVC pipe in some cases. The deflected shape curves are generally consistent with a restrained-head boundary condition. Some rotation is observed, but the rotation is small relative to a free-head pile subjected to the same load levels (see single pile test results). It appears that the shape arrays were long enough to extend below the depth where lateral displacements dropped off to zero.

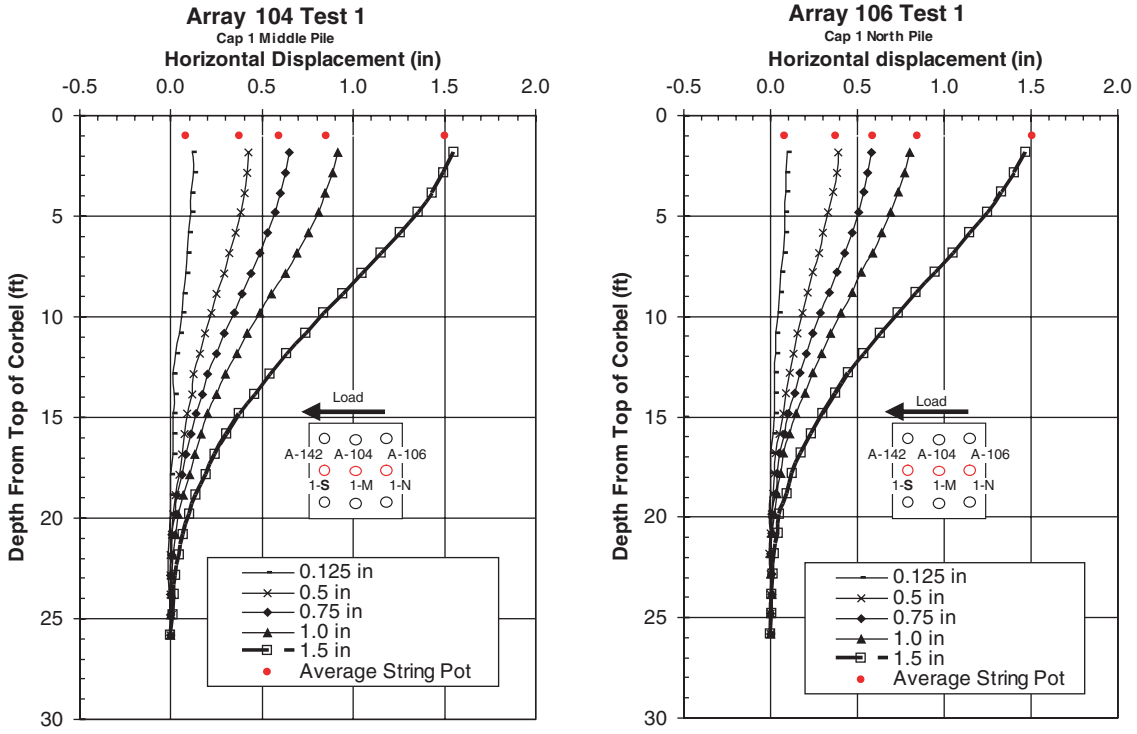

Figure 3-18. Deflection vs depth curves at several deflection increments for Pile Cap 1 during Test 1.

Figure 3-18 provides comparisons between the displacement versus depth curves obtained from the shape arrays and the two inclinometer pipes in Pile Cap 1. Since inclinometer soundings were only taken at the maximum displacement, comparisons are only provided for one increment. Because the inclinometer soundings required 20 minutes to perform the displacement profiles from the shape arrays are sometimes different than the values for the 1.5-in. displacement increments shown in Figure 3-19. The displacement profiles from the shape arrays are quite consistent with the profiles from the inclinometers. These results provide increased confidence in the accuracy of the profiles. It should be noted, however, that the inclinometer profiles, which extend deeper into the pile, indicate that some negative displacement is occurring below the base of the shape arrays.

Maximum Moment versus Load Curves

Figures 3-20 and 3-21 provide plots of the maximum negative and positive bending moments versus applied pile cap load, respectively, for Cap 2 during Test 1. Moment data come from both shape array and strain gauge data when available. Initially, the curves are relatively linear; however, the bending moment tends to increase more rapidly with load at the higher load levels as soil resistance is overcome. The curves from the strain gauges provide relatively consistent moment versus load curves with little evidence of strong group interaction effects for the displacement levels involved. The agreement between the curves computed by the strain gauges and shape arrays varies.

Test 2 Results after Excavation Adjacent to Pile Cap

As previously indicated, the two pile caps were pulled back to zero displacement at the end of Test 1. However, when the load was released, the caps relaxed back toward the direction they had previously been pushed leaving a residual (negative) displacement offset of about 0.3 in. at the start of Test 2. Because the pile caps during Test 2 were pushed in the opposite direction to those from Test 1, the residual deflection is given a negative sign. Figure 3-22 provides a comparison between the load-displacement curves for Caps 1 and 2 during Tests 1 and 2. The load-displacement curves for Test 2 have been shifted right slightly (0.15 in.) to account for gap effects so that the curve for Cap 2 matches the curves for Caps 1 and 2 during Test 1 at larger displacements than would be expected. A comparison of load-displacement curves for Cap 1 with and without passive force on the pile cap can then be made and the results indicate that the passive force is approximately 50 kips. Based on the curves in Figure 3-22, the passive force versus displacement curve shown in Figure 3-23 has been developed,

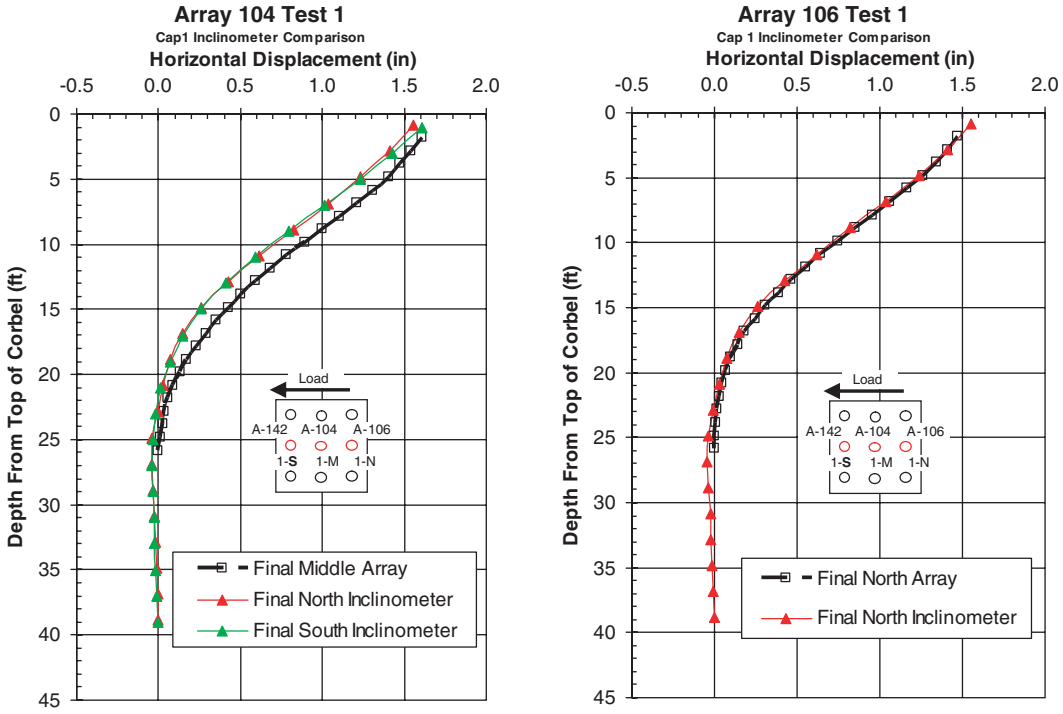

Figure 3-19. Comparison of displacement vs depth curves measured by shape arrays and inclinometers for Cap 1 during Test 1.

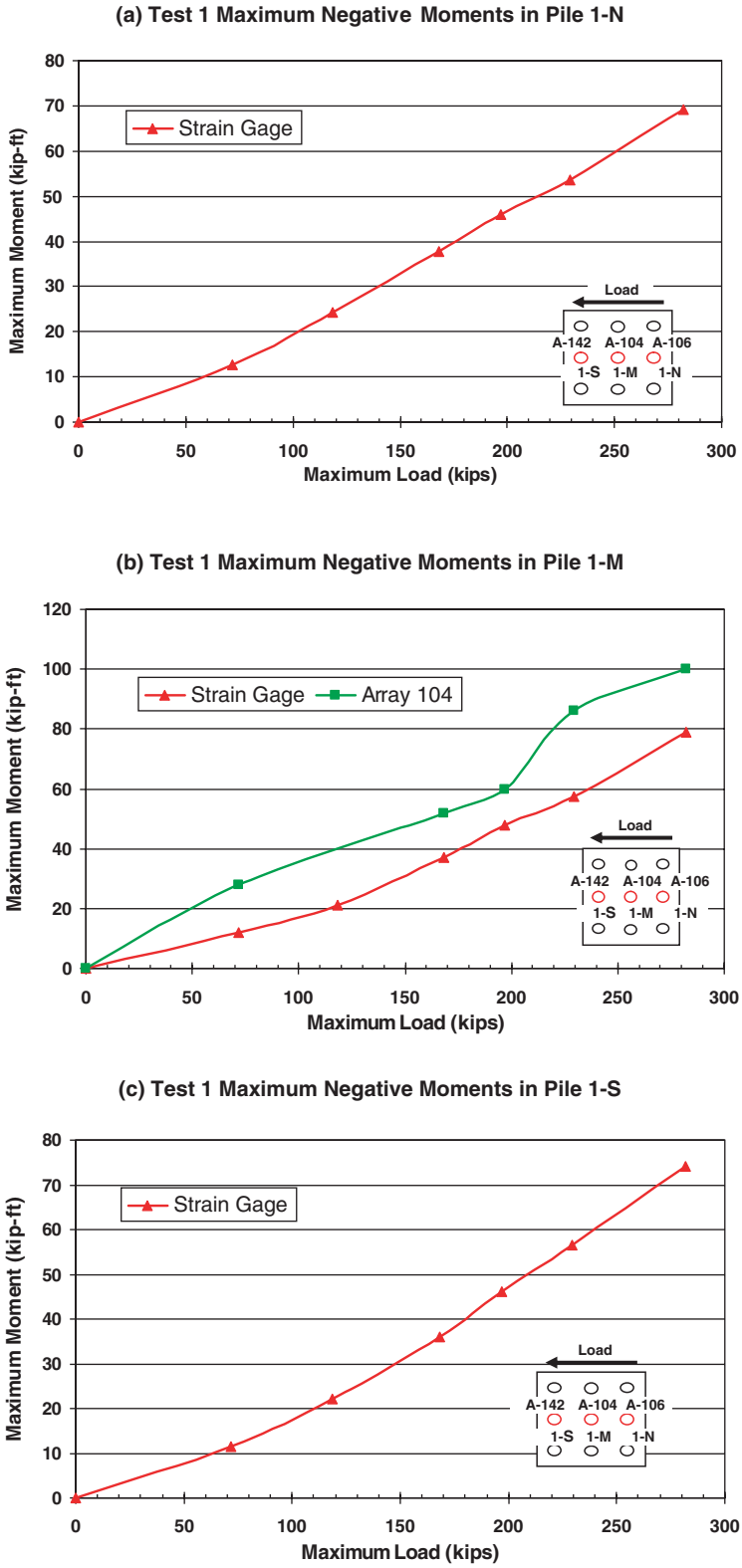

Figure 3-20. Maximum negative moment vs total pile cap load for Piles (a) 1-N, (b) 1-M, and (c) 1-S in Cap 2 during Test 1.

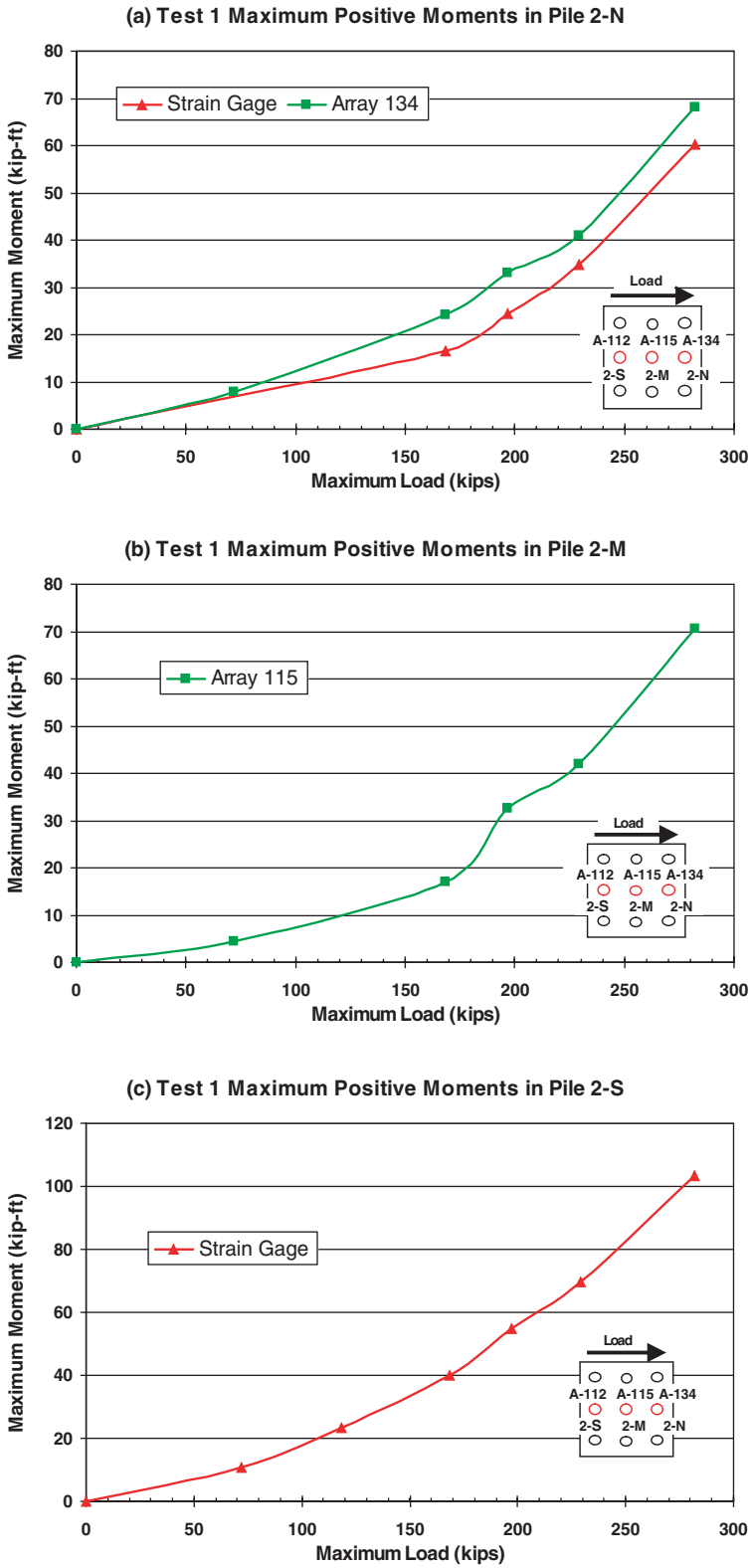

Figure 3-21. Maximum positive moment vs total pile cap load for piles (a) 2-N, (b) 2-M, and (c) 2-S in Cap 2 during Test 1.

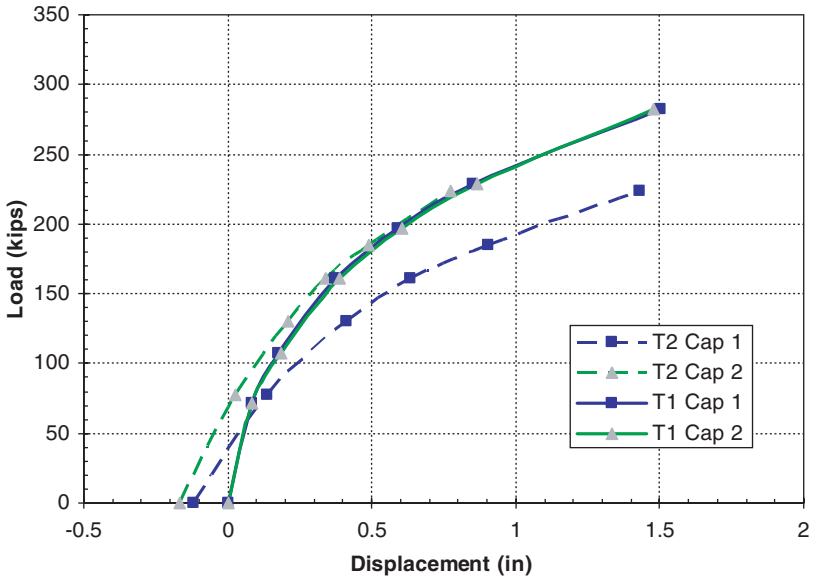

Figure 3-22. Comparison of peak pile cap load vs pile head deflection curves for Caps 1 and 2 during Tests 1 and 2.

which indicates that the full passive force was essentially developed with a displacement of about 0.75 in. Additional test results for Test 2 are provided in Adsero (2008, Appendix 2).

3.7 Pile Group Load Tests Involving Jet Grouting

Plan and profile views of the jet grout columns around Pile Caps 1 and 2 are shown in Figure 3-24. Jet grouting treatment for Pile Cap 1 involved treatment adjacent to the pile group. Treatment for Pile Cap 2 involved treatment below and around the pile group. A single-hole double fluid jet grouting technique was employed to form the grout columns and each of the columns was constructed with identical installation parameters. The jet grout drill head was initially advanced to the base of the treatment zone using water jets and a drill bit located at the bottom of the drill rod. Subsequently, the drill head was rotated and pulled upward at a constant rate, while cement slurry was injected at a specified pressure and flow rate from the inner orifice of the drill nozzle. Concurrently, compressed air was injected from the outer orifice of the drill nozzle to form a protective shroud around the slurry jet to improve the

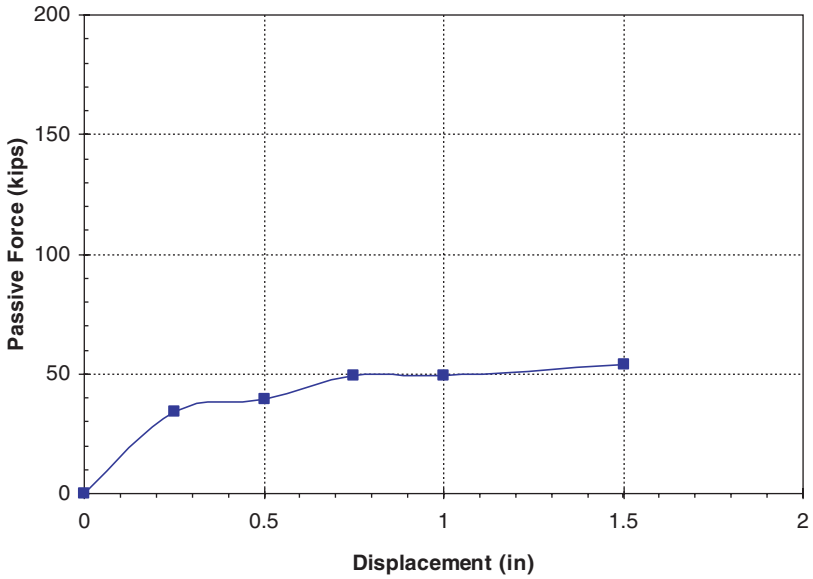

Figure 3-23. Interpreted passive force vs deflection curves based on comparison of Tests 1 and 2 on Pile Cap 1.

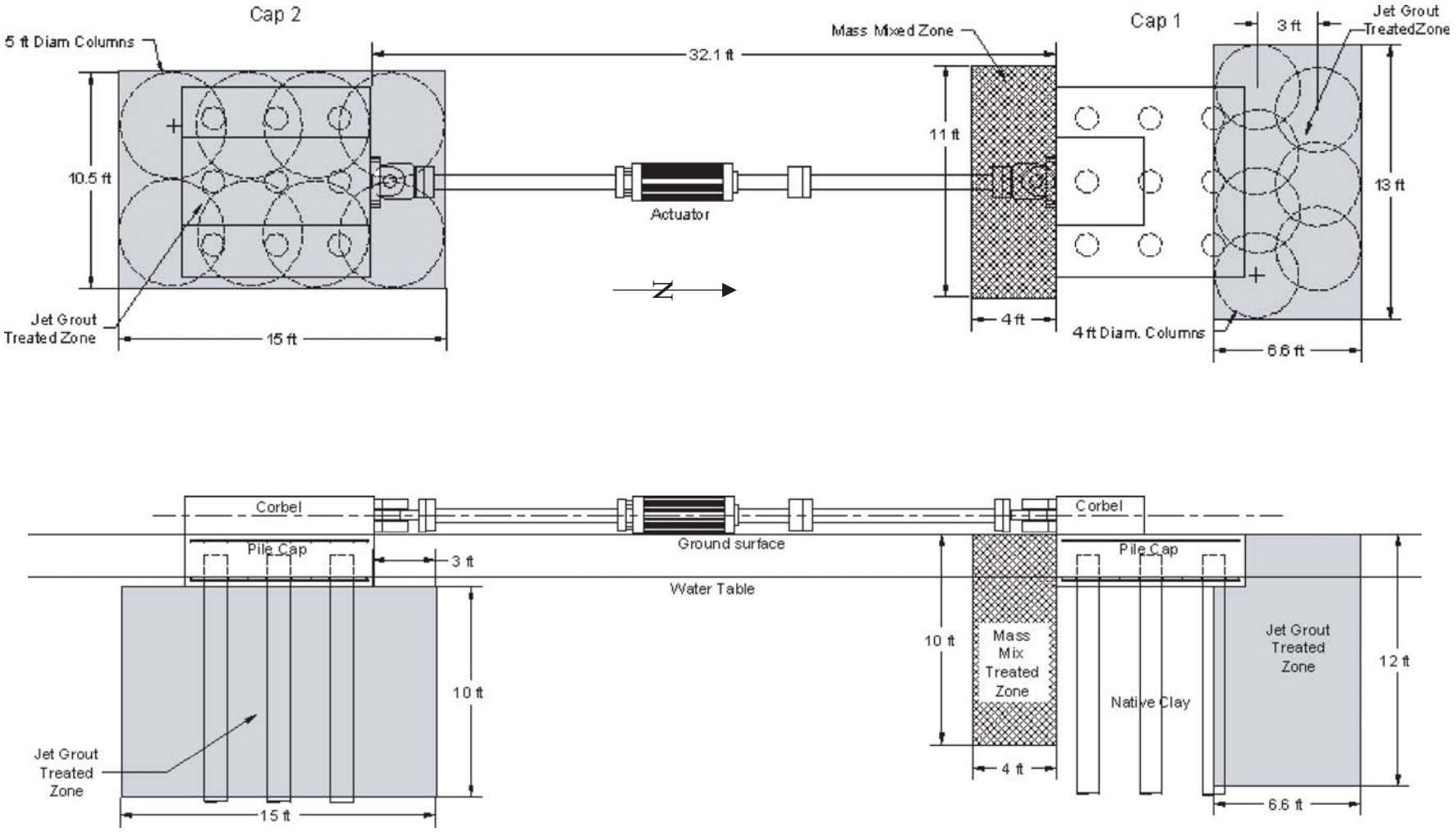

Figure 3-24. Plan and profile views of Pile Groups 1 and 2 after treatment with jet grouting.

erosive capacity of the cement slurry jet. The grout slurry mix had a specific gravity of 1.52, which is equivalent to a 1:1 water to cement ratio by weight.

Jet Grout Treatment below Pile Cap 2

A total of eight 5-ft diameter soilcrete columns were installed beneath and around Pile Cap 2 to a depth of 10 ft below the bottom of the pile cap. Four of the columns were installed at the periphery of the pile cap, and an additional four were installed through the cap itself. During construction of the pile cap, four 6-in. diameter PVC pipes were placed in the pile cap between the rebar to allow easy access to the jet grout pile after construction. After constructing the cap, backfill soil was placed over the cap to allow the jet grout rig to move over the cap. Four PVC pipes were extended to the ground surface to provide the jet grout drill rod with an unobstructed path through the fill material and the pile cap. For retrofit projects these access holes would have to be drilled through the pile cap. The jet grout columns were spaced at approximately 3 ft center-to-center in the north-south direction and 5 ft center-to-center in the east-west direction. This likely produced a 2-ft overlap between columns in the north-south direction, but there was little or no overlap between columns in the east-west direction. The grout treatment extended about 3 ft beyond the front and back ends of the cap and somewhat beyond the cap on the top and bottom sides.

Each of the columns was constructed with identical installation parameters. These parameters are summarized in Table 3-2. One rotation of the high-pressure nozzles occurred in a 0.11-in. lift. Based on the column diameter, flow rates, pull rates, and rotation rates, the cement content for the jet grout columns would be expected to be about 26 lbs/ft^3 or about 20% by weight.

Jet Grout Treatment Below Cap 1

A total of seven soilcrete columns were installed in two rows to create a wall along one edge of the foundation. Plan and profile views of the jet grout columns adjacent to Pile Cap 1 are shown in Figure 3-24. The target diameter of each of the columns was 4 ft and they were spaced 3-ft-on-center in a triangular pattern. This created an overlap between columns of approximately 1 ft. Each jet grout column extended from the top of the pile cap to a depth of 12 ft below the top of the pile cap. The centers of the first row of jet grout columns were positioned so that the jet could cut underneath the pile cap and produce a soilcrete wall that would intersect the front row of piles. Based on the target column diameter, the soilcrete columns likely extended about 1.5 ft under the pile cap, or about to the middle of the outside row of piles.

Each of the columns was constructed using identical construction parameters that are summarized in Table 3-3. One rotation of the high-pressure nozzles occurred in a 0.14-in. lift. Based on the column diameter, flow rates, pull rates, and rotation rates, the cement content for each jet grout column would be expected to be about 24 lbs/ft^3 or about 20% cement by weight.

Table 3-2. Jet grouting installation parameters for columns created beneath Pile Cap 2.

Column Length	10 ft
Estimated Column Diameter	5 ft
Grout Pressure	6000 lbs/in.^{2}
Grout Flow Rate	90 gallons/min
Rotation Speed	7 revolutions/min
Pull Rate	0.79 in./min

Table 3-3. Jet grouting installation parameters for columns installed adjacent to Pile Cap 1.

Column Length	12 ft
Estimated Column Diameter	4 ft
Grout Pressure	6000 psi
Grout Flow Rate	90 gallons/min
Rotation Speed	8 revolutions/min
Pull Rate	1 in./min

Compressive Strength Testing of Jet Grout Columns

Wet grab samples were taken from five completed columns below Cap 2 and two columns adjacent to Cap 1. The samples were taken from locations near the top, middle, and bottom of the columns. In addition, core samples were taken from the top of two columns adjacent to Cap 1 a few weeks after treatment. Prior to testing, the cored samples measured 4 in. in diameter with an approximate length to diameter ratio of 2.0.

The unconfined compressive strength of the soilcrete produced by the jet grouting process was evaluated using the wet grab samples as well as core samples. Figure 3-25 provides a summary of the compressive strength test results as a function of time after treatment. Although there is significant scatter to the data, which is typical for soilcrete columns installed using jet grouting, there is a trend of increasing strength with curing time. Although the compressive strength of the untreated soil prior to treatment was approximately 4 psi, the average compressive strength after jet grout treatment reached about 680 psi with mean ±1 standard deviation bounds ranging from about

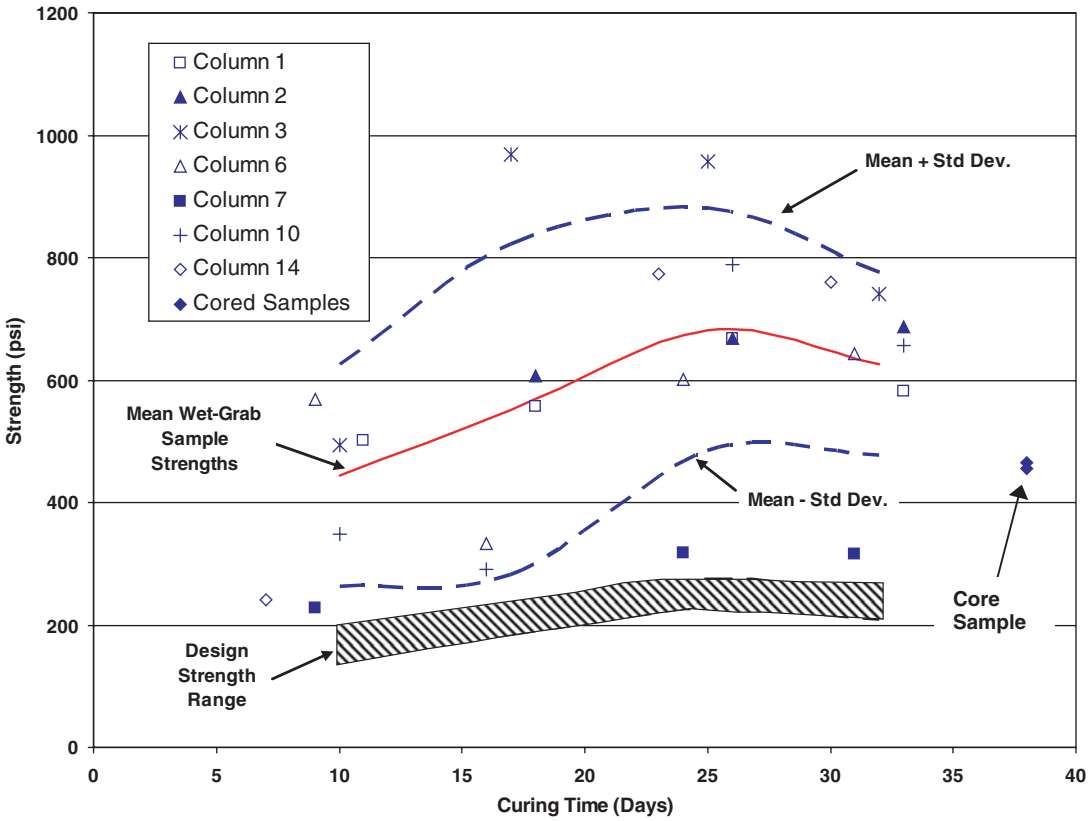

Figure 3-25. Compressive strength of jet grout columns as a function of time after treatment along with design strength values typically employed by geotechnical specialty contractors.

500 to 800 psi. These strength gains are typical for jet grouting applications in similar soils (Burke, 2004). Ground improvement specialty contractors typically use a design value of about one-third the value measured from field test specimens to account for variations in properties within the treated zone. Using this approach, the compressive strength of the jet grouted zone would be about 250 psi; however, even cored specimens had strengths of 480 psi as shown in Figure 3-25. The average strength from two cored samples is about 30% lower than the strength obtained from the wet grab samples. The strength from the core samples is likely more representative of in-situ conditions and is attributable to the poorer mixing produced by the jet grouting process relative to the hand mixing employed with the wet grab samples.

Test Results for Cap 1 (Jet Grouting Adjacent to Cap)

Treating the soil adjacent to Pile Cap 1 with jet grouting increased the lateral resistance of the pile cap substantially. The results from Test 3 and Test 6 were combined to create a composite load-displacement curve for the pile cap following jet grouting. The combined curve is presented in Figure 3-26. The combined curve had a maximum load of 612 kips at a pile cap displacement of 0.72 in., which is 398 kips greater than the 214 kip maximum load from the virgin curve for the same displacement. This represents an increase in lateral resistance of 185% at the maximum measured deflection.

Tests were also performed on Pile Cap 1 after the soil adjacent to the pile cap had been excavated. Despite excavation of the soil, the load-displacement curve was essentially the same after consideration of reloading effects (typically a 10% reduction). Although the soilcrete mass was not connected to the pile cap, it was connected to the piles below because jet grouting extended under the cap. Therefore, lateral movement of the piles engaged the soilcrete mass and produced the same lateral resistance.

Test Results for Pile Cap 2 (Jet Grouting below the Cap)

Figure 3-27 presents a plot of the load-displacement curve for Pile Cap 2 after jet grouting in comparison with the virgin load-displacement curves. Comparing the resistance at a displacement of 1.5 in., jet grouting increased the lateral pile cap resistance from 282 kips to nearly 782 kips. This increase of

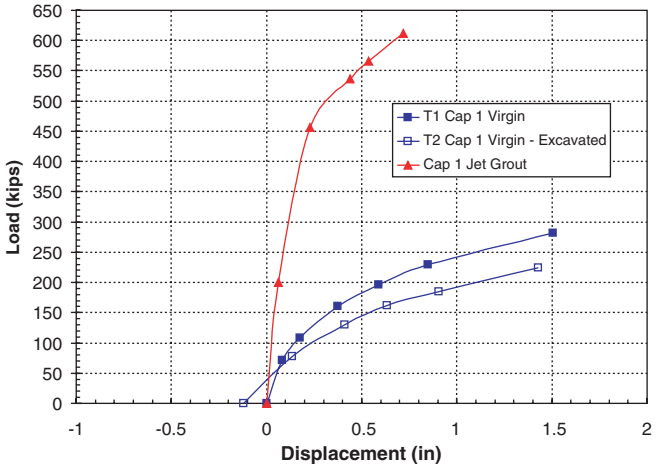

Figure 3-26. Combined load-displacement curves for all tests performed on Pile Cap 1 following jet grouting. The results from the virgin test also are shown for comparison.

500 kips equates to an increase in total resistance of about 2.6 times or 160%. In addition, the initial stiffness of the load-displacement curve after jet grouting is considerably higher than the initial stiffness during virgin loading. The pile cap only displaced 0.016 in. at a load of 200 kips. The load-displacement curve can be separated into three distinct parts. The initial 0.3 in. of the curve are fairly linear. At a displacement of about 0.3 in. the curve shows an abrupt change in slope. A second, relatively linear portion of the curve extends from 0.3 to about 1.6 in. of displacement. The third portion of the curve following 1.6 in. of displacement is flat with a slight drop off in strength after 2.1 in. of displacement. This shape is much different than the hyperbolic shape of the load-displacement curve for the virgin tests and is likely associated with the different deflections required to mobilized adhesive resistance on the soilcrete mass (0.25 in.) relative to that for passive force (2 in.).

The load-displacement curve after excavation to a depth of 7 ft in front of the jet grout zone is also shown in Figure 3-27. Initially, the stiffness is not much greater than that for the pile group in untreated virgin soil; however, the ultimate resistance exceeds 600 kips at a displacement of 3 in.

To produce a more readable report, additional plots, similar to those presented for the pile group in virgin clay are not presented here but are available in Adsero (2008, Appendix 2).

3.8 Pile Group Load Tests Involving Soil Mixing

Construction Details

Plan and profile drawings of the pile group with a soil mix wall on one side of Pile Cap 1 are provided in Figure 3-24. The soil mixed wall adjacent to the cap was 10 ft deep, 11 ft wide, and extended 4 ft in front of the cap. Because of the small size of the wall, economics did not permit the mobilization of a dedicated soil mixing rig to the site. Instead, a procedure was applied to produce a volume of soil with a compressive strength and consistency typical of that produced by soil mixing. The native soil was first excavated to a depth of 5 ft below the top of the cap using a trackhoe. The excavation was then filled to the top of the cap with jet grout spoils from the opposite side of the cap. Afterward, the remaining intact soil from

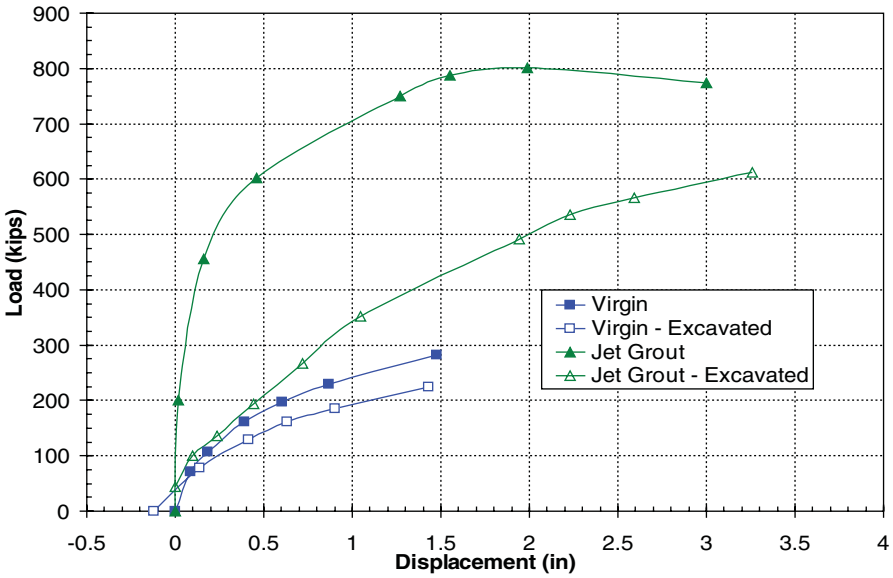

Figure 3-27. Combined load-displacement curves for tests performed on Pile Cap 2 following jet grouting. The results from the virgin test also are shown for comparison.

5 to 10 ft below the top of the cap was progressively excavated with the excavator bucket and mixed with the jet grout spoils. Mixing was accomplished by repeatedly stirring the native soil and grout spoil until the consistency of the mixture became relatively homogeneous and no large blocks were obvious in the mixture. This process required approximately 10 to 15 minutes of mixing and provided a 1:1 ratio of soil to grout spoil mixture.

The grout used in the jet grouting procedure was designed to have a specific gravity of approximately 1.52, which is the equivalent of a 1:1 water to cement ratio by weight using normal Type I cement. The cement content per volume of jet grout slurry was computed to be about 24 lbs/ft^3. Mixing the jet grout slurry with the underlying clay at a 1:1 ratio by volume reduced the cement content of the resulting soilcrete wall to approximately 12 lbs/ft^3. This corresponds to about 10% cement by weight. Six core samples obtained from the soilcrete wall indicate that the mean compressive strengths were 130 and 140 psi after 30 and 60 days of curing, respectively. This strength gain is consistent with past experience for soil mixed walls (Terashi, 2003).

Test Results for Pile Cap 1 with Soil Mixing

Figure 3-28 presents plots of the load-displacement curves for Cap 1 in untreated virgin clay and Test 3 after the mass mix soil improvement. With the soil mix wall, the pile cap resisted 452 kips compared to the 282 kips resisted by the pile cap in the virgin clay at a displacement of 1.5 in. This represents an increase of 60% in the lateral resistance provided by the pile cap. It also is interesting to evaluate the increase in initial stiffness due to the mass mixing. Prior to treatment, the secant stiffness of the load-displacement curve at a displacement of

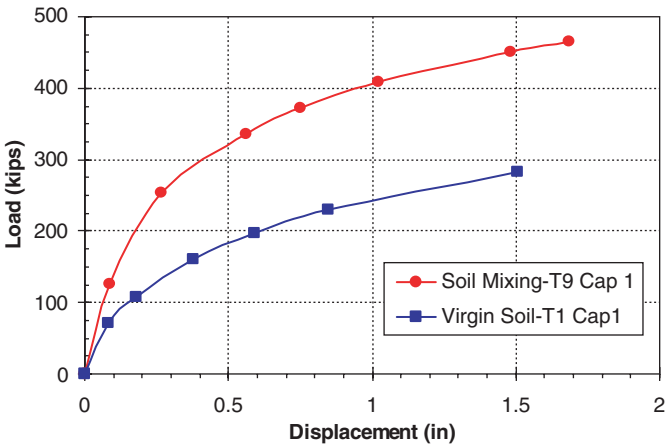

Figure 3-28. Comparison of measured load-displacement curves for Cap 1 in virgin soil and after construction of a soil mix wall on one side of the cap.

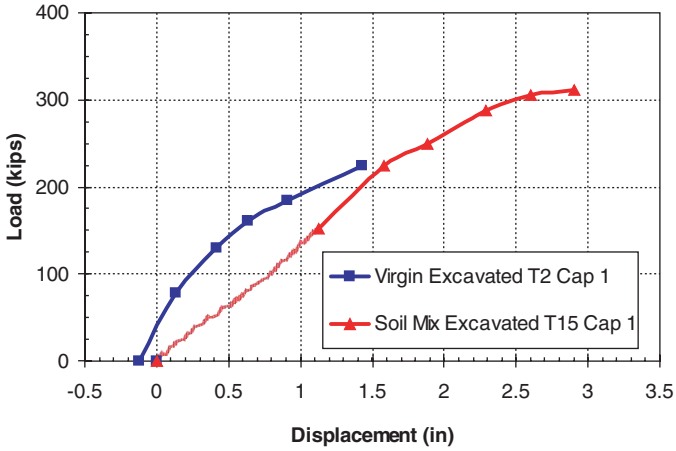

Figure 3-29. Comparison of measured load-displacement curves for Cap 1 in virgin soil and after construction of a soil mix wall on one side of the cap followed by excavation of soil adjacent to the cap.

0.1 in. was 800 kips/in.; after soil mixing the stiffness increased to 1300 kips/inch. This represents an increase in stiffness of about 62%.

Figure 3-29 provides plots of the load-displacement curves for Cap 1 during Test 2 in virgin clay and Test 4 after the mass mix wall construction. In contrast to Tests 1 and 3, in these two tests the soil adjacent to the cap was excavated to the base of the cap. Because the soil had been previously loaded, the load-displacement curve for the pile cap with the mass mix wall is actually lower than that for the pile cap in virgin clay. However, as displacement increases to the maximum previous displacement, the load-displacement curve appears to follow the load-displacement curve for the pile cap in virgin clay with little apparent increase. Because the soil adjacent to the pile cap had been excavated, the pile cap no longer pushed the soil-mixed wall laterally; hence, no increase in lateral resistance was produced. This behavior is in contrast with that for Pile Cap 2 where jet grouting allowed the soilcrete to extend underneath the pile cap and contact the piles themselves.

To produce a more readable report, additional plots, similar to those presented for the pile group in virgin clay are not presented here but are available in Herbst (2008, Appendix 3).

3.9 Pile Group Load Tests Involving Flowable Fill

Several sets of lateral load tests were performed after excavating and replacing the soil around Pile Cap 3 with flowable fill. One set of tests was performed for the case where the soil below the pile cap was excavated and replaced with flowable fill prior to driving the test piles. The technique would represent an approach for improving lateral resistance for new construction. Plan and profile drawings for this case are shown in Figure 3-30. In this case the flowable fill extended

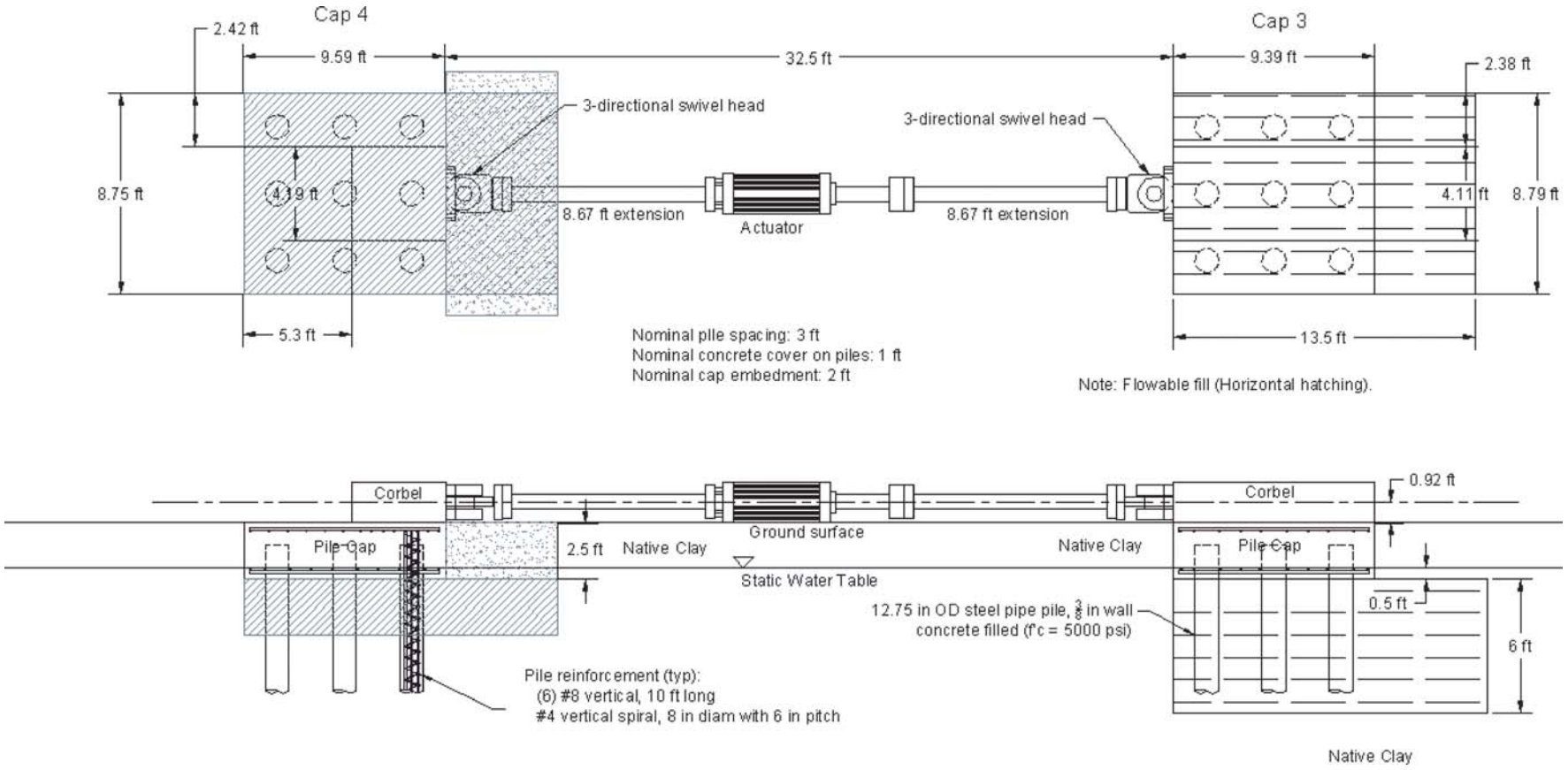

Figure 3-30. Plan and profile views of Cap 3 (right) and Cap 4 (left) during Tests 3 and 5.

directly below the cap to a depth of 6 ft below the base of the pile cap. The fill was flush with the edge of the pile cap on one side but extended 5 ft beyond the pile cap on the other side to evaluate the effect of improvement width in front of the pile groups. The flowable fill zone was originally intended to be deeper, but the depth had to be reduced to prevent failure of the excavation in the weak clay layers. Although the flowable fill was designed to have an unconfined compressive strength of about 100 psi, only one of the six test cylinders was intact enough to be tested and that test cylinder only had a compressive strength of 30 psi. Therefore, the flowable fill was probably closer to a weakly cemented sand at a medium relative density. For Test 3, the two pile groups were pushed apart but for Test 5 the pile groups were pulled together.

Because of the lower than expected compressive strength of the original flowable fill zone, a second set of lateral load tests was subsequently performed after constructing a flowable fill wall adjacent to the pile cap. This technique would represent an approach for improving lateral pile group resistance after construction. Plan and profile drawings for this case are provided in Figure 3-31. The flowable fill zone was only 6 ft deep, 12 ft wide, and extended 6 ft in front of the pile cap. The flowable fill was designed to have a compressive strength of 150 psi; however, the average of four test cylinders was 137 psi. For Test 10, the pile groups were pushed apart but for Test 12 the pile groups were pulled together.

Some concern has been expressed about long-term strength loss of flowable fill in saturated conditions with groundwater flow. Therefore, three flowable fill cylinders were kept in a fog room and tested 700 days after placement. The test results for these cylinders were very consistent and yielded an average compressive strength of 57 psi, which represents a 56% decrease in strength over 2 years' time. Visual observations of the test cylinders did indicate that indeed some of the cementitious material had leached out. Leaching was observed as white streaks on the outside of the samples. The leaching occurred because water was able to flow into the flowable fill. If the flowable fill had higher cement content the leaching would have been reduced. Also, if the water did not flow over the flowable fill, the leaching would have been reduced or possibly eliminated.

Load Test Results

Figure 3-32 shows the load-displacement curves for Cap 3 during Test 3 after treatment with flowable fill compared to Test 1, Cap 2 in untreated virgin soil with soil to the top of the pile cap. In these tests, the pile caps were both in contact with the adjacent soil. Both curves have the same general hyperbolic shape; however, the flowable fill treatment increased the resistance by about 20 to 30 kips or about 10% relative to the pile cap in untreated soil. Figure 3-33 provides a plot of the load-displacement curves for Cap 3 during Test 5 after treatment with flowable fill compared to Cap 1 during Test 2 in untreated virgin soil. In both cases, the soil adjacent to the pile cap was excavated. The ultimate resistance for the cap with flowable fill was once again about 30 kips greater than that for the pile cap in untreated clay. This represents an increase of about 10% relative to the pile cap in untreated clay. These results indicate that excavating the weak clay and replacing it with the weakly cemented sand provided only minimal increases in lateral resistance.

Figure 3-34 provides a comparison of the lateral load-displacement curves for Cap 3 for Test 10 where the flowable fill extended to the top of the pile cap and for Test 12 where a 1-ft wide slot was excavated to the base of the pile cap immediately adjacent to the cap. The flowable fill wall increased the lateral resistance at a displacement of 1.85 in. by about 150 kips. This represents an increase in lateral resistance of about 50% with relatively little cost or effort.

Figure 3-35 provides a comparison of the lateral load-displacement curve for Cap 3 after excavation of the slot relative to the curve for Cap 1 in untreated clay after excavation adjacent to the cap. The load-displacement curves for both cases are relatively comparable, suggesting that the increase in resistance was achieved when the pile cap impacted the flowable fill wall and caused it to move into the surrounding ground. As the wall moved laterally, both passive force on the back of the wall and adhesive resistance on the side of the wall could produce increased lateral resistance. When the slot was excavated next to the cap, the cap did not impact the wall and the resistance was about the same as that for the cap in untreated clay.

The load test results for the flowable fill wall are very similar to those obtained for the soil mixed wall and suggest that the mechanism of increased resistance is produced by passive force and adhesive shear on the side walls as the wall is pushed into the surrounding soil rather than by increased lateral pile-soil resistance. The results also suggest that the treated zone may only need to have an unconfined compressive strength of 140 psi to effectively behave as a "rigid wall" in developing increased lateral resistance. To produce a more readable report, additional plots, similar to those presented for the pile group in virgin clay are not presented here but are available in Miner (2009, Appendix 3).

3.10 Pile Group Load Tests Involving Excavation and Replacement

Excavation and Replacement with Compacted Fill

Plan and profile drawings showing the layout of Pile Cap 4 with compacted fill are provided in Figure 3-36. Tests on this

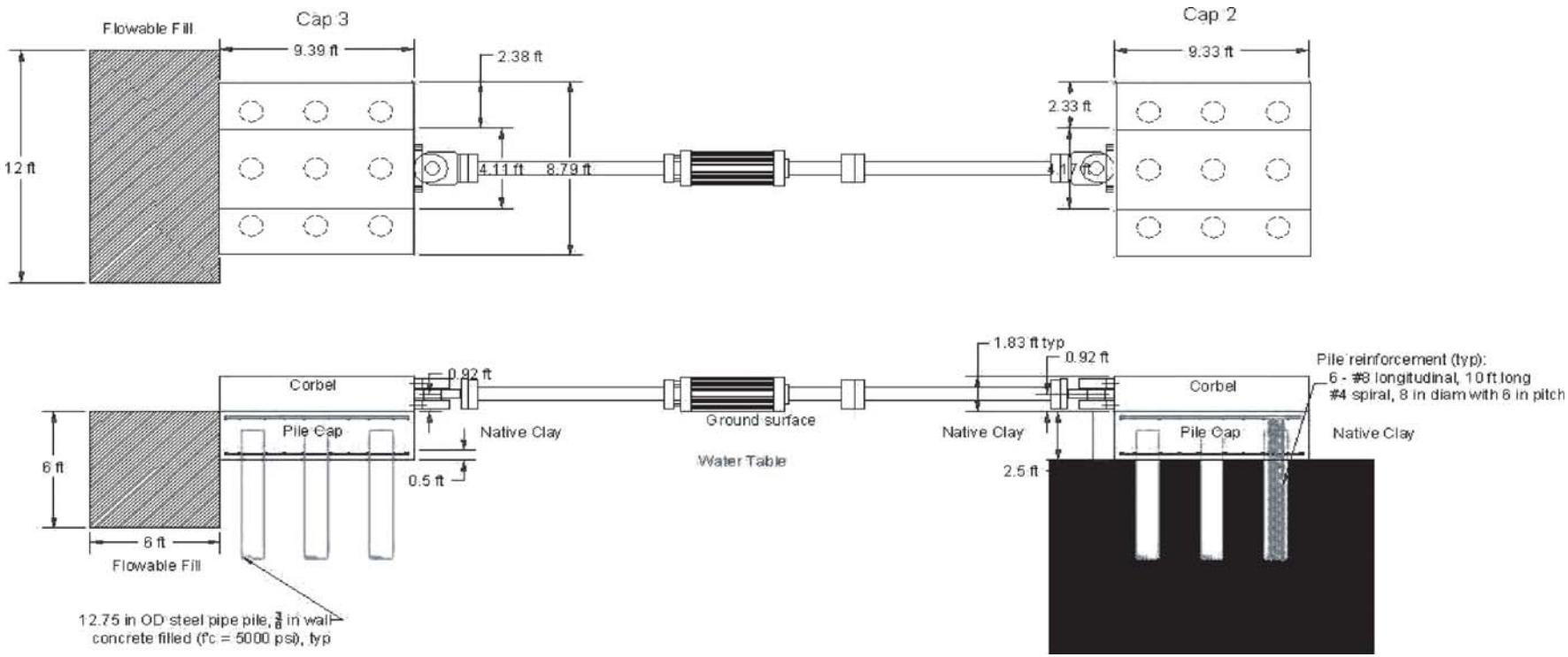

Figure 3-31. Plan and profile views of Cap 3 (left) and Cap 2 (right) during Tests 10 and 12. Test 10 performed with flowable fill adjacent to pile cap and Test 12 performed after excavation of flowable fill adjacent to cap.

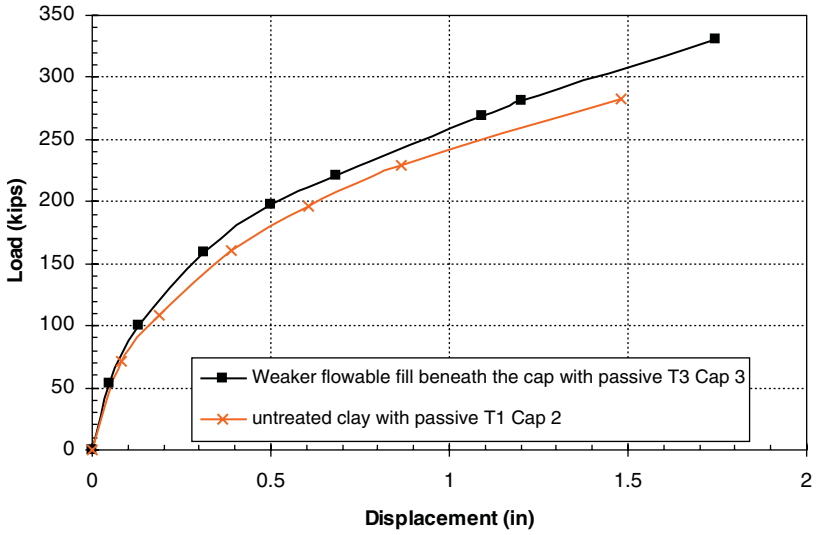

Figure 3-32. Load vs displacement results comparing Test 3 on Cap 3 (weak flowable fill below the cap) to Test 1 on Cap 2 (untreated clay).

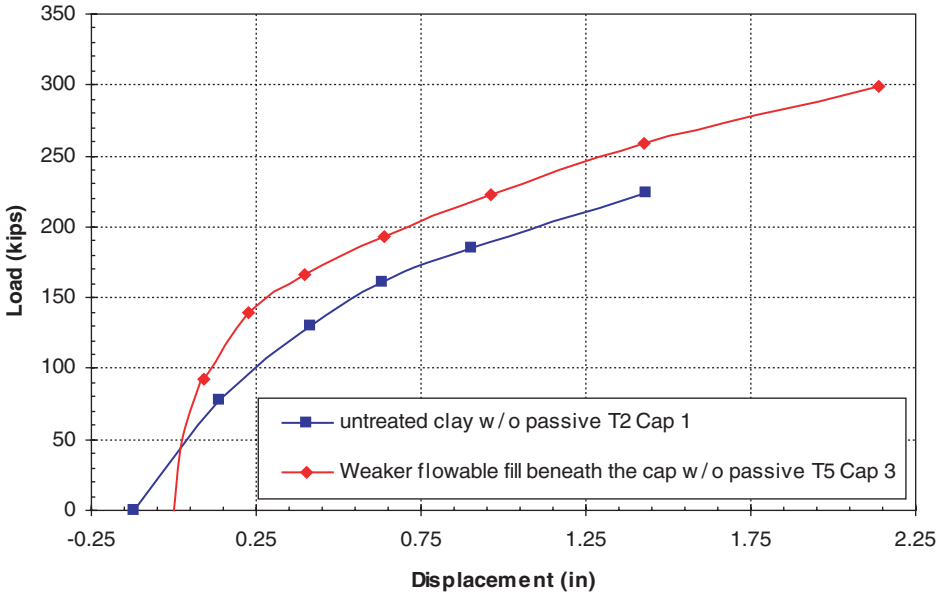

Figure 3-33. Load vs displacement curves for Test 5 on Cap 3 (weak flowable fill below the cap excavated to base of cap) to Test 2 on Cap 1 (untreated clay excavated to base of cap).

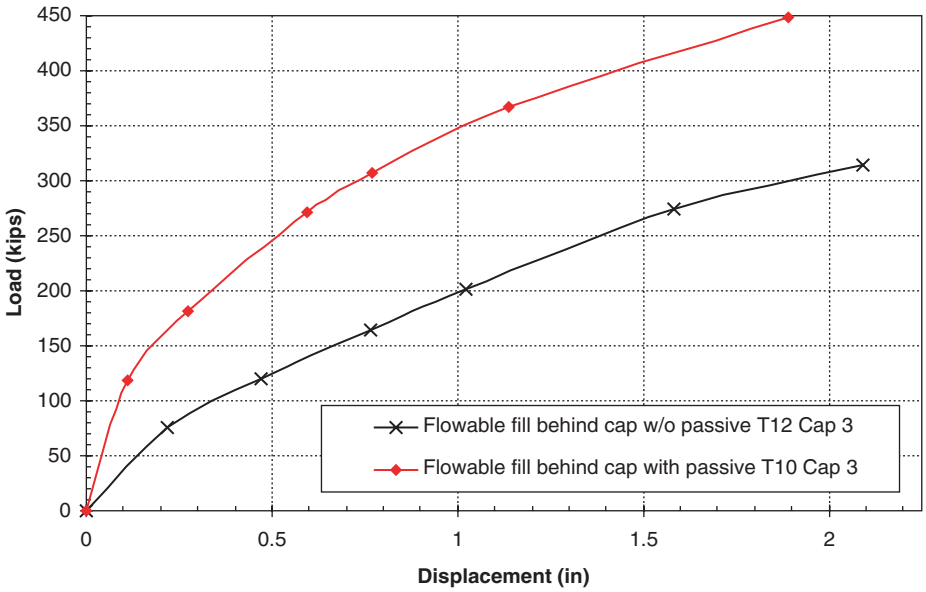

Figure 3-34. Load vs displacement results comparing Tests 12 and 10.

pile group were designed to determine the increased strength that could be provided by excavating the soft clay and replacing it with compacted sand. Prior to pile driving, clay was excavated to a depth of 6.25 ft and replaced with compacted fill up to the base of the pile cap. Clean concrete sand, meeting ASTM C-33 specifications, was used as the backfill material. The sand was compacted in 6- to 8-in. lifts using a hydraulic plate compactor attached to the end of a trackhoe. Based on nuclear density measurements, the sand was compacted to an average in-place dry density of 104.2 lb/ft^3, which is 93.7% of the modified Proctor density ($\gamma_{d\,max}$ = 111 lbs/ft^3). Plans originally called for excavation and replacement to greater depth; however, caving of the soft clay precluded deeper excavation. When the piles were installed, the ground heaved and, in order to maintain the correct pile cap thickness, approximately 0.75 ft of backfill had to be removed, leaving approximately 3 ft of sand under the cap. The sand fill extended 5 ft beyond the cap face on one side to evaluate the increased pile-soil resistance from extending the

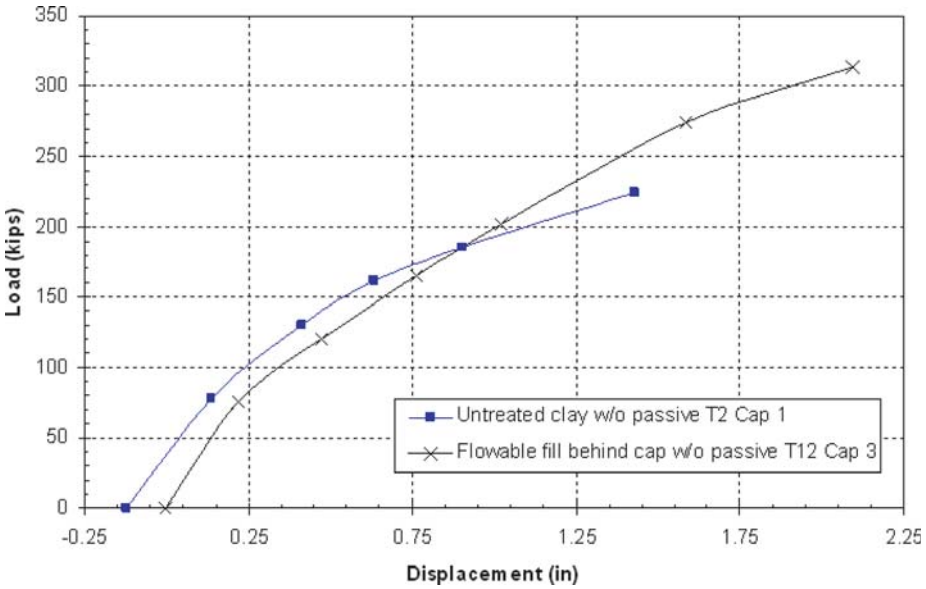

Figure 3-35. Load vs displacement results comparing Test 2 on Cap 1 to Test 12 on Cap 3.

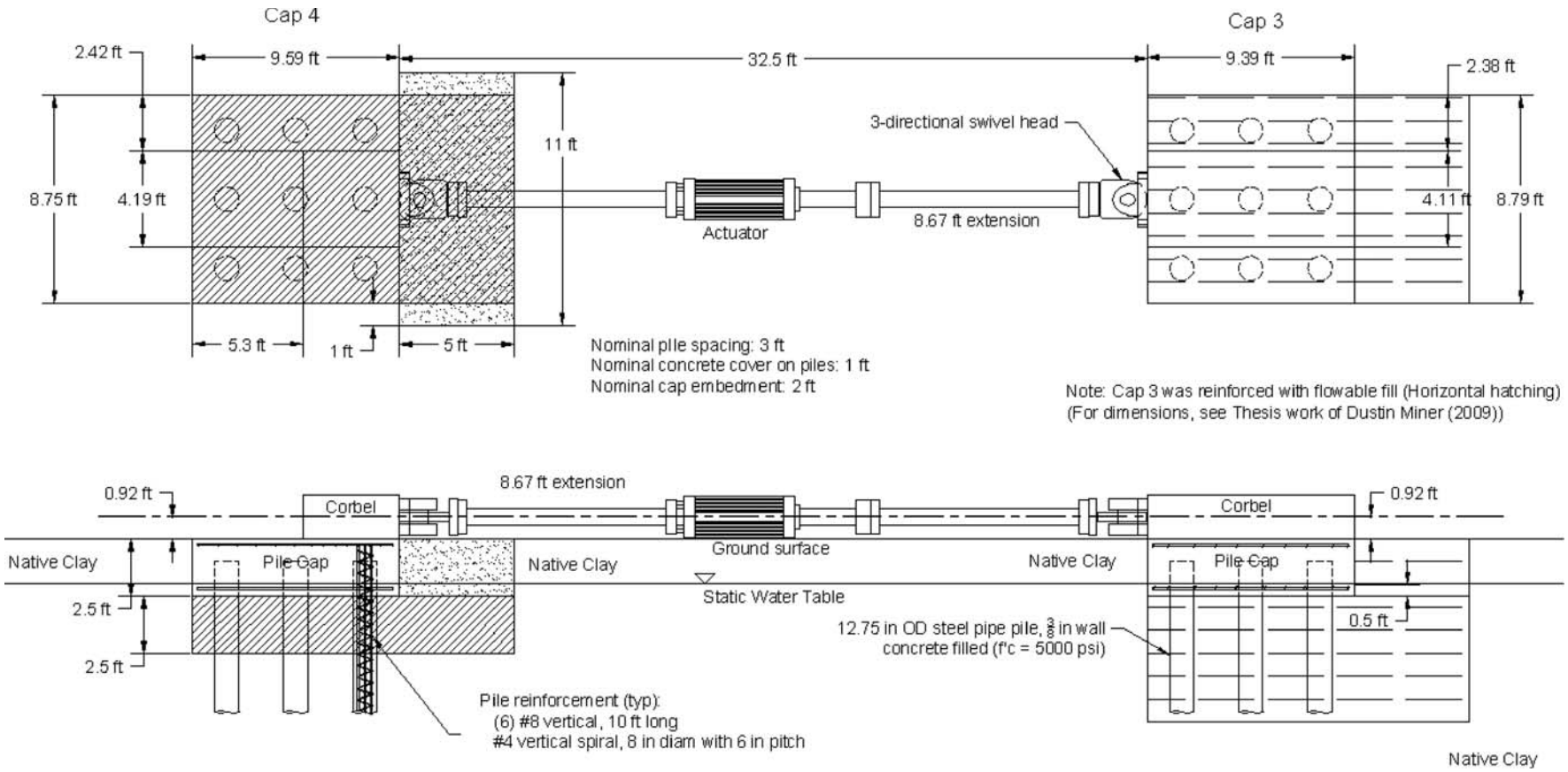

Figure 3-36. Plan and profile views of Pile Caps 3 and 4 after excavation and replacement with compacted fill around Pile Cap 4 and placement of flowable fill under Pile Cap 3.

sand fill. Lateral load tests were performed in both directions. Comparison with the pile caps in Tests 1 and 2 allow a determination of the increased resistance for sand fill.

Test Results for Compacted Fill

A comparison of the load-displacement curves for Tests 1 and 5 is provided in Figure 3-37. Test 1 involves the pile cap in untreated clay; compacted sand was placed directly below the pile cap for Test 5. The comparison shows an increase in lateral resistance of about 23 kips at a displacement of 1.5 in. resulting from placing compacted fill directly below the pile cap. This represents an 8% increase in resistance relative to the total resistance from soil-pile interaction and passive force or a 10% increase in resistance relative to soil-pile resistance alone.

Figure 3-38 provides a comparison of the load-displacement curves for Test 3 relative to Test 2. In contrast with Test 5 where the compacted fill stopped at the end of the pile cap, the compacted fill extends 5 ft beyond the end of the cap for Test 3. For both Tests 2 and 3 the soil adjacent to the pile cap was excavated so no passive resistance was present in either test. A comparison of the two curves indicates that the compacted fill increased the lateral soil-pile resistance by about 40 kips. As expected, extending the compacted fill 5 ft beyond the cap increased the lateral resistance; however, the increase was relatively small. The increased resistance represents an increase of 18% relative to a comparable pile group in untreated clay. This increase in lateral resistance can only be attributed to increased soil-pile resistance because there was no soil adjacent to the pile cap. The increase of 18% is comparable to results reported by Brown et al. (1986, 1987) when a stiff clay was replaced with compacted sand at a relative density of 50%.

Greater improvement could potentially have been achieved if the compacted fill could have extended deeper; however, this would have required flatter excavation slopes to prevent caving and more backfill material, which would increase the cost. Finite element studies conducted by Weaver and Chitoori (2007) suggest that most of the benefit from compacted fill around a pile occurs for fill materials extending five pile diameters below the ground surface based on FEM analysis. In this case, the fill extended about three pile diameters.

Figure 3-39 provides a comparison of the load-displacement curves for Test 3 and Test 4. The only difference between the two tests is that for Test 4 sand was compacted adjacent to the pile cap extending 5 ft beyond the cap. Therefore, the difference between the two tests represents the passive force that the 5-ft wide and 2.5-ft thick layer of sand produced. A comparison between the load-displacement curves for Tests 3 and 4 at the greatest displacements indicates that the ultimate passive force with the sand backfill was approximately 32 kips. This passive force is actually less than the 50-kip passive force measured when the native clay was left in place adjacent to the pile cap face in Test 1, as discussed previously. This decrease in passive force occurs because the native clay in the upper 2.5 ft of the profile is desiccated and relatively strong. However, if the clay in the upper 2.5 ft of the profile were softer, excavation and replacement with compacted sand could have increased the passive force. For example, if the clay surface layer had an undrained shear strength of only 500 psf, the passive force in the clay would only have been about 25 kips.

Rammed Aggregate Pier Construction

Rammed aggregate piers (RAPs) are a shallow alternative to deep foundations. They create a dense gravel column that

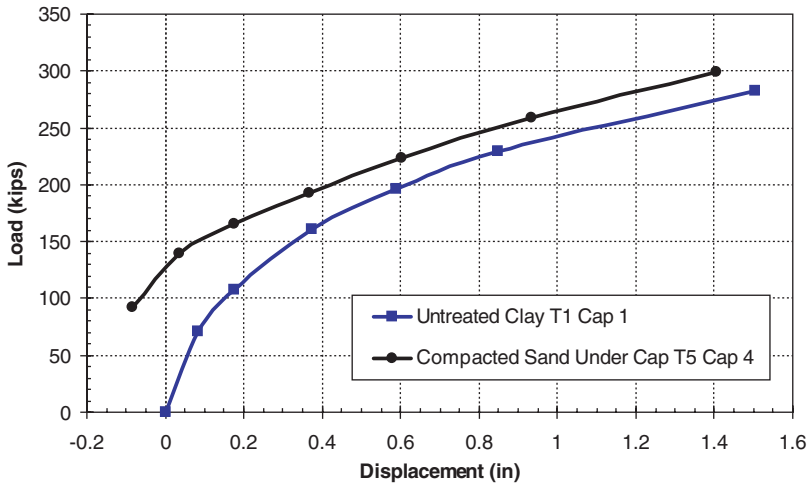

Figure 3-37. Load displacement comparison of Test 1 with Test 5 (shifted to the right 0.4 in.).

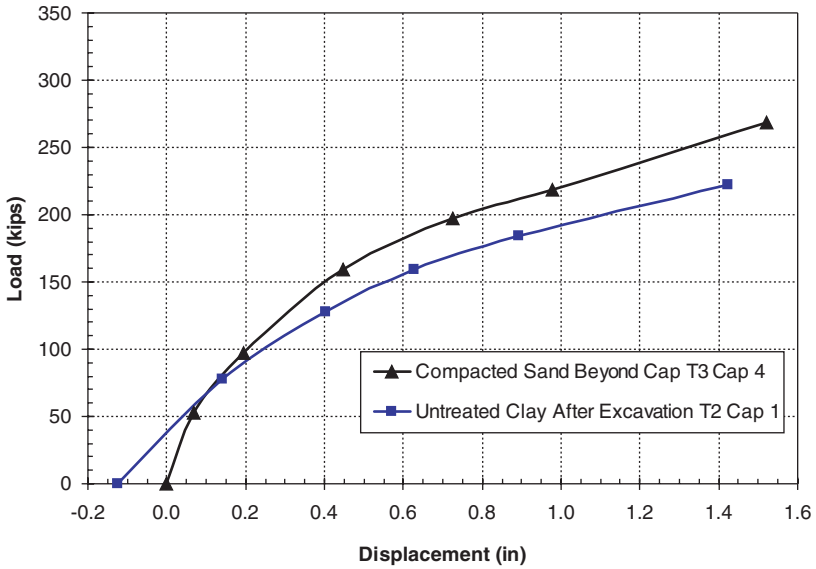

Figure 3-38. Comparison of load-displacement curves for Pile Cap 4 with compacted sand extending 5 ft beyond the cap and Pile Cap 1 in native clay without soil adjacent to cap.

reinforces the surrounding soil. In addition, they increase the normal stress in the surrounding soil and compact the surrounding soil if it is cohesionless. When testing was complete on the compacted fill, 30-in. diameter geopiers were installed in a grid pattern south of Pile Cap 4. Plan and profile drawings are shown in Figure 3-40. The RAPs were spaced at 36 in. center to center (c-c) in the direction of loading and 40 in. c-c in the direction transverse to loading. The 13-pier configuration consisted of 4 piers next to the cap, 5 piers in the middle row, and 4 piers in the row farthest from the cap. The row farthest from the cap was installed first and the row closest to the cap was installed last. Each column extended to a depth of 12.5 ft below the top of the pile cap. Dynamic cone penetration tests were performed on three of the columns and penetration resistance exceeded 40 blows per 1.75-in.

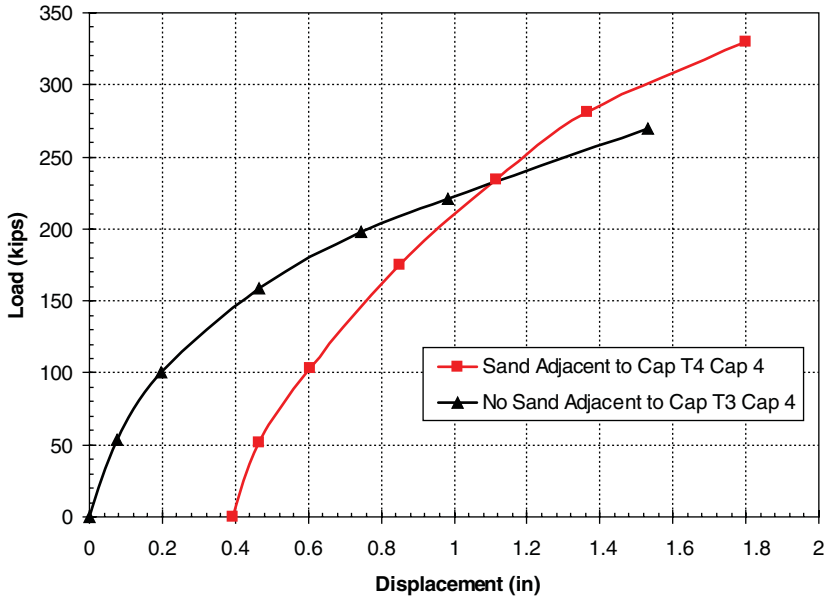

Figure 3-39. Comparison of load-displacement curves for Pile Cap 4 with and without sand adjacent to the pile cap.

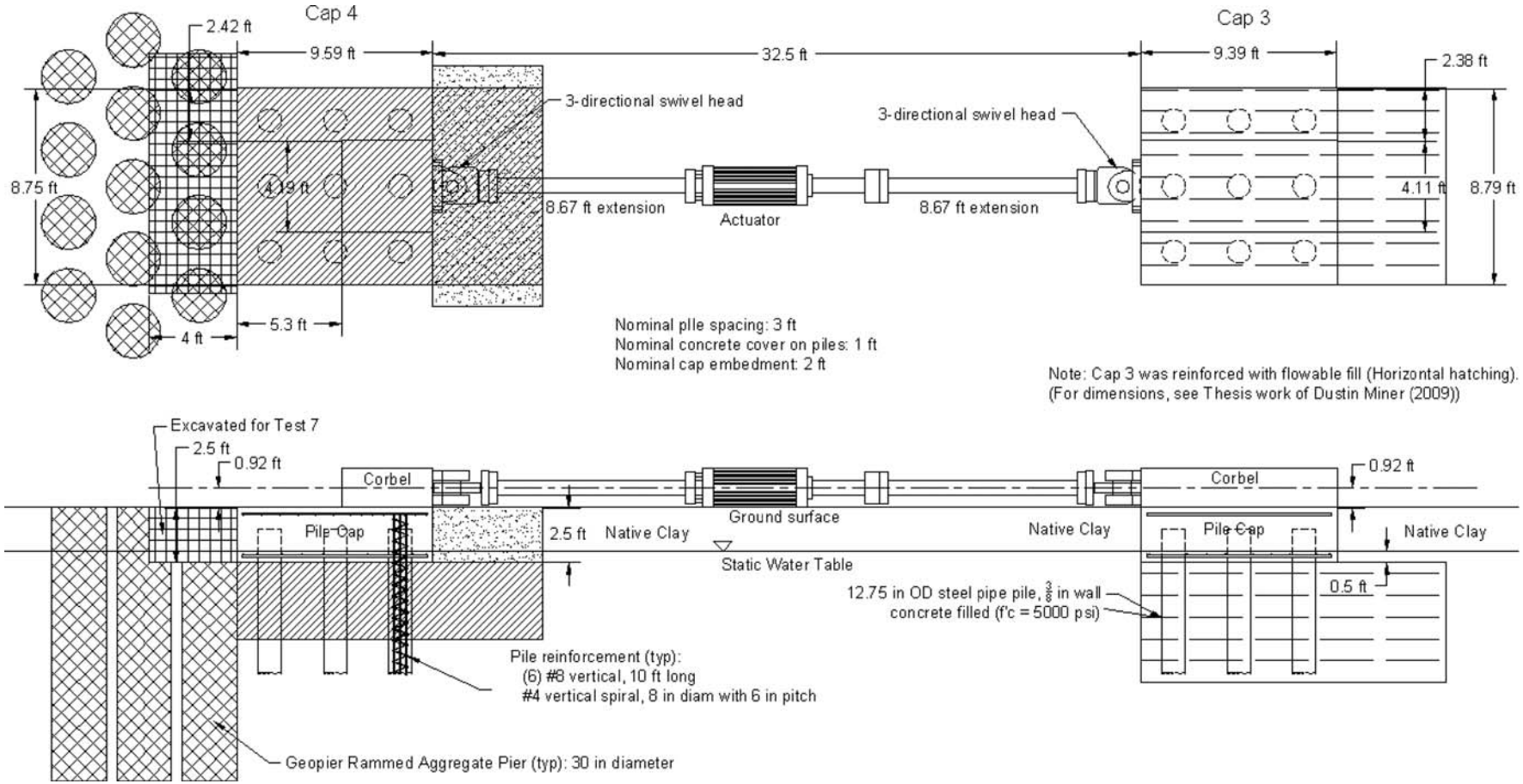

Figure 3-40. Plan and profile view of Pile Cap 4 showing the locations of the rammed aggregate piers and location of excavated zone for subsequent test.

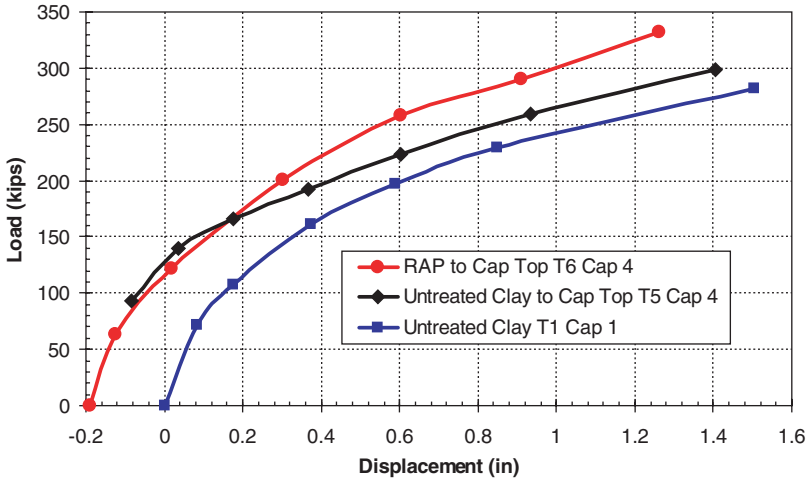

Figure 3-41. Comparison of load-displacement curves for Pile Cap 4 with RAP extending to the top of the cap relative to tests on Cap 4 without RAP columns and Cap 1 in untreated native clay.

RAPs are a relatively inexpensive means of retrofitting a pile cap, but they are not designed specifically to increase lateral resistance. Nevertheless, comparison tests were performed to explore the potential for increasing lateral resistance using this approach.

Test Results for Rammed Aggregate Piers

Figure 3-41 provides a comparison of the lateral load-displacement curves for Cap 4 after treatment with RAP columns (Test 6) in comparison with the same cap without the columns (Test 5). At a displacement of about 1.3 in., the addition of the RAP columns increased the total lateral resistance by about 40 kips. This represents an increase of about 15% relative to the cap without the RAP columns. Figure 3-42 plots the load-displacement curves for Cap 4 after treatment with RAP columns before (Test 6) and after excavation (Test 7) of the soil adjacent to the pile cap. Because of reloading effects, the curves for Test 7 at small displacements are not particularly meaningful; however, at larger displacements they appear to be reasonable based on comparison with similar tests. The difference between the curves for Tests 6 and 7 would represent the

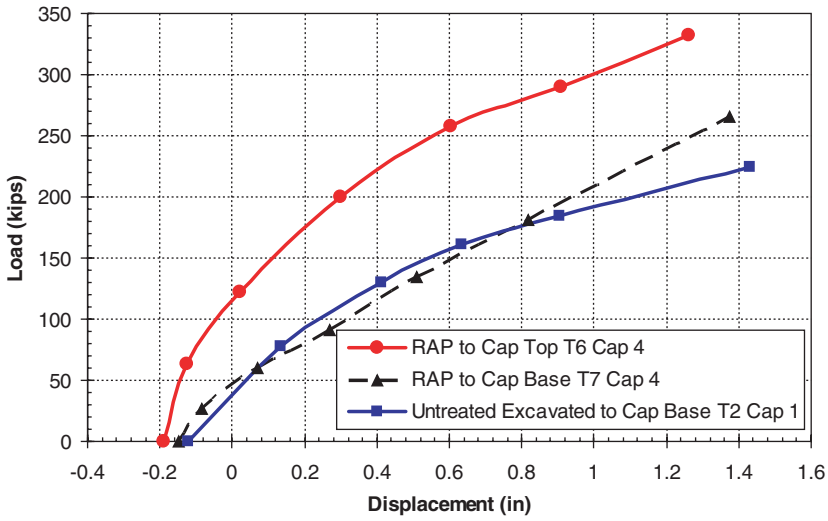

Figure 3-42. Comparison of load-displacement curves for Pile Cap 4 after RAP treatment with and without soil adjacent to the pile cap.

passive force contributed by the clay with RAP columns. At a displacement of 1.25 in., the interpreted passive force is about 85 kips. This is about 35 kips higher than the passive force (50 kips) obtained when clay alone was acting against the pile cap. This result indicates that nearly all of the increased resistance provided by the RAP columns was a result of increased passive force against the pile cap and only about 10% of the increase was a result of increased soil-pile resistance below the pile cap. This result seems consistent based on the results of previous soil improvement tests in which little improvement in lateral pile resistance was achieved unless the soil improvement extended to the face of the piles. The increase of 35 kips in the passive force alone represents an increase of about 70% relative to the passive resistance provided by the clay alone.

To produce a more readable report, additional plots, similar to those presented for the pile group in virgin clay are not presented here but are available in Lemme (2010, Appendix 4).

3.11 Summary of Increased Resistance from Soil Improvement Methods and Cost Considerations

A summary of the geometries of the various soil improvement techniques and the increase in lateral resistance that they produced is provided in Table 3-4. The greatest increase in lateral load (400 to 500 kips) was produced by the jet grouting method. Soil mixing and flowable fill also produced significant increases in lateral resistance (140 to 170 kips). Excavation and replacement techniques produced a relatively small increase in lateral resistance (20 to 40 kips).

It should be noted that the treatments producing the greatest improvement were typically those that involved the larger volumes of treated soil and the greatest cost to implement; however, this is not always the case. To provide some indication of the cost effectiveness of the various treatment methods relative to driving more piles, some simplified cost estimates were produced for the various approaches. A complete cost assessment is beyond the scope of this investigation and would be dependent on a number of factors that would vary from location to location. In addition, the geometries could potentially be further optimized to produce greater resistance relative to the geometries used in the field tests. Furthermore, it may be possible to reduce the cost of ground improvement obtained by jet grouting by using lower strength mixes or by using more economical approaches such as soil mixing, as will be investigated subsequently. Nevertheless, this simple comparison provides a first estimate of the economic viability of the ground improvement approaches for increasing lateral pile group resistance.

One common alternative to soil improvement would be to simply add more piles and increase the size of the pile cap. According to the test results for Cap 1 during Test 2, the maximum lateral load resisted by the nine-pile group was about 230 kips. Assuming this load is distributed evenly, each pile would have carried about 26 kips. Therefore, to obtain the same lateral resistance of 500 kips that was achieved through jet grouting beneath the pile cap, 20 piles would have to be added. Similar calculations have been made for each improvement approach. The cost of the additional piles, neglecting mobilization costs, were estimated by assuming a typical pile length of 80 ft, pipe pile costs of $30/ft, and driving costs of $12/ft. In addition, the cost of concrete fill and reinforcing steel cages in the piles was estimated assuming $150/cubic yard of concrete. Finally, adding more piles will require an increase in the size of the pile cap and an estimate of this cost also was made for each case assuming 3-ft center-to-center pile spacing.

The cost of jet grouting was estimated to be roughly $475 per cubic yard for the 20% by weight cement content used in this study. Mobilization costs are highly variable and were not included in the cost because mobilization costs also were excluded from the pile driving costs. Soil mixing was assumed

Table 3-4. Summary of treatment geometries and increased resistance provided by the various soil improvement methods.

Treatment Method	Treatment Dimensions (LxWxD)	Treatment Volume (cu. Yds.)	Untreated Resistance (kips)	Increase in Resistance (kips)	Percent Increase in Resistance	Comments
Jet Grouting Below Cap	15'x10.5'x10'	58.3	282	500	160	
Jet Grouting Adjacent to Cap	6.6'x13'x12'	38.1	214	398	185	
Soil Mixing Adjacent to Cap	4'x11'x10'	16.3	282	170	60	
Weak Flowable Fill Below Cap	13.5'x8.8'x6'	26.4	232	24	10	
Flowable Fill Adjacent to Cap	6'x12'x6'	16.0	265	145	55	
Compacted Fill to Edge of Cap	9.6'x8.75'x3.5'	10.9	232	23	10	
Compacted Fill 5 ft beyond Edge of Cap	14.6'x8.75'x3.5'	16.6	232	40	18	
Rammed Aggregate Piers Adjacent to Cap Top	13-2.5' dia x 13' deep	29.5	285	40	14	
Rammed Aggregate Piers Adjacent to Cap Top	13-2.5' dia x 10.5' deep	23.6	50	35	70	1

Note 1: Increase in resistance is for passive resistance only

Table 3-5. Summary of increased resistance provided by the various soil improvement methods along with cost savings relative to providing additional piles.

Treatment Method	Increase in Resistance (kips)	Equivalent Number of Pipe Piles	Add'l Pile/Cap Cost	Ground Improvement Cost	Savings Relative to Piles	Percent Savings	Ground Improvement Cost/kip	Comments
Jet Grouting Below Cap	500	20	$84,200	$28,500	$55,700	66	$57	
Jet Grouting Adjacent to Cap	398	16	$69,360	$38,000	$31,360	45	$95	1
Soil Mixing Adjacent to Cap	170	7	$30,345	$10,000	$20,345	67	$59	1
Weak Flowable Fill Below Cap	24	1	$4,335	$3,180	$1,155	27	$133	
Flowable Fill Adjacent to Cap	145	6	$26,010	$3,600	$22,410	86	$25	1
Compacted Fill to Edge of Cap	23	1	$4,335	$544	$3,791	87	$24	
Compacted Fill 5 ft beyond Edge of Cap	40	2	$8,670	$828	$7,842	90	$21	
Rammed Aggregate Piers Adjacent to Cap Top	40	2	$8,670	$4,225	$4,445	51	$106	
Rammed Aggregate Piers Adjacent to Cap Top	35	2	$8,670	$4,225	$4,445	51	$121	2

Note 1: Cost of soil improvement doubled to account for increased resistance in opposite direction
Note 2: Increase in resistance is for passive resistance only
Note 3: Cost/kip for pile/pile cap = $182/kip

to cost about $300 per cubic yard for the 10% by weight cement content, and flowable fill was assumed to cost $75 per cubic yard in addition to excavation costs. For the treatments adjacent to the pile cap, the cost was doubled assuming that a similar improvement zone would be required on the opposite side to account for load in the opposite direction.

The excavation and replacement cost was assumed to be $50 per cubic yard for the small volumes involved and the cost of RAPs was assumed to be $50 per ft of length. The estimates of improvement costs associated with each treatment method are shown in Table 3-5. In addition, the cost savings associated with soil improvement compared to providing additional piles is listed for each case along with the percent savings relative to additional piles. In all cases, the ground improvement method provided cost savings, although in some cases, the cost savings are small, as is the increase in resistance. This is particularly true for the excavation and replacement approaches. Finally, the cost per kip of increased lateral resistance was computed for each case to provide another indication of the cost-effectiveness of the various approaches. For comparison purposes, the cost per kip for the pipe pile alternative was $182/kip. All of the ground improvement methods had lower costs per kips than that for the piles. The lowest cost per kips was provided by the excavation and replacement method because of the low cost of the treatment method. However, it must be recognized that despite the low cost per kip for this treatment method, the potential for increasing resistance also was quite limited.

CHAPTER 4

Finite Element Modeling of Single Pile Load Test

The soils in the field are all clays typically classified as CL or CH according to the borehole log shown in Figure 3-3(a). The soil is modeled up to a depth of 45 ft. The soil was divided into 13 layers. The top 9 layers are all 2.5 ft thick, the next 3 layers are 5 ft thick, and the last layer is 7.5 ft thick, as shown in Table 4-1.

Since all of these 13 soil layers are primarily clays, the soils are modeled with a von Mises model without hardening. A total of 13 sets of material parameters for von Mises type elastoplasticity were estimated from the lab or in-situ tests. In the finite element model, the elastic Young's moduli and compression strengths are needed. The elastic Young's moduli can be estimated from the following relationships:

$$G = r_d \frac{\gamma}{g} v_s^2 \tag{6}$$

$$E = 2(1+\nu)G \tag{7}$$

where

G is the shear modulus;
v_s is the shear wave velocity measured from the downhole seismic cone testing;
γ is the total soil unit weight that can be estimated by averaging from the lab data along the depth;
g is the gravity constant;
r_d is a reduction factor that accounts for the large deformation effect and remolding effect, here a value of 0.25;
E is the Young's modulus in the elastic part of the von Mises model; and
The Poisson's ratio, v, is assumed as 0.45 due to the nearly undrained condition of the clay during the tests.

The yield strength in the von Mises yield function is twice the measured undrained strength, as follows:

$$k = 2s_u \tag{8}$$

The simplified distributions of shear wave velocity and undrained shear strength based on the test data are plotted in Figures 4-1 and 4-2, respectively.

The total length of the pile is 46.5 ft and the pile toe depth is 45 ft in the soil. The pile is modeled as a 1-D linear elastic beam-column element. For the steel pipe pile with concrete fill, the composite EI is required. The pile EI is calculated as 1.41×10^7 kip-in^2, using a compressive strength of 5150 psi based on compression tests on concrete cylinders at the time of testing. The steel cross-sectional area is computed based on an outside diameter of 12.75 in. and a 0.375-in. wall thickness. Young's modulus for the pile is 29,000 ksi and the Poisson's ratio is 0.20.

Since the 1-D beam-column element has no physical dimension in the cross-sectional plain, special measures were taken to include the diameter effects of the pile by connecting the soil nodes with pile nodes using radially rigid "spokes," which also are modeled by a very stiff elastic beam-column element.

Non-extension spring elements link the outer ends of the spokes and the soil nodes to model the gapping between the pile and the soil. The compression stiffness of these spring elements is very large but the extension stiffness is zero. To avoid possible numerical instability, a very small extension stiffness value is used in the finite element model.

The soil was modeled as 3456 3-D solid element accounting for large deformation and large strain effects. The pile was modeled using 36 1-D elastic beam elements. The pile and the surrounding soil were linked by 468 non-extension spring elements. A total of 4,717 nodes were in the FEM mesh, which is shown in Figure 4-3. The nodes on the outside surface of the cylinder are restrained against horizontal movements. The nodes on the bottom surface are restrained against movement in any directions. The movements of the nodes in the middle plane are restricted to embody the load and geometry symmetry.

A displacement control method is used for this problem. The node on the pile top is selected for the displacement

Table 4-1. Model parameters used for FEM model.

Layer #	Top Depth (Ft)	Bottom Depth (Ft)	Thickness (Ft)	Su (psf)	Vs (Fps)
1	0.0	2.5	2.5	950	416
2	2.5	5.0	2.5	325	389
3	5.0	7.5	2.5	350	357
4	7.5	10.0	2.5	400	338
5	10.0	12.5	2.5	450	355
6	12.5	15.0	2.5	500	425
7	15.0	17.5	2.5	525	495
8	17.5	20.0	2.5	550	565
9	20.0	22.5	2.5	600	550
10	22.5	27.5	5.0	655	500
11	27.5	32.5	5.0	750	500
12	32.5	37.5	5.0	845	500
13	37.5	45.0	7.5	940	500

Notes: Su is undrained shear strength; Vs is shear wave velocity; and Fps is feet per second.

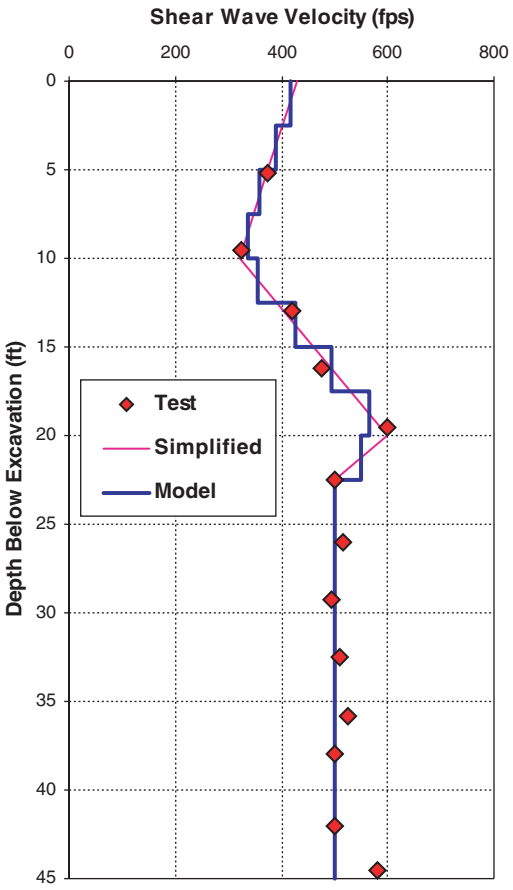

Figure 4-1. Tested, simplified, and model shear wave velocity distribution.

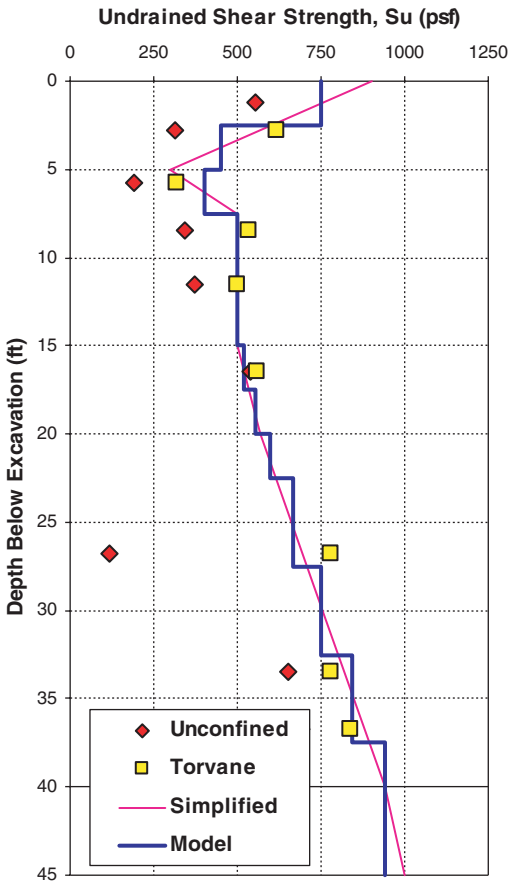

Figure 4-2. Tested, simplified, and model undrained shear strength distribution.

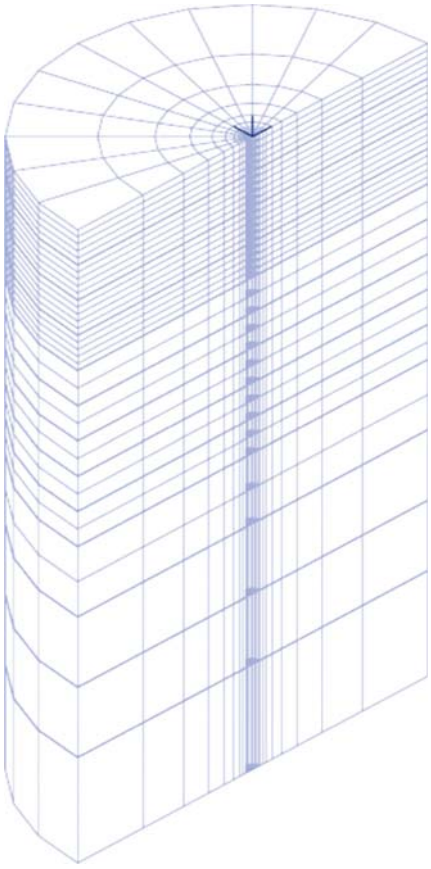

Figure 4-3. FEM mesh used for analysis of single pile lateral load test.

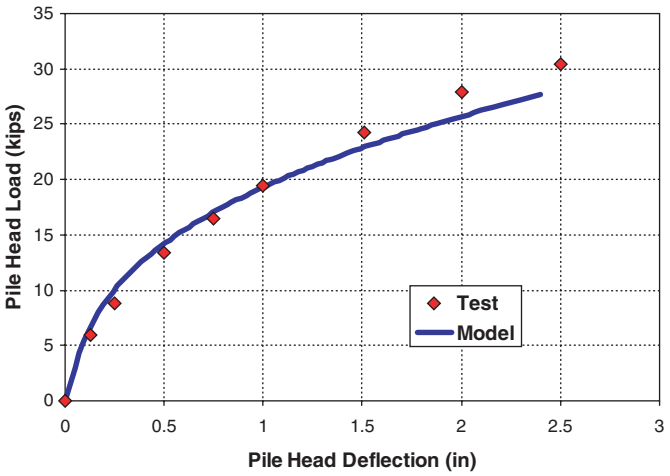

Figure 4-4. Simulated and tested data on pile head load vs pile head displacement.

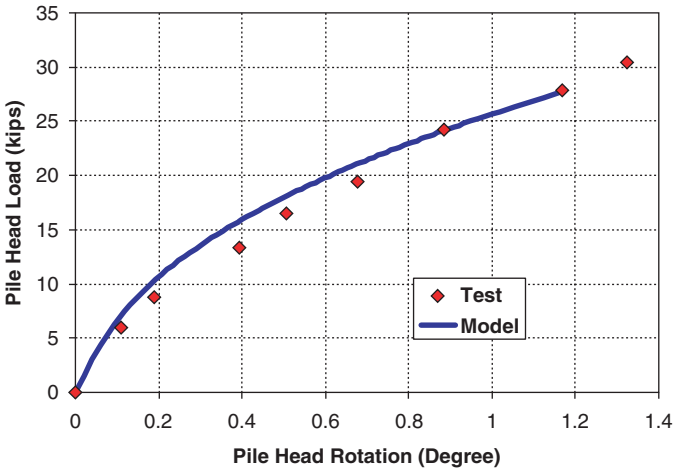

Figure 4-5. Simulated and tested data on pile head load vs pile head rotation.

control, which is laterally pushed up to 2.5 in. The pile head is considered to be a free-head boundary with no rotational constraint. The static loading step number is 50 with pile head lateral displacement of 0.05 in. per loading step.

The simulated pile head load versus pile head displacement and pile rotation are shown in Figures 4-4 and 4-5, respectively. The loads have been doubled to account for symmetry. The curves exhibit the conventional hyperbolic shape that would be expected for soft clay and are in good agreement with the test data. This suggests that the single pile in clay under lateral loading can be satisfactorily simulated using the simple von Mises soil model with the above-mentioned parameters. The calibrated parameters for the soil and pile will be used for the later pile group analysis.

CHAPTER 5

Finite Element Modeling of Pile Group Load Tests

5.1 Pile Group FEM Mesh Design

The FEM mesh design for the pile group simulation is tedious and time consuming. Since a considerable amount of parametric study will be conducted, making a specific FEM mesh for each case is not reasonable. Our strategy was to make a general mesh that reserves the same element groups for soil improvements. A MATLAB program was coded for this purpose. The mesh schematic is shown in Figure 5-1. According to geometrical symmetry, only one-half of the domain was considered. The soil block is of 54 ft in. length (31.5 ft in the lateral load direction and 22.5 ft in the direction opposite to the lateral load direction), 22.5 ft width (half of the whole soil block) and 45 ft depth. The pile cap side is 9 ft square with a depth of 2.5 ft. The pile caps were constructed by excavating 2.5 ft into the virgin clay. In the tests, a corbel was constructed on each cap to allow the actuator to apply load above the ground surface without affecting the soil around the pile cap. The corbel extended the full length of the pile cap for Cap 2 but was only about half of the pile length in Cap 1. The load was 0.92 ft above the cap surface. In the FEM model, the 0.92 ft corbel was added to the cap thickness and the load was considered to be applied on the surface middle of the cap with 3.42 (2.5 + 0.92) ft thickness. Considering symmetry, the cap length, width and depth dimension are $9 \times 4.5 \times 3.42$ ft in the half FEM mesh shown in Figure 5-1.

The soil improvement zones in the FEM model are located below the cap and on one side of the cap and can extend to a depth of 12.5 ft. The model can accommodate a combination of soil improvement below and beside the cap. The soil improvement zone is fixed at a width of 4.5 ft, which is the same as the width of the cap. However, the length of the soil improvement zone is variable. The soil is also layered for different soil properties at different depths, as was the case for the FEM model for the single pile simulation. For tests of soil improvement, the material model of some zones can be changed from that of the virgin soil to that of the improved mass. This mesh design is advocated here for its generality and its convenience for parametric studies.

The basic mesh for pile group simulation is shown in Figure 5-2. For boundary settings, all nodes at $x = -22.5$ (left side surface of the model) and 31.5 ft (right side surface of the soil model) have a zero displacement constraint in the x direction; all nodes at $y = 0$ (symmetric plain of the soil block and toward side surface of the model) and 22.5 ft (the forward side surface of the model) have a zero displacement constraint in the y direction; all nodes $z = -45$ ft (the bottom surface) have a zero displacement constraint in the z direction.

Since the cap concrete is much stiffer in comparison with the clays, it will introduce little error to the load-displacement relationship to model the cap as linear elastic material with a relatively high Young's modulus. In our model, a typical concrete Young's modulus of 7.2×10^8 psf and a typical Poisson's ratio of 0.2 were used for the cap. The cap concrete was poured against vertical soil faces on the front and back sides of each pile cap. This construction procedure made it possible to evaluate passive force against the front and back faces of the pile caps. In contrast, plywood forms were used along the sides of each cap and were braced laterally against the adjacent soil face. This construction procedure created a gap between the cap sidewall and the soil so that side friction would be eliminated. In the FEM model, the front face of the cap is linked with the soil by non-extension springs while the nodes at the other face of the cap are modeled with different node numbers but with the same coordinates as the adjacent soil nodes.

Similar to the single pile model, the piles are modeled as 1-D elastic beam elements. The pile is connected with the soil nodes by radial rigid "spokes," which also are modeled by very stiff elastic beam elements. Non-extension spring elements link the outer ends of the spokes and the soil nodes to model the gapping between the pile and the soil. The compression stiffness of these spring elements is very large but the extension stiffness is zero. To avoid possible numerical instability, very small extension stiffness is alternatively input in the finite element model.

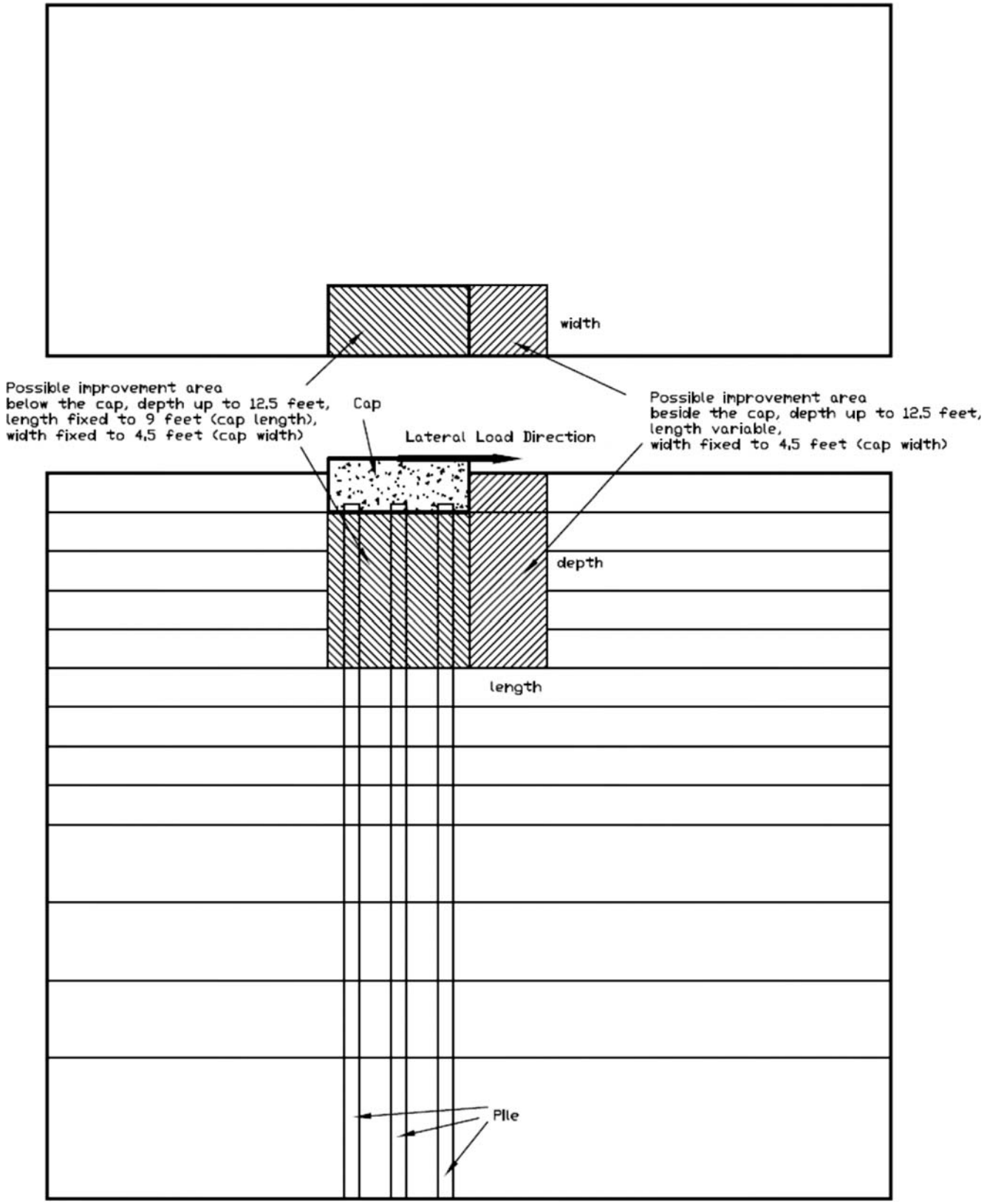

Figure 5-1. FEM profile for the pile group.

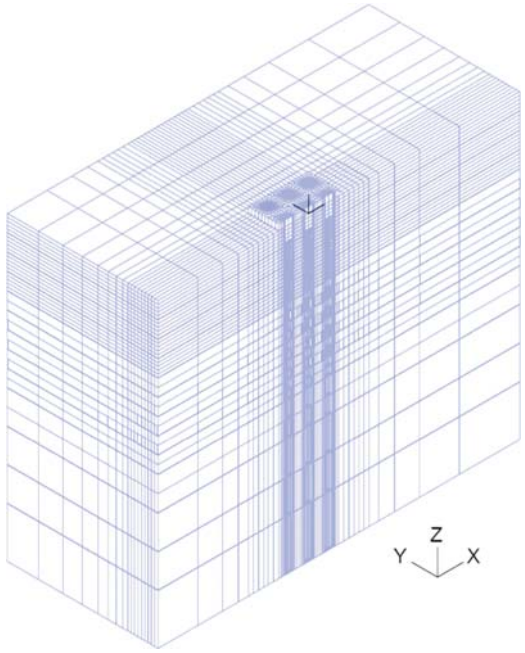

Figure 5-2. Finite element mesh for model of pile group in virgin soil.

The pile heads are extended into the cap base for 0.5 ft to account for the cap pinning effects on the pile head rotation.

5.2 FEM Model for Pile Group Model in Virgin Clay

The pile group in virgin clay provides the basic data for comparison with the pile group with soil improvements. The mesh used for the FEM pile group model in virgin soil is shown in Figure 5-2. A total of 50,247 nodes and 44,796 elements were in the FEM mesh. A displacement control method is used in analyzing the pile group test. The node on the pile top is selected for the displacement control, which is laterally pushed up to a maximum displacement of 1.5 in. The static displacement is applied in 50 steps with a pile head lateral displacement of 0.03 in. per loading step.

The load-displacement response curves computed by the FEM are plotted in Figure 5-3 in comparison with the measured curve. Generally, they exhibit good agreement with test data from both Cap 1 and 2 of Test 1. The load-rotation response curve computed by the FEM is plotted in Figure 5-4 and the results seem to plot between the test data Cap 1 and 2 of Test 1 at the beginning loading stage and thereafter tend to be close to test data of Cap 2 and has considerable discrepancy to the test data of Cap 1. However, the load rotation test data of Cap 1 was somewhat smaller than that of Cap 1; it was unclear whether this resulted from measurement errors or from the fact that the corbel on Cap 1 did not extend across the entire cap as did the corbel for Cap 2.

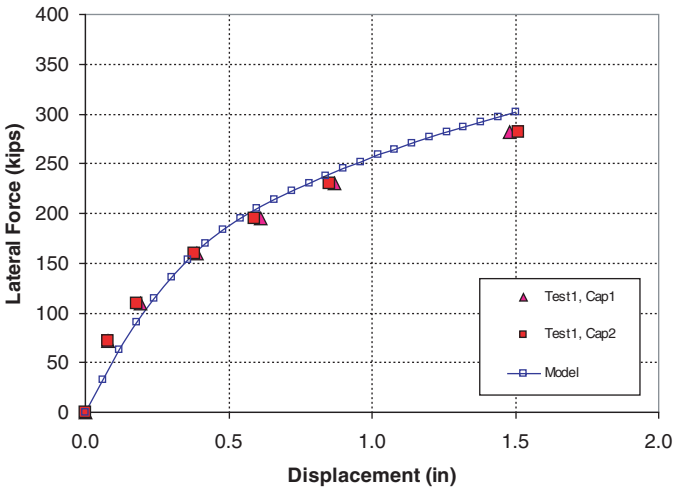

Figure 5-3. Simulated and tested displacement-load results for pile group in virgin clay.

It can be seen that the soil parameters calibrated from the single pile test in virgin clay appear to be appropriate to the pile group test. The FEM model of pile group in virgin clay can simulate the essential load-displacement response of the test.

5.3 Pile Group Model in Virgin Clay with Excavation

The pile group in virgin clay with excavation provides the estimation of the passive force by the unsaturated clay against the pile group. A similar mesh design strategy was followed for the FE model of pile group in virgin clay without excavation. Once again, a displacement control method was used for this problem. The node on the pile top was selected for the displacement control, which is laterally displaced to 1.5 in. The maximum displacement was produced using 50 loading

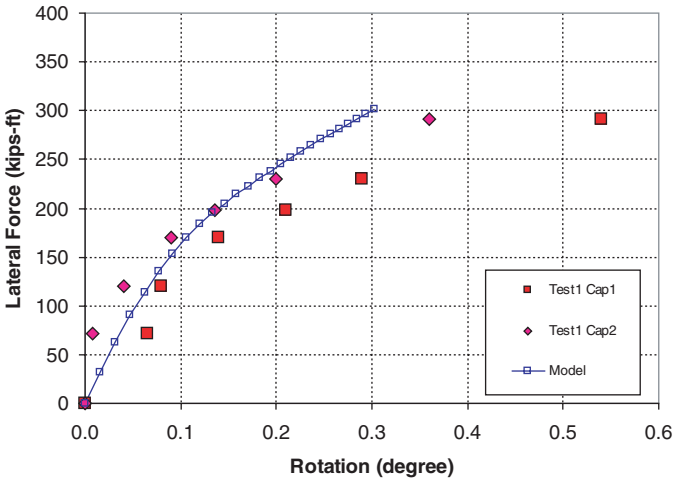

Figure 5-4. Simulated and tested load-rotation response curve results for pile group in virgin clay.

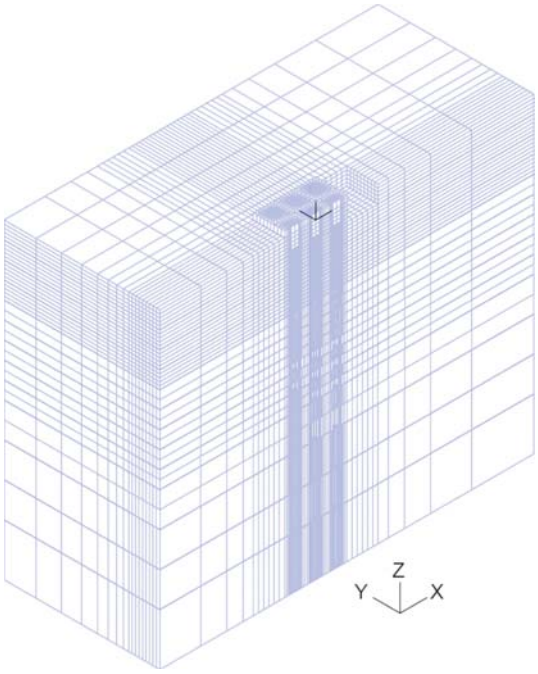

Figure 5-5. Finite element mesh for model of pile group with excavation adjacent to cap.

steps with pile head lateral displacement of 0.03 in. per loading step.

The mesh of the FEM pile group model in virgin soil with excavation adjacent to the cap is shown in Figure 5-5. A total of 49,977 nodes and 44,666 elements were in the FEM mesh. The load-displacement curves computed using the FEM model with and without excavation adjacent to the cap were used to produce the passive force-displacement curve. The passive force on the pile cap was obtained by subtracting the load with excavation from that without excavation. The simulated passive force-displacement curve is compared with the measured curve in Figure 5-6. The simulated force is greater than the measured force for displacements less than about 0.3 in., which is as expected for small displacement due to the residual displacement. However, the agreement is satisfactory for displacements more than 0.3 in.

5.4 FEM Model of Pile Group with Mass Mixing

The mass mixing treatment zone in the FEM model is shown in Figure 5-7. The modeled zone is 10 ft deep, 4 ft long in the direction of the lateral loading direction, and 11 ft wide transverse to the loading direction. These dimensions are the same as in the field test.

Six 3-in. diameter core samples were extracted and tested after 38 and 63 days of curing. The test results indicated an average strength of 131 psi after 38 days and an average strength of

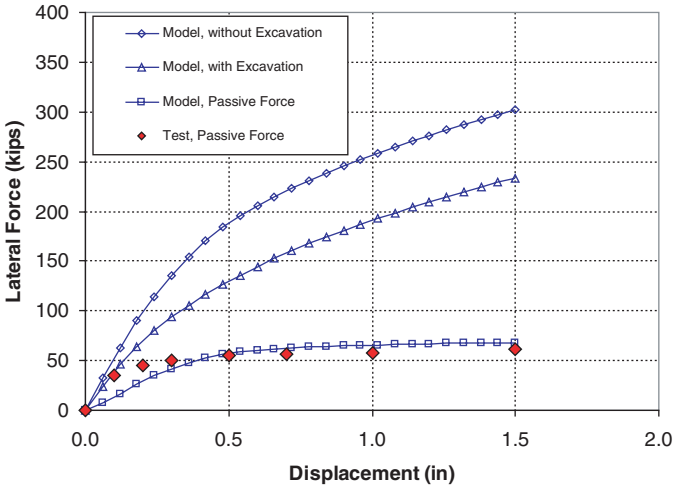

Figure 5-6. Simulated and tested pile cap passive pressure.

about 140 psi after 63 days with a standard deviation of about 8 psi. Assuming that the soil-cement mixture cured at the same rate as concrete alone, the compressive strength of the mixture at the time of testing would be approximately 126 psi.

Preliminary analyses suggested that the shear strength of the mass mixed wall was sufficient to allow the wall to behave essentially as a rigid block. Based on this conclusion and the fact that the mass mix has much higher strength than the clay, the mass mix is modeled as elastic material. This assumption will introduce little error to the pile load-displacement response against a more complicated material model for the mass mix. The Young's modulus of the mass mix zone is estimated as 6.4×10^5 psi from the compressive strength of the mixture at the time of testing (126 psi) with the assumption that the Young's modulus can be estimated with the same formula as that for concrete [$E = 57000(f'_c)^{0.5}$]. The Poisson's ratio of the mass mix is assumed to be 0.2.

A comparison of load-displacement curves from the test data and the FEM model is provided in Figure 5-8. The FEM model provides very good agreement with the measured results. These results indicate that the linear elastic material model with the material properties described previously can reasonably represent the lateral resistance of the pile group after treatment with mass mixing. Furthermore, this result provides confidence that additional parametric studies can be used as "virtual load tests" for the purpose of developing a simplified model.

5.5 Pile Group Model with Jet Grouting

Soil improvement using jet grouting was undertaken in Test 8. For Cap 1, improvement was limited to zones in the front and back sides of the pile cap, while for Cap 2 the improve-

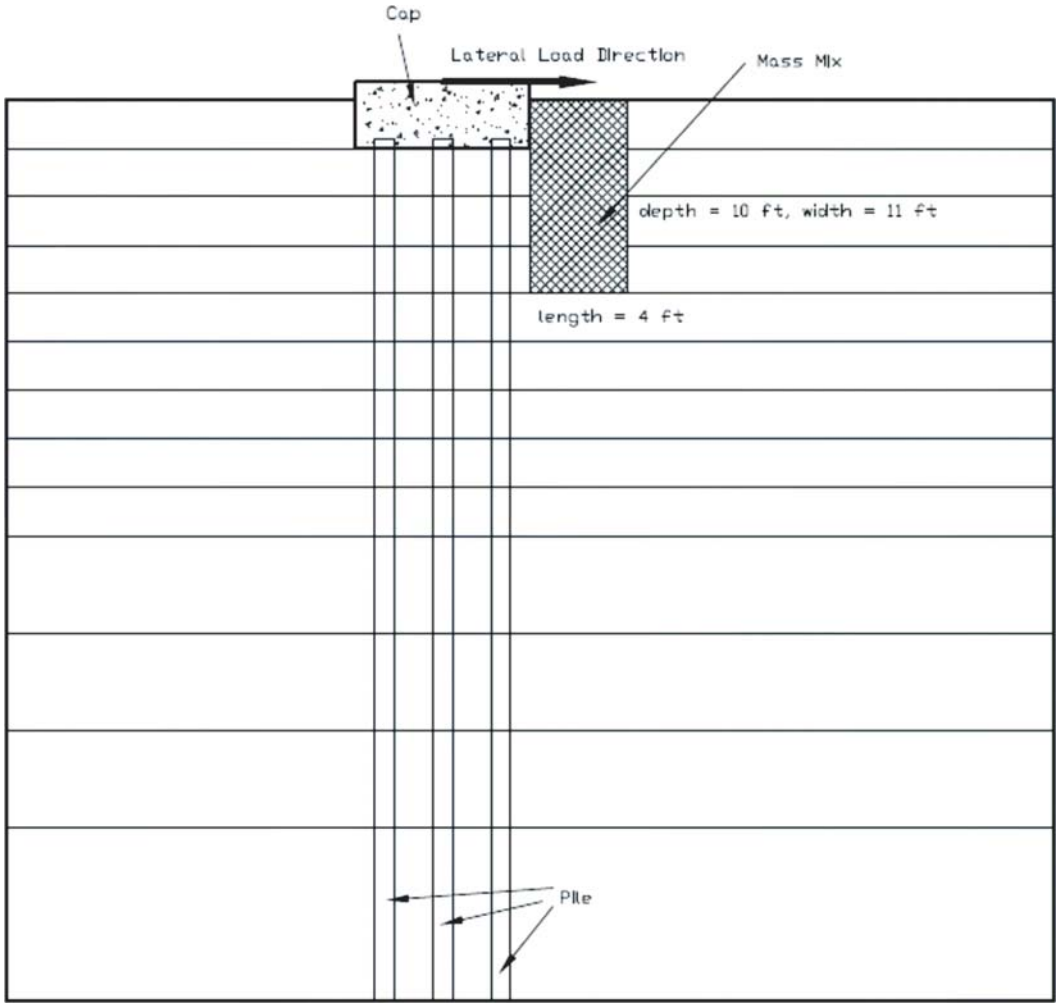

Figure 5-7. FEM model profile with mass mix treatment zone beside the cap—mass mix zone is 10 ft deep, 4 ft long, and 11 ft wide transverse to loading.

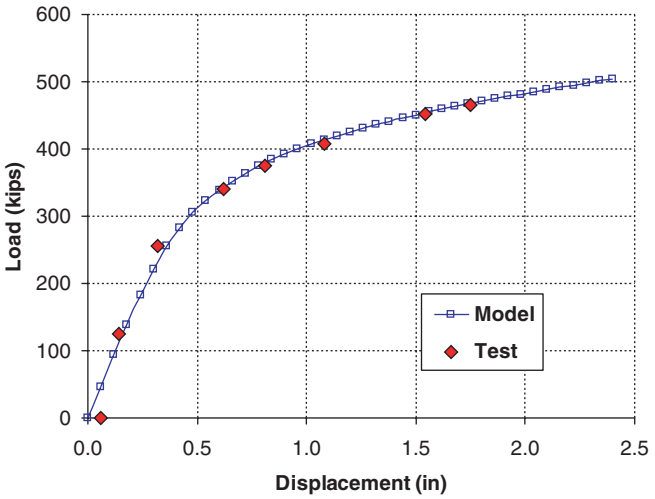

Figure 5-8. Comparison of load-displacement curves from FEM model and field test with mass mix zone adjacent to the pile cap.

ment extended underneath the entire pile cap as shown in Figure 5-9.

Figure 5-10 shows a schematic profile diagram of the FEM model with the jet grout treatment zone. The model shown in Figure 5-2 was used to model the pile with jet grout treatment after appropriate elements in the model were assigned the properties corresponding to the soilcrete. Analyses suggested that the shear strength of jet grouting soilcrete was sufficient to allow the soilcrete zone to behave as a rigid block. Based on this conclusion and the fact that the soilcrete has a much higher strength than the clay, the soilcrete was modeled as an elastic material. This assumption will introduce little error into the pile load-displacement response relative to a more complicated material model for jet grouting soilcrete. The Young's modulus of the soilcrete is estimated as 1.4×10^6 psi based on the compressive strength of the mixture at the time of testing, which would be approximately 600 psi. This modulus value is based on the assumption that the Young's

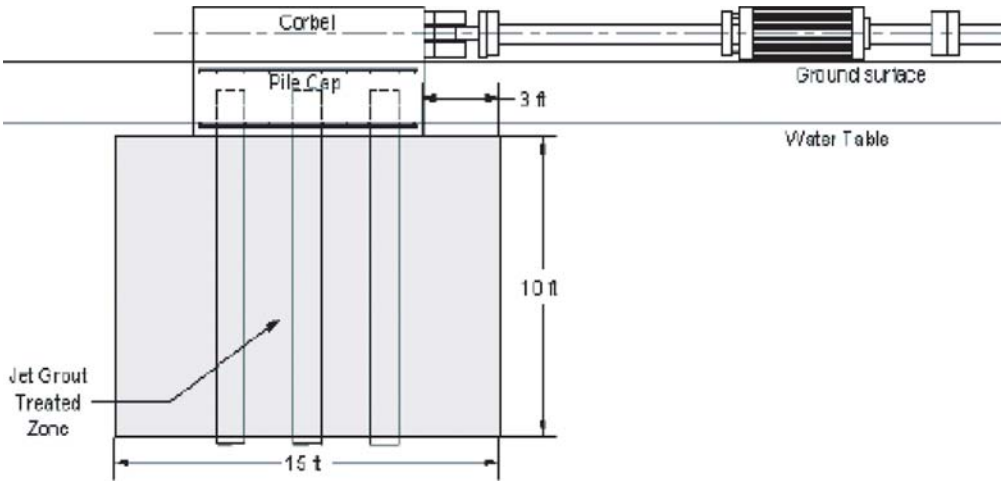

Figure 5-9. Layout of test using jet grouting under Cap 2.

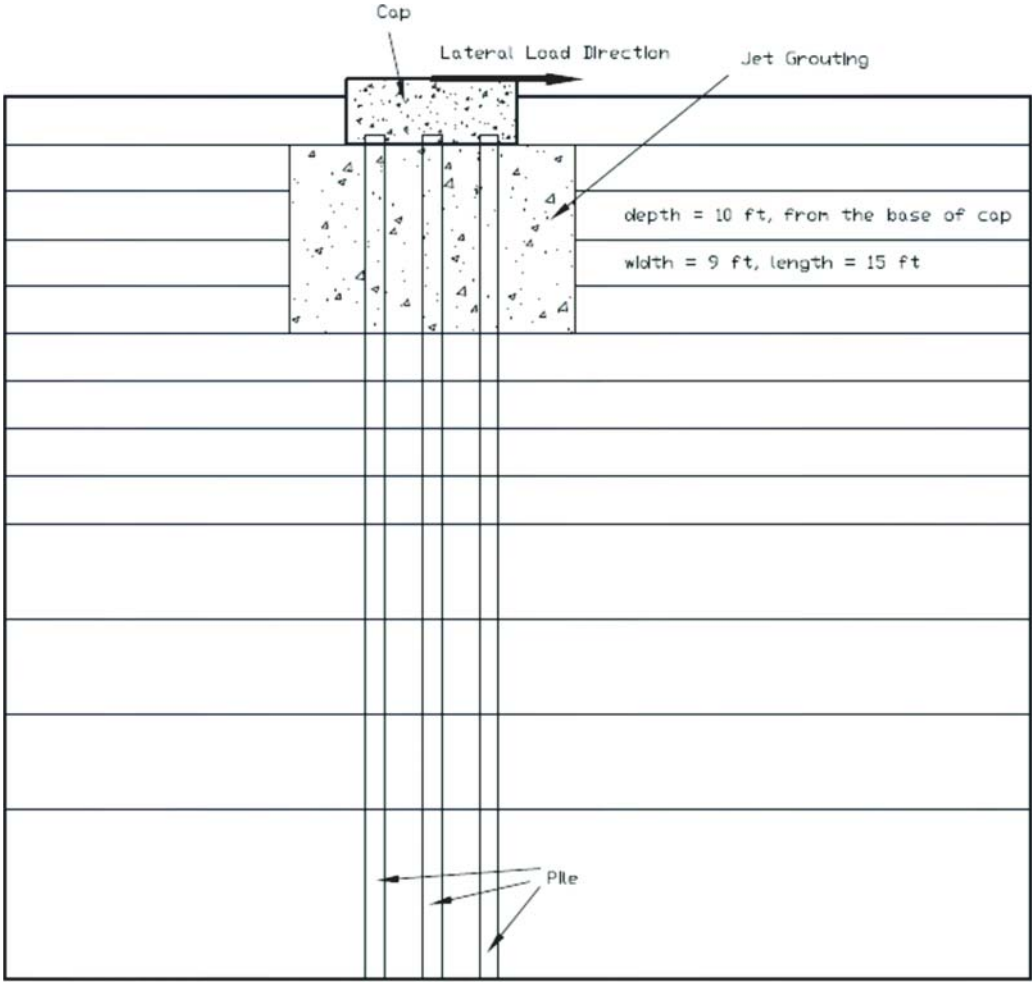

Figure 5-10. Schematic profile drawing of FEM model with jet grouting beside and/or underneath the cap.

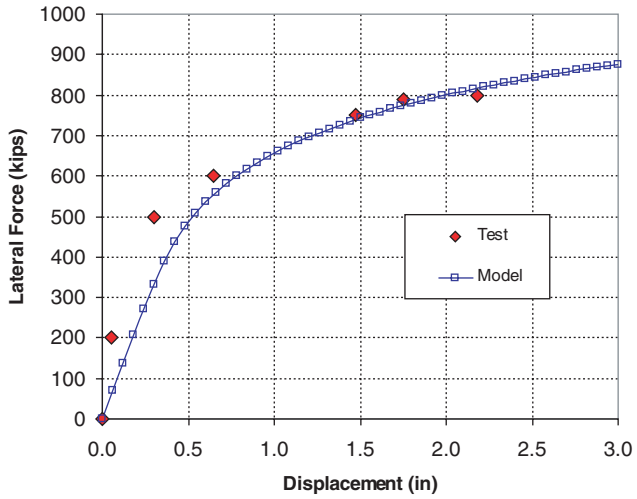

Figure 5-11. Comparison of FEM computed and measured load-displacement curve with jet grouting below and beside the cap. The jet grouting soilcrete has a depth of 10 ft from the cap base, a length of 15 ft, and a width of 9 ft.

modulus can be reasonably well estimated based on the same formula as that for concrete, $E = 57000(f'_c)^{0.5}$. The Poisson's ratio of the mass mix is assumed to be 0.2.

A comparison of the measured load-displacement curve with that computed with the FEM model is provided in Figure 5-11. Once again, the agreement between measured and computed results is generally satisfactory especially for pile cap displacement more than 0.5 in. The researchers noted that for small displacements of the cap less than 0.5 in., the load-displacement curve from the test is somewhat stiffer than the curve obtained by the FEM model. This could be due to the linkage between the pile cap and jet grouting soilcrete. Once again, the relatively good agreement suggests that using the linear elastic material model with the above-mentioned properties can produce reliable estimates of the measured load-deflection curve obtained from the field tests with jet grout treatment around the pile group. Therefore, the same model can be used for parametric studies using the variations on geometries to expand our understanding of the increased lateral resistance provided by jet grouting.

CHAPTER 6

Parametric Studies

The parametric studies provide numerical simulation of the behavior of the pile group subjected to lateral loading and eliminate the cost of additional field tests. The basic approach for the parametric studies is to develop calibrated soil and pile parameters based on the results of the field testing. Then, using these calibrated parameters, the depth, width, and strength of the improved ground can be systematically varied to determine the effect on computed pile group response such as load-deflection curves, maximum moment-load curves, etc. This chapter describes parametric studies associated with the various soil improvement methods.

6.1 Mass Mix Depth Effect (Beside the Cap) on Lateral Resistance

The first parametric study involved an investigation of the depth of the mass mix block produced by soil improvement on the pile group capacity. The mass mix block is assumed to be immediately adjacent to the pile cap but does not contact the piles themselves. As shown in Figure 6-1, the mass mix block length was held constant at 4 ft in the direction of loading with a width of 9 ft (cap width) perpendicular to the lateral load direction while the depth was increased. The top of the mass mix was assumed to be at the same depth as the cap top, which is at a depth of zero ft. Analyses were performed for mass mix blocks with bottom depths of 2.5, 5.0, 7.5, 10.0, and 12.5 ft (about 2.4D, 4.7D, 7.0D, 9.4D, and 11.8D, where D is the pile diameter). Other soil and pile parameters were kept the same as described in Section 5.4.

The load-displacement curves calculated by the FEM analysis for each soil mix depth are plotted in Figure 6-2. The percent increase in lateral resistance for improved soil relative to the virgin soil at a reference lateral displacement of 1.5 in. is 14%, 27%, 33%, 36%, and 41% for the mass mix bottom depth of 2.5, 5.0, 7.5, 10.0, and 12.5 ft, respectively. It is readily apparent that the lateral load increases as the depth of the block increases; however, the increase is not uniform, indicating that a greater proportion of the lateral resistance is carried by the upper part of the mass mix block.

The improvement ratio is defined as the lateral load in the improved soil over the lateral load in the virgin soil at a reference cap lateral displacement of 1.5 in. Figure 6-3 provides a plot the improvement ratio versus the depth of the mass mix zone adjacent to the cap. An equation for the trend line computed using the least square method is also shown in Figure 6-3. The slope of the trend line becomes flatter as the depth of the mass mix depth increases, which suggests increasing the depth is becoming less effective in increasing the lateral resistance. Beyond a certain limit, increasing the depth of mass mix treatment provides only a relatively limited increase in lateral capacity. These results suggest that the optimal soil improvement depth of mass mixing beside the pile cap would be about 10 pile diameters for a similar soil and pile profile.

6.2 Mass Mix Depth Effect (Below the Cap) on Lateral Resistance

The second parametric study investigated the effect of the depth of a mass mix layer below the pile cap on the lateral pile group resistance. The mass mix block is assumed to have the same cross section as the cap (length of 9 ft in the direction of loading and a width of 9 ft perpendicular to loading), and has variable depths along the depth direction. The top of the mass mix block is at the base of the pile cap (a depth of 2.5 ft) and the bottom of the mass mix block is at depths of 5.0, 7.5, 10.0, and 12.5 ft (see Figure 6-4). Other soil and pile parameters remain the same as described in Section 5.4. There is no linkage between base of the cap and the top of the mass mix block.

The load-displacement curves computed with the FEM model are presented in Figure 6-5. The depth of the mass mix block below the cap has a significant effect on the lateral capacity of the pile group. The increased lateral capacity at the reference cap lateral displacement of 1.5 in. is 41%, 60%, 75%, and

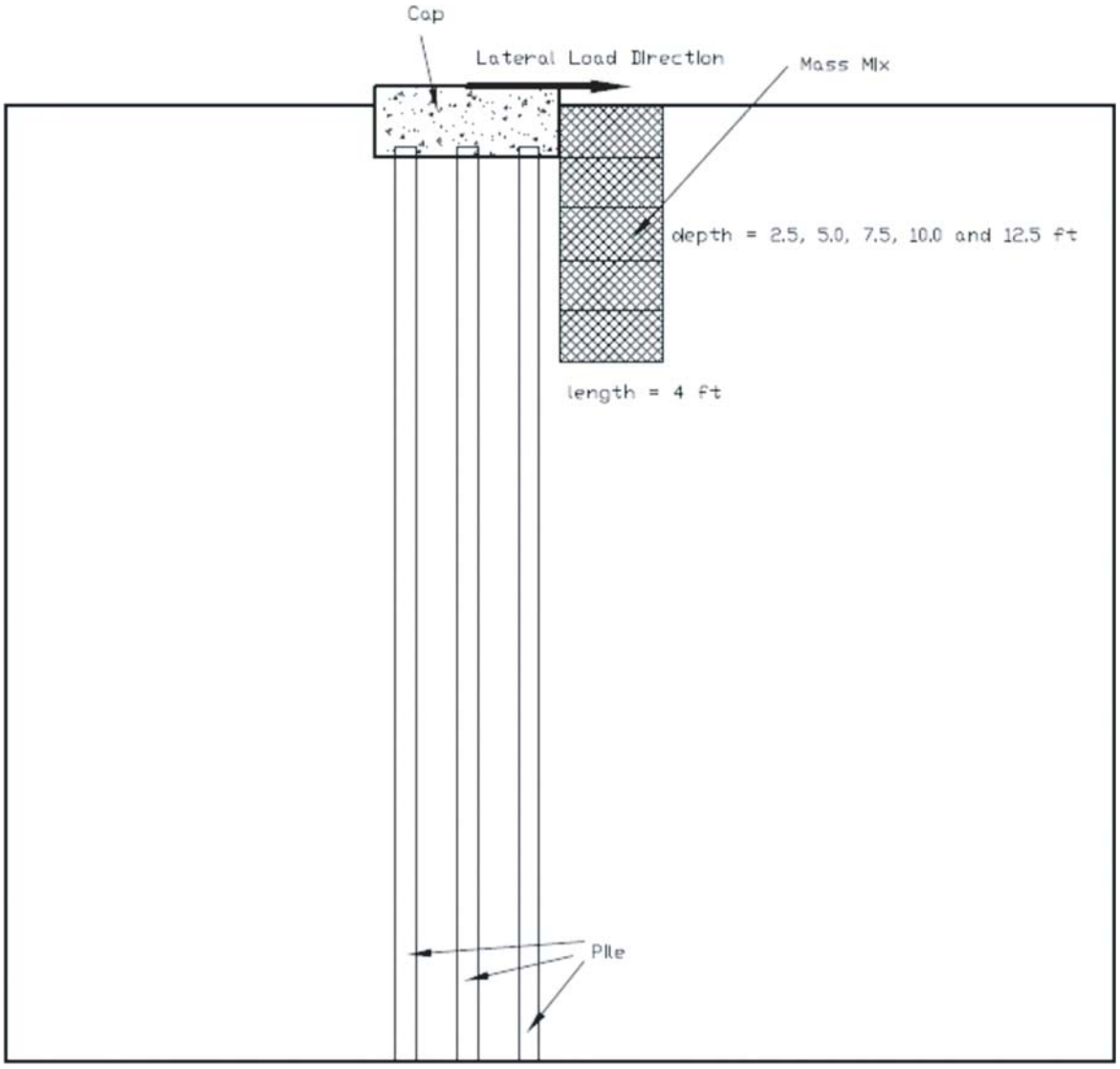

Figure 6-1. Mass mixing depth intervals adjacent to cap for parametric study.

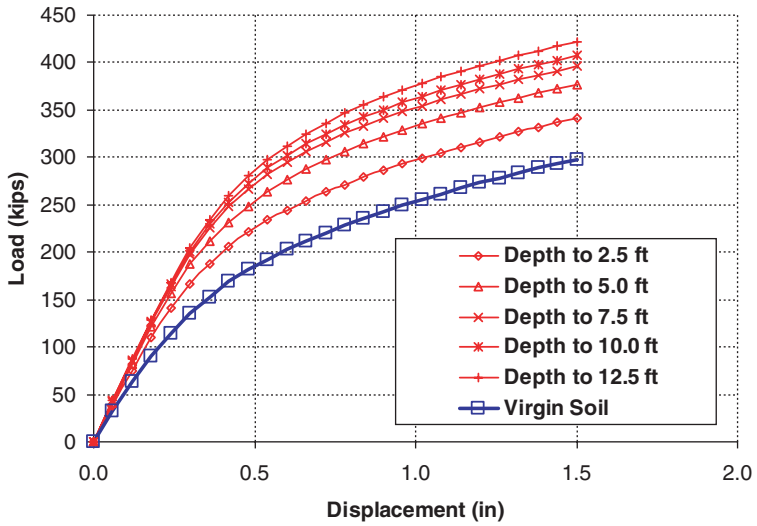

Figure 6-2. Parametric study of mass mix depth adjacent to the cap on the computed load-displacement curve.

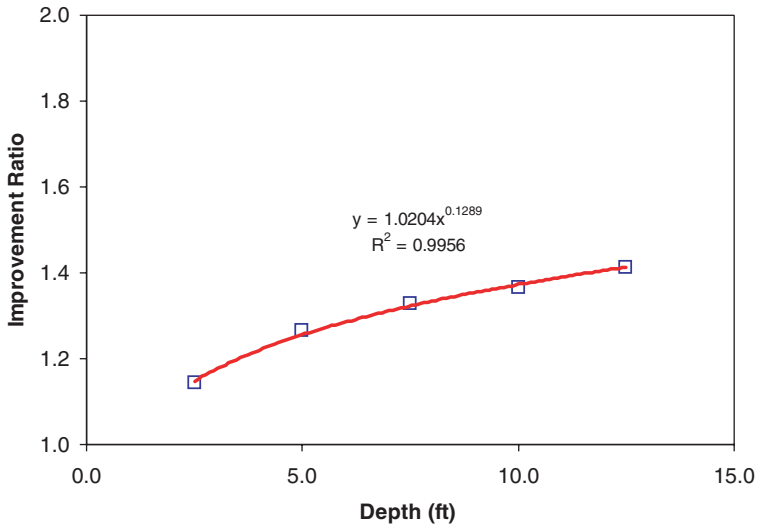

Figure 6-3. Improvement ratio as a function of mass mix depth adjacent to cap.

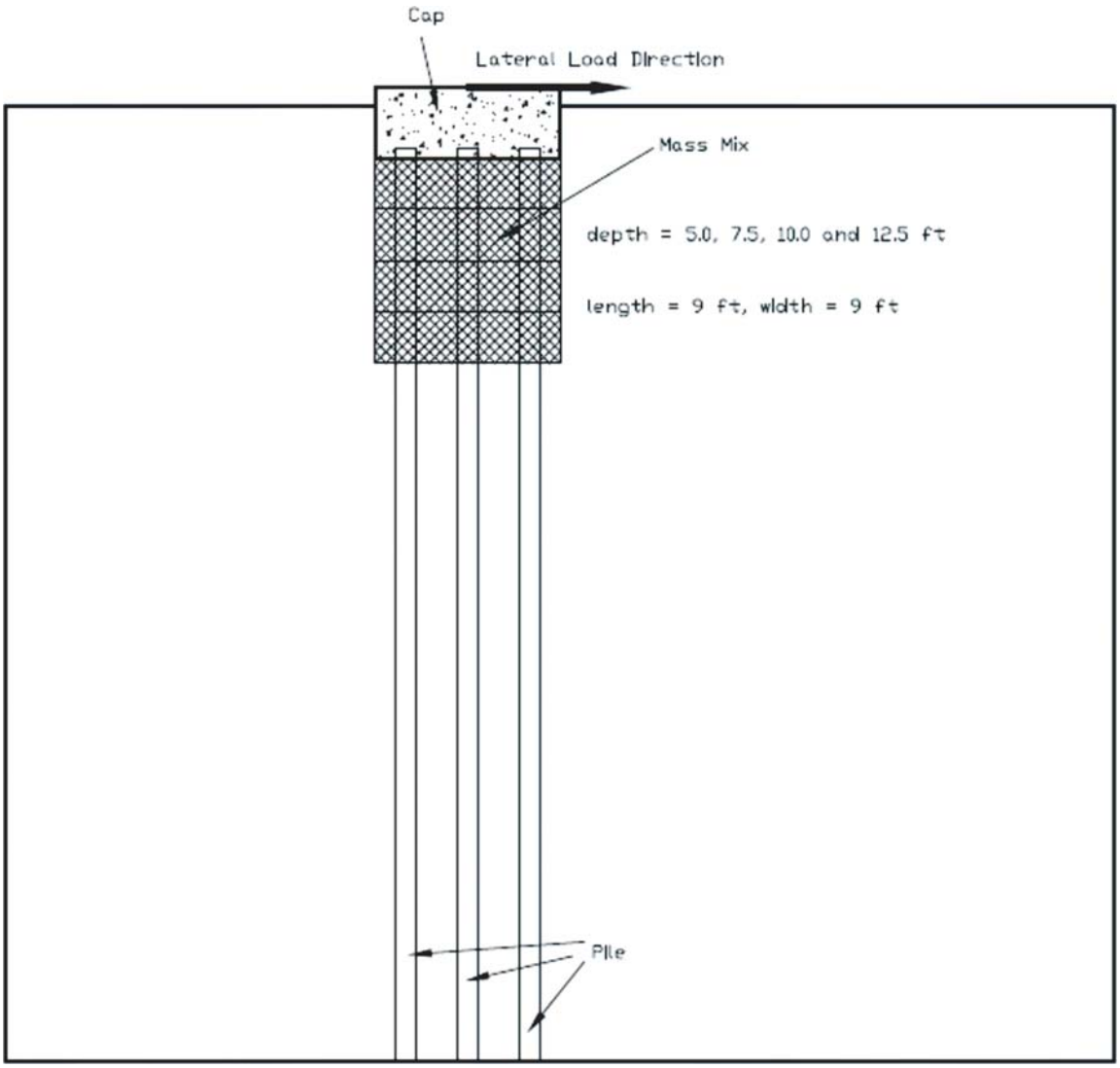

Figure 6-4. Mass mixing depth intervals below cap for parametric study.

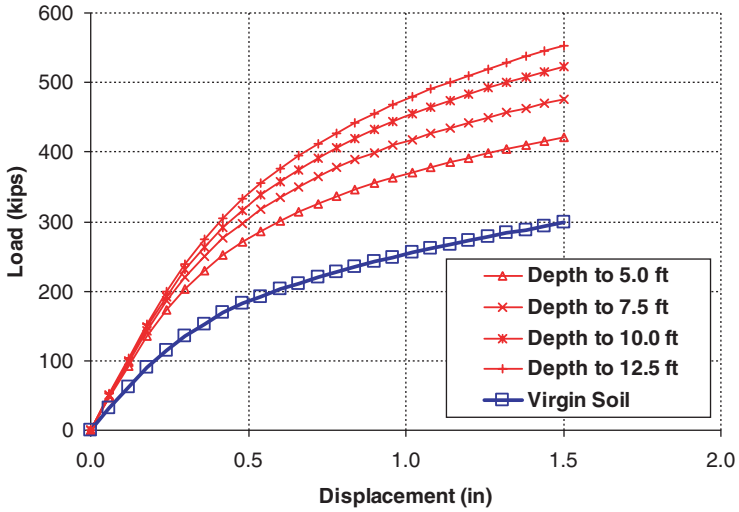

Figure 6-5. Results of parametric study of the effect of the mass mix depth below the cap on the computed load-displacement curve.

86% for the mass mix depths of 5.0, 7.5, 10.0, and 12.5 ft, respectively.

Figure 6-6 provides a plot of the improvement ratio versus the depth of the mass mix below the cap using a best-fit trend line. These results suggest that mass mixing below the cap will dramatically increase the lateral capacity of the pile group relative to that in virgin clay. For mass mix zones with thicknesses ranging from 2.5 ft to 10.0 ft (2.4D to 9.4D) underneath the cap, the lateral resistance will increase by approximately 40% to 86% for similar soil and pile profiles. The increased resistance from the soil treatment is partially due to the increased passive area and partially due to constraint of piles by the mass mix (so that the mass mix and the piles can be considered as an integrated block). The slope of the trend line flattens somewhat as the depth of the mass mix zone increases, which suggests that the upper mass mix zone provides more lateral resistance, as expected.

It should also be noted that the improvement ratio produced by mass mixing below the cap is much higher than that produced by mass mixing beside the cap for the same depth of treatment. This may be due to the larger cross section (9×9 ft for mass mix below the cap in this section, 9×4 ft for mass beside the cap as in Section 6.1) as well as the constraint of piles by the mass mix. However, in practical design, since the external load (e.g., wind or earthquake load) direction is very random, the soil improvement beside the cap should be preformed on all four sides of the cap. In contrast, the mass mix below the cap will resist external load in any direction.

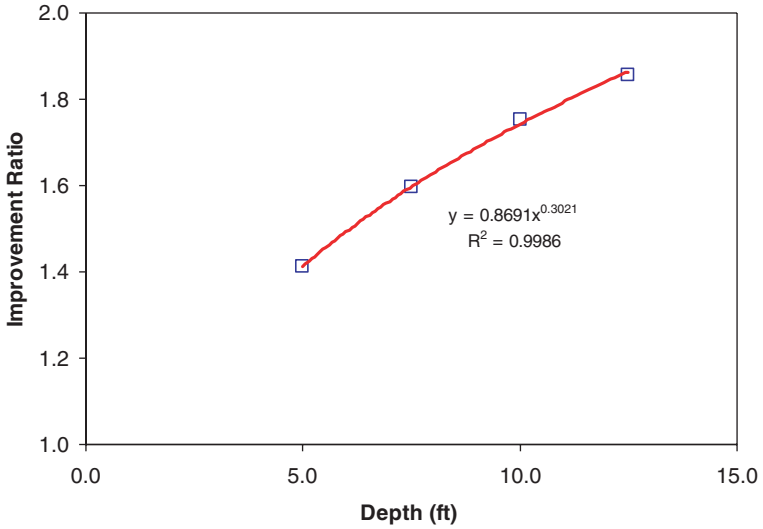

Figure 6-6. Improvement ratio as a function of mass mix depth below the cap.

6.3 Mass Mix Length Effect (Beside the Cap) on Lateral Resistance

The third parametric study involved an investigation of the length of the mass mix block in the direction of the loading on the increase in lateral pile group resistance. In this case, the mass mix block also was assumed to be beside the pile cap but not in contact with the piles. The depth of the block was fixed at 12.5 ft and the width was taken as 9.0 ft perpendicular to the lateral load direction (4.5 ft in the FEM model due to symmetry), which is equal to the pile cap width. Other soil and pile parameters were kept the same as described in Section 5.4. Finite element analyses were then performed for mass mix block lengths ranging from 3 ft to 7 ft in the direction of lateral loading as illustrated in Figure 6-7.

The load-displacement curves calculated with the FEM model are plotted in Figure 6-8. As the length of the mass mix zone increases, the lateral resistance gradually increases in a rather consistent fashion. Figure 6-9 provides a plot of the improvement ratio as a function of the length of the mass mix block in the direction of the lateral loading relative to the virgin clay resistance at a lateral displacement of 1.5 in. The improvement ratio is 1.36, 1.42, 1.47, 1.54, and 1.60 for the mass mix lengths of 3.0, 4.0, 5.0, 6.0, and 7.0 ft, respectively. As observed in Figure 6-9, the improvement ratio increases almost linearly with the mass mix length. This is considerably different from the nonlinear trend lines obtained from the parametric studies relative to mass mix depth presented in Sections 6.1 and 6.2. The correlation equation shows that each additional foot of length leads to an additional increase in the improvement ratio of about 0.06. Since the passive pressure area is the same for various lengths of the mass mixes, the increase in the lateral capacity is considered to be a result of the increase in the shear area of the mass mix block. However,

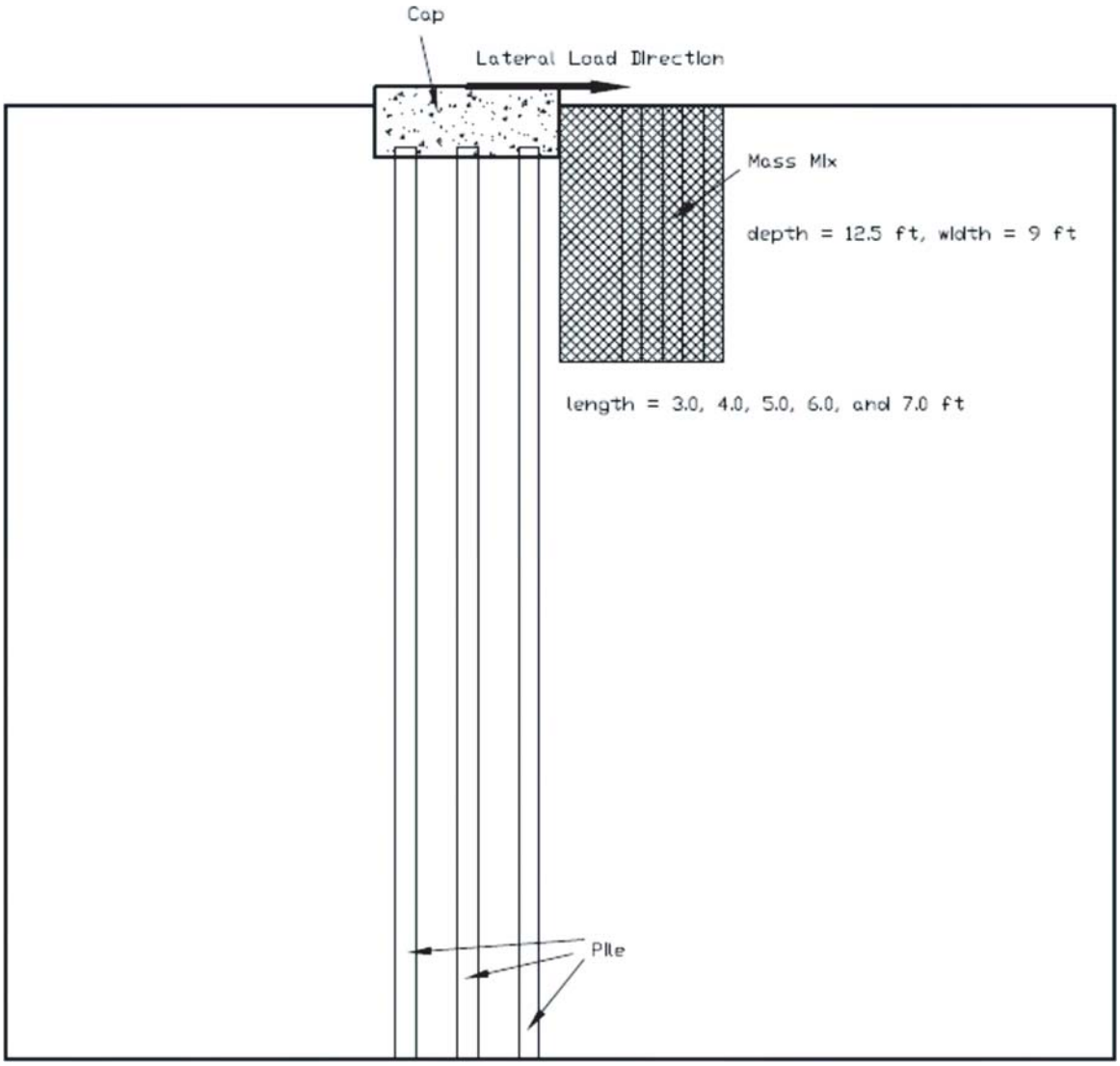

Figure 6-7. Mass mix length intervals beside cap for parametric study.

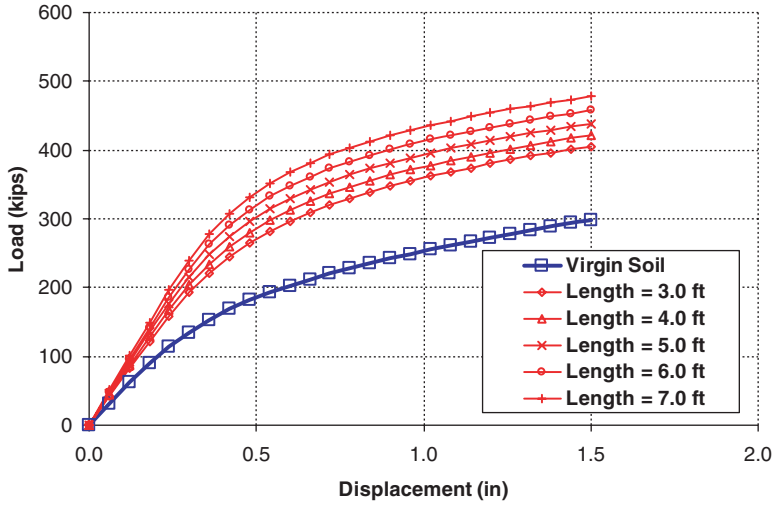

Figure 6-8. Results of parametric study on the length of the mass mix zone beside the pile cap on the computed load-displacement curve.

increasing mass mix length will increase the cost. The optimal length requires a balance analysis between engineering capacity and economic efficiency.

6.4 Jet Grout Depth Effect (Beside the Cap) on Lateral Resistance

This parametric study is very similar to that conducted for the mass mix treatment except that the improved soil is now soilcrete produced by jet grouting, which has a higher strength than that from the soil mixing. The jet grout soilcrete is assumed to be at the side of the pile cap and has a length of 4 ft in the direction of loading with a width of 9 ft transverse to the lateral load direction (see Figure 6-10). FEM analyses are conducted for variable soilcrete depths. The top of the soilcrete is assumed to be at the ground surface and the bottom of the soilcrete is at depths of 2.5, 5.0, 7.5, 10.0, and 12.5 ft as shown in Figure 6-10. Other soil and pile parameters are the same as those described in Section 5.5.

The load-displacement curves computed by the FEM model are presented in Figure 6-11. The depth of the jet grout beside the cap has a significant effect on the lateral resistance of the pile group. The increased lateral resistance (or improvement ratio minus 1) at the cap lateral displacement of 1.5 in. is 13%, 25%, 31%, 35%, and 40% for the mass mix depth of 2.5, 5.0, 7.5, 10.0, and 12.5 ft, respectively.

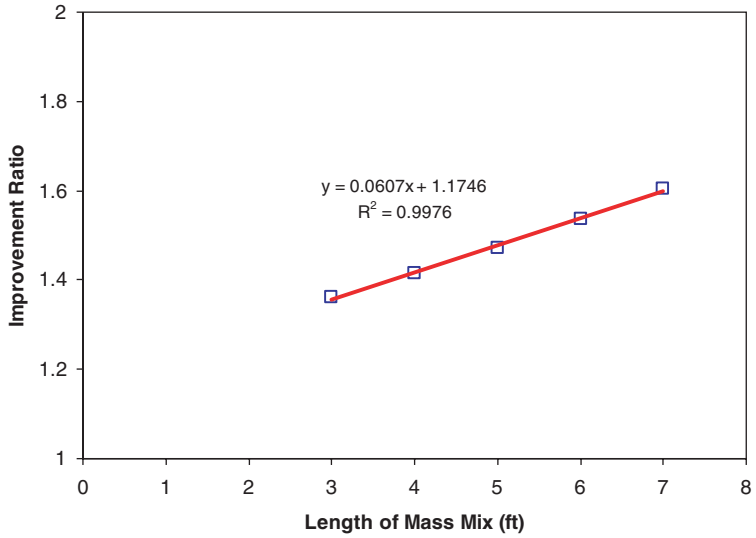

Figure 6-9. Improvement ratio as a function of mass mix length adjacent to the cap.

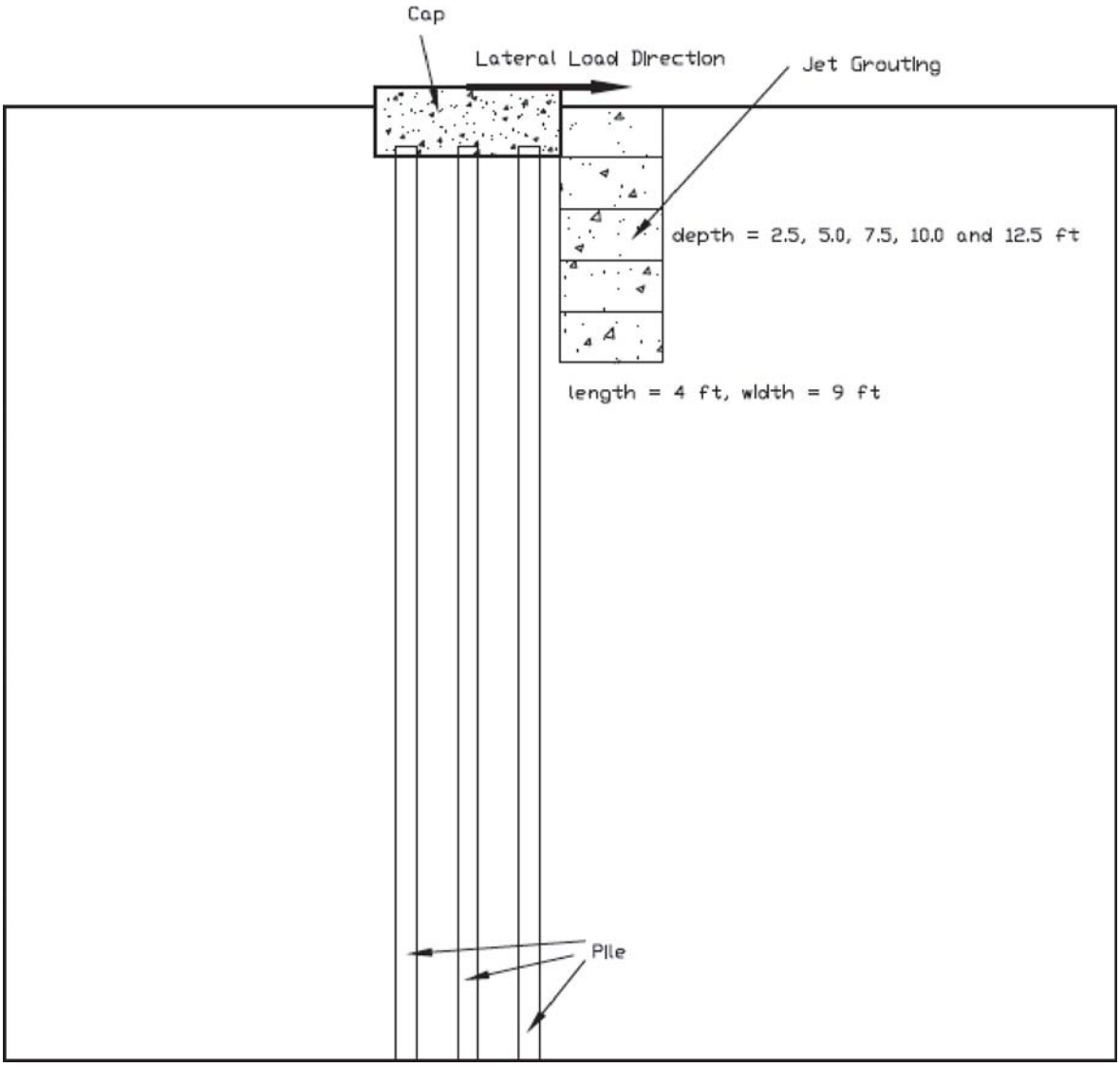

Figure 6-10. Jet grout soilcrete depth intervals beside cap for parametric study.

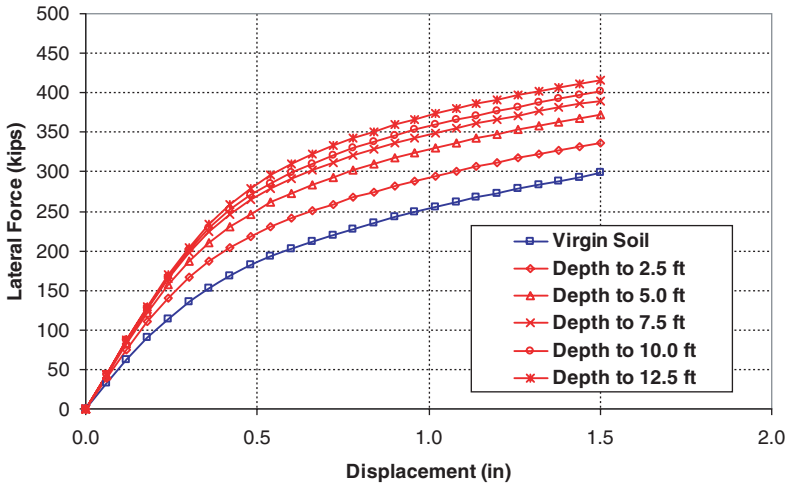

Figure 6-11. Parametric study of jet grout depth adjacent to the cap on the computed load-displacement curve.

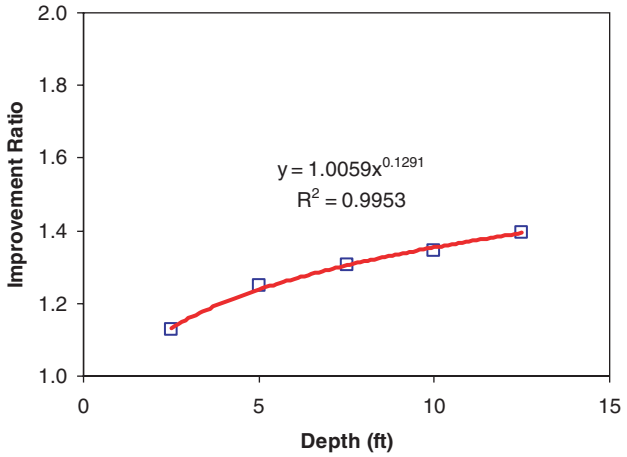

Figure 6-12. Effect of jet grout depth beside the cap on the improvement ratio for a lateral displacement of 1.5 in.

Figure 6-12 plots the improvement ratio versus the depth of the jet grout beside the cap. The equation for the best-fit trend is a power function. As was the case for the mass mix treatment, the slope of the trend line flattens as the depth of the jet grout soilcrete increases. This result suggests that the upper soilcrete zone carries more lateral resistance. Increasing the depth of the jet grout zone beside the cap will increase the lateral capacity of the pile group; however, when the depth reaches a certain value (roughly 10 times that of the pile diameter), increasing additional depth will only provide limited increases in lateral pile group resistance relative to virgin clay.

6.5 Jet Grout Depth Effect (Below the Cap) on Soil Improvement

For the numerical tests of the jet grout below the cap, the jet grout soilcrete has the same cross section as the cap (length of 9 ft in direction of loading and width of 9 ft perpendicular to the direction of loading). The bottom of the soilcrete block is at depths of 5.0, 7.5, 10.0, and 12.5 ft below the ground surface as shown in Figure 6-13. There is no linkage between the base of the cap and the top of the jet grouting block. Other soil and pile parameters remain the same as described in Section 5.5.

Figure 6-14 provides load-displacement curves computed by the FEM model. Again, the depth of the jet grout treatment below the cap is found to have a significant impact on the lateral resistance of the pile group. At a lateral pile cap displacement of 1.5 in. the lateral capacity is increased by 40%, 59%, 74%, and 85% for the mass mix depths of 5.0, 7.5, 10.0, and 12.5 ft, respectively.

Figure 6-15 provides a plot of the improvement ratio versus the depth of the soilcrete below the cap. A best-fit curve and the accompanying equation also are provided. These results suggest that the soil improvement method of jet grouting soilcrete below the cap will dramatically increase the lateral capacity of the pile group in virgin clay. A jet grouting soilcrete with the height of 2.5 ft to 10 ft (2.4D to 9.4D) will increase the lateral capacity by approximately 40% to 85% for similar soil and pile profiles. The slope of the trend line flattens somewhat as the soilcrete depth increases, which suggests that the upper layers in the improved zone provide more lateral resistance than do the lower layers.

It should be noted that the improvement ratio produced by jet grout below the cap (1.40 to 1.85) is much higher than that produced by jet grout beside the cap for the soilcrete with the same depth. This result is likely a result of the larger cross section (9×9 ft for the jet grouting soilcrete below the cap in this section, 9×4 ft for jet grout beside the cap as in section 6.4) as well as the constraint of piles by the jet grouting. Again, the improved soil below the cap will resist external load in any direction.

It also is important to note that the increase in lateral resistance for the soilcrete produced by jet grouting was very similar to that obtained for the soilcrete produced by mass mixing despite the lower compressive strength. This result suggests that lower strengths that can be produced by less expensive treatment approaches might still be effective in improving the lateral resistance. This issue will be investigated further in a subsequent parametric study.

6.6 Jet Grout Length Effect (Beside the Cap) on Soil Improvement

This parametric investigation focuses on the block length effect on the pile group lateral capacity for the jet grout mix beside the cap. The jet grouting soilcrete has a fixed depth of 12.5 ft and a width of 9 ft (4.5 ft in the FEM model due to symmetry) perpendicular to the lateral load direction, and has variable length from 3 ft to 7 ft along the lateral loading direction (see Figure 6-16). Other soil and pile parameters are kept the same as described in Section 5.5.

The load-displacement curves calculated with the FEM model are presented in Figure 6-17 and the improvement ratio versus soilcrete length is provided in Figure 6-18. As the length increases, the load-displacement curves increase relatively consistently. The improvement ratios are 1.34, 1.40, 1.45, 1.51, and 1.58 for the jet grouting soilcrete lengths of 3.0, 4.0 5.0, 6.0, and 7.0 ft, respectively. The trend line in Figure 6-18 shows that the improvement ratio versus the jet grout soilcrete length is roughly linear, which is different from the nonlinear trend lines associated with the jet grout depth as presented previously. The correlation equation shows that each additional foot of jet grouting soilcrete length will cause the improvement ratio to increase by 0.06. This result is identical to that found for the parametric study of soilcrete length with soil mixing. Since the passive pressure area is the same for various lengths of the soil-

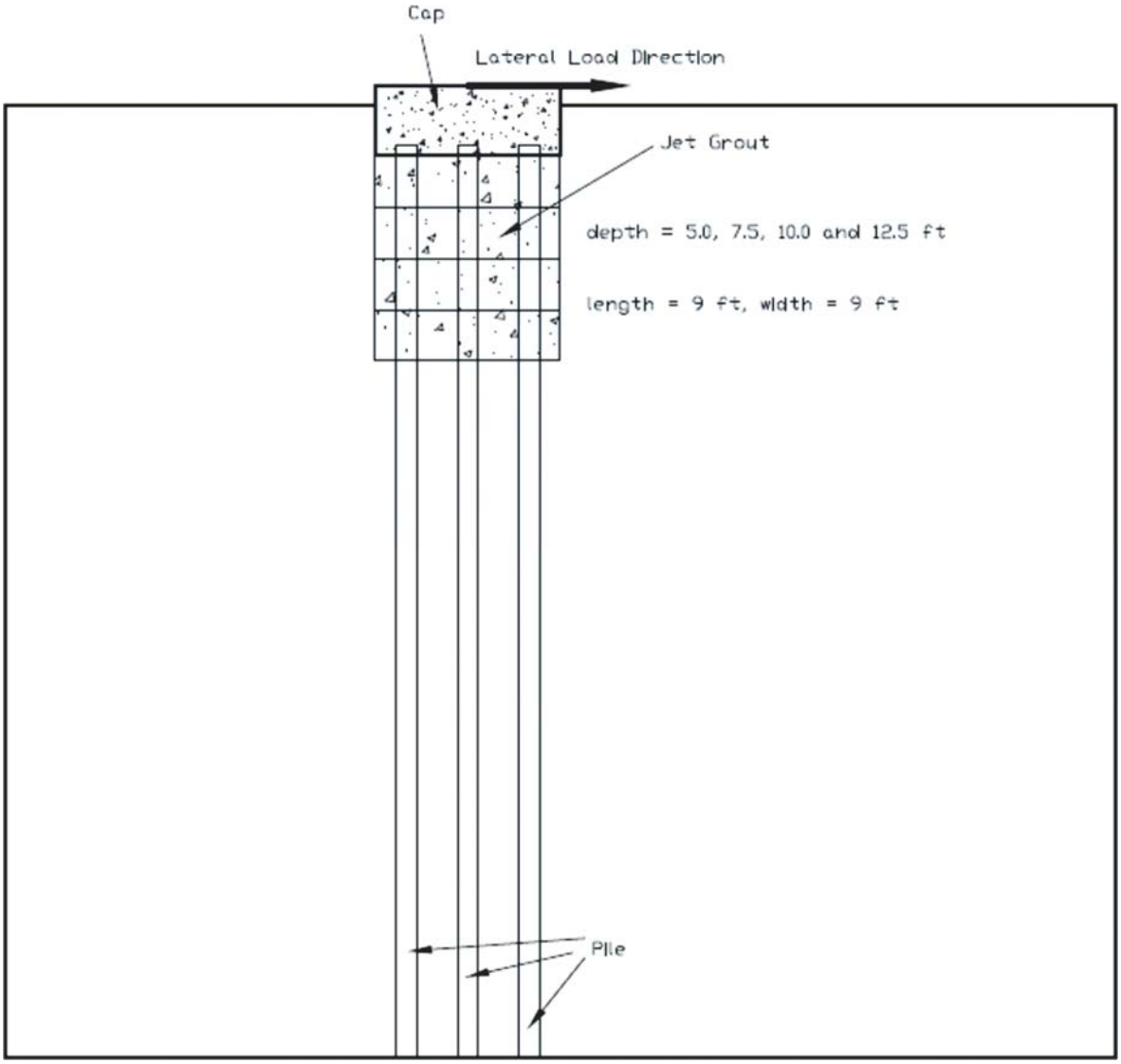

Figure 6-13. Jet grout depth intervals below cap for parametric study.

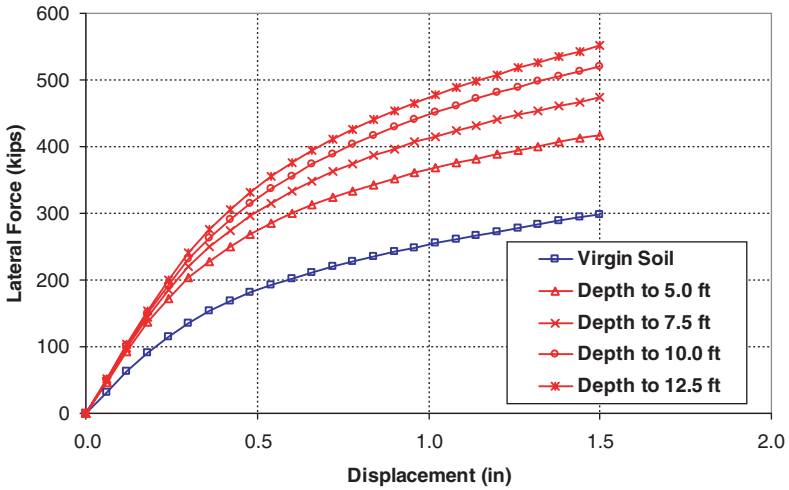

Figure 6-14. Results of parametric study of the effect of the mass mix depth below the cap on the computed load-displacement curve.

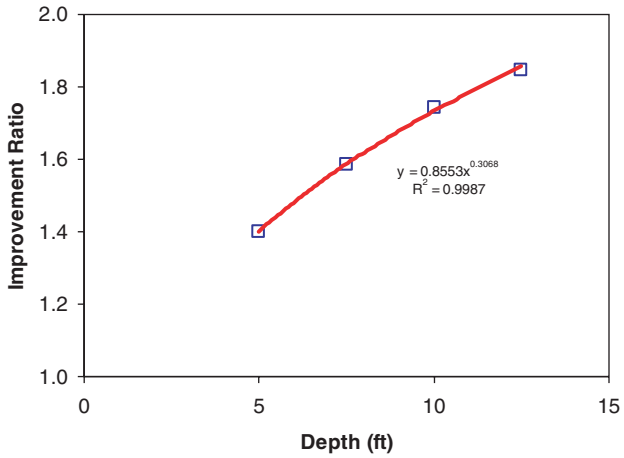

Figure 6-15. Improvement ratio as a function of jet grout treatment depth below the cap.

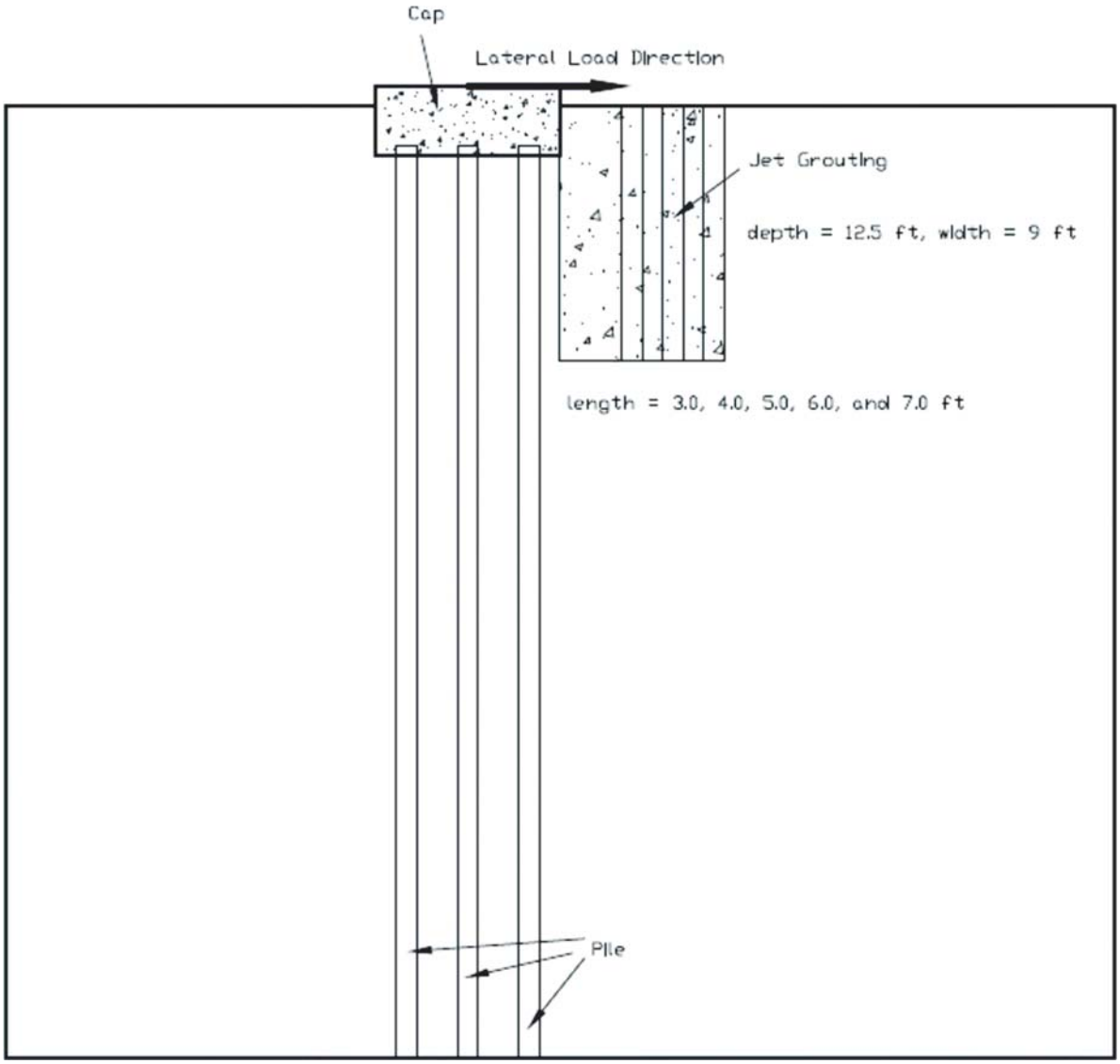

Figure 6-16. Jet grout treatment length intervals beside cap for parametric study.

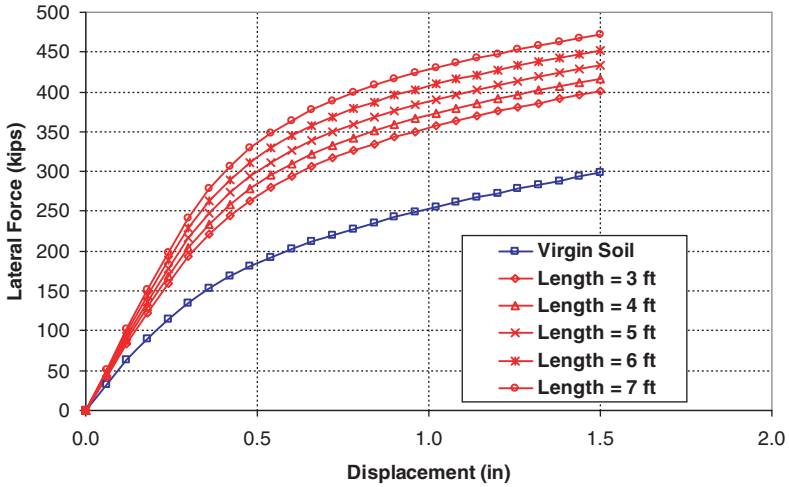

Figure 6-17. Results of parametric study on the length of the jet grout treatment zone beside the pile cap on the computed load-displacement curve.

crete, the increase of the lateral capacity is mainly caused by the increase of the shear area of the jet grouting soilcrete. Therefore, these results indicate that a lower strength soilcrete, which could be produced with a lower cost treatment method, could produce the same adhesive resistance as that obtained with jet grouting. This finding increases the potential that soil improvement methods can be a cost-effective approach for increasing lateral pile group resistance.

6.7 Material Strength Effect on Lateral Pile Group Resistance

Based on the results from the previous parametric studies, another set of parametric studies was performed to investigate the effect of the strength of the soil improvement zone on the increase in lateral pile group resistance. For the first of these studies, the improved soil block is assumed to be at the side of the pile cap and have a length of 4 ft in the direction of loading, a width of 9 ft perpendicular to the loading direction, and a depth of 12.5 ft (see Figure 6-19).

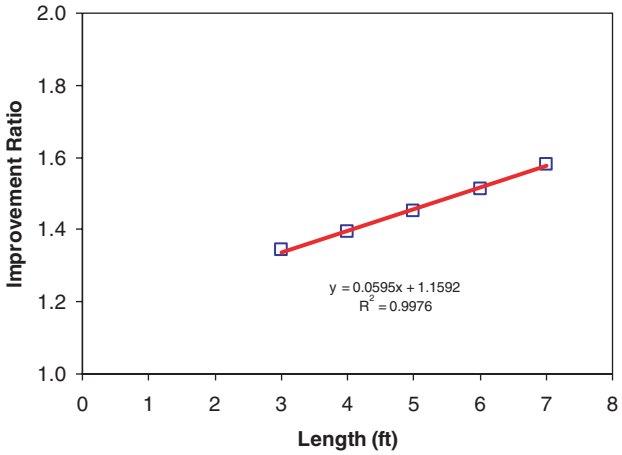

Figure 6-18. Improvement ratio as a function of jet grout treatment length adjacent to the cap.

The compressive strength of the improved soil (f'_c) is assumed to vary over a wide range between 21 and 7700 psi. Young's modulus is assumed to abide by the same relation as that of conventional concrete [$E = 57000(f'_c)^{0.5}$] and is in the range of 260 to 5000 ksi, which covers the typical strengths of mass mixed and jet grouted soil (see Table 6-1). Since the improved soils with the Young's moduli shown in Table 6-1 are much stiffer than the virgin clay, the improved soils have been modeled as linear elastic materials.

The load-displacement curves computed using the FEM model are presented in Figure 6-20 and the improvement ratio is plotted versus compressive strength in Figure 6-21. As shown in Figure 6-20, the load-displacement curves all plot on top of each other for the range of compressive strengths investigated. As a result, the improvement ratio is essentially constant relative to the compressive strength of the treated zone as shown in Figure 6-21. These results show that the lateral capacity of the pile group is not sensitive to the compressive strength of the treated zone, which is as expected since all of the improved soils are much stiffer than the virgin clay. Therefore, for practical purposes, the improved soils can be considered to act as a rigid block for the range of material properties in Table 6-1. The numerical model suggests that the lateral capacity of the pile group is sensitive to the geometry of the improved soil, but not to the material strength (or Young's Modulus), provided the improved soil is much stiffer than the virgin clay. The typical mass mix and jet grouting soilcrete are much stiffer than the soft clay.

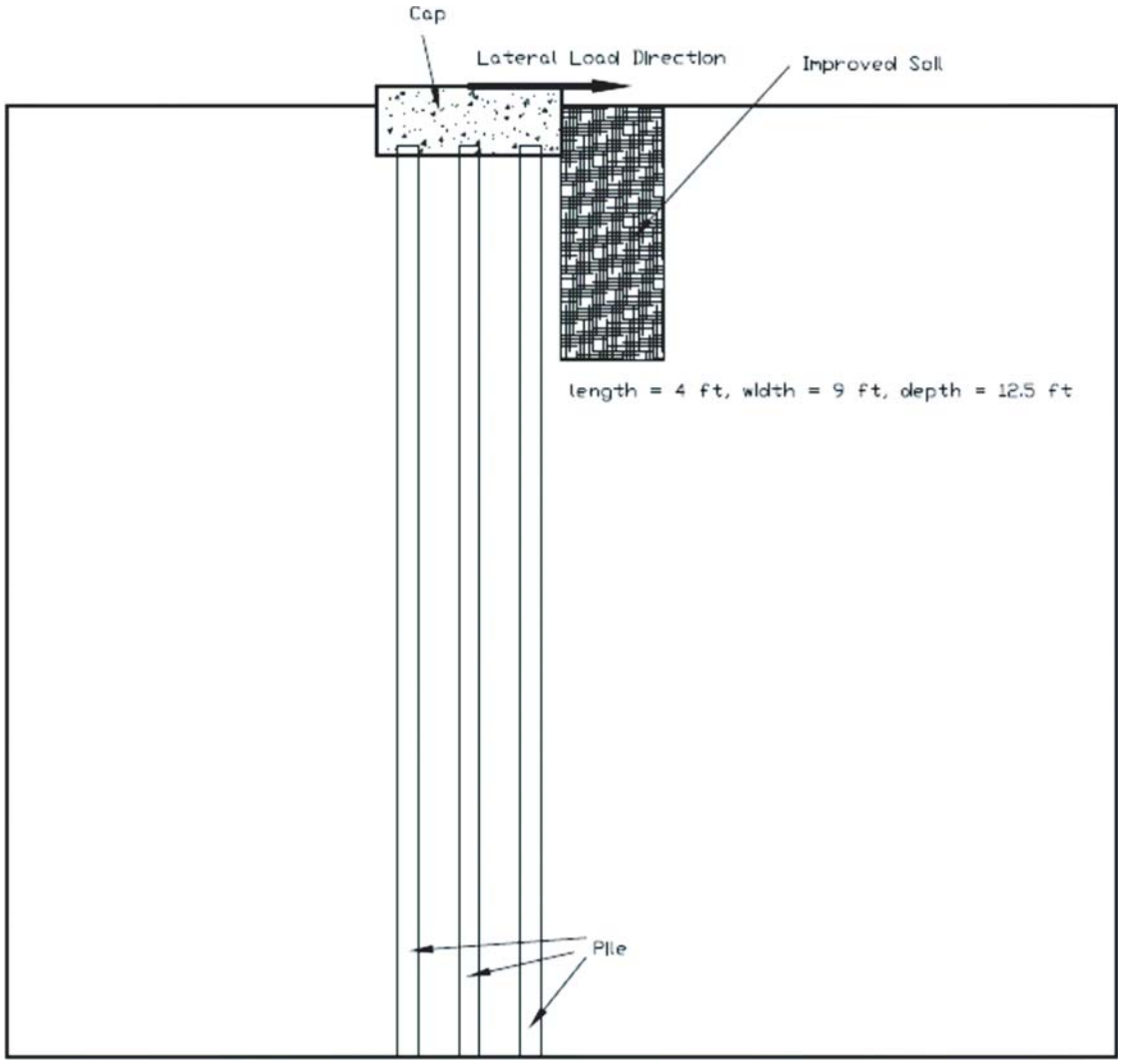

Figure 6-19. Treatment zone relative to pile group for parametric study involving the effect of compressive strength of the improved soil beside the cap.

The final set of parametric studies involved varying the compressive strength of the soilcrete zone directly below the pile cap as shown in Figure 6-22. As shown, the soilcrete zone was 9 ft square in plan view and extended 12.5 ft below the ground surface. As in the previous case, the computed load-displacement curves plot on top of each other as shown in Figure 6-23 and the improvement ratio shown in Figure 6-24 is nearly constant with strength. These results indicate that the lateral resistance is relatively insensitive to the soilcrete strength, provided the soilcrete is much stiffer than the virgin clay.

Table 6-1. Material strength of the improved soil.

Strength (psi)	Young's Modulus (ksi)	Note
21	261	
63	452	
126	640	Typical mass mix
252	905	
300	987	
600	1400	Typical jet grout
900	1710	
1200	1980	
4000	3600	
7700	5000	Typical concrete

6.8 Conclusions Based on Parametric Studies

Verification and validation procedure was conducted for the finite element model before the parametric studies. Mesh and boundary sensitivity analyses were performed and the soil material properties were carefully calibrated by comparison with the test data for the single pile and pile groups. The load-displacement curves obtained from the numerical models fit satisfactorily with the test data. Parameter studies were then performed to examine the sensitivity of the depth (beside and

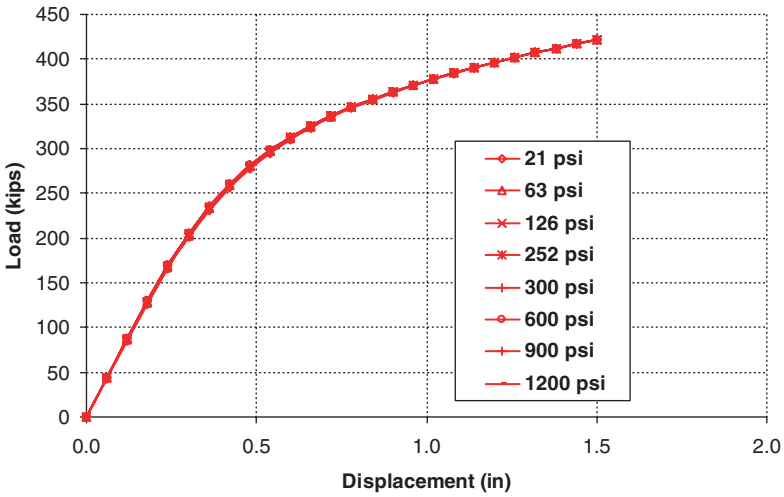

Figure 6-20. Load-displacement curves computed using the FEM model assuming a variety of compressive strength values for the soil improvement zone beside the cap.

below the cap) and the length of the improved soil, including mass mix and jet grout, as well as the sensitivity of the material strength of the improved soil. Based on the parametric analyses some important conclusions have been developed, as follows:

1. The lateral resistance of the pile group is not sensitive to the material strength of the improved soil (including mass mix and jet grouted soilcrete), provided that the improved soil is much stiffer than the virgin clay. When the stiffness is high relative to the surrounding clay, the soilcrete behaves more like a rigid block within the surrounding soil. This result suggests that soilcrete with lower strength, which can be produced by less expensive treatment approaches, can still produce the same increases in lateral pile group resistance as a higher strength soilcrete.
2. A relatively narrow zone of improved soil adjacent to the pile group increased the lateral resistance relative to untreated clay by 15% to 40% for improved soil block depths of 2.5 to 12.5 ft (2.4D to 11.8D), respectively. The trend line of the improvement ratio versus depth is a power function and flattens considerably for depths greater than 8D to 10D. As a result, the upper improved layer provides more lateral resistance than the deeper layers.
3. For the improved soil beside the cap to a depth of 12.5 ft below the ground, the lateral resistance increased 36% to

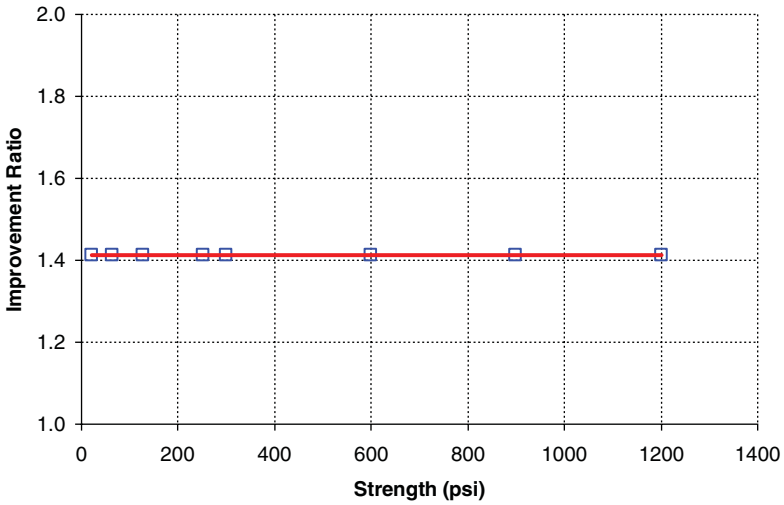

Figure 6-21. Effect of material strength of improved soil beside the cap on improvement ratio relative to untreated clay at a lateral cap displacement of 1.5 in.

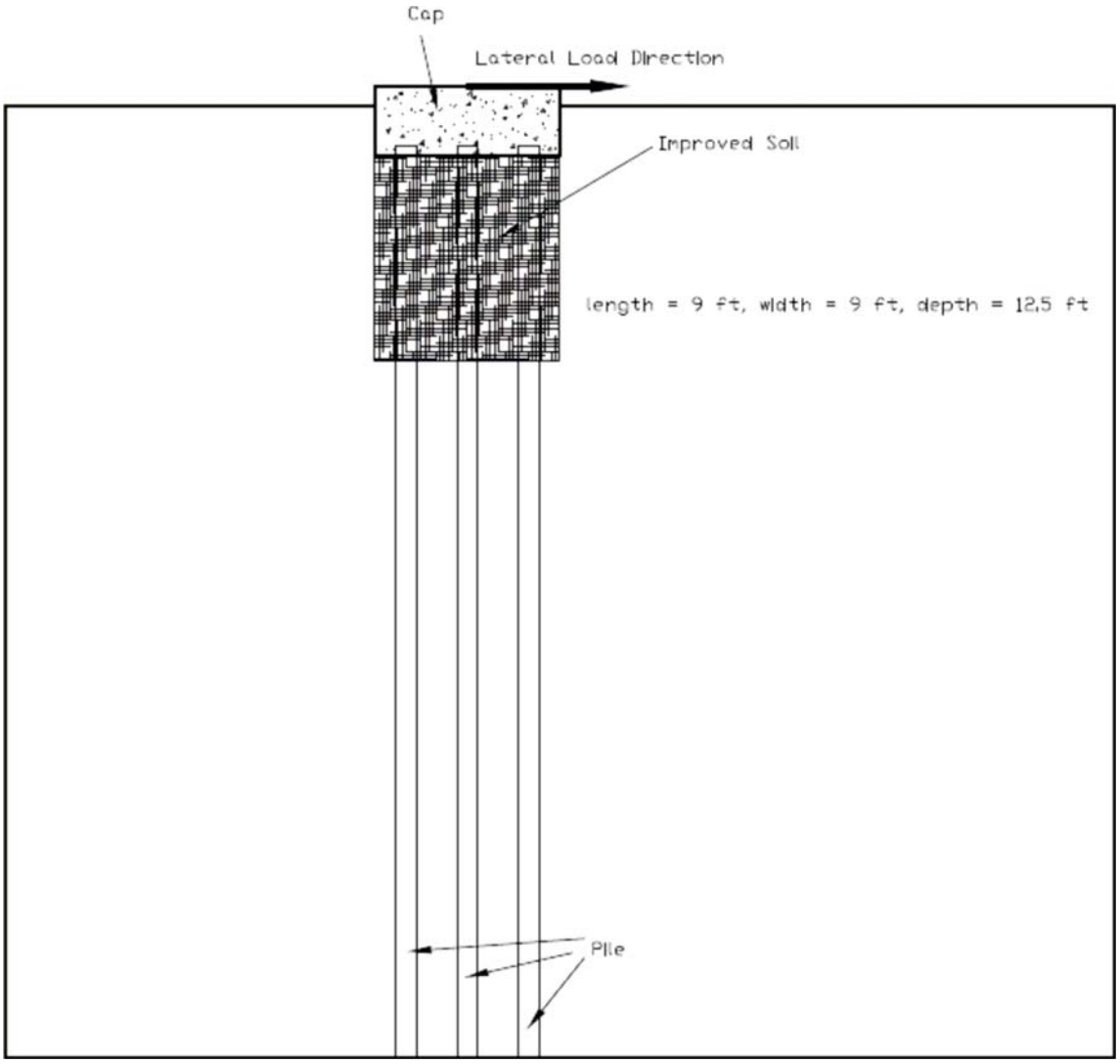

Figure 6-22. Treatment zone relative to pile group for parametric study involving the effect of compressive strength of the improved soil below the cap.

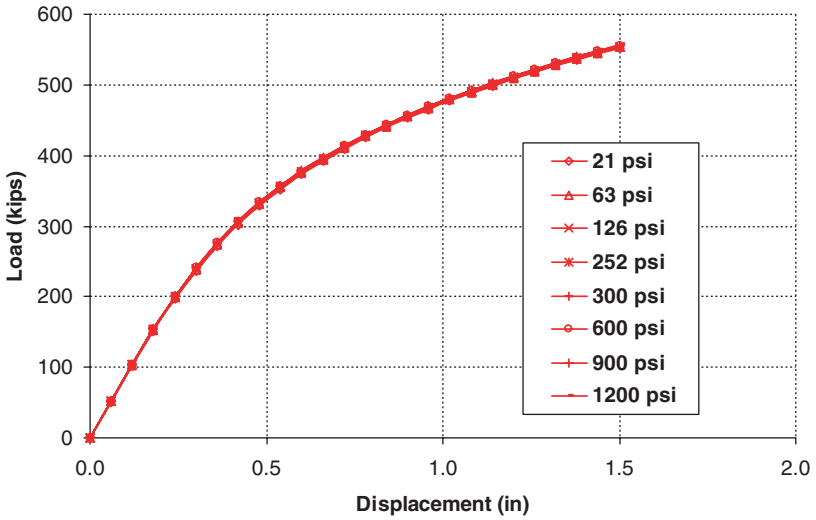

Figure 6-23. Load-displacement curves computed using the FEM model assuming a variety of compressive strength values for the soil improvement zone beneath the cap.

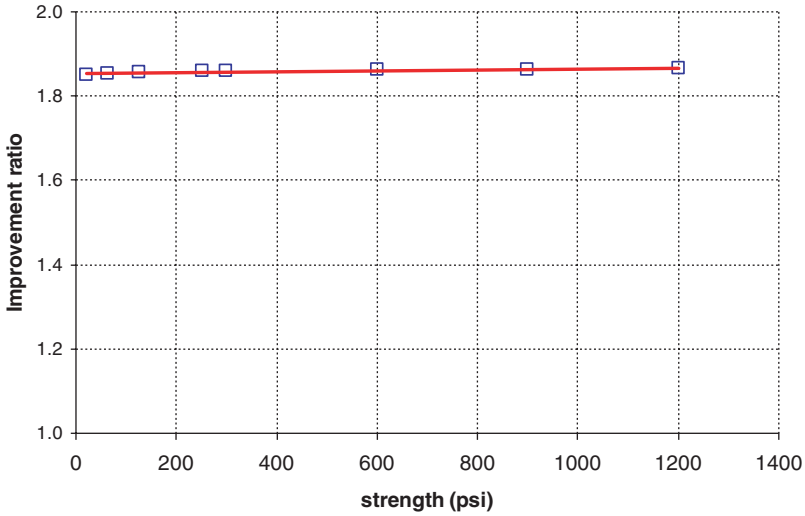

Figure 6-24. Effect of material strength of improved soil below the cap on improvement ratio relative to untreated clay at a cap lateral displacement of 1.5 in.

60% for soil block length ranging from 3 to 7 ft. The improvement ratio versus the soil block length is roughly linear and increasing the length of the block 1 ft produced an increase in the improvement ratio of 0.06. This increase is likely associated with increased side and base shear since the passive resistance remains constant with a constant width.

4. Improving the soil directly below the pile cap increased lateral resistance by 40% to 85% relative to untreated clay for the improved soil depths of 5.0 to 12.5 ft (4.7D to 11.8D). The trend line of the improvement ratio versus depth is roughly a power function and flattens somewhat with depth. As a result, the upper improved soil layers provide more lateral resistance than do the deeper layers, but increasing the depth can still provide significant increases in resistance. Another advantage of the improved soil below the cap is that the soil improvement will increase the lateral capacity of the pile group in any direction and increase the constraint on the piles themselves.

Generally, increasing the depth and length of the improved soil block will increase the lateral capability of the pile group. On the other hand, increasing the dimension of the improved soil also increases the volume of the improved soil and accordingly increases the economic cost. The optimal dimension of the improved soil is expected to be a balanced one that comprehensively considers the engineering demand and the economic budget.

It should be mentioned that the above conclusions were based on the conditions described in this report. Any extrapolation of these conclusions should be carefully evaluated to take into account sensitivity of improved soil geometry and position, the properties of soil and pile, numerical method limitations, and other factors.

CHAPTER 7

Development of Simplified Model

The purpose of the work included herein is to provide the practicing engineer a simplified approach to estimate the performance of a pile group exposed to lateral loading considering various ground improvement techniques. A simple approach for design purposes is needed because FE modeling is somewhat cost-prohibitive for routine projects. Additionally, because of the complex nature of numerical modeling in general, the use of FE analytical techniques can be misleading, counter-productive, and possibly unconservative without a substantial effort by well-qualified individuals who must perform the analyses.

7.1 Calibration GROUP Analysis Model

A soil model was developed for application with relatively simple (as compared to sophisticated FE techniques) pile-foundation analysis software packages. Such packages are commercially available and widely used. This study employed GROUP (Reese, Wang, Arrellaga et al., 2004b), produced by Ensoft, Inc. The GROUP model was generated by matching the software output to the observed test behavior. Initially, Test 2 (virgin soil, cap not embedded) was used to develop and calibrate the model. Test 2 was selected such that the unknown passive resistance generated by an embedded pile cap was not included.

The subsurface profile used in the analyses is shown in Table 7-1, with 0 depth corresponding to the ground surface. Groundwater was at a depth of 24 in. beneath the ground surface. The existing p-y curve formulations available in GROUP were used. Layer 1 used the stiff clay model without free water. Layers 2 and 3 used the soft clay model with K values of 30 pounds per cubic inch (pci) and 100pci, respectively.

The axial resistance of the piles is an important parameter affecting the observed rotation of the pile cap. Because the piles are embedded in soft to stiff clay, the nominal axial resistance of the piles used in the GROUP model was estimated using an alpha coefficient of 0.85 for unit side resistance and a bearing coefficient of 9 for unit base resistance.

The pile-group effects were modeled using user-specified p-multipliers as suggested by Rollins et al. (2005). Based on the soil type, pile diameter, and pile spacing, the p-multipliers used in the GROUP model were taken as 0.85, 0.70, and 0.50 for the leading row, middle row, and trailing row of piles, respectively. These values are generally higher than those that would be computed internally from the default values used in the software. The default p-multipliers provided by the software, on average (3-D model), for the group tested in this research are 0.81, 0.51, and 0.50 for the leading row, middle row, and trailing row of piles, respectively.

The 3×3 pile groups shown in Figure 3-14 protrude a little more than 41 ft beneath the bottom of the pile cap. The piles are closed-ended pipe piles filled with reinforced concrete (non-reinforced concrete in the bottom 33.5 ft). The pipes are 12.75-in. diameter with 0.375-in. wall thickness and were impact driven with a hydraulic hammer. The embedment of the pile heads into the cap along with reported details of the connection suggest modeling the group with "fixed conditions" is appropriate.

The center row of piles contained strain gages mounted externally. An angle iron was attached to protect the instrumentation. Therefore, the EI of the piles in the center row is 1.41×10^7 k-in^2. The EI of the outer row piles is 1.23×10^7 k-in^2.

7.2 Comparison with Results from Tests in Virgin Soil

Using the GROUP model presented above, the observed behavior during full-scale testing and predicted behavior using GROUP was evaluated. Several iterations were required in which c_u, ϵ_{50}, and α were varied until an acceptable fit of both deflection and cap rotation was obtained for Test 2. Note the various model inputs that provided the best fit are in good agreement with typically used values and are consistent with

Table 7-1. Summary of soil properties used in GROUP analysis.

Layer	Depth (in)		Undrained Shear Strength (psi)		ε_{50} (%)		Total Unit Weight (pcf)
	Top	Bottom	Top	Bottom	Top	Bottom	
1	0	30	11.0	5.5	0.005	0.01	117.5
2	30	66	5.5	3.3	0.01	0.015	109
3	66	600	3.3	8.0	0.015	0.005	118

data obtained during the subsurface investigation. The final values obtained are those shown in Table 7-1.

Using the soil model described previously, adequate agreement between the observed behavior during full-scale testing and predicted behavior using GROUP is obtained as can be seen in Figures 7-1 and 7-2. Figure 7-1 compares the observed versus modeled pile head deflection for Test 2. Test 2 was the horizontal test conducted without passive resistance of the pile caps (e.g., soil adjacent to the pile cap was excavated prior to the test so the cap was not embedded). Figure 7-2 compares the observed versus modeled pile cap rotation for Test 2.

The lower magnitude horizontal loads were not investigated because Test 2 was conducted in the opposite direction of Test 1, and because Test 1 was performed first. It is

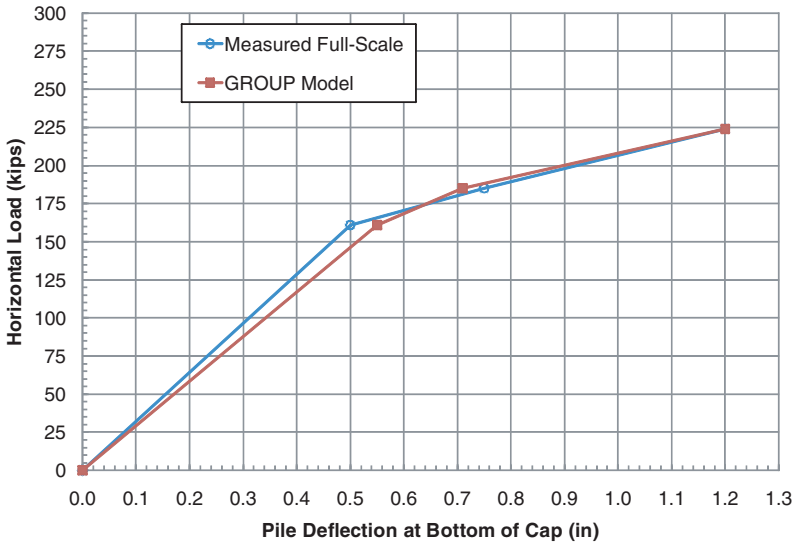

Figure 7-1. Comparison of measured and computed load-deflection for Test 2 (virgin soil, pile caps not embedded).

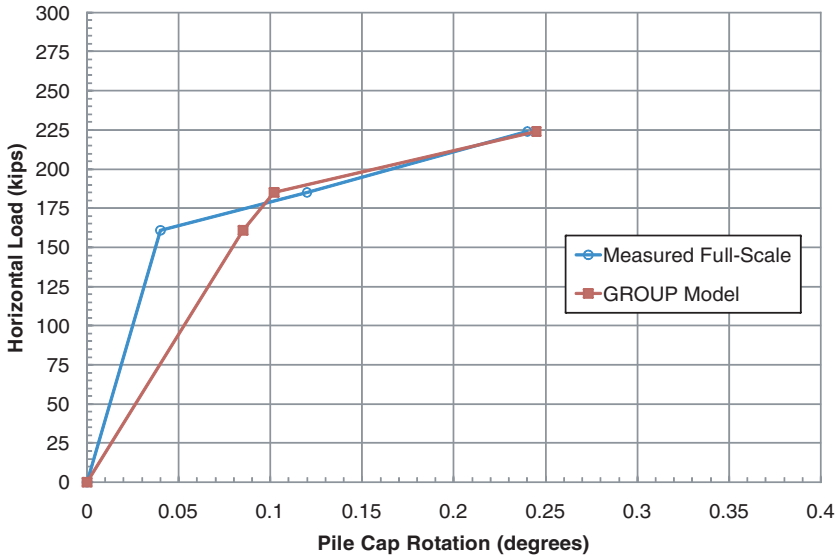

Figure 7-2. Comparison of measured and computed load-rotation curves for Test 2 (virgin soil, pile caps not embedded).

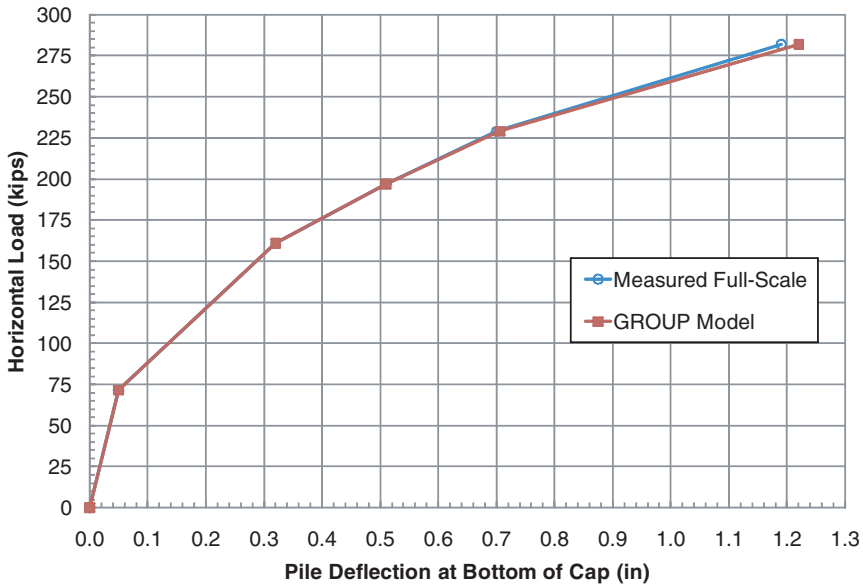

Figure 7-3. Comparison of measured and computed load-deflection curves for Test 1 (virgin soil, pile caps embedded).

believed that performing Test 1 prior to Test 2, but in the opposite direction, may have impacted the lower magnitude results.

After matching the Test 2 deflection and rotation via an iterative approach, the model was used to evaluate Test 1 (virgin soil, pile cap embedded) to evaluate the effect of the embedded cap on the total lateral resistance of the group. For these analyses, the magnitude of the applied horizontal force was reduced until the field-measured deflection and GROUP model deflection were nearly equal, as shown in Figure 7-3. This procedure was performed for each loading increment. The passive resistance provided by the pile cap at various deflections is computed as the difference between the actual applied horizontal force in the field load test and the applied horizontal force in the calibrated model.

The pile cap rotation predicted by the GROUP model also was compared to the measured rotation, as shown in Figure 7-4. Although not perfect, the agreement between the two curves is reasonable and provides further validation of the GROUP model.

The passive resistance is equal to the difference between the load applied during the test and the load applied in GROUP

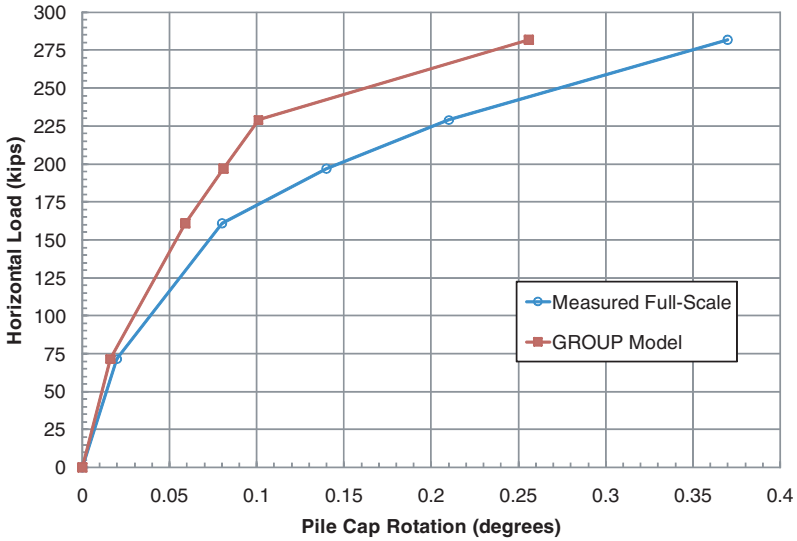

Figure 7-4. Comparison of measured and computed load-rotation curves for Test 1 (virgin soil, pile caps embedded).

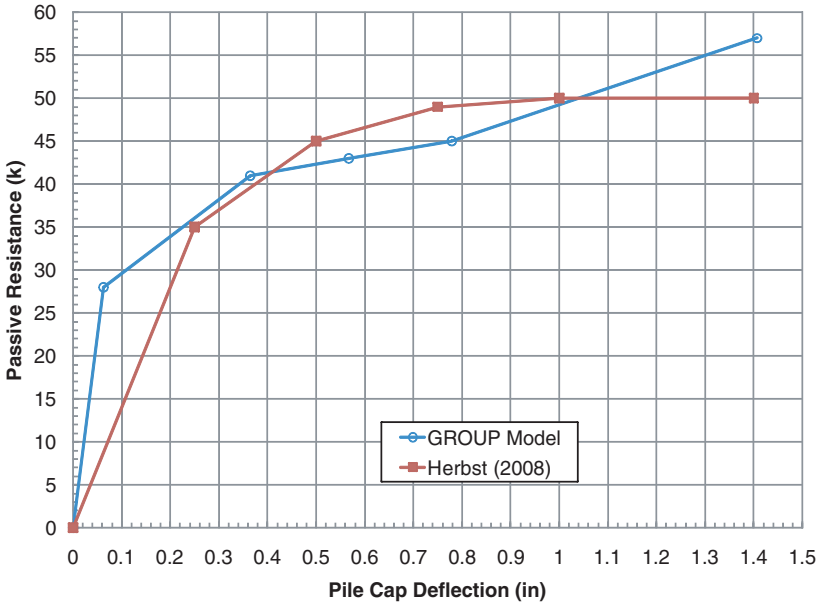

Figure 7-5. Computed passive resistance acting on pile cap in virgin soil.

to displace the cap the same distance. A comparison between the passive resistance reported and that computed by the GROUP model is shown in Figure 7-5. The good agreement appears to further validate the GROUP model.

7.3 Comparison with Results from Tests Involving Mass Mixing

The calibrated model and the procedure for estimating the contribution of the pile cap to lateral resistance described above provides a means of directly evaluating the benefit of using mass mix soil improvement adjacent to a pile cap. Mass mix soil improvement was performed adjacent to Pile Cap 1. In plan view, the treatment was 4 ft parallel to, and 11 ft perpendicular to, the direction of loading. The treatment depth was 10 ft, which resulted in improved soil adjacent to and 7.5 ft beneath the bottom of the pile cap. Details of the mass mix procedure are provided in Section 3.8 and Herbst (2008, Appendix 3). The unconfined compressive strength of the mass mix material was reportedly on the order of about 130 psi and was therefore substantially stronger than the in-situ fine-grained soil.

Similar to the approach used for Test 1 (virgin soil, pile cap embedded), the magnitude of the applied horizontal load was reduced in the GROUP model until the field-measured deflection and GROUP model deflection were nearly equal, as shown in Figure 7-6. This procedure was performed for each loading increment. The passive resistance provided by the pile cap plus mass mix at various deflections was computed as the difference between the actual applied horizontal force in the field load test and the applied horizontal force in the calibrated model.

The pile cap rotation predicted by the GROUP model was then compared to that which was measured, as shown in Figure 7-7. Although not perfect, adequate agreement between the two exists. These results again seem to confirm the applicability of the GROUP model.

The additional resistance provided by the mass mix is equal to the difference between the load applied during the test and the load applied in GROUP to displace the cap the same distance. A comparison between the virgin soil (passive) resistance and that observed during the mass mix test (computed by the GROUP model) is shown in Figure 7-8. The magnitude of additional resistance provided by the mass mix is considered to be a combination of passive resistance acting on a portion of the leading edge of the mass mix block and adhesion along the sides of the block.

7.4 Development of Simplified Method

The simplified method proposed for design is based on estimating the contribution of the treated ground around the pile group using a limit equilibrium analysis of the treated soil mass. This analysis includes passive resistance acting against the face of the treated soil mass and adhesion acting on the sides of the treated soil mass as lateral displacement mobilizes the passive soil resistance.

To model the effect of ground treatment using generally available computer software, the contribution of the treated

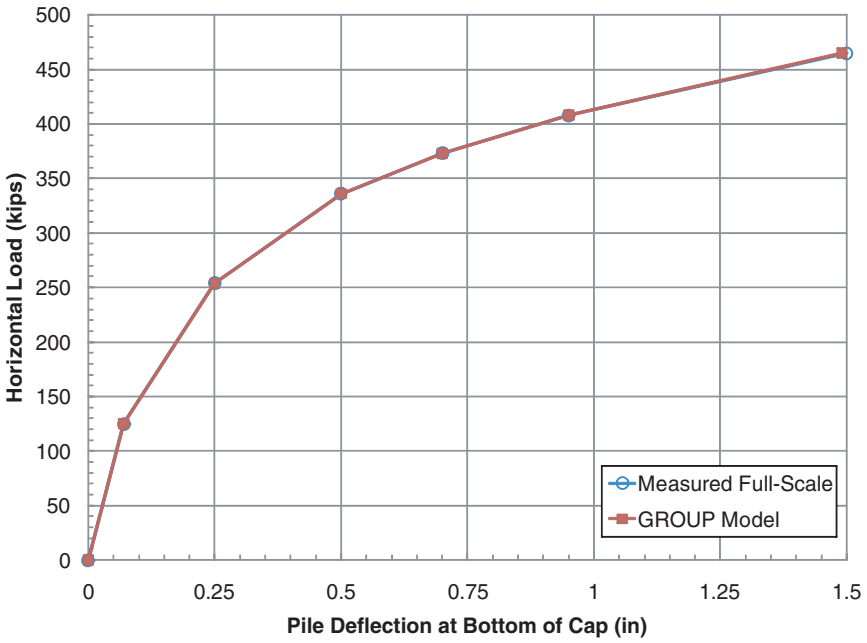

Figure 7-6. Comparison of load-deflection curves for pile group test involving mass mixing.

soil to the lateral resistance of the foundation is modeled by reducing the magnitude of horizontal load applied to the foundation by the estimated amount of passive and adhesive resistance provided by the improved (treated) area. The limit equilibrium analysis is used to estimate the magnitude of passive resistance acting on the leading face of the treated block and the amount of adhesive resistance acting on the sides and the base of the block. The geometry of the treated soil mass is subject to limitations on the projected area and the depth of the treated area relative to the width of the group.

Passive Resistance Acting on the Face of the Treated Soil Mass

Based upon the computed magnitude of passive resistance acting against the leading face of the pile cap (50 kips at 1-in.

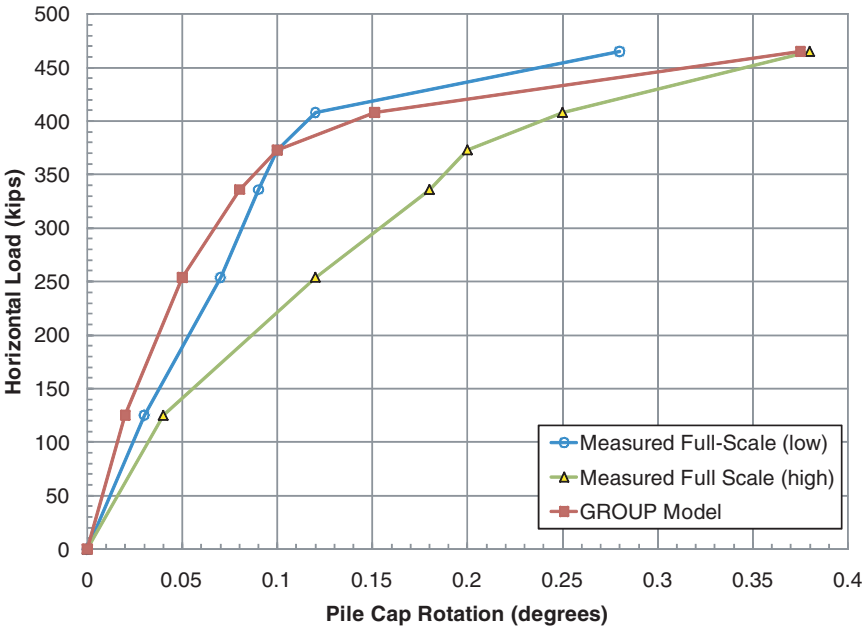

Figure 7-7. Comparison of measured and computed load-rotation curves for test involving mass mixing.

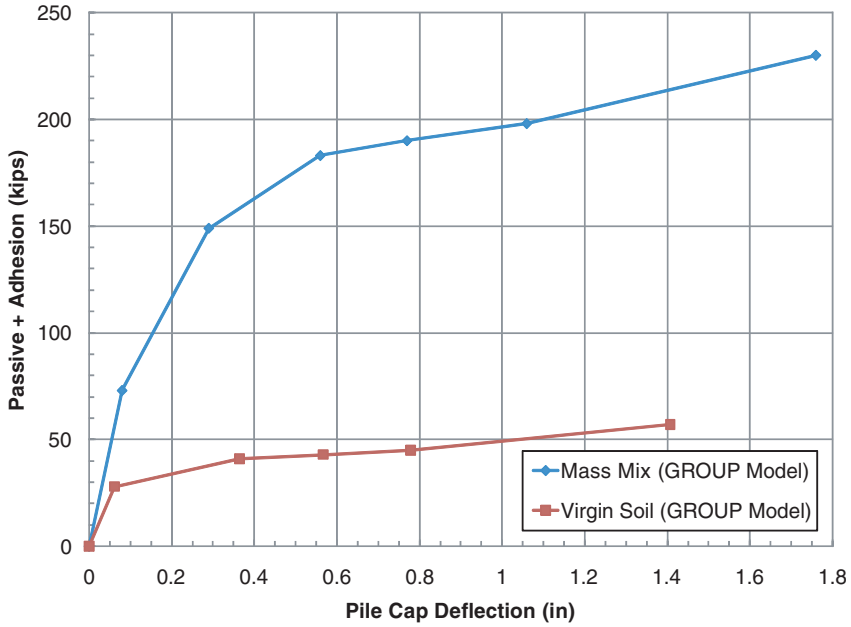

Figure 7-8. Additional lateral resistance provided by mass mixing estimated by the GROUP model.

deflection), and the dimensions of the embedded cap (8.75 ft by 2.5 ft), a unit value for passive resistance acting against the cap in virgin soil can be computed as follows:

$$p_p = 50\text{k}/(2.5\text{ ft} \times 8.75\text{ ft}) = 2.29\text{ksf} \quad (9)$$

Because of observed desiccation of the crust and associated cracks in the soil matrix, it is considered likely that the effective shear strength contributing to passive lateral resistance in the upper 1 ft of the soil mass would be slightly less than the strength measured using the relatively small cone penetrometer or laboratory tests on relatively small samples.

With the computed unit passive resistance determined above, Rankine earth pressure theory can be used to determine the undrained shear strength profile over the depth of the pile cap. Note that the details of the strength profile within this depth range do not change the calibrated GROUP model discussed previously because the piles are embedded beneath this zone and are not affected by the shear strength surrounding the pile cap (cap not embedded in the GROUP model).

The following expression for Rankine passive resistance was used to correlate the relationship between the undrained shear strength of the soil and the lateral soil resistance acting against the cap:

$$p_p = 2c_u + \sigma'_v \quad (10)$$

Below the top 1 ft of soil, this relationship was used with the shear strength profile used in the GROUP model. In the upper 1 ft of soil, the shear strength profile was back-calculated using this relationship so as to provide a total lateral resistance against the cap equal to that determined from the previous comparisons of measured contribution of the pile cap. Since p_p has been determined to provide an average value of 2.29 ksf and σ'_v can be estimated from the unit weight of the soil, c_u can be determined in the upper foot. The undrained shear strength profile used to estimate passive and adhesive resistance is shown in Figure 7-9, along with the effective vertical stress and unit passive resistance (Rankine 2-D) profiles.

Adhesion Acting on the Sides and Base of the Treated Soil Mass

The parametric study using finite element analyses provided an evaluation of the effect of treatment depth on the lateral resistance contributed by the treatment. One of these analyses considered treatment only to the bottom of the cap (depth of 2.5 ft) and adjacent to the leading face of the cap. The zone of treatment in the model was 4 ft in the direction of loading and 9 ft perpendicular to the direction of loading, slightly smaller than actually tested due to limitations in the geometry of the model. The results indicate that 45k of additional resistance resulted from creating this treated block above the magnitude of the resistance provided by virgin soil. This additional resistance is likely to have been developed by adhesion along the two sides and the base of the treatment block, assuming the unit passive resistance acting on the leading face of the block is equal to that of the pile cap with identical dimensions.

Because the dimensions of the treated block are known and the magnitude of additional resistance provided by adhesion

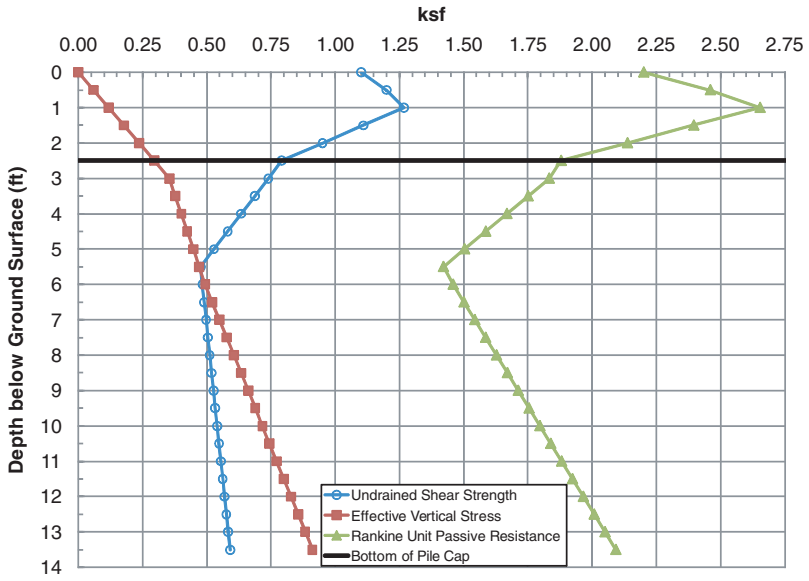

Figure 7-9. Variation of undrained strength, effective vertical stress and Rankine unit passive resistance vs depth at the virgin soil profile.

on the block is known, an adhesion factor (α_{pass}) can be determined based on a comparison of the adhesion acting on the block with the undrained shear strength of the soil. This adhesion factor represents the ratio of the adhesion to the undrained shear strength, a parameter that is similar but not identical to the alpha factor (α) used for the axial resistance of the driven piles (which was 0.85). Of course, considering the different construction methods and materials, there is no reason to assume that the adhesion on the treated block would be the same as the adhesion on a driven steel pile. From Figure 7-9, the average undrained shear strength acting along the depth of the pile cap (0 to 2.5 ft) is 1.07 ksf; the undrained shear strength adjacent to the bottom of the pile cap is 0.79 ksf. The adhesion factor (α_{pass}) can then be estimated as follows:

$$45\text{k} = (2\ \text{sides} \times 2.5\ \text{ft} \times 4\ \text{ft} \times 1.07\text{ksf} \times \alpha_{pass}) + (1\ \text{base} \times 9\ \text{ft} \times 4\ \text{ft} \times 0.79\text{ksf} \times \alpha_{pass})$$

$$\alpha_{pass} = 0.9 \quad (11)$$

Accordingly, a simplified approach to estimate the additional lateral resistance provided by a block of improved soil adjacent to the pile cap in the direction of loading has been developed. This simplified approach has been calibrated to the parametric studies conducted using an FE model and is presented in Chapter 6. The parametric studies, which utilized a model calibrated to the full-scale load test results, investigated the relative improvement of lateral resistance gleaned by varying both the width and depth of treatment. The results of these studies are shown in Figures 7-10 and 7-11.

Limitations Related to the Geometry of the Treated Soil Mass

The parametric FE studies generally indicate a linear increase in lateral resistance when the improvement dimension parallel to the direction of loading increases. Intuitively, this linear increase should continue to an upper bound that is defined by the entire soil layer around the pile cap and having the properties of the treated soil.

Alternatively, the relative amount of improvement with increasing depth of treatment is observed to decrease. Beyond a depth of about three times the pile cap embedment depth (equal to 7.5 ft for this study), relatively little increase in lateral resistance is observed. The small amount that is observed is likely a result of the treatment affecting the lateral behavior of the piles as opposed to only providing additional resistance to the cap. The simplified design approach presented herein conservatively neglects the slight additional resistance that may exist beneath a depth of three times the pile cap embedment depth.

Iterative analyses indicate the geometry of the constructed block (treated soil) is not identical to the constructed dimensions with regard to surface area available for passive and adhesive resistance. For this purpose, a "projected area" is proposed. The projected area is defined by a line projecting at a 52° angle from the heel of the leading edge of the pile cap through the treated block. All surface area above this projected line is available for either passive resistance or adhesion. This projected area is shown relative to the FE parametric study in Figures 7-12 and 7-13.

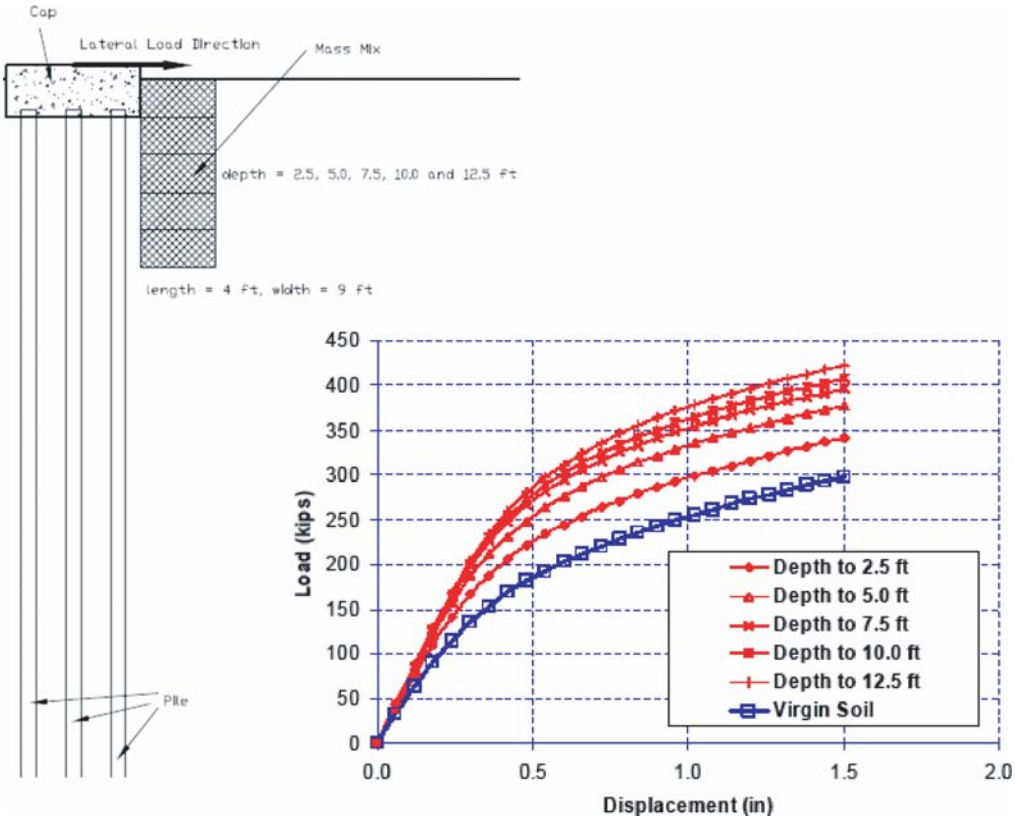

Figure 7-10. Results from FE parametric depth study for soil mixing.

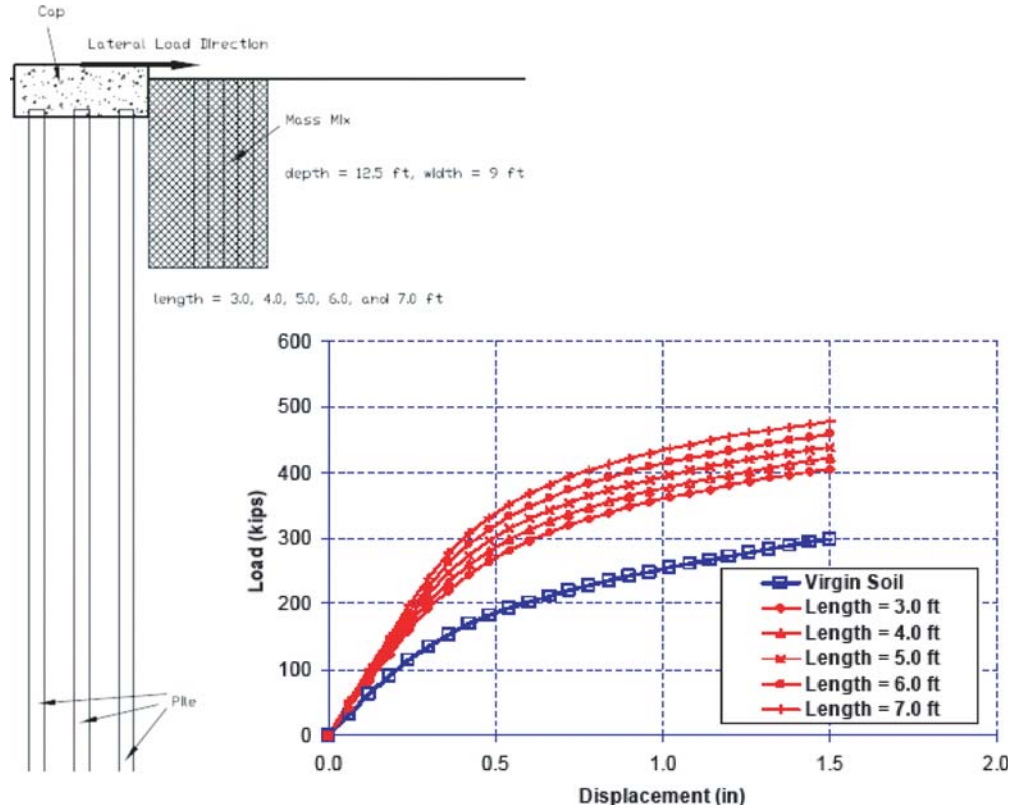

Figure 7-11. Results from FE parametric length study for mass mixing.

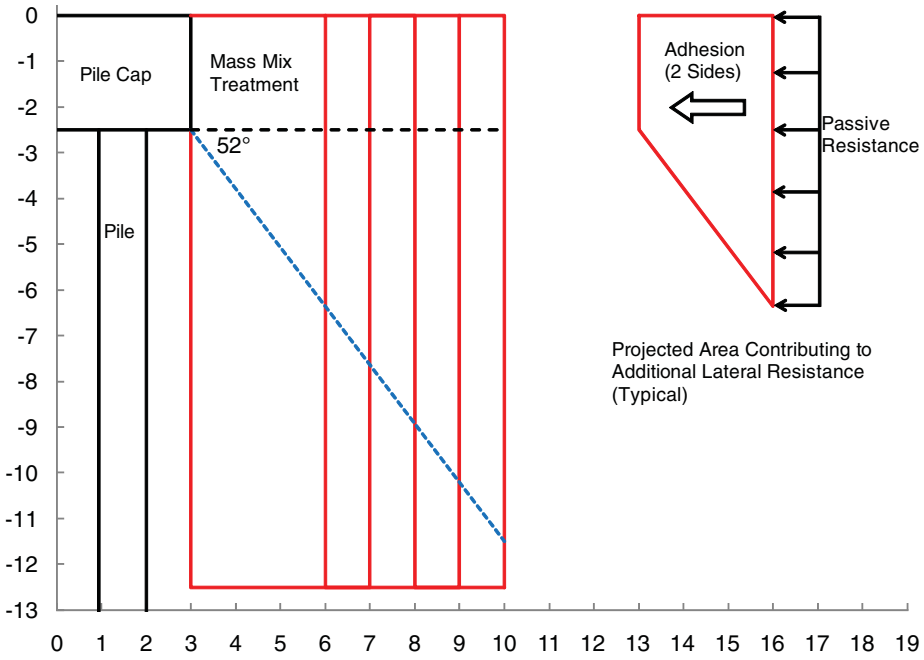

Figure 7-12. Projected area available for passive and adhesive resistance (1 of 2).

The 52° angle defining the projected area was determined to provide a best fit with respect to a comparison between the results of the parametric study and the simplified method. For design purposes, the projected area can conservatively be defined using a 45° angle, which is recommended. Furthermore, based on results of the FE parametric study as well as the investigated treatment geometries using a projected area defined by a 52° angle, the benefit of treatment and applicability of this simplified approach should be truncated at a depth equal to 3 times the pile cap embedment depth assuming the depth dimension of the treatment controls.

Note that the sides of the contributing treatment block defined by the projected area are trapezoidal in shape. Accordingly, a three-dimensional weighted average is necessary for

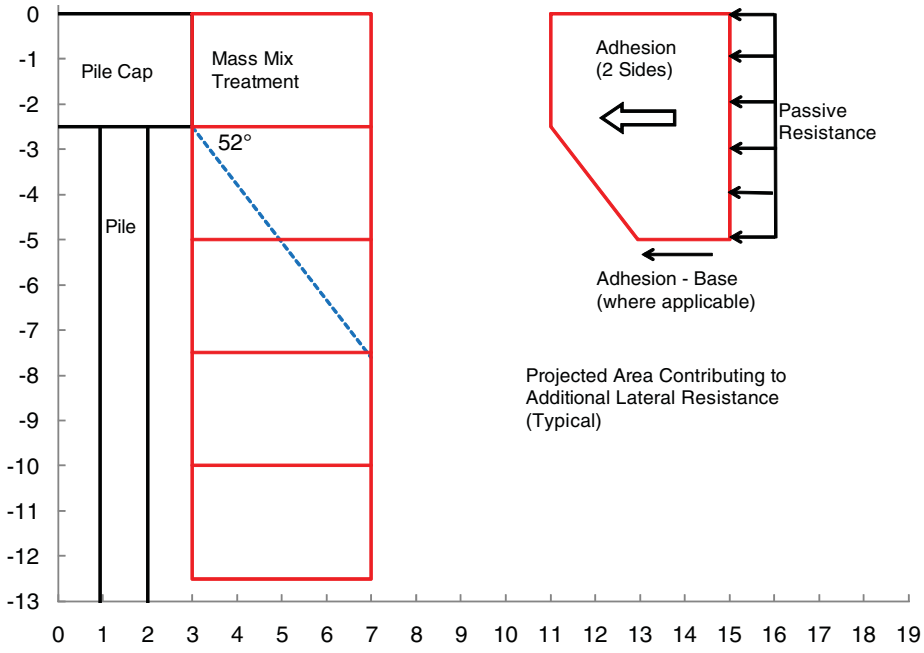

Figure 7-13. Projected area available for passive and adhesive resistance (2 of 2).

estimating the undrained shear strength acting along the sides (assuming the shear strength profile varies with depth). If the treatment block projected area contains a horizontal base, the adhesion acting on the base of the block also should be included. If the treatment depth is deeper, a tension crack is expected to develop behind the trapezoidal block beneath the bottom of the pile cap, thereby nullifying any base adhesion.

Incorporation of the Lateral Resistance from the Treated Soil Mass into the Analysis of the Pile Group

The proposed method decouples the limit equilibrium analysis of the treated soil mass from the analysis of the pile group. The magnitude of lateral resistance provided by the projected area is computed in accordance with the methodology outlined previously. In order to incorporate this contribution into the analysis of the foundation response using available software (such as GROUP or similar), the magnitude of the applied horizontal force acting on the pile group is reduced by the contribution of the treated soil mass.

To illustrate the applicability of this simplified approach, Figures 7-14 and 7-15 have been developed for comparison purposes. The plots in Figure 7-14 provide a comparison of results including the FE parametric studies involving changes in the treatment dimension parallel to the direction of loading. The FE results and projected area dimensions were presented in Figures 7-10 and 7-12, respectively. For all cases, the simplified approach is within 15% of the FE model. Less agreement is apparent for increasing dimensions of treatment, so extrapolation beyond the results investigated herein is not recommended. With any simplified approach, some discrepancy is anticipated, and 15% would appear to be within the realm of sufficient accuracy and precision for general design purposes.

The graph in Figure 7-15 provides a comparison of results including the FE parametric studies involving changes in the treatment depth. The FE results and projected area dimensions were presented in Figures 7-11 and 7-13, respectively. For all cases, excellent agreement is obtained and further substantiates truncating the projected area depth at three times the embedded pile cap depth.

7.5 Evaluation for Jet Grouting Cases

Similar to the mass mix tests, jet grout ground improvement techniques were performed in or around the pile groups and tested to evaluate the benefit on performance of the group under lateral loading. Jet grout ground improvement was constructed adjacent to Pile Cap 1 and the leading row of piles in the group, as shown in Figure 7-16. It also was constructed beneath Pile Cap 2 around the piles in the group.

The plan dimensions provided in Figure 7-16 indicate a treatment area of 10 ft perpendicular to the direction of loading and 15 ft parallel to the loading. The profile dimensions indicate ground improvement from the bottom of the pile cap to a depth of 12.5 ft below ground surface. All dimensions defining jet grout ground improvement must be considered as estimates only. Neat lines do not exist considering the nature of the jet grout process.

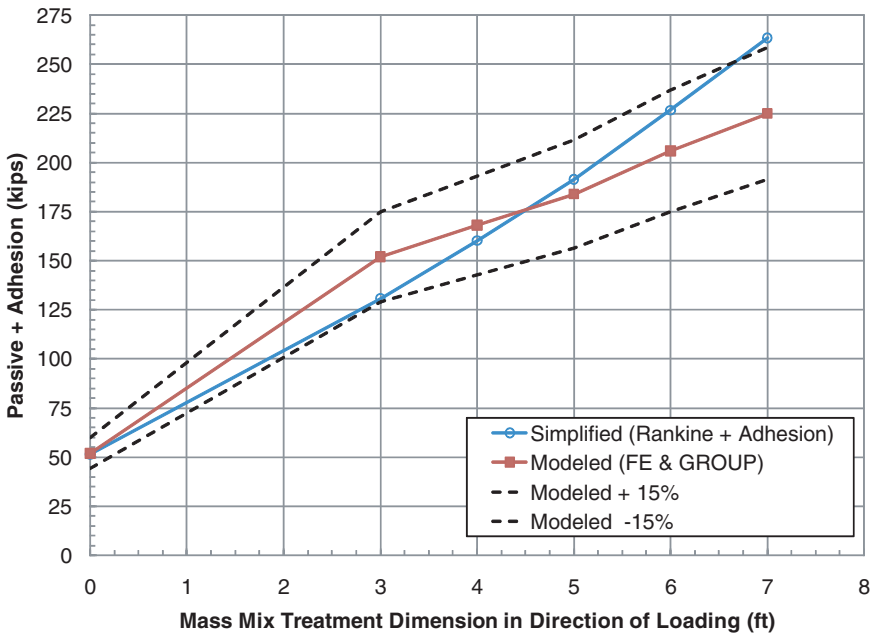

Figure 7-14. Simplified and FE results with varying treatment width.

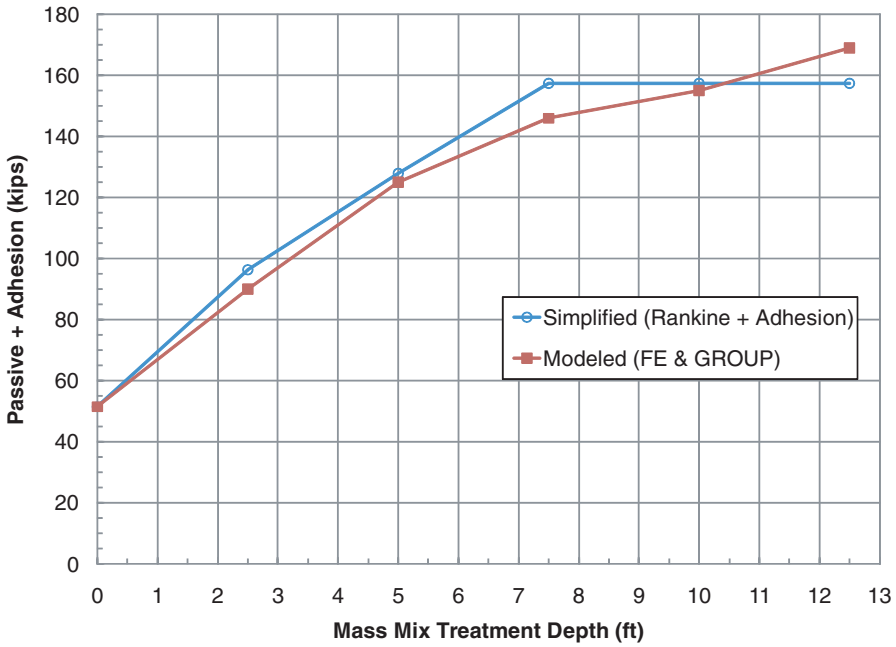

Figure 7-15. Simplified and FE results with varying treatment depth.

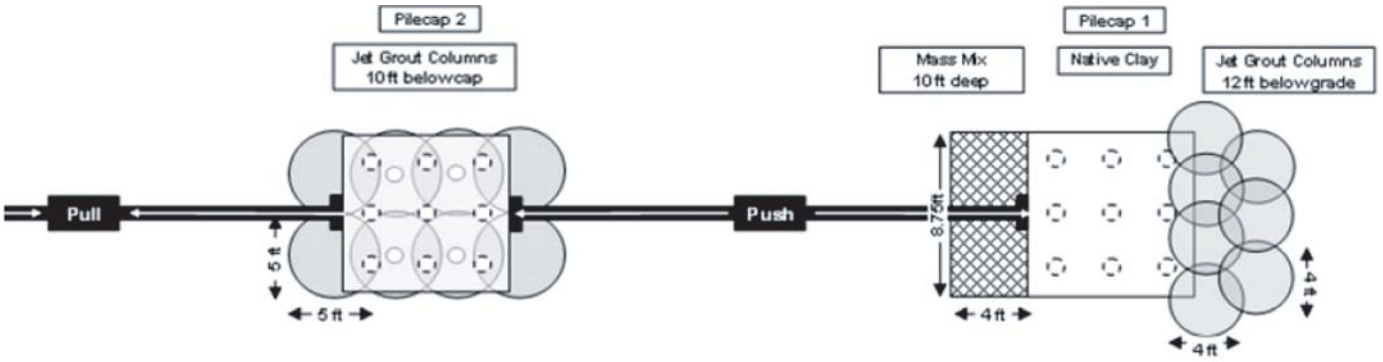

Schematic plan view of Test 4.

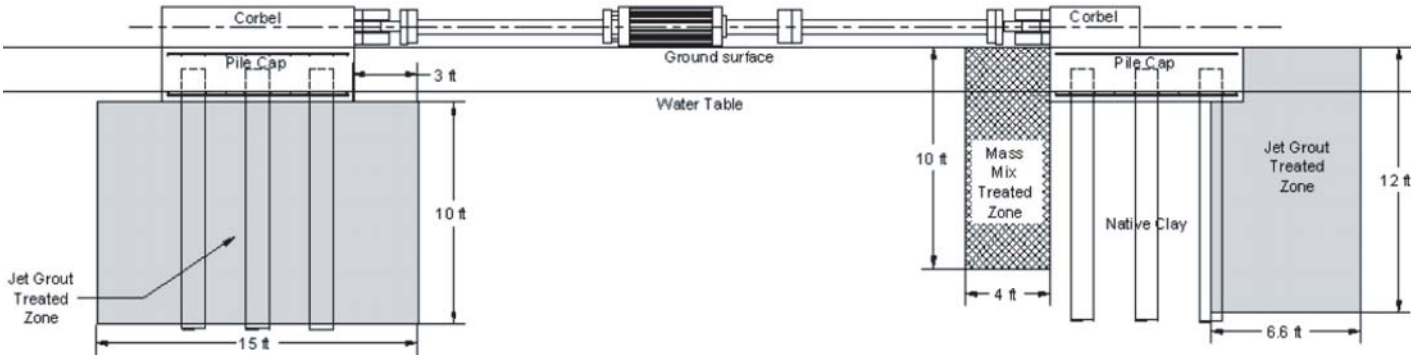

Figure 7-16. Layout of test for pile group with jet grout treatment.

The unconfined compressive strength of the jet grout improved soil at the time of the tests is estimated to be greater than 600 psi. Further discussion of the strength is provided in Chapter 4. However, the results of these analyses, as with the FE analyses, are not sensitive to the strength of the jet grout improved soil since it is significantly stronger than the in-situ soil.

The first attempt at testing the two groups was not successful. Because only one actuator was initially used, the load to produce significant deflection was not available. Accordingly, an additional actuator was used in series with the first to double the horizontal load applied to Cap 2. However, additional loading capacity was not available for Cap 1. The measured load-displacement curves for Caps 1 and 2 are provided in Figures 3-26 and 3-27, respectively. The maximum loading magnitude applied to Caps 1 is about 450k, slightly more than half the 800k maximum load applied to Cap 2. The 800k maximum load applied to Cap 2 appears to initiate an ultimate, or limit state, condition with excessive deflection under constant load.

The simplified procedure described previously is compared with the results of the jet grout ground improvement, based on the results measured at Cap 2 (jet grout beneath cap and around piles). Insufficient load versus deflection data exist for Cap 1 to draw definitive conclusions. However, based on the similar load-deflection behavior observed at both caps at relatively small displacements, and the applicability of the simplified procedure to mass mix or jet grout improved soils, it is considered reasonable that the simplified procedure is appropriate for conditions tested at Cap 1.

The lateral resistance provided by the jet grout ground improvement is estimated using a limit equilibrium approach, and the contribution of the improved soil incorporated into the analysis by reducing the magnitude of the applied force by the contribution to lateral resistance from the block of improved ground. This reduced force is then used in GROUP (or equivalent) to compute the response of the pile group separately from the contribution of the improved ground.

The passive resistance is estimated using Rankine earth pressure theory and should be truncated at a depth equal to the width of the group from outside pile edge to outside pile edge perpendicular to the direction of loading. The adhesive resistance along the sides of the treatment block, also truncated with depth, is estimated using α_{pass}=0.9 times the undrained shear strength. The undrained shear strength may be computed using a weighted average over the surface of the block. The adhesive resistance along the base should also be included in a similar manner to that along the sides. This simplified procedure is shown graphically in Figures 7-17 and 7-18 for the actual and simplified cases, respectively.

Considering the jet grout ground improvement geometry beneath Cap 2 and the unit passive resistance and shear strength versus depth data presented in Figure 7-9, the summation of passive and adhesive resistance can be estimated as follows for the truncated depth:

- Passive Resistance: 10 ft × 7.5 ft × 1.85ksf = 139k
  - where 10 ft is the treatment dimension perpendicular to loading,
  - where 7.5 ft is the truncated depth, and

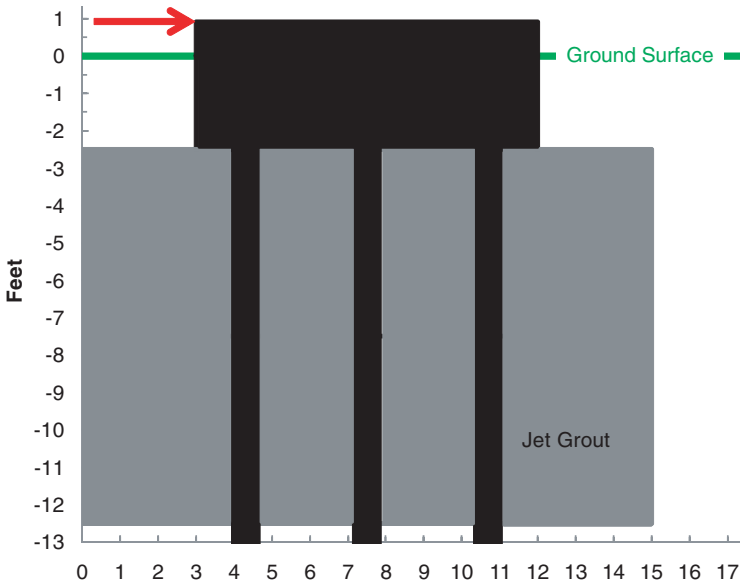

Figure 7-17. Jet grout test as performed (Cap 2).

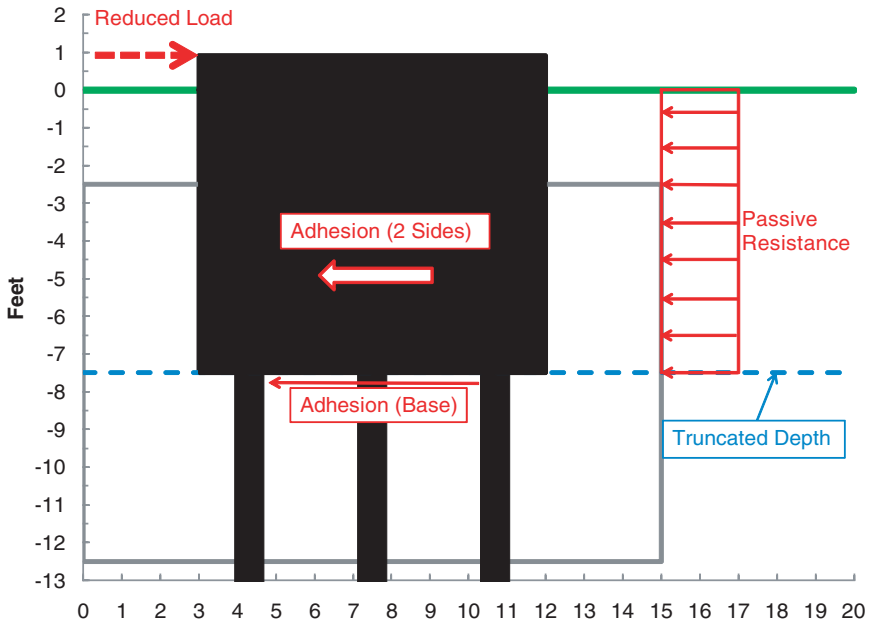

Figure 7-18. Forces on pile cap for simplified procedure for jet grout test.

  - where 1.85 ksf is the average unit passive resistance over the truncated depth.
- Adhesive Resistance (sides): 2 sides × 5 ft × 15 ft × 0.9 × 0.58ksf = 78k
  - where 5 ft is the truncated treatment depth beneath the cap (note the sides of the cap are not in contact with the soil),
  - where 15 ft is the treatment dimension parallel to loading,
  - where 0.9 is α_{pass}, and
  - where 0.58 ksf is the average undrained shear strength over this depth.
- Adhesive Resistance (base): 10 ft × 15 ft × 0.9 × 0.50ksf = 68k
  - where 10 ft is the treatment dimension perpendicular to loading,
  - where 15 ft is the treatment dimension parallel to loading,
  - where 0.9 is α_{pass}, and
  - where 0.50 ksf is the undrained shear strength at this depth.
- Therefore, reduce the applied load by: 139k + 78k + 68k = **285k**.

Alternatively, if the depth were not truncated, the summation of passive and adhesive resistance would be estimated as follows for the entire treatment depth:

- Passive Resistance: 10 ft × 12.5 ft × 1.84ksf = 230k
  - where 10 ft is the treatment dimension perpendicular to loading,
  - where 12.5 ft is the treatment depth, and
  - where 1.84ksf is the average unit passive resistance over the treatment depth.
- Adhesive Resistance (sides): 2 sides × 10 ft × 15 ft × 0.9 × 0.56ksf = 151k
  - where 10 ft is the truncated treatment depth beneath the cap (note the sides of the cap are not in contact with the soil),
  - where 15 ft is the treatment dimension parallel to loading,
  - where 0.9 is α_{pass}, and
  - where 0.56 ksf is the average undrained shear strength over this depth.
- Adhesive Resistance (base): 10ft × 15ft × 0.9 × 0.58ksf = 78k
  - where 10 ft is the treatment dimension perpendicular to loading,
  - where 15 ft is the treatment dimension parallel to loading,
  - where 0.9 is α_{pass}, and
  - where 0.58 ksf is the undrained shear strength at this depth.
- Therefore, reduce the applied load by: 230k + 151k + 78k = **459k**.

If the magnitude of the applied load is reduced by the amounts listed above (285k for truncated depth and 459k for full treatment depth), and applied considering the appropriate effective cap depth (7.5 ft and 12.5 ft beneath ground surface, respectively) using the GROUP model discussed above, good agreement with measured performance is obtained. A comparison of the results predicted using the aforementioned simplified procedure versus the measured data is provided in Figure 7-19.

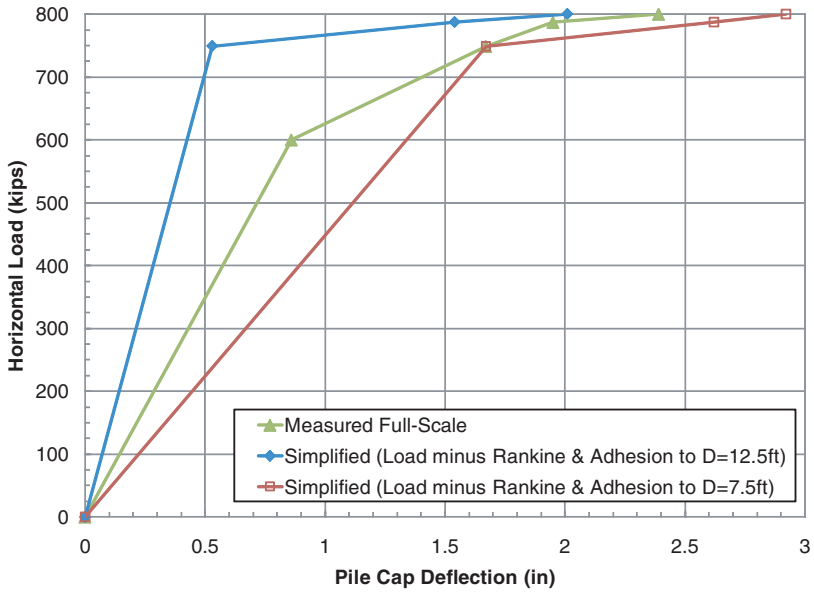

Figure 7-19. Comparison of simplified procedure to measured results.

Note that the simplified procedure as presented requires adjustment at lower magnitude loading because full passive resistance is not mobilized at small deflections. To compute the contribution of the treated block at less than full passive resistance, the method requires that the passive resistance be reduced to the mobilized resistance as a function of deflection. This condition would require an iterative approach using estimates of the mobilized passive resistance versus deflection.

A comparison of the measured and modeled (simplified procedure in conjunction with GROUP) behavior of the cap and center pile in the leading row is provided in Table 7-2. The proposed simple design procedure appears to provide reasonable agreement with full-scale test measurements, sufficient for general design purposes.

The results shown in Figure 7-19 indicate that the proposed procedure for truncating the depth of treated soil for design purposes produces a design that is slightly conservative. This slight conservatism seems appropriate for design, particularly when a simplified method is employed. Furthermore, the reduced benefit of treatment with depth is indicated by parametric analyses conducted using an FE model.

The results from the parametric FE model study are shown in Figure 7-20. Note that the ground improvement dimensions evaluated in the FE parametric study are slightly different to those constructed and tested in-situ. The effect of increasing the depth of treatment on lateral resistance is shown in Figure 7-20 where depth is relative to the ground surface. As indicated in Figure 7-20, the relative magnitude of the improvement in lateral resistance does not increase linearly in proportion to the depth of treatment. These results suggest that the proposed use of a truncated depth is a suitable simplification. Recall that the simplified procedure truncates the treated soil block at a depth equal to the outside-to-outside dimension of the piles in the group perpendicular to the direction of loading.

7.6 Design Recommendations

Pile Group Improved with Cemented Soils or Flowable Fill

Assuming that the treated soil has a compressive strength of at least 75 psi, the following simplified design approach is recommended for the purpose of estimating the additional lateral resistance provided by the ground improvement:

1. Based on the proposed geometry of the treatment area, compute the magnitude of passive resistance acting on

Table 7-2. Comparison of results from full-scale test and simplified procedure.

	Measured	Simplified
Pile Cap Rotation	0.76°	0.96°
Pile Deflection at a Depth of 7.5 ft beneath Ground Surface	1.14in	1.22in
Maximum Bending Moment in Leading Row, Center Pile	100 to 160 k-ft	195 k-ft
Depth to Maximum Moment beneath Ground Surface	15.5ft	13.5ft

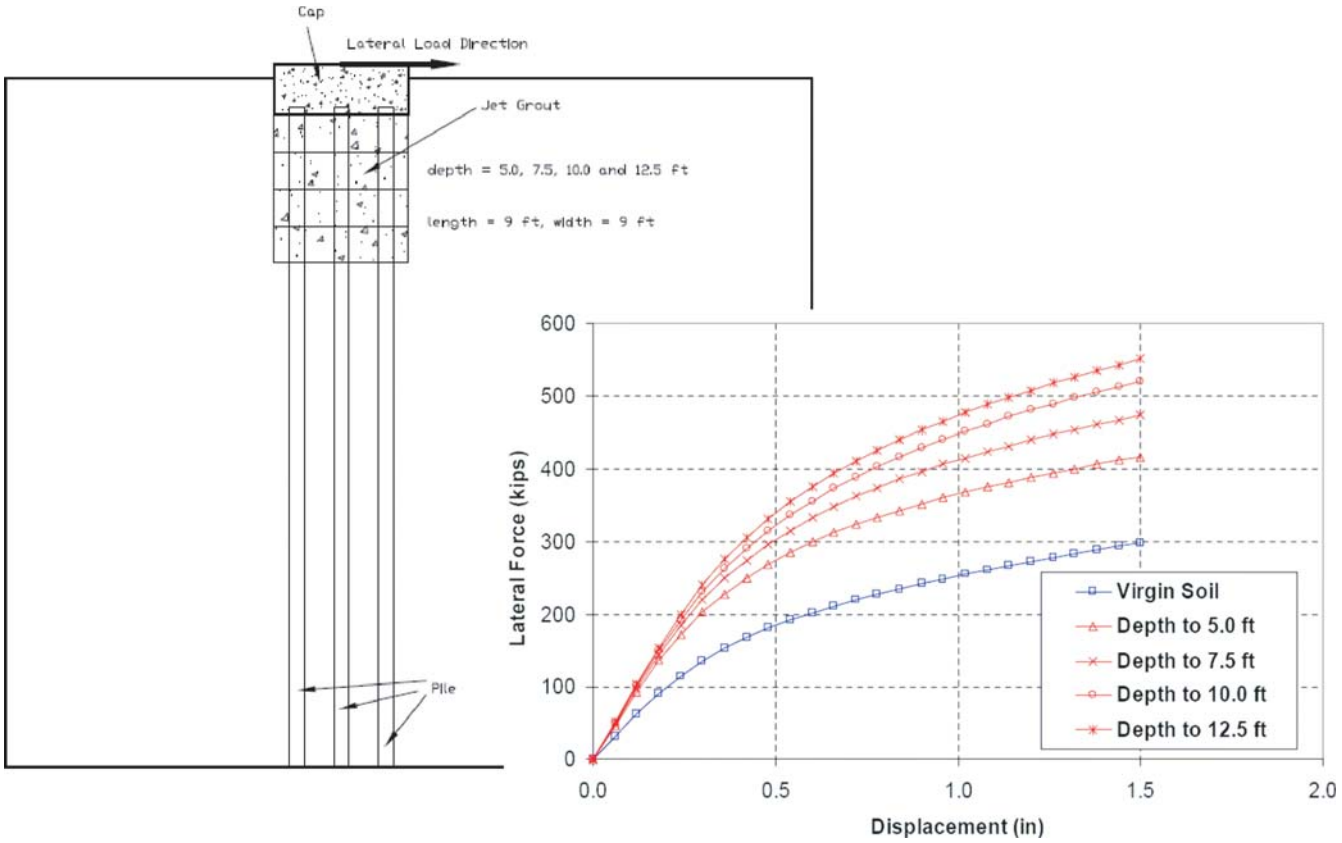

Figure 7-20. Summary of results from FEM parametric study of jet grout treatment.

the leading face of the block using Rankine earth pressure theory with the following constraints:

- The surface area of the leading face for passive resistance calculations should be the projected area defined by a 45° angle projecting from the pile cap (in all directions) if ground improvement is adjacent to the pile cap.
- The depth dimension of the projected area should be truncated at a depth below ground surface equal to the outside-to-outside dimension of the piles in the group perpendicular to the direction of loading.

2. Compute the magnitude of adhesion acting along the sides of the treatment block using $\alpha_{pass} = 0.9$. The sides of the contributing treatment block (defined by a 45° angle from the pile cap) are trapezoidal in shape and limited to the geometric constraints noted in Step 1. A three-dimensional weighted average is used to estimate the undrained shear strength acting along the sides (assuming the shear strength profile varies with depth). If the treatment block projected area contains a horizontal base, the adhesion acting on the base of the block also should be included. If the treatment depth is deeper and/or the base is not horizontal, a tension crack is expected to develop behind the trapezoidal block beneath the bottom of the pile cap, thereby nullifying any base adhesion.
3. Compute the total lateral resistance contributed by the treated block as the sum of the passive resistance and adhesion acting on the projected area of the treatment block. Reduce the external horizontal loading force magnitude applied to the pile cap by the lateral resistance contributed by the treated block.
4. Use the reduced horizontal forces described in Step 3 in GROUP (or a similar software package) to estimate the contribution of the pile group to the total foundation performance (e.g., deflection, moment, shear, etc.).
5. The total foundation resistance to force effects is the sum of the lateral resistance provided by the treated soil block and the lateral resistance provided by the pile group, (i.e., the unreduced foundation forces from Step 4).
6. If force-deflection calculations are necessary, the side shear can be assumed to develop with a displacement of approximately 0.25 in. and the passive force-displacement curve can be computed using a hyperbolic curve as described by Duncan and Mokwa (2001).

Example 1—Soil Cement Wall Adjacent to Pile Group

Consider a typical existing foundation for a bridge pier that includes a 3 × 4 group of 1-ft diameter piles spaced at

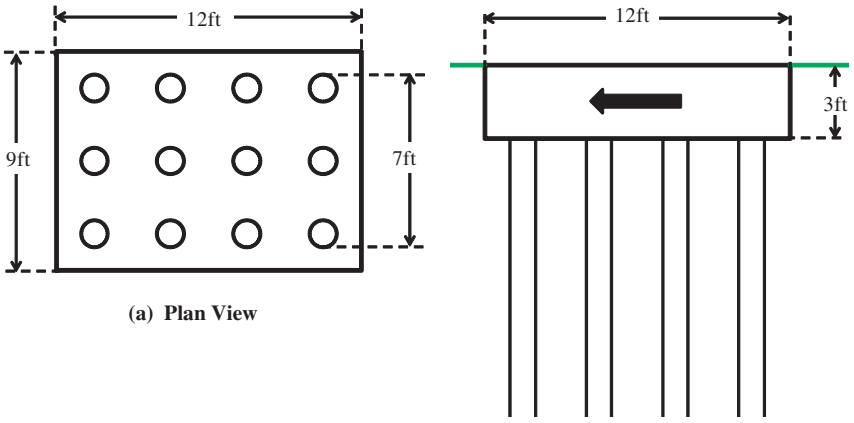

(a) Plan View

(b) Elevation View

Figure 7-21. Existing foundation prior to ground improvement.

a 3-ft center-to-center spacing in both directions as shown in Figure 7-21. The piles are structurally fixed (full moment connection) to a 3-ft-thick reinforced concrete pile cap. The top of the pile cap is at the ground surface. The direction of horizontal loading induced by the structure is as shown.

The soil is soft to medium clay with a uniform undrained shear strength of 500 lb/ft^2. The total unit weight of the soil is 110 lb/ft^3 and the water table is at a depth of 10 ft beneath the ground surface.

Due to an anticipated increase in structural demand applied to the foundation, the lateral resistance (geotechnical) provided by the existing foundation requires enhancement. Therefore, ground improvement is being considered as shown in Figure 7-22. The ground improvement involves introducing and mixing Portland cement into the virgin soil such that a mass of treated soil is created that substantially exceeds the in-situ strength of the virgin soil.

To model the geotechnical benefit provided by the ground improvement, the simplified method described herein is used to compute the additional resistance provided by the ground improvement. This additional resistance is then subtracted from the lateral demand imposed on the foundation. Upon determining the reduced lateral demand, the problem can be modeled as one would typically do using commercially available software such as GROUP, or similar. Note that when using GROUP, the option for considering an "embedded pile cap" should not be activated.

Analysis Procedure

1. Compute the magnitude of passive resistance acting on the projected area at the leading face of the ground

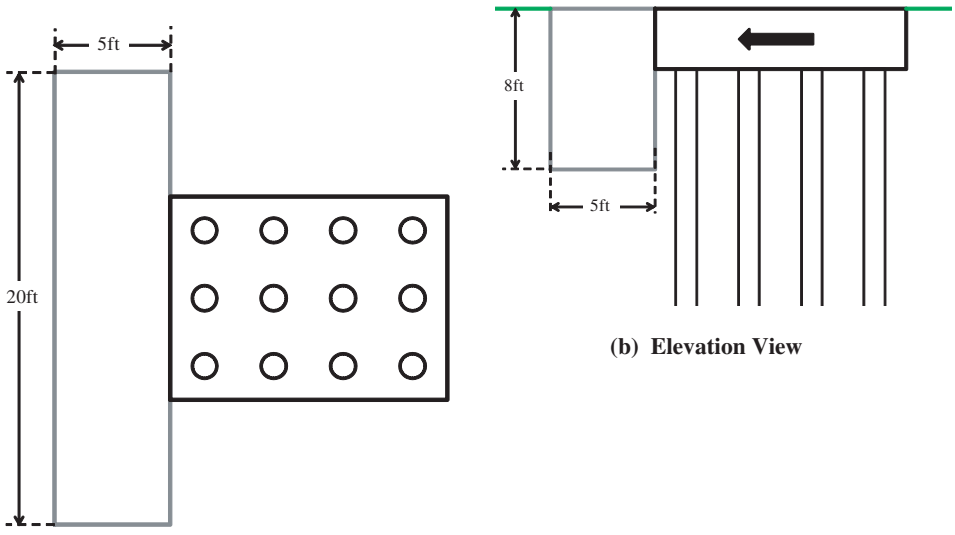

(a) Plan View

(b) Elevation View

Figure 7-22. Existing foundation after ground improvement.

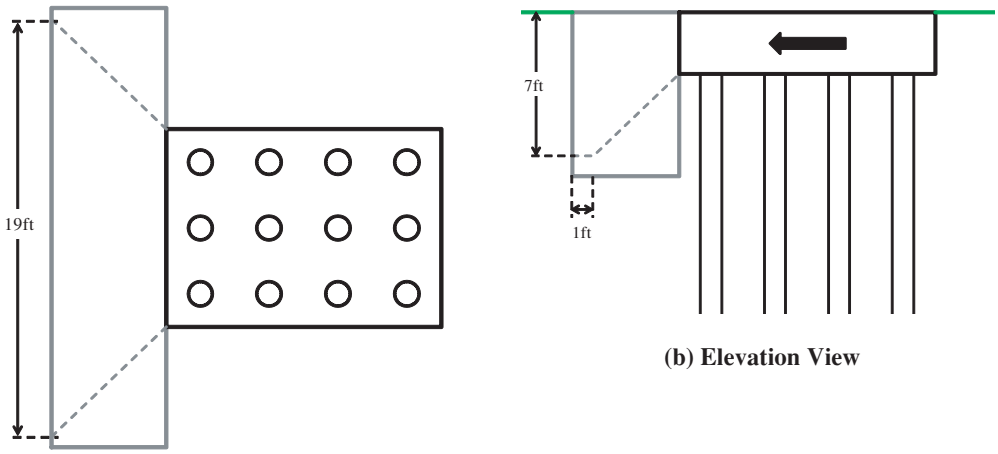

(a) Plan View

(b) Elevation View

Figure 7-23. Existing foundation after ground improvement with projected areas.

improvement block. The projected area is defined by 45° angles projecting from the pile cap edges (in all directions) and is truncated a depth below ground surface equal to the outside-to-outside pile spacing perpendicular to the direction of loading as follows (see Figure 7-23):

a. Projected Area of Leading Face, A_{LF}:

$$A_{LF} = 19\text{ ft} \times 7\text{ ft} = 133\text{ ft}^2$$

b. Average Effective Vertical Stress at Leading Face of Projected Area, σ'_v:

$$\sigma'_v = 110\text{ lb/ft}^3 \times 3.5\text{ ft} = 385\text{ lb/ft}^2$$

c. Passive Pressure Acting on Leading Face of Projected Area, p_p:

$$p_p = 2c_u + \sigma'_v = (2 \times 500\text{ lb/ft}^2) + 385\text{ lb/ft}^2 = 1{,}385\text{ lb/ft}^2$$

d. Passive Force Acting on Leading Face of Projected Area, F_p:

$$F_p = A_{LF} \times p_p = 133\text{ ft}^2 \times 1{,}385\text{ lb/ft}^2 = \mathbf{184k}$$

2. Compute the magnitude of adhesion acting along the sides and horizontal base (if applicable) of the projected area of the treatment block using an adhesion factor, α_{pass}, equal to 0.9.

a. Projected Area of Sides, A_S:

$$A_s = 2\text{ sides} \times [(5\text{ ft} \times 3\text{ ft}) + (1\text{ ft} \times 4\text{ ft}) + (\tfrac{1}{2} \times 4\text{ ft} \times 4\text{ ft})]$$
$$= 54\text{ ft}^2$$

b. Adhesion along Sides, $F_{\alpha s}$:

$$F_{\alpha s} = A_s \times \alpha_{pass} \times c_u = 54\text{ ft}^2 \times 0.9 \times 500\text{ lb/ft}^2 = 24\text{k}$$

c. Projected Area of Horizontal Base, A_b:

$$A_b = 19\text{ ft} \times 1\text{ ft} = 19\text{ ft}^2$$

d. Adhesion along Base, $F_{\alpha b}$:

$$F_{\alpha b} = A_b \times \alpha_{pass} \times c_u = 19\text{ ft}^2 \times 0.9 \times 500\text{ lb/ft}^2 = 9\text{k}$$

e. Cumulative Adhesion along Sides and Base, F_a:

$$F_\alpha = F_{\alpha s} + F_{\alpha b} = 24\text{k} + 9\text{k} = \mathbf{33k}$$

3. Compute the total lateral resistance contributed by the treated block, F, as the sum of the passive resistance, F_p, and cumulative adhesion, F_α, acting on the projected area of the treatment block:

$$F = F_p + F_a = 184\text{k} + 33\text{k} = \mathbf{217k}$$

4. Compute the reduced horizontal load to be used in foundation analyses, $P_{reduced}$, by subtracting the total lateral resistance contributed by the treated block, F, from the external horizontal loading force magnitude applied to the foundation, P:

$$P_{reduced} = P - F = \mathbf{P - 217k}$$

5. Use $P_{reduced}$ to analyze the foundation using commercially available software such as LPILE, GROUP, FBPier, etc.

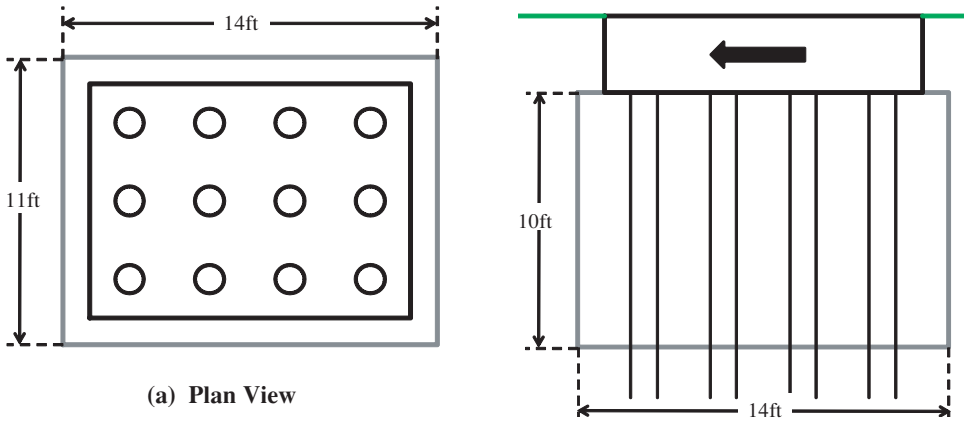

(a) Plan View

(b) Elevation View

Figure 7-24. Existing foundation after ground improvement.

Example 2—Soil Cement Wall Around a Pile Group

Consider the same pile group foundation and soil profile described in Example 1. Due to an anticipated increase in structural demand applied to the foundation, the lateral resistance (geotechnical) provided by the existing foundation requires enhancement. The ground improvement involves introducing and mixing Portland cement into the virgin soil beneath the cap and around the piles as shown in Figure 7-24 such that a mass of treated soil is created that substantially exceeds the in-situ strength of the virgin soil.

To model the geotechnical benefit provided by the ground improvement, the simplified method described herein is used to compute the additional resistance provided by the ground improvement (see Figure 7-25). This additional resistance is then subtracted from the lateral demand imposed on the foundation. Upon determining the reduced lateral demand, the problem can be modeled as one would typically do using commercially available software such as GROUP, or similar. Note that when using GROUP, the option for considering an embedded pile cap should not be activated.

Analysis Procedure

1. Compute the magnitude of passive resistance acting on the projected area at the leading face of the ground improvement block. The projected area is defined by 45° angles projecting from the outer edges of the piles and is truncated at a depth below ground surface equal to the outside-to-outside pile spacing perpendicular to the direction of loading as shown in:
   a. Projected Area of Leading Face, A_{LF}:

$$A_{LF} = 11\text{ ft} \times 7\text{ ft} = 77\text{ ft}^2$$

   b. Average Effective Vertical Stress at Leading Face of Projected Area, σ_v':

$$\sigma_v' = 110\text{ lb/ft}^3 \times \left[3.5\text{ ft} + \left(7\text{ ft} \div 2\right)\right] = 715\text{ lb/ft}^2$$

   c. Passive Pressure Acting on Leading Face of Projected Area, p_p:

$$p_p = 2c_u + \sigma_v' = \left(2 \times 500\text{ lb/ft}^2\right) + 715\text{ lb/ft}^2 = 1{,}715\text{ lb/ft}^2$$

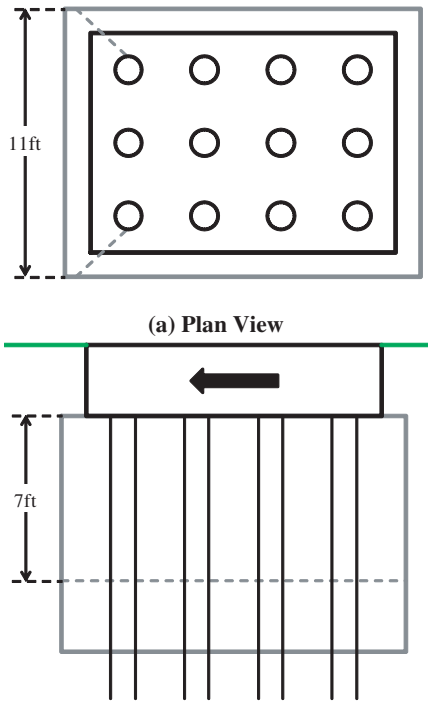

(a) Plan View

(b) Elevation View

Figure 7-25. Existing foundation after ground improvement with projected areas.

d. Passive Force Acting on Leading Face of Projected Area, F_P:

$$F_p = A_{LF} \times p_p = 77\ ft^2 \times 1{,}715\ lb/ft^2 = \mathbf{132k}$$

2. Compute the magnitude of adhesion acting along the sides and base of the projected area of the treatment block using an adhesion factor, α_{pass}, equal to 0.9.
   a. Projected Area of Sides, A_S:

$$A_s = 2\ sides \times (14\ ft \times 7\ ft) = 196\ ft^2$$

   b. Adhesion along Sides, $F_{\alpha s}$:

$$F_{\alpha s} = A_s \times \alpha_{pass} \times c_u = 196\ ft^2 \times 0.9 \times 500\ lb/ft^2 = 88k$$

   c. Projected Area of Base, A_b:

$$A_b = 11\ ft \times 14\ ft = 154\ ft^2$$

   d. Adhesion along Base, $F_{\alpha b}$:

$$F_{\alpha b} = A_b \times \alpha_{pass} \times c_u = 154\ ft^2 \times 0.9 \times 500\ lb/ft^2 = 69k$$

   e. Cumulative Adhesion along Sides and Base, F_a:

$$F_\alpha = F_{\alpha s} + F_{\alpha b} = 88\ k + 69k = \mathbf{157k}$$

3. Compute the total lateral resistance contributed by the treated block, F, as the sum of the passive resistance, F_p, and cumulative adhesion, F_α, acting on the projected area of the treatment block:

$$F = F_p + F_a = 132\ k + 157k = \mathbf{289k}$$

4. Compute the reduced horizontal load to be used in foundation analyses, $P_{reduced}$, by subtracting the total lateral resistance contributed by the treated block, F, from the external horizontal loading force magnitude applied to the foundation, P:

$$P_{reduced} = P - F = \mathbf{P - 289k}$$

5. Use $P_{reduced}$ to analyze the foundation using commercially available software such as LPILE, GROUP, FBPier, etc.

Adaptation for Pile Groups with Bent Caps

Some states use pile bents where piles extend from the ground to a support beam under the deck without including a pile cap in the ground. The piles then extend down below the bent cap, often through water, and into the ground without having a cap that comes in contact with the ground. The results of the field tests conducted during this study indicate that even though a pile cap is not present, the piles and cemented soil still function as a composite block, which increases the lateral resistance of the group. To apply the simplified method to this case, we recommend that an equivalent "pile cap" geometry be constructed to the outside edges of the pile group as illustrated in Figure 7-26. In this case, the base of the equivalent pile cap would be the top of the cemented soil zone. Using this equivalent pile cap geometry, the resistance can be estimated using the same approach as that described for the case with the piles in Examples 1 and 2.

Construction Considerations

For new construction, ground improvement can be performed most economically and efficiently if it is performed prior to foundation construction. Clearly, if piles or drilled shafts are not in place, then a wider variety of treatment methods can be employed to create a soilcrete block. For example, in the absence of piles, the soil could be treated to a depth of 5 meters using mass soil mixing. For high-moisture-content soils, the dry method could be used while the wet method could be used for other soils. Wet or dry mixing by column methods could be performed to much deeper depths, if necessary. Piles could be driven through the treated soil if driving was performed within a day or two after treatment, otherwise, pre-drilling might be required. If new piles were driven prior to soil treatment, soil mixing techniques could still be used to treat the soil around the periphery of the pile group prior to construction of the cap so that the treated soil would be in direct contact with the exterior piles. However, jet grouting would be required to treat the soil between the piles to create intimate contact between the interior piles and the treated soil. Because jet grouting is more expensive than other treatment methods and the piles would restrict access, the cost of treatment would be high.

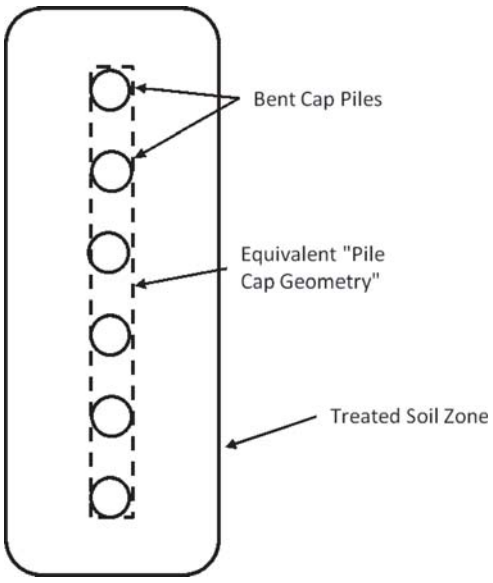

Figure 7-26. Equivalent pile cap geometry for use with piles with a bent cap.

For retrofit of existing structures where piles and pile caps are already in place, soil mixing methods could be used to create a soilcrete wall adjacent to the pile cap, but contact would not be achieved between the underlying piles and the treated soil. Jet grouting would allow the creation of a soilcrete zone around the periphery of the pile group that would also be in contact with the piles below the cap to improve lateral resistance. Core drilling through the pile cap would be required to allow jet grouting to be performed below the pile cap that would again increase the cost of treatment.

Pile Group Improved by Excavating Clay and Replacing with Compacted Granular Fill

Based on available test results and limited numerical results, the compacted granular zone should extend at least 6 pile diameters below the ground surface and 10 pile diameters beyond the edge of the pile face in the direction of loading. The lateral resistance can then be analyzed using the properties of the compacted fill with a computer program such as GROUP.

Pile Group Improved by Compacting Narrow Dense Granular Soil Adjacent to the Pile Cap in Loose Sand

The dense compacted granular zone should have a minimum width of 3 ft and extend 2 ft below the base of the pile cap or abutment back wall. In addition, the granular zone should be compacted to a minimum of 95% of the modified Proctor maximum unit weight. The passive resistance for the pile cap can then be computed using the following procedure:

1. Compute the ultimate passive force per width (E_p) for the dense granular zone using the pile cap or abutment backwall height (H) and unit weight (γ) of the dense granular soil using the equation:

$$E_p = 0.5\gamma H^2 K_p \cos\delta \quad (12)$$

   Use the log-spiral method to compute the Kp value with the friction angle of the dense granular zone and a wall friction (δ) equal to 0.7 times the friction angle of the soil.
2. Compute the passive force ratio (PFR) for geometry and frictional properties of the dense and loose granular soils using Equation 1.
3. Multiply the passive force computed in Step 1 by the PFR to obtain the horizontal passive force per length for the combined geometry.
4. For long abutments, multiply the passive force per length by the actual length of the abutment wall to obtain the total horizontal passive force on the wall. For pile caps, multiply the passive force per length by the effective width of the cap, which is equal to the actual width of the cap multiplied by the R_{3D} factor to account for 3D end shear effects.

CHAPTER 8

Conclusions

Based on the results of the literature review, full-scale field testing, numerical analyses, and—finally—the simplified analyses, the following conclusions have been developed:

1. Significant increases in the lateral resistance of bridge foundations can be achieved by soil improvement techniques. The greatest benefits will typically be achieved when improving soft clays; however, significant improvement is also possible with loose sands.
2. Excavating soft clay and replacing it with compacted granular fill increases the lateral pile-soil resistance as well as the lateral passive resistance on the pile cap. Typical increases in lateral resistance are 10% to 50%, with the highest increases occurring when the contrast in strength is the greatest. The compacted granular fill should extend 5 pile diameters below the ground surface and 10 pile diameters beyond the face of the piles to obtain the full lateral resistance of the granular soil.
3. Ground improvement techniques such as soil mixing and jet grouting can create a cemented volume of "soilcrete" in-situ with compressive strengths of 100 to 600 psi. This soilcrete block is most effective when it encompasses the entire pile group below the cap, although significant improvement also can be obtained with soilcrete walls around the periphery of the pile group. During full-scale lateral load testing, jet grouting below a pile cap increased lateral resistance by 500 kips or (160%) relative to the 280 kip lateral resistance in untreated clay. Soilcrete walls produced by jet grouting and soil mixing adjacent to a pile group produced increases of 400 kips (185%) and 170 kips (60%), respectively, relative to untreated conditions.
4. Under lateral loading, the soilcrete zone tends to move as a block and develop increased lateral resistance from passive force on the back of the block and adhesion on the sides of the block, rather than increased pile-soil resistance. This lateral resistance can be computed using the principles of basic soil mechanics for passive force and side shear under undrained conditions with some adjustments. Numerical analyses suggest that soilcrete block depths greater than about 10 ft will provide limited increased benefit for a lateral deflection limit of 1.5 in. at the pile cap.
5. A cemented block also can be efficiently created by excavating soft clay and replacing it with flowable fill. The flowable fill can be placed below a pile cap prior to pile driving or around the periphery of the pile group after driving. In comparison with in-situ treatments, it is necessary to maintain a stable excavation after excavation, which may be difficult in soft clay. In this study, problems were encountered in obtaining a consistent compressive strength of the flowable fill. In addition, tests performed 2 years after treatment showed strength degradation in test specimens.
6. Numerical analyses suggest that the lateral resistance of the soilcrete block is relatively insensitive to the strength of the soilcrete. Therefore, soil improvement techniques that can produce a compressive strength greater than 100 psi may be sufficient for practical purposes. Shear calculations can be used to check the minimum strength requirement.
7. Full-scale field tests and FEM analyses indicate that placement of a narrow dense compacted granular zone adjacent to a pile cap or abutment in loose sand can significantly increase the lateral passive resistance provided by the cap. Typically, when the width of the dense zone is equal to the cap height, the passive resistance is increased to about 60% of that which would be obtained for a homogenous dense backfill extending about four times the height of the cap. A generalized equation can be used to compute the percentage of the passive force as a function of backfill width, dense sand friction angle, and loose sand friction angle.
8. Simple cost comparisons indicate that ground improvement techniques have the potential to produce increased lateral pile group resistance at significantly less cost than would be obtained by simply driving more piles and extending the pile cap. Although costs are expected to vary with locality, these results make it clear that engineers should investigate this alternative as part of their overall effort to produce a cost-effective foundation solution.

References

Adsero, M. E., "Effect of Jet Grouting on the Lateral Resistance of Soil Surrounding Driven-Pile Foundations" (M. S. Thesis, Brigham Young University, Provo, UT, 2008).

ASCE (1997), "Ground Improvement, Reinforcement and Treatment: A Twenty Year Update and Vision for the 21st Century," ASCE Geo-Institute Conference, July 1997 (*Geotechnical Special Publication No. 69*).

Ashford, S. A., Rollins, K. M, and Baez, J. I. (2000a), "Comparison of Deep Foundation Performance in Improved and Non-Improved Ground Using Blast-Induced Liquefaction," ASCE, *Geotechnical Special Publication 107,* Soil Dynamics and Liquefaction 2000, 35–57.

Ashford, S. A., Rollins, K. M., Bradford, S. C., Weaver, T. J., Baez, J. I. (2000b), *Transportation Research Record 1736: Liquefaction Mitigation Using Stone Columns Around Deep Foundations: Full-Scale Test Results,* Transportation Research Board, Washington, D.C., 110–118.

Brown, D. A., Morrison, C., and Reese, L. C. (1988), "Lateral Load Behavior of a Pile Group in Sand," *Journal of Geotechnical Engineering,* ASCE, 114(11): 1261–1276.

Brown, D. A., Reese, L. C., and O'Neill, M. W. (1987), "Behavior of a Large Scale Pile Group Subjected to Cyclic Lateral Loading," *Journal of Geotechnical Engineering,* ASCE, 113(11): 1326–1343.

Burke, G. (2004), "Jet Grouting Systems: Advantages and Disadvantages," *ASCE Geotechnical Special Publication No. 12:* 875–886.

Cole, R. T and Rollins, K. M. (2006), "Passive Earth Pressure Mobilization During Cyclic Loading," *Journal of Geotechnical and Geoenvironmental Engineering,* 132(9): 1154–1164.

Duncan, J. M. and Mokwa, R. L. (2001), "Passive Earth Pressures: Theories and Tests," *Journal of Geotechnical and Geoenvironmental Engineering,* ASCE 127(3): 248–257.

Gerber, T. M., Rollins, K. M., Cummins, C. R., and Pruett, J. M. (2010), *Dynamic Passive Earth Pressure on Abutments and Pile Caps.* Final report prepared for Utah Department of Transportation Research Division Lead Agency for Pooled-Fund Study. Unpublished raw data.

Herbst, M. A. "Impact of Mass Mixing on the Lateral Resistance of Driven-Pile Foundations" (M. S. Thesis, Brigham Young University, Provo, UT, 2008).

Kulhawy, F. H. and Mayne, P. W. (1990), *Manual on Estimating Soil Properties for Foundation Design,* Report EPRI EL-6800, Electric Power Research Institute, Palo Alto, CA.

Lemme, N. A., "Effectiveness of Compacted Fill and Rammed Aggregate Piers on Lateral Resistance of Pile Foundations" (MS Thesis, Brigham Young University, Provo, UT, 2010).

Miner, D. E., "The Effect of Flowable Fill on the Lateral Resistance of Soil Surrounding Driven-Foundations" (MS Thesis, Brigham Young University, Provo, UT, 2009).

Mitchell, J. K. (1981), "Soil Improvement – State-of-the-Art Report," *Proceedings of the Tenth International Conference on Soil Mechanics and Foundation Engineering,* Stockholm, Sweden, June 1981, 509–565.

Mokwa, R. L. and Duncan J. M. (2001). "Experimental Evaluation of Lateral-Load Resistance of Pile Caps," *Journal of Geotechnical and Geoenvironmental Engineering,* ASCE 127(2): 185–192.

Reese, L. C., Wang, S. T., Isenhower, W. M., and Arrellaga, J. A. (2004a), "LPILE Plus v5.0 for Windows: A Program for the Analysis of Piles and Drilled Shafts under Lateral Loads," *Technical Manual,* Ensoft, Inc., Austin, TX.

Resse, L. C., Wang, S. T., Arrellaga, J. A., and Hendrix, J. (2004b), *GROUP Version 5.0 for Windows: Users Manual,* Ensoft, Inc. Austin, TX.

Rollins, K. M. and Cole, R. T. (2006), "Cyclic Lateral Load Behavior of a Pile Cap and Backfill," *Journal of Geotechnical and Geoenvironmental Engineering,* ASCE 132(9): 1143–1153.

Rollins, K. M., Gerber, T. M., and Ku Hyun Kwon (2010), "Increased Lateral Abutment Resistance from Gravel Backfills of Limited Width," *Journal of Geotechnical and Geoenvironmental Engineering,* ASCE 136(1): 230–238.

Rollins, K. M., Snyder, J. L., and Broderick, R. D. (2005), "Static and Dynamic Lateral Response of a 15 Pile Group," *Proceedings, 16th Intl. Conf. on Soil Mechanics and Geotech. Engineering,* Millpress, Rotterdam, The Netherlands, Vol. 4: 2035–2040.

Rollins, K. M., Snyder, J. L., and Walsh, J. M. (2010), "Increased Lateral Resistance of Pile Group in Clay Using Compacted Fill," Proceedings, GeoFlorida 2010: Advances in Analysis, Modeling and Design, (*Geotechnical Special Publication No. 199*) ASCE 1602–1611.

Rollins, K. M. and Nasr, M. (2010), "Numerical Analysis of the Effectiveness of Limited Width Gravel Backfills in Increasing Lateral Passive Resistance." *Dynamic Passive Earth Pressure on Abutments and Pile Caps.* Final report prepared for Utah Department of Transportation Research Division Lead Agency for Pooled-Fund Study.

Rollins, K. M., Olsen, R. J., Egbert, J. J., Jensen, D. H., Olsen, K. G., and Garrett, B. H. (2006), "Pile Spacing Effects on Lateral Pile Group Behavior: Load Tests," *Journal of Geotechnical and Geoenvironmental Engineering,* ASCE 132(10): 1262–1271.

Terashi, M. and Juran, I. (2000), "Ground Improvement—State of the Art," In: *GeoEng2000: An International Conference on Geotechnical and Geological Engineering,* 19–24 November 2000, Melbourne, Vol. 1: 461–519.

Terashi, M. (2003), "The State of Practice in Deep Mixing Methods," *Grouting and Ground Treatment, Proceedings of the 3rd Intl. Conference,* L. F. Johnsen, D. A. Bruce, and M. J. Byle, eds., ASCE (Geotechnical Special Publication No. 120), Vol. 2: 25–49.

Weaver, T. J., Ashford, S. A., and Rollins, K. M. (2005), "Lateral Resistance of a 0.6 m Drilled Shaft in Liquefied Sand," *Journal of Geotechnical and Geoenvironmental Engineering,* ASCE 131(1): 94–102.

Weaver, T. J. and Chitoori, B. (2007), "Influence of Limited Soil Improvement on Lateral Pile Stiffness," *Proceedings, Geo-Denver, Soil Improvement,* (*Geotechnical Special Publication 172*) ASCE, Reston, VA, CD.

APPENDIX A

Schematic Drawings Showing the Layout of the 16 Lateral Pile Group Tests

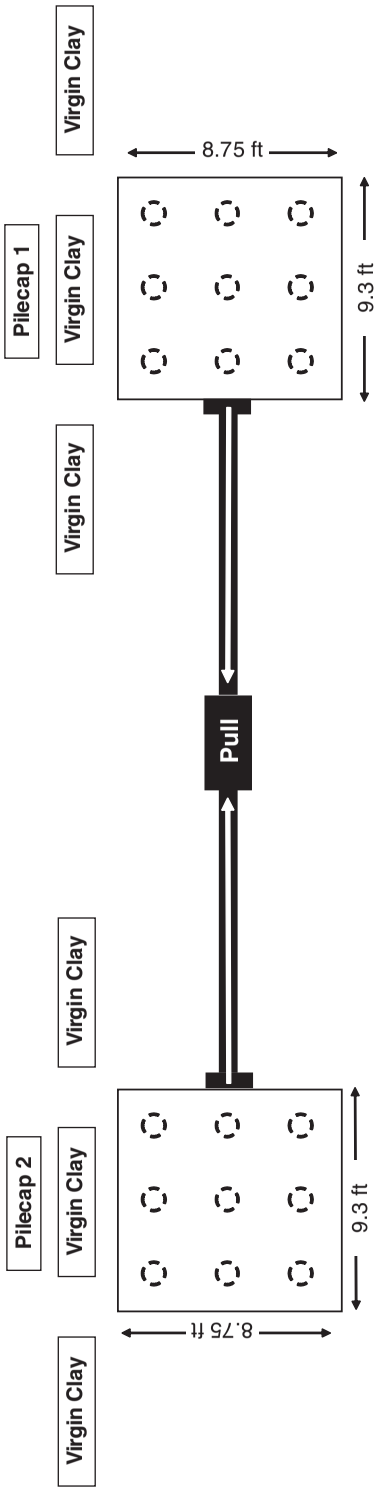

Figure A-1. Schematic layout of pile caps and soil treatments for Test 1.

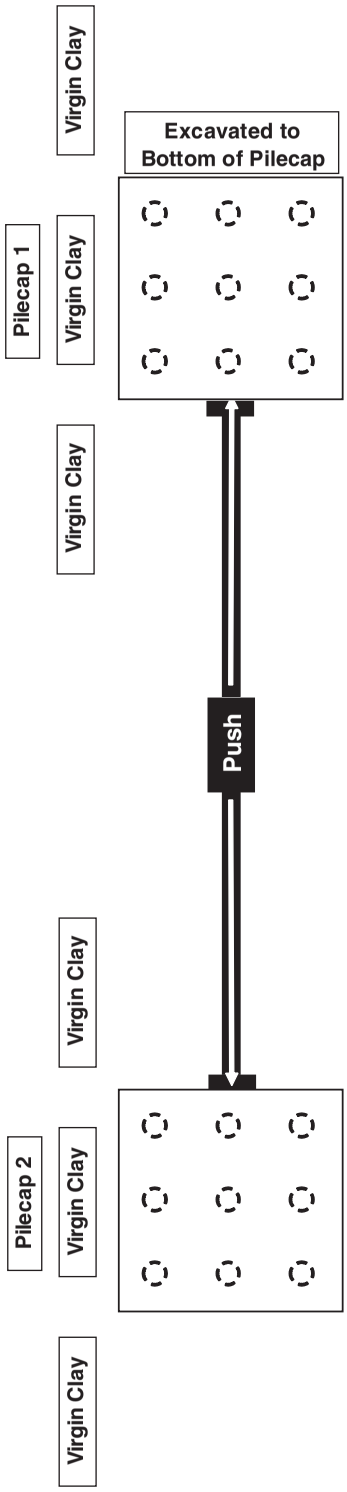

Figure A-2. Schematic layout of pile caps and soil treatments for Test 2.

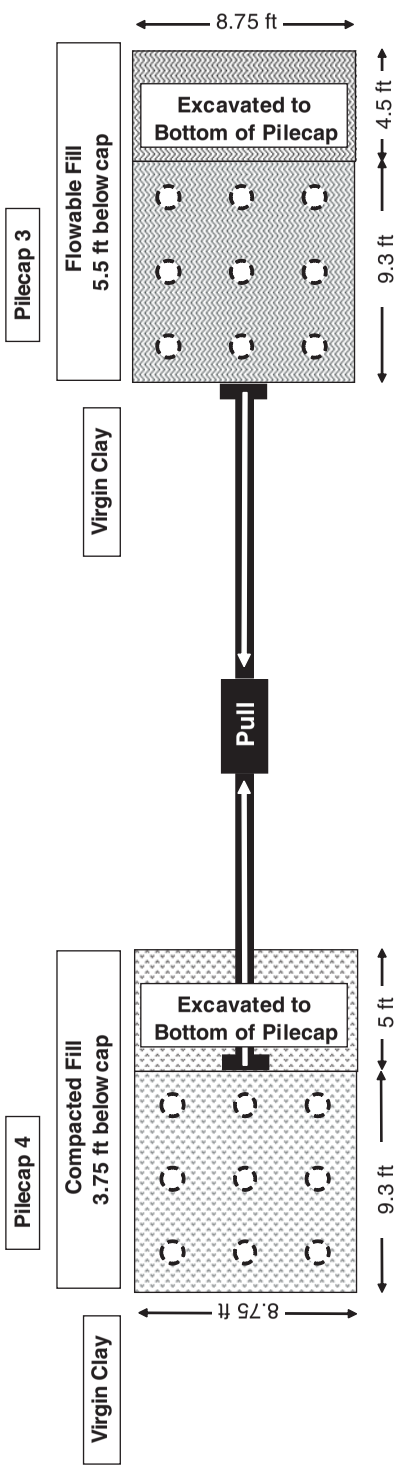

Figure A-3. Schematic layout of pile caps and soil treatments for Test 3.

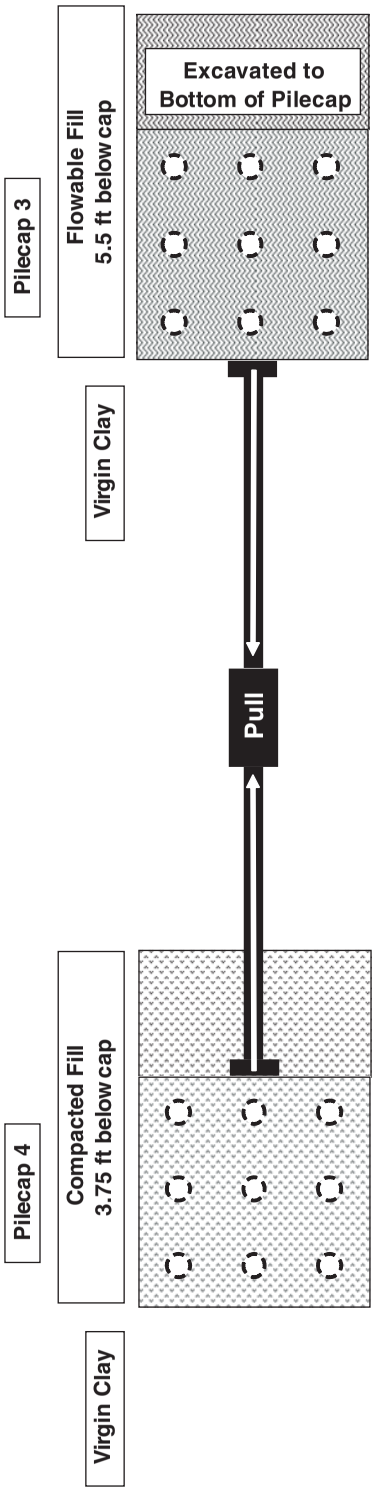

Figure A-4. Schematic layout of pile caps and soil treatments for Test 4.

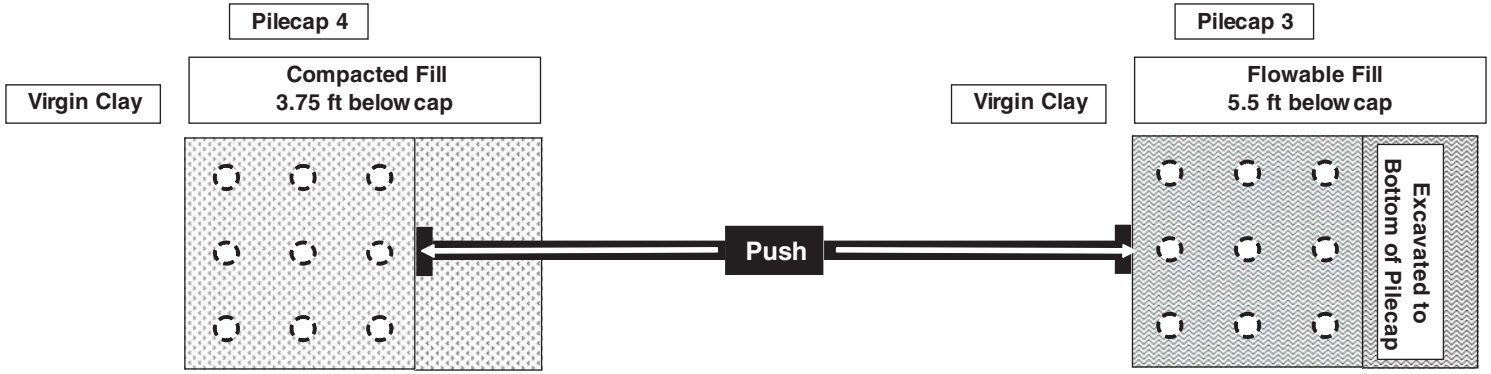

Figure A-5. Schematic layout of pile caps and soil treatments for Test 5.

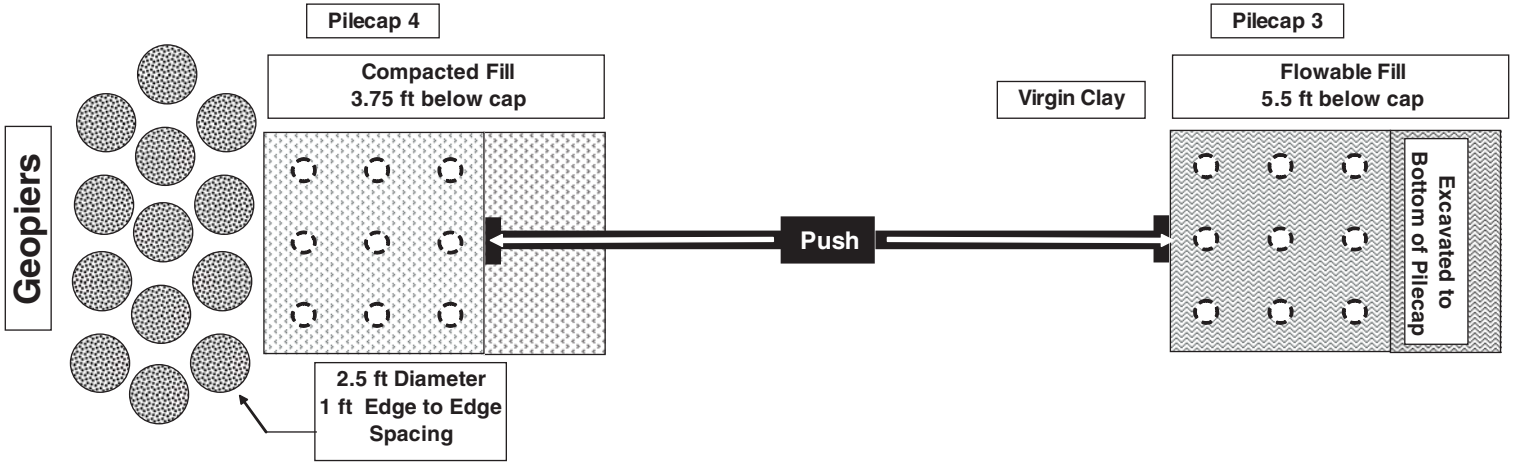

Figure A-6. Schematic layout of pile caps and soil treatments for Test 6.

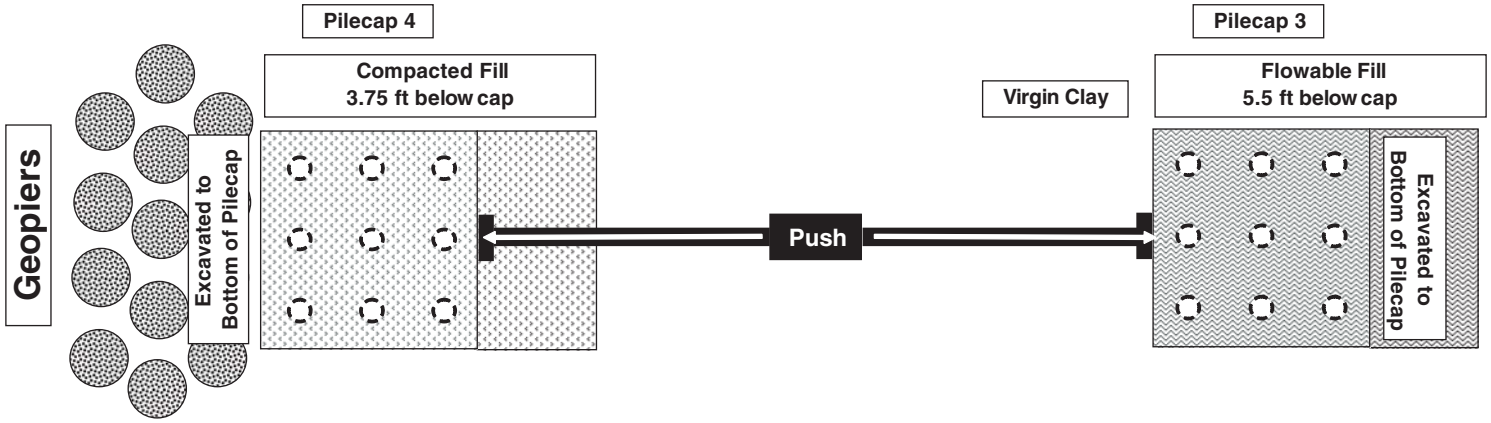

Figure A-7. Schematic layout of pile caps and soil treatments for Test 7.

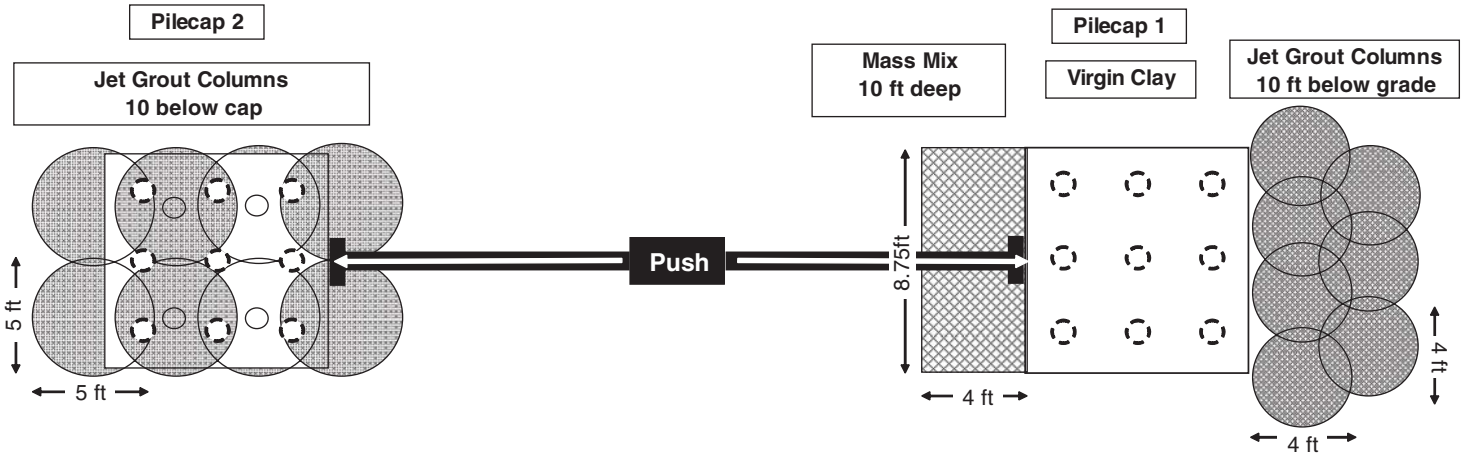

Figure A-8. Schematic layout of pile caps and soil treatments for Test 8.

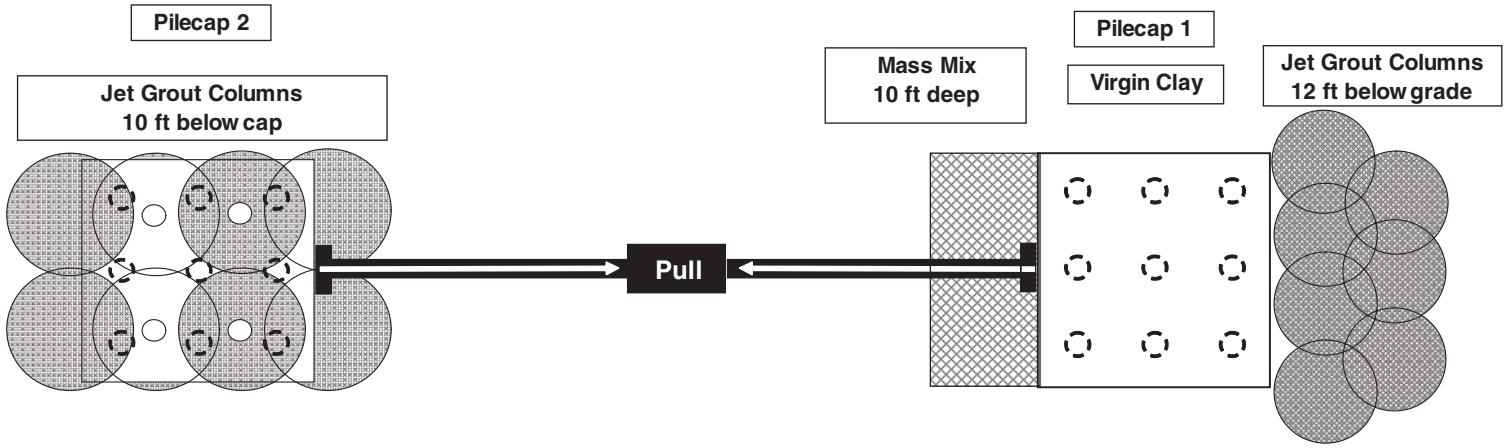

Figure A-9. Schematic layout of pile caps and soil treatments for Test 9.

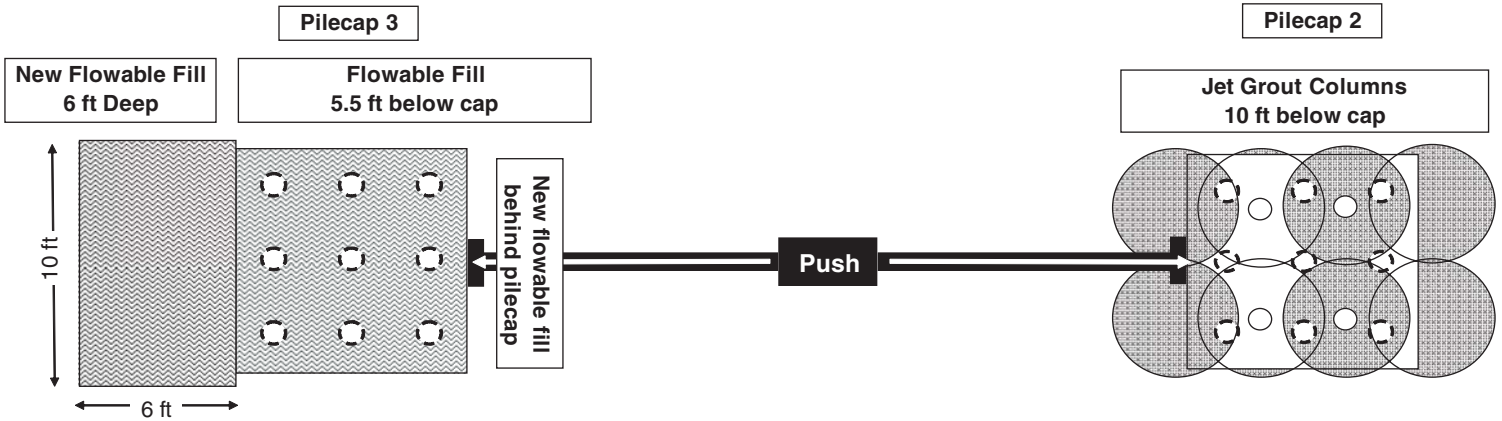

Figure A-10. Schematic layout of pile caps and soil treatments for Test 10.

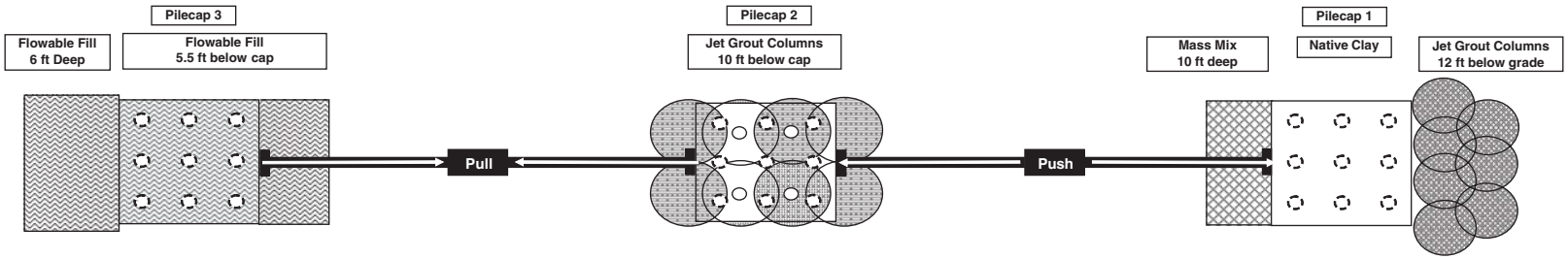

Figure A-11. Schematic layout of pile caps and soil treatments for Test 11.

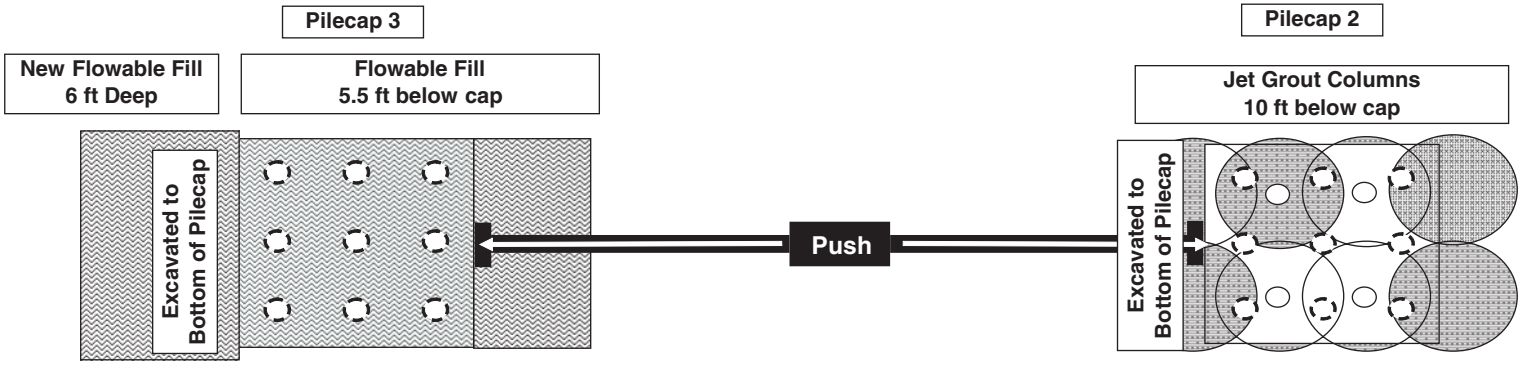

Figure A-12. Schematic layout of pile caps and soil treatments for Test 12.

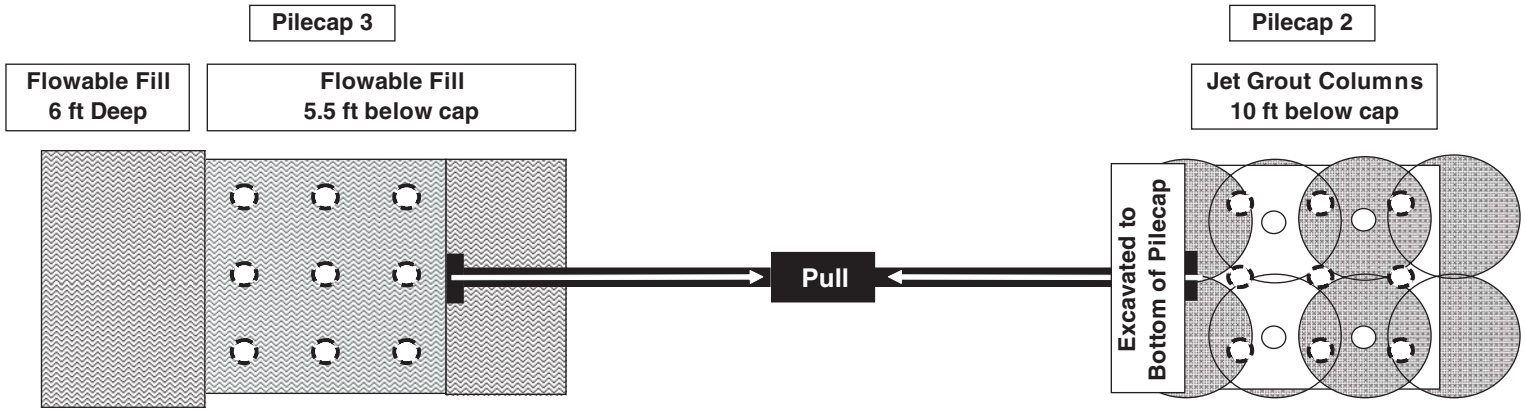

Figure A-13. Schematic layout of pile caps and soil treatments for Test 13.

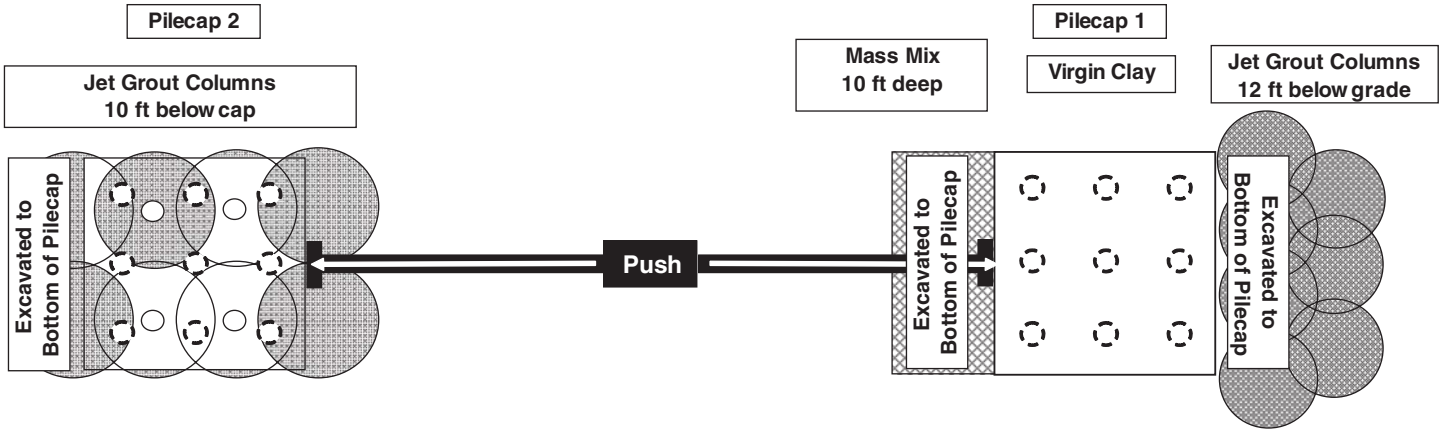

Figure A-14. Schematic layout of pile caps and soil treatments for Test 14.

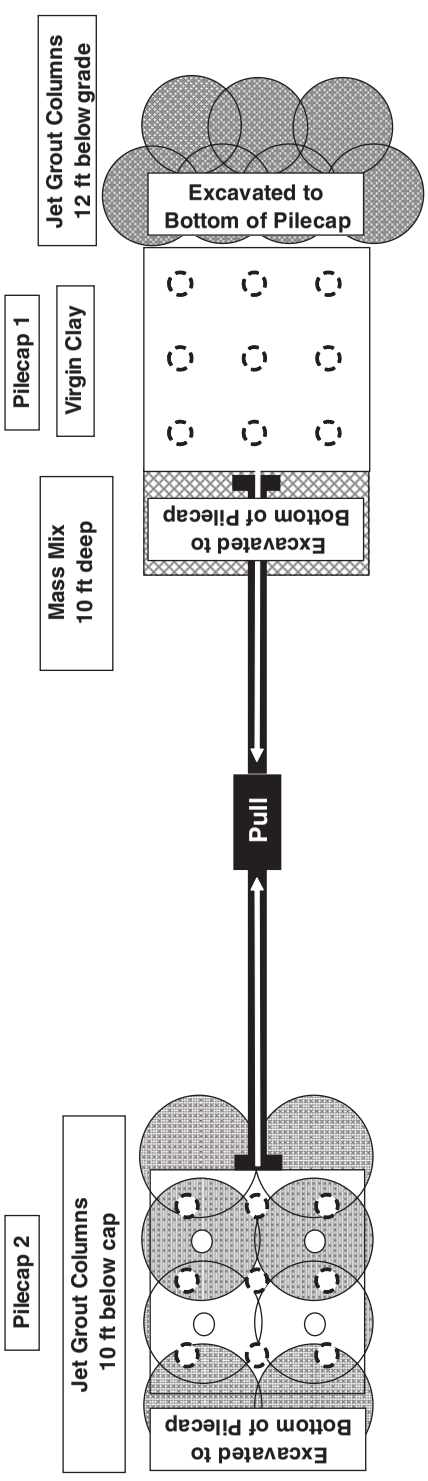

Figure A-15. Schematic layout of pile caps and soil treatments for Test 15.

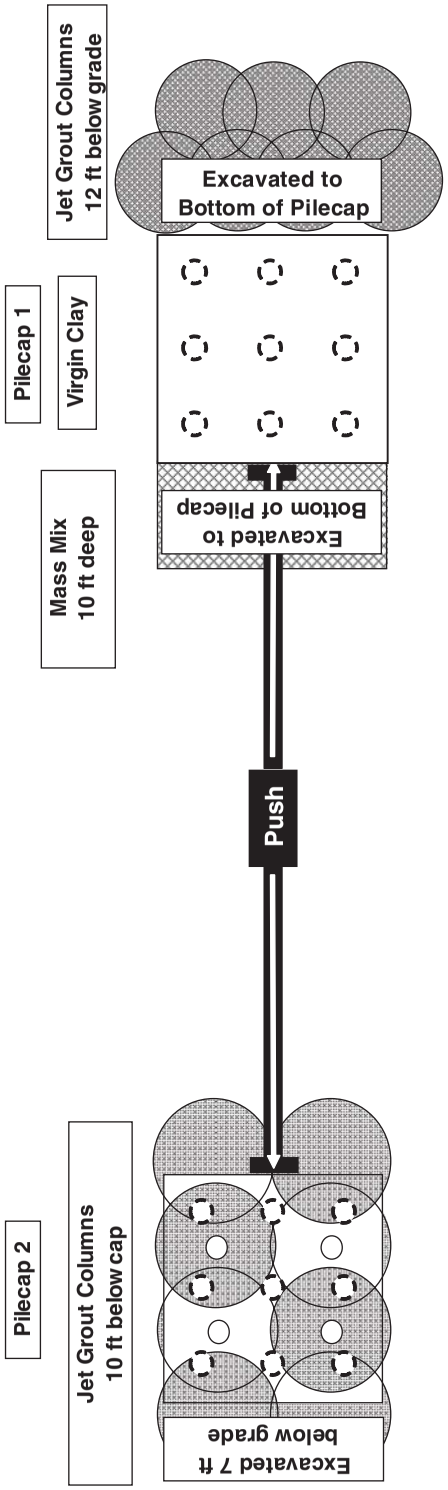

Figure A-16. Schematic layout of pile caps and soil treatments for Test 16.

Abbreviations and acronyms used without definitions in TRB publications:

AAAE	American Association of Airport Executives
AASHO	American Association of State Highway Officials
AASHTO	American Association of State Highway and Transportation Officials
ACI–NA	Airports Council International–North America
ACRP	Airport Cooperative Research Program
ADA	Americans with Disabilities Act
APTA	American Public Transportation Association
ASCE	American Society of Civil Engineers
ASME	American Society of Mechanical Engineers
ASTM	American Society for Testing and Materials
ATA	Air Transport Association
ATA	American Trucking Associations
CTAA	Community Transportation Association of America
CTBSSP	Commercial Truck and Bus Safety Synthesis Program
DHS	Department of Homeland Security
DOE	Department of Energy
EPA	Environmental Protection Agency
FAA	Federal Aviation Administration
FHWA	Federal Highway Administration
FMCSA	Federal Motor Carrier Safety Administration
FRA	Federal Railroad Administration
FTA	Federal Transit Administration
HMCRP	Hazardous Materials Cooperative Research Program
IEEE	Institute of Electrical and Electronics Engineers
ISTEA	Intermodal Surface Transportation Efficiency Act of 1991
ITE	Institute of Transportation Engineers
NASA	National Aeronautics and Space Administration
NASAO	National Association of State Aviation Officials
NCFRP	National Cooperative Freight Research Program
NCHRP	National Cooperative Highway Research Program
NHTSA	National Highway Traffic Safety Administration
NTSB	National Transportation Safety Board
PHMSA	Pipeline and Hazardous Materials Safety Administration
RITA	Research and Innovative Technology Administration
SAE	Society of Automotive Engineers
SAFETEA-LU	Safe, Accountable, Flexible, Efficient Transportation Equity Act: A Legacy for Users (2005)
TCRP	Transit Cooperative Research Program
TEA-21	Transportation Equity Act for the 21st Century (1998)
TRB	Transportation Research Board
TSA	Transportation Security Administration
U.S.DOT	United States Department of Transportation